Alma Mater Studiorum – Università di Bologna

DOTTORATO DI RICERCA IN

Ingegneria Civile, Ambientale e dei Materiali

Ciclo XXVIII

Settore Concorsuale di afferenza: 09/D1

Settore Scientifico disciplinare: ING-IND 22

NEW PHOSPHATE-BASED TREATMENTS FOR CARBONATE STONE CONSOLIDATION AND PROTECTION

Presentata da: **Gabriela Graziani**

Coordinatore Dottorato

Prof. A. Lamberti

Relatore

Dott. Ing. E. Franzoni

Correlatori

Dott. Ing. E. Sassoni

Prof. G.W.Scherer

Esame finale anno 2016

TABLE OF CONTENTS

Summary

When building materials are exposed to environment, weathering phenomena seriously compromise their integrity and cohesion, leading to relevant loss of material. This is a critical issue, especially in the field of cultural heritage conservation. For this reason, consolidants (aimed at restoring the material's cohesion and mechanical properties) and protectives (aimed at protecting the substrate from weathering agents) are used.

However, none of the products commercially available presently fulfills all of the requirements that stone consolidants and protectives must fulfill, namely efficacy, compatibility and durability (in general, traditional inorganic products lack efficacy, while organics lack compatibility and durability). To overcome the limitations of currently available treatments, in 2010 a novel hydroxyapatite-based consolidant was proposed for limestone consolidation and recently for marble protection. Hydroxyapatite (HAP) has very low solubility and dissolution rate and it also has lattice parameters close to those of calcite, hence epitaxial nucleation of HAP on calcite is expected to occur. HAP can be obtained by a mild wet chemical route by reacting a phosphatic salt (generally diammonium hydrogen phosphate) with calcium ions, either deriving from millimolar dissolution of the stone or externally added. Reaction can occur at room temperature, without using acidic pH or toxic products. Results obtained so far are very promising, but because the treatment is of very recent introduction, all the aspects concerning a systematic evaluation of its efficacy, compatibility and durability when applied to different substrates, as well as the determination of a treatment protocol, are yet to be performed. Moreover, no application to real historical artifacts nor on-site application had been performed. One critical feature of the treatment that needs specific evaluation is the fact that not only HAP, but several metastable calcium phosphate phases can be formed by the reaction, some of which have high solubility and can be detrimental for the treatment success. Moreover, HAP can easily incorporate foreign ions (mostly carbonates) that might alter its crystallinity and solubility, together with the morphology of the treated layer. For this reason, a systematic evaluation of the composition of the phases that form and of the morphology of the treated layers that are obtained by varying the treatment parameters also needs to be performed.

Therefore, the present research was devoted to the systematic investigation of the novel HAP treatment as a consolidant and protective for carbonate stones (limestone and marble). Specific treatment procedures were set up for each of the tested conditions and all the aspects concerning treatments efficacy, compatibility and durability were evaluated for different substrates. Results were compared to those obtained by using either ethyl silicate or ammonium oxalate, i.e. the commercial products most widely used in the on-site practice for the relevant lithotypes. The

effects of varying the treatment parameters and/or the substrate to which the coating is applied were evaluated, in terms of composition and morphology of the new phases. Limestone and marble were selected because of their different composition (almost 100% calcite in the case of marble, calcite and quartz in the case of limestone) and microstructural features (almost no open porosity in the case of marble, porosity up to 40% in the case of limestone). These different features make the two types of stones prone to different weathering phenomena and lead to different consolidant uptake and distribution, so that using the same treatment on different substrates may lead to significantly different treatment outcomes.

In the case of limestone, weathering processes related to its porous structure (e.g., freezing-thawing and salt crystallization cycles) were identified as critical. These weathering actions cause severe phenomena such as flaking, scaling, erosion and alveolization, all leading to significant decreases in mechanical properties and loss of cohesion, with loss of substantial parts of material that make consolidation necessary. For this reason, the first part of the thesis *("Part 1: Limestone Consolidation")* was devoted to the investigation of limestone consolidation. First, the best application conditions were investigated to maximize the treatment performance; then, for limestone treated with the selected application method, the HAP-treatment efficacy, compatibility and durability were evaluated in comparison with ethyl silicate, currently the most used consolidant for this lithotype.

In the case of marble, loss of grain cohesion due to anisotropic deformation of calcite caused by thermal weathering (the so-called "sugaring") and dissolution in acidic rain were identified as the most severe weathering phenomena. For this reason, the second part of the thesis *("Part 2: Marble Consolidation")* was devoted to consolidation of sugaring marble and the last part *("Part 3: Marble Protection")* to marble protection against corrosion in acidic rain.

In *"Part 2"*, different formulations of the HAP-treatment were first investigated and the effects evaluated in terms of composition and morphology of the new phases. Then, the efficacy and the compatibility of the treatment were evaluated and compared to those of ammonium oxalate and ethyl silicate. Tests were carried out on artificially weathered samples, in laboratory conditions. Afterwards, the treatment protocol exhibiting the most promising results was applied to a naturally weathered real historical artifact, where possible presence of contaminants, surface roughening and non-uniform weathering conditions could affect the treatment outcome. Efficacy and compatibility of the HAP-treatment when applied to the real historic artifact were compared to those obtained on laboratory samples. Particular attention was devoted to differences in phase formation as a result of the presence of contaminants and of weathering features. Finally, based on the encouraging results obtained in the previous phases, a pilot application of the HAP-based treatment was carried out on

site, on the historic Rolandino De' Passeggeri Tomb in Bologna (XIII century). In this case, efficacy and compatibility were evaluated by non-destructive tests.

In *"Part 3"*, the effect of several treatment parameters on the morphology, composition and acid resistance of the HAP-coating was investigated, with the aim of creating a continuous, non-porous, crack-free HAP layer on top of calcite, so as to suppress marble dissolution in acidic rain. In particular, the parameters taken into consideration were concentration and pH of the starting solution, inorganic and organic additions, possibility to couple subsequent layers with different properties. The most promising treatment procedure was selected by evaluating surface morphology and composition of the coating and by measuring the acid resistance of treated samples. At this step, tests were performed on calcite powders, then the most promising formulations were applied to Carrara Marble specimens and tested by a simulated rain apparatus, that allows reproducing both dissolution and mechanical action exerted by rain on site.

The HAP-based treatment was found to give excellent results for all the aims tested, namely limestone consolidation, marble consolidation and marble protection.

In particular, for limestone consolidation, the best treatment procedure was identified, which allowed to obtain remarkable efficacy and compatibility. The efficacy was found to be highly dependent on the application procedure, which influences consolidant uptake and retention in the stone pores, mechanical properties, aesthetical outcome of the treatment and also redistribution of the consolidant in the phases following the treatment application. When compared to ethyl silicate, the HAP-treatment exhibited improved compatibility and a slightly lower efficacy. Efficacy, however, was counterbalanced by a much higher durability, which causes initial benefit of ethyl silicate to be rapidly lost. No metastable phases but only HAP formation was detected as a result of the proposed treatment.

Remarkable efficacy and compatibility were assessed also for marble consolidation, both on laboratory samples, naturally weathered samples and on site. This indicates that HAP exhibits a good performance on several substrates with very variable characteristics. One of the most important findings of "*Part 2*" is that phase formation on real historical objects might be remarkably different from that assessed in laboratory conditions: in fact, it seems that presence of gypsum contamination, in combination with increased surface roughness caused by weathering, favor the formation of HAP instead of other calcium phosphate phases. This is a very important finding, as combination of gypsum presence and surface roughening are very common on site, due to the presence of black crusts. Finally, the possibility of obtaining a continuous crack-free HAP coating over calcite, that enhanced marble acid resistance, was highlighted. In particular, ethanol

additions were found to enhance surface coverage without crack formation and to increase remarkably marble resistance to dissolution. None of the other tested parameters have shown a beneficial effect; however, changes in pH of the starting solution and millimolar cationic and anionic additions were found to completely alter surface morphology, composition and acid behavior of the coatings. The effect of the solution concentration and of the resulting coating thickness on crack formation was also envisaged. Finally, the results obtained on powders were verified by testing the most promising formulations on coarse Carrara marble specimens, by means of a simulated rain apparatus: the beneficial effect of ethanol was confirmed, though improvements were less dramatic than for the powders, and the most promising formulation have shown reduced dissolution compared to untreated marble and ammonium oxalate.

State of the art and research aims

Materials on site suffer from weathering due to the interactions with the environment [1]. Weathering results in alterations of the material characteristics, generally connected with a gradual reduction in mechanical properties and an increase in porosity, pore size and water absorption that, in turn, favor further weathering [2-4].

The morphology and extent of decay depend on a multitude of parameters, including environmental factors (such as the type and extent of environmental actions that affect the materials) and characteristics of the materials themselves (mostly in terms of composition, microstructure, transport properties and tensile strength) [5]. Microstructural, physical and mechanical properties of the materials, together with their mineralogical composition, determine the relevance and extent of damage caused by each weathering factor.

These phenomena are particularly relevant as they affect historic materials, such as natural stones and mortars used in architecture and sculpture [4], with consequent damage of objects of inestimable artistic and historical value (examples of weathering in historic artifacts are in figure 1). Weathering, in fact, may be very severe and lead to phenomena such as flaking, scaling, pulverization and detachments, that cause the loss of significant parts of the original material, thus seriously compromising the integrity of historic artworks.

Figure 1: Examples of weathering phenomena affecting materials on site. In particular, biological decay, salt weathering and erosion, marble disgregation, sugaring of marble, plaster flaking and masonry erosion, efflorescence and black crusts are reported.

For these reasons, consolidation and protection interventions are often needed. Consolidation and protection are two of the phases of Conservation practice [5], together with cleaning and preconsolidations, when needed: cleaning, however, is beyond the scope of the present thesis and will not be discussed.

Consolidation treatments aim at restoring materials integrity by binding loose grains, improving their cohesion and bonding to the substrate, and thus enhancing mechanical properties [6-10]. To be effective, a consolidant must distribute homogeneously in depth in the stone, so as to reach the unweathered substrate, and bind it to the consolidated layer [6,7,11]. No mismatch should occur between the two parts, so as to prevent incompatibility and possible detachments.

Protection, instead, is meant to prevent aggressive interactions between the historical artifacts and the surrounding environment. Surface protection consists in the application of a superficial layer over stone, which acts as a barrier protecting the substrate from weathering agents, such as rainwater and/or pollutants, without altering the appearance of the stone [6,12,13]. Stone protectives can either create a superficial layer that would impede or at least slow down stone dissolution, or protect stone by making it water repellent [14], as the great majority of weathering phenomena are caused or enhanced by the presence of moisture [15].

Both consolidants and protectives must fulfill fundamental conservation principles, namely efficacy, compatibility, durability and retreatability [4,7,11]. Moreover, they must not be toxic or harmful for either the substrate or the environment, nor lead to the formation of noxious byproducts [7,11,16].

To be considered *effective*, a consolidant must distribute in depth in the stone, so as to bind the disaggregated part of the stone to the sound substrate, thus improving the mechanical properties of the material and enhancing its resistance to further decay [6,7,11]. A protective, instead, is generally required to create a continuous, non-porous, non-cracked layer on top of the stone, which enhances stone resistance to solubilization. To do so, it must either have low solubility or be hydrophobic.

In terms of *compatibility*, consolidants and protectives must not alter materials characteristics in a negative sense or to too great an extent [17]. All aesthetic, physical, microstructural and thermal properties need to be taken into consideration when evaluating compatibility [11,17,18].

Durability, instead, requires that the consolidant or protective not loose effectiveness, suffer detrimental alterations or give rise to harmful by-products as a result of weathering [7]. Moreover, it must not cause incompatibility with the substrate due to ageing [5,19]. That is to say that durability takes into consideration both the resistance of the consolidant itself and its capability to protect the substrate from further weathering. In fact, as previously mentioned, materials susceptibility to

weathering depend on a multitude of factors, also connected to materials mechanical, physical and microstructural properties [20-24]: when consolidants and/or protectives are applied to a weathered material, they might alter several of these characteristics, hence making it even harder to predict durability of treated materials, to such an extent that they might even increase materials' susceptibility towards weathering [5].

Conservation principles also require *reversibility*, i.e. the possibility to undo any intervention at any date after its application [6,16], as one of the fundamental requirements; however, stone consolidants and protectives are generally not reversible, apart from some thermoplastic organic resins that can be dissolved in solvents. Also in the latter case, a complete removal of the products from stone pores is very unlikely and is expected to cause severe harm to the stone [11]. For this reason, stone consolidants and protectives are required to be retreatable, which means that their application must not prevent the possibility to retreat the stone with the same or other products at a later time [16].

Each of these requirements imply that the product must comply with a series of demands; however, which parameters should be taken into consideration to evaluate compliance to demands and the extent of modification that is desired for those parameters is debated, hence evaluation of effectiveness, compatibility and durability is quite challenging [11,16,18].

As stone consolidants and protectives are generally to be considered non-reversible and because incorrect applications of these products have often resulted in acceleration of material decay [20,25,26], the search for suitable products for stone consolidants and protectives is a particularly urgent task.

Several materials have been proposed both as stone consolidants and/or protectives, generally distinguished between organic and inorganic products [6,8,27]. Traditional inorganic products are generally compatible but lack efficacy. Organics, on the other hand, exhibit limited compatibility and/or durability [28,29]. For this reason, no fully satisfactory products are available at the present stage.

Recent studies have investigated the possibility to enhance compatibility and durability of organic products [12,30]; however, inorganics are generally preferred. Briefly, traditional inorganic products include barium hydroxide-based and, mostly, lime-based consolidants (such as lime-milk and lime-water). Lime-based products aim at producing calcium carbonate in the stone pores due to reaction with atmospheric CO_2 [31,32]. Calcium carbonate, being the main component of multiple stone types, is highly compatible and is hence expected to bind loose grains as calcium carbonate matrix actually does in natural stones. However, small penetration depth, slow carbonation and limited solubility in water make the effectiveness of these products very limited [33]. Dimensional

reduction to the nano-scale has been proposed to increase penetration depth [34,35], but results obtained so far are not very satisfactory. For this reason, nanolimes currently find applications where only limited penetration depth is required (such as in the case of paintings), while no promising results have so far been achieved for stone consolidation.

At the present stage, ethyl silicate (ES) is the most used consolidant for stone [36,37]. Ethyl silicate belongs to the class of alkoxysilanes [26]. Alkoxysilanes, which also include methyltrimethoxysilane (MTMOS) and methyltriethoxysilane (MTEOS), have been extensively investigated in the last decades as stone consolidants and protectives, due to some of their intrinsic properties, namely low viscosity allowing a good penetration depth [26,38,39], ability of forming Si–O–Si bonds with the substrate significantly improving stone mechanical properties [26] and absence of harmful reaction by-products. They are an intermediate class between organic and inorganic products, and do not suffer from the main drawbacks of the latter ones, as Si-O-Si bonds allow high stability and good durability [26,38-40]. Alkoxysilanes containing methyl groups are hydrophobic and hence can be used as stone protectives; however, due to some issues especially regarding their safe use by the operator, they are not frequently used [26].

The consolidating action of ES occurs due to hydrolysis and condensation reactions that finally lead to the formation of silica gel in the stone pores [16,41]. More in detail, ethyl silicate, ($Si(OC_2H_5)_4$) is introduced into the pores where it undergoes hydrolysis reaction, that cause ethoxy groups (OC_2H_5) to be substituted by hydroxyl groups (OH) [31]. Then a condensation reaction takes place that leads to the formation of silica gel [32]. Silica gel, despite not being identical to quartzitic fractions in stone, can be regarded as compatible with quartz-containing stones: moreover it does not cause too dramatic a pore occlusion, thus further boosting the widespread use of this consolidant [4].

When silicate fractions are present in the stone, and hence hydroxyl groups are available on grains surfaces, chemical bonding (in the form of covalent bonds) may form between silica gel formed from ES and the substrate [25,32]. However, in the absence of a silicate fraction, that is to say in the case of carbonate materials (such as marble, limestone, calcareous sandstone and lime-based mortars), no chemical bonding occurs but only physical-mechanical bonding, thus resulting in very limited efficacy [42].

Moreover, ES exhibits some further drawbacks mainly owing to the tendency to crack and to very slow curing reactions (even in presence of a catalyst) [3,7,27], that are also the cause of temporary hydrophobicity of the substrate. Curing reactions, in fact, occur due to the reaction with atmospheric moisture and can require up to 6-7 months to be complete [43,44]. Ethoxy groups make the stone hydrophobic, hence temporary hydrophobicity lasts until curing reactions are

complete [32]. Hydrophobicity is only temporary, thus not suitable for the use of ES as a protective, plus it might give rise to some issues, such as impossibility to perform water-based treatments (such as cleaning or repair by mortars and grouts) for several months after its application, and can also give rise to incompatibility if a water source is present behind the consolidated layer [16]. In fact, water, possibly carrying salts, would be impeded from exiting the stone, thus possibly causing detachments.

In brief, ethyl silicate is highly effective on quarzitic stones, but its effectiveness on carbonate stones, such as marble and limestone, may be very limited. To enhance ES efficacy on carbonate stones coupling-agents have been proposed (e.g., tartaric acid, organoalkoxysilanes, etc.), having an anchor group on the one end that can bond to calcite, and an OH- group on the other end, to bond with silica gel [3,7].

Despite its limited efficacy on carbonate stones, ES is still largely used on these lithotypes, mostly due to the lack of more suitable alternatives [20]. Carbonate stones, however, have been used since ancient times in architecture and sculpture and are subject to several and very severe weathering mechanisms [32], mostly due to the susceptibility of calcite, that is their main constituent. Calcite in fact, has relatively high solubility, which makes it prone to dissolution in acidic rain, suffers anisotropic deformation due to thermal cycles, that cause phenomena such as bowing and sugaring of marble, and is also prone to sulphatation and formation of black crusts. Moreover, carbonate stones may be highly porous, thus susceptible to other phenomena, such as freeze-thaw cycles or salt crystallization.

For these reasons, the study of suitable products for consolidation and protection of carbonate stones is of paramount importance in the field of cultural heritage conservation and was the aim of this PhD thesis.

For consolidation and protection of calcitic substrates, several products are currently under study; among the others, ammonium oxalate is that most widely investigated [45-48]. The idea of using calcium oxalate (calcium oxalate monohydrate, whewellite, $CaC_2O_4 \cdot H_2O$) as a protective for stone was first proposed by Matteini et al. [45]. Calcium oxalate can be formed by a mild chemical reaction between calcite and a solution of ammonium oxalate that is applied to the stone. Ammonium oxalate does not induce chromatic alterations on stone surface; however, results obtained so far are not as promising as expected, for various reasons [31]. First, a significant mismatch exists between the lattice parameters of calcite and oxalate, that prevents epitaxial growth of calcium oxalate on calcite and hence can lead to the formation of patchy and/or porous layers.

Second, ammonium oxalate is not remarkably less soluble than calcite, so it was found to be effective in delaying weathering but not in preventing it [32].

For this reason, in 2010 a novel treatment was proposed for limestone consolidation and lately investigated for marble protection. The treatment consists in the formation of hydroxyapatite (HAP), that is the main constituent of mineralized tissue of mammals (bone, enamel and dentine) and can be formed by reaction with calcite by a mild chemical reaction [32]. Hydroxyapatite, $Ca_5(PO_4)_3(OH)$, is usually indicated as $Ca_{10}(PO_4)_6(OH)_2$, as the crystal unit cell comprises two formula units [32].

HAP, as well as calcium oxalate, is one of the constituents of adherent and protective mineral patinas found on ancient monuments, probably originated by slow weathering of ancient treatments (for example milk-based coatings [49,50]). The existence of these patinas themselves after centuries of exposure to environmental agents indicate a good durability of the material. Different from calcium oxalate, HAP has a much lower lattice mismatch with calcite and is much less soluble [31].

Specifically, the efficacy of HAP for stone consolidation and protection was hypothesized on the basis of the following considerations [32]:

- HAP solubility and dissolution rate are much lower than those of calcite: solubility products at 25 °C being $K_sp = 1.6 \cdot 10^{-117}$ for HAP [51] and $K_{sp} = 3.4 \cdot 10^{-9}$ for calcite [52]. Because the formula for HAP contains 18 ions and that of calcite contains 2, the solubility of the "molecule" is $c_{HAP} = K_{sp}^{1/18} \approx 3.25 \times 10^{-7}$ M and $c_{Calcite} \approx 5.83 \times 10^{-5}$ M (in terms of grams/liter or moles of Ca^{2+} dissolved in a liter of solution, HAP is about 18 times less soluble than calcite). HAP dissolution rate [53-55] is about 4 orders of magnitude lower than that of calcite [56];
- HAP has a hexagonal unit cell [57], while calcite has a rhombohedral unit cell, but is often described as hexagonal [26]. In terms of lattice parameters: for HAP a = b = 9.43 Å and c = 6.88 Å (two unit cells are considered), for calcite a = b = 9.96 Å and c = 17.07 Å [59,60]). This good lattice match should favor the epitaxial formation of a HAP layer on top of calcite.

A wide variety of deposition techniques have been proposed in the literature for deposition of HAP [51,61-65], mostly for use in the biomedical field: however, the great majority of those is not suitable for use in the field of cultural heritage, because of the application at high temperature, in acidic conditions or involving use of toxic compounds. Moreover, surfaces of large dimensions might need to be treated, hence techniques using deposition chambers need to be discarded. This also implies that large amounts of product can be used, which makes the aspects connected to the health of the operator and the non-toxicity for the environment of paramount importance and also has an economical impact.

One suitable procedure for on-site application is available, consisting in the reaction of a phosphate

salt (generally diammonium hydrogen phosphate, DAP, $(NH_4)_2HPO_4$) with calcium ions that can either derive from partial dissolution of the stone or can be externally added [31,32,66,67]. This way, HAP is not introduced into marble as already formed particles (not even at the nanoscale) that could affect penetration depth of the solution, but it is formed directly at grain boundaries or in micro-cracks on the surface of calcite grains. Moreover, the solution has low viscosity, further enhancing its penetration in porous substrates. The solution is water-based and non-toxic for the operator and the environment.
The reaction, that occurs at room temperature is reported below [68]:

$10CaCO_3 + 5(NH_4)_2HPO_4 \rightarrow Ca_{10}(PO_4,CO_3)_6(OH,CO_3)_2 + 5(NH_4)_2CO_3 + 3CO_2 + 2H_2O$,
where PO_4^{3-} and OH^- can be partially replaced by CO_3^{2-}.

The so-formed HAP is generally non-stoichiometric (several substitutions are often found, the most common being that of carbonate ions) and several metastable calcium phosphate phases [51,71-75], eventually converting into HAP [69,70], can be formed by the reaction (see Table 1). Those phases have different Ca/P ratio and solubility, and are all more soluble than HAP for the relevant pH range (that is above pH 4), thus their formation instead of HAP is generally undesired.

Compound		Formula	Ca/P ratio	Solubility at 25°C [g/l]
HAP	Hydroxyapatite	$Ca_{10}(PO_4)_6(OH)_2$	1.67	~0.0003
CDHA	Calcium-deficient HAP	$Ca_{10-x}(HPO_4)_x(PO_4)_{6-x}(OH)_{2-x}$ (0<x<1)	1.5-1.67	~0.0094
ACP	Amorphous calcium phosphate	$Ca_xH_y(PO_4)_z \cdot nH_2O$ (n=3-4.5, 15-20% H_2O)	1.2-2.2	n.a.
β-TCP	β-Tricalcium phosphate (or calcium phosphate tribasic)	β-$Ca_3(PO_4)_2$	1.5	~0.0005
OCP	Octacalcium phosphate	$Ca_8(HPO_4)_2(PO_4)_4 \cdot 5H_2O$	1.33	~0.0081
DCPD	Dicalcium phosphate dihydrate (or brushite)	$CaHPO_4 \cdot 2H_2O$	1	~0.088
DCPA	Dicalcium phosphate anhydrous (or calcium phosphate dibasic)	$CaHPO_4$	1	~0.0048
MCPM	Monocalcium phosphate monohydrate	$Ca(HPO_4)_2 \cdot H_2O$	0.5	~18
MCPA	Monocalcium phosphate anhydrous (or calcium phosphate monobasic)	$Ca(HPO_4)_2$	0.5	~17

Table 1: Overview of the most diffused calcium phosphates [76]

HAP is prone to incorporation of both anionic and cationic substitutions that can alter its lattice and its properties, mostly in terms of crystallinity and solubility [66,67,77,78]. For this reason, they might be employed to modify the properties of the HAP layer that is formed.

Preliminary experiments on the use of HAP for limestone consolidation have shown promising results [31,32], as HAP was found to have good efficacy without substantially modifying the microstructure and appearance of stone. Moreover, mechanical strength is achieved in just 48 hours curing, which is another important advantage of this technique.

However, when research for the present the PhD thesis was started, all the aspects connected to the setup of a treatment procedure and the systematic investigation of efficacy, compatibility and durability of the proposed treatment, when applied to different substrates, was yet to be determined. At the same time, no application to real historic artifacts or on-site testing had been performed.

Given all the aspects discussed so far, the present thesis was divided into three main parts:

- *Part 1: Limestone consolidation*
- *Part 2: Marble consolidation*
- *Part 3: Marble protection*

Marble and limestone were chosen because they exhibit remarkably different microstructural features that cause, on the one hand, susceptibility to different decay phenomena (examples of use and weathering of Limestone and Marble are in figure 2 and figure 3, respectively) and, on the other hand, different absorption and distribution of the consolidant and hence different performances. Moreover, the different composition and morphological features of the two lithotypes is also expected to influence the phases that form as a result of the treatment and the morphology of the treated layer.

Figure 2: Globigerina Limestone used in Santa Caterina degli Italiani Church (Malta) and examples of weathering (alveolization) in the same stone.

Figure 3: Marble columns and façade in San Pietro Church (Rome, Italy) and examples of weathered marble (black crusts, grain disaggregation and material loss). San Pietro columns have recently undergone protective treatment for preventing corrosion.

The main factors that cause decay of porous limestone are salt crystallization and freeze-thaw cycles, both largely depending on stone tensile strength and microstructure [79-83]. The latter is particularly relevant as it determines not only the amount of water/saline solution that is absorbed by the materials, but it also influences the crystallization pressure, which controls the material's decay [5]. The pore system of the stone also determines consolidant absorption and redistribution in the substrate and, as a consequence, penetration depth, homogeneity in the distribution in depth, mechanical properties and physical-microstructural alterations. These modification caused by the consolidants, in turn, affect further resistance to weathering.

Globigerina limestone was chosen for the tests on limestone consolidation, in view of its high porosity and water uptake that make it prone to severe decay, due to flaking and powdering and a very severe form of alveolization, i.e. a combination of salt crystallization and wind erosion [84].

Globigerina limestone (''Franka'' variety [43]) has a very high carbonate content (93 wt.%), owing to calcite crystals and fossils, bonded by calcareous cement and it also contains traces of quartz and possibly clays [3,21]. The microstructure of the stone is characterized by very high open porosity (~ 40%), mainly owing to coarse pores, which leads to very high sorptivity [3,21].

Part 1 "Limestone consolidation" comprises Chapters I to IV. In Chapter I, a treatment protocol will first be set up, so as to determine the most effective procedure for HAP application on porous limestone. In fact, several aspects (such as the precursor to be used and its concentration, the eventual addition of calcium ions and the application method) do have an impact on the treatment outcome and need to be specifically evaluated. For all the tests, stone is artificially weathered prior to the tests, in order to reproduce the weathering damage that materials exhibit on site. In Chapter II, the distribution of the consolidant inside the porous network of the material as function of the application method will be evaluated. This aspect is relevant as it determines the penetration depth and the uniformity of distribution inside the substrate and also influences phase formation as a

result of the reaction.
In Chapters III and IV, the efficacy, compatibility and durability of the novel treatment will be systematically investigated, in comparison with that of ethyl silicate, which is currently the most used consolidant for limestone consolidation. By doing so, it will be determined whether or not the new HAP-based treatment is a valuable option for limestone consolidation or if the treatment needs further optimization. Prior to the evaluation, the requirements to be obtained will be discussed. Then, a preliminary investigation about retreatability and toxicity of the two consolidants will be performed.

In the case of marble, thermal weathering, causing disaggregation of calcite grains (the so-called "sugaring") and chemical weathering, leading to calcite dissolution in acidic rain, are the most significant phenomena [84,85]. Therefore, consolidation of sugaring marble is the object of *Part 2*, while protection against dissolution in acidic rain is discussed in *Part 3*.

Part 2 "Marble consolidation" comprises Chapters V to VII. In Chapter V, a protocol for marble consolidation will be first set up in laboratory by using artificially weathered samples. Morphology and phase composition of the treated layer were evaluated to determine the most promising procedure. Then, efficacy and compatibility of the most promising treatments were tested in comparison with ammonium oxalate and ethyl silicate. Then, as reported in Chapter VI, the treatment was applied to a naturally weathered sample, coming from the Monumental Cemetery in Bologna (the Cemetery is part of the Association of Significant Cemeteries of Europe-ASCE). This allowed testing of the treatment efficacy and compatibility and, especially, phase composition and layer morphology change when the treatment is applied to real historical samples that are affected by contaminations, which often cannot be completely removed, and by non-uniform weathering conditions.
Finally, as described in Chapter VII, an application on site was performed, on Rolandino De' Passeggeri Tomb in Bologna (XIII century). In this case, the application was made even more difficult because environmental parameters could be monitored, but unexpected environmental conditions could occur. Moreover, only non-destructive tests could be used for evaluation of the weathering conditions and the treatment outcome.

In *Part 3*, constituted by Chapters VIII and IX, marble protection against corrosion in an acidic environment was investigated. The aim was achieving a continuous uncracked and nonporous layer of hydroxyapatite over marble, so as to prevent its dissolution. First, the effects of precursor concentration, organic and inorganic additions and pH of the starting solution on the morphology,

composition and acid resistance of treated samples were investigated. Double treatments were also investigated to obtain superimposed layers with different properties. At this step, powders were used to speed up dissolution processes and hence reduce the impact of other processes that might occur alongside dissolution. Moreover powders allowed to examine a very high number of grains with different crystallographic orientation and impurities. By doing so, it was possible to determine the best treatment procedure to be applied. Results were compared to those obtained for Ammonium Oxalate (AmOx).
Then, the most promising formulations were tested on Carrara marble specimens with a simulated rain apparatus, so as to get closer to real conditions on site.

By doing so, a systematic evaluation of the HAP-treatment for consolidation and protection of carbonate stones was achieved, in comparison with products currently available for stone conservation.
Efficacy, compatibility and durability of the treatment, as well as phase formation, as a result of different treatment parameters and different characteristics of the substrate, were evaluated and discussed.
Finally, feasibility and performance of the proposed treatment were evaluated from laboratory testing to on site application.

References

[1] Graziani G., Sassoni E., Franzoni E., Consolidation of porous carbonate stones by an innovative phosphate treatment: mechanical strengthening and physical-microstructural compatibility in comparison with TEOS-based treatments, Herit Sci 3 (2015)

[2] Tugrul A., The effect of weathering on pore geometry and compressive strength of selected rock types from Turkey. Eng Geol 75 (2004) 215–27.

[3] Franzoni E., Sassoni E., Scherer G.W., Naidu S., Artificial weathering of stone by heating. J Cult Herit 14S (2013) e85–93.

[4] Sassoni E., Graziani G., Franzoni E., An innovative phosphate-based consolidant for limestone. Part 1: Effectiveness and compatibility in comparison with ethyl silicate, Constr Build Mater 102 (2016) 918-930

[5] Graziani G., Sassoni E., Franzoni E., Experimental study on the salt weathering resistance of fired clay bricks consolidated by ethyl silicate, Materials and Structures (2015) DOI 10.1617/s11527-015-0665-8

[6] Amoroso G.G., Fassina V., Stone decay and conservation. New York: Elsevier; 1983.

[7] Lazzarini L., Laurenzi Tabasso M., Il restauro della pietra. Padua: CEDAM; 1986.

[8] Zendri E., Biscontin G., Nardini I., Riato S., Characterization and reactivity of silicatic consolidants. Constr Build Mater 21 (2007) 1098–106.

[9] Toniolo L., Paradisi A., Goidanich S., Pennati G., Mechanical behaviour of lime based mortars after

surface consolidation. Constr Build Mater 25 (2011) 1553–9.

[10] Vacchiano C.D., Incarnato L., Scarfato P., Acierno D., Conservation of tuff-stone with polymeric resins. Constr Build Mater 22 (2008) 855–65.

[11] Italian Recommendation NORMAL 20/85. Conservazione dei materiali lapidei: Manutenzione ordinaria e straordinaria, Istituto Centrale per il Restauro (ICR), Rome; 1985.

[12] Cardiano P., Ponterio R.C., Sergi S., Lo Schiavo S., Piraino P., Epoxy-silica polymers as stone conservation materials. Polymer 46 (2005) 1857-1864

[13] Tsakalof A., Manoudis P., Karapanagiotis I., Chryssoulakis I., Panayiotou C., Assessment of synthetic polymeric coatings for the protection and preservation of stone monuments. J Cult Herit 8 (2007) 69-72

[14] Matteini M., Inorganic treatments for the consolidation and protection of stone artifacts. Conserv Sci Cult Herit 8 (2008): 13–27

[15] Lourenço P.B., Luso E., Almeida M.G., Defects and moisture problems in buildings from historical city centres: a case study in Portugal. Build Environ 41(2006) 223-234

[16] Scherer G.W., Wheeler G.S., Silicate consolidants for stone. Key Eng Mater 391 (2009) 1–25.

[17] Van Balen K., Papayanni I., Van Hees R., Binda L., Waldum A., Introduction requirements for and functions and properties of repair mortars. Mater Struct 38 (2005) 781–5.

[18] Cnudde V., Cnudde J.P., Dupuis C., Jacobs PJS., X-ray micro-CT for the localization of water repellents and consolidants inside natural building stones. Mater Charact 53 (2004) 259-71.

[19] Sassoni E., Graziani G., Franzoni E., An innovative phosphate-based consolidant for limestone. Part 2. Durability in comparison with ethyl silicate. Constr Build Mater 102 (2016) 931-942

[20] Maravelaki-Kalaitzaki P., Kallithrakas-Kontos N., Korakaki D., Agioutantis Z., Maurigiannakis S., Evaluation of silicon-based strengthening agents on porous limestones. Progr Org Coat 57 (2006) 140-148

[21] E. Sassoni, E. Franzoni, Influence of porosity on artificial deterioration of marble and limestone by heating, Appl Phys A Mater 115 (2014) 809–16

[22] E. Sassoni, E. Franzoni, Carrara marble consolidation by hydroxyapatite and behavior towards thermal weathering after consolidation, Proceedings of "Built Heritage 2013. Monitoring Conservation Management" Springer International Publishing Switzerland, Editors: Lucia Toniolo, Maurizio Boriani, Gabriele Guidi, pp.379-389

[23] C. Miliani, M.L. Velo-Simpson, G.W. Scherer, Particle-modified consolidants: a study on the effect of particles on sol–gel properties and consolidation effectiveness, J Cult Herit 8 (2007) 1–6

[24] Tsui N., Flatt R.J., Scherer G.W., Crystallization damage by sodium sulfate. J Cult Herit 4 (2003) 109-115

[25] Maravelaki-Kalaitzaki P., Kallithrakas-Kontos N., Agioutantis Z., Maurigiannakis S., Korakaki D., A comparative study of porous limestones treated with silicon-based strengthening agents, Progr Org Coat 62 (2008) 49-60

[26] Wheeler G., Alkoxysilanes and the consolidation of stone. Los Angeles: The Getty Conservation

Institute; 2005.

[27] Ferreira Pinto A.P., Delgado Rodriguez J., Stone consolidation: the role of treatment procedures. J Cult Herit 9 (2008) 38–53.

[28] Favaro M, Mendichi R, Ossola F, Russo U, Simon S, Tomasin P, et al. Evaluation of polymers for conservation treatments of outdoor exposed stone monuments. Part I. Photo-oxidative weathering. Polym Degrad Stabil 91 (2006) 3083–96.

[29] Carretti E., Dei L., Physicochemical characterization of acrylic polymeric resins coating porous materials of artistic interest. Prog Org Coat 49 (2004) 282–9.

[30] Esposito Corcione C., Striani R., Frigione M., UV-cured siloxane-modified methacrylic system containing hydroxyapatite as potential protective coating for carbonate stones, Prog Org Coat 76 (2013) 1236-1242

[31] Sassoni E., Naidu S., Scherer GW., The use of hydroxyapatite as a new inorganic consolidant for damaged carbonate stones. J Cult Herit 12(2011) 346–55.

[32] Sassoni E., Franzoni E., Pigino B., Scherer G.W., Naidu S. Consolidation of calcareous and siliceous sandstones by hydroxyapatite: comparison with a ES based consolidant. J Cult Herit 14S (2013) e103–8.

[33] Daniele V., Taglieri G., Quaresima R., The nanolimes in Cultural Heritage conservation: characterization and analysis of the carbonatation process. J Cult Herit 9 (2008) 294-301

[34] F. Yang, B. Zhang, Y. Liu, W. Guofeng, H. Zhang, W. Cheng, Z. Xu, Biomimic conservation of weathered calcareous stones by apatite, New J Chem 35 (2011) 887–892.

[35] Liu Q., Zhang B., Synthesis and characterization of a novel biomaterial for the conservation of historic stone building and sculptures. Mater Sci Forum 675–677 (2011) 317–320.

[36] Franzoni E., Pigino B., Leemann A., Lura P. (2013) Use of TEOS for fired-clay bricks consolidation. Mater Struct 47 (2014): 1175-1184

[37] Liu R., Han X., Huang X., Li W., Luo H. Preparation of three-component TEOS-based composites for stone conservation by sol-gel processes. J Sol-Gel Sci Tech 68 (2013) 19-30.

[38] Salazar-Hernandez C., Zarraga R., Alonso S., Sugita S., Calixto S., Cervantes J., Effect of solvent type on polycondensation of TEOS catalysed by DBTL as used for stone consolidation. J Sol-Gel Sci Tech (2009)49:301-310.

[39] Mosquera M.J., Pozo J., Esquivias L., Stress during drying of two stone consolidants applied in monumental conservation. J Sol-Gel Sci Tech 26 (2003)1227-1231.

[40] Baglioni M., Berti D., Teixeira J., Giorgi R., Baglioni P., Nanostructured surfactant-based systems for the removal of polymers from wall paintings: A small-angle neutron scattering study. Langmuir 28 (2012) 15193-15202.

[41] Xu F., Li D., Effect of the addition of hydroxyl-terminated polydimethylsiloxane to TEOS-based stone protective materials. J Sol-Gel Sci Tech 65 (2013) 212-219.

[42] Donatti D., Vollet D.R., Effects of the water quantity on the solventless TEOS hydrolysis under ultrasound transmission. J Sol-Gel Sci Tech 17 (2000) 19-24.

[43] Franzoni E., Graziani G., Sassoni E., TEOS-based treatments for stone consolidation: acceleration of hydrolysis-condensation reactions by poulticing. J Sol-Gel Sci Tech 74 (2015) 398-405

[44] Naidu S., Liu C., Scherer G.W., New techniques in limestone consolidation: Hydroxyapatite based consolidant and the acceleration of hydrolysis of silicate-based consolidants. J Cult Herit 16 (2015) 94-101

[45] Matteini M., Moles A., Giovannoni S., Calcium oxalate as a protective mineral system for wall paintings: methodology and analyses, III Int. Symp. Conservation of Monuments in the Mediterranean Basin, ed. V. Fassina, H. Ott, F. Zezza, 1994.

[46] Conti C., Colombo C., Dellasega D., Matteini M., Realini M., Zerbi G., Ammonium oxalate treatment: Evaluation by μ-Raman mapping of the penetration depth in different plasters. J Cult Herit 12 (2011) 372-379

[47] Doherty B., Pamplona M., Selvaggi R., Miliani C., Matteini M., Sgamellotti A., Brunetti B., Efficiency and resistance of the artificial oxalate protection treatment on marble against chemical weathering. Appl Surf Sci 253 (2007) 4477-4484

[48] Matteini M., Rescic S., Fratini F., Botticelli G., Ammonium phosphates as consolidating agents for carbonatic stone materials used in architecture and cultural heritage: preliminary research. Int J Archit Herit: Conservation, Analysis, and Restoration 5 (2011) 717-736

[49] Polikreti K., Maniatis Y., Micromorphology, composition and origin of the orange patina on the marble surfaces of Propylaea (Acropolis, Athens). Sci Total Environ 308 (2003) 111–119

[50] Alvarez de Buergo M., Fort Gonzalez R., Protective patinas applied on stony facades of historical buildings in the past, Constr Build Mater, 17 (2003) 83–89

[51] Dorozhkin S.V., Calcium orthophosphates in nature, biology and medicine, Materials 2 (2009) 399–498

[52] Lide D.R. (Ed.), CRC Handbook of Chemistry and Physics, The Chemical Rubber Co, Boca Raton, FL (1999)

[53] Harouiya N., Chaïrat C., Köhler S.J., Gout R., Oelkers E.H., The dissolution kinetics and apparent solubility of natural apatite in closed reactors at temperatures from 5 to 50°C and pH from 1 to 6. Chem Geol 244 (2007) 554–568.

[54] Nelson D.G.A., Featherstone J.D.B., Duncan J.F., Cutress T.W., Effect of carbonate and fluoride on the dissolution behavior of synthetic apatites, Caries Res 17 (1983) 200–211.

[55] Zhu Y., Zhanga X., Chena Y., Xiea Q., Lana J., Qiana M., He N., A comparative study on the dissolution and solubility of hydroxylapatite and fluorapatite at 25°C and 45°C. Chem Geol 268 (2009) 89–96.

[56] Brady P.V., Ch. 4 in Physics and Chemistry of Mineral Surfaces, ed. P.V. Brady CRC Press, Boca Raton, FL, 1996.

[57] Boivin G., The hydroxyapatite crystal: a closer look. Medicographia 29 (2007) 126–132.

[58] Skinner A.J., LaFemina J.P., Hansen H.J.F., Structure and bonding of calcite: a theoretical study. Am. Mineral 79 (1994) 205–214.

[59] Mathew M., Takagi S., Structures of biological minerals in dental research, J Res Natl Inst Stand Technol 106 (2001) 1035–1044.

[60] Maslen E.N., Streltsov V.A., Streltsova N.R., Ishizawa N., Electron density and optical anisotropy in rhombohedral carbonates. III. Synchroton X-ray studies of $CaCO_3$, $MgCO_3$ and $MnCO_3$. Acta Crystallogr B51 (1995) 929–939.

[61] Liu C., Huang Y., Shen W., Cui J., Kinetics of hydroxyapatite precipitation at pH 10 to 11. Biomaterials 22 (2001) 301–306.

[62] Osaka A., Miura Y., Takeuchi K., Asada M., Takahashi K., Calcium apatite prepared from calcium hydroxide and orthophosphoric acid. J Mater Sci Mater Med 2 (1991) 51–55.

[63] Brendel T., Engel A., Russel C., Hydroxyapatite coatings by a polymeric route. J Mater Sci Mater Med 3 (1992) 175–179.

[64] Yoshimura M., Suda H., Okamoto K., Ioku K., Hydrothermal synthesis of biocompatible whiskers. J Mat Sci 29 (1994) 3399–3402.

[65] Slòsarczyk A., Stobierska E., Paskiewicz Z., Gawlicki M., Calcium phosphate materials prepared from precipitates with various calcium: phosphorous Molar Ratios. J Am Ceram Soc 79 (1996) 2539–2544.

[66] Naidu S., Scherer G.W., Nucleation, growth and evolution of calcium phosphate films on calcite. J Colloid Interf Sci 435 (2014) 128-137

[67] Naidu S., Blair J., Scherer G.W., Acid attack mechanism on Carrara marble and efficacy of a protective hydroxyapatite film. J Am Ceram Soc (in press)

[68] Kamiya M., Hatta J., Shimida E., Ikuma Y., Yoshimura M., Monma H., AFM analysis of initial stage of reaction between calcite and phosphate. Mater Sci Eng B 111 (2004) 226–231.

[69] Mathew M., Takagi S., Structures of biological minerals in dental research. J Res Natl Inst Stand Technol 106 (2001) 1035–1044.

[70] M.S.A. Johnsson, G.H. Nancollas, The role of brushite and octacalcium phosphate in apatite formation, Crit Rev Oral Bio M 3 (1992) 61–82.

[71] Dorozhkin S.V., Amorphous Calcium Orthophosphates: Nature, Chemistry and Biomedical Applications. Int J Mater Chem 2 (2012) 19-46

[72] Dorozhkin S.V., Biphasic, triphasic and multiphasic calcium orthophosphates. Acta Biomater 8 (2012) 963–977

[73] Dorozhkin S.V., Calcium orthophosphate coatings on magnesium and its biodegradable alloys. Acta Biomater 10 (2014) 2919–2934

[74] Dorozhkin S.V., Calcium orthophosphates. Biomatter 1:2 (2011) 121-164

[75] Doherty B., Pamplona M., Selvaggi R., Miliani C., Matteini M., Sgamellotti A., Brunetti B., Efficiency and resistance of the artificial oxalate protection treatment on marble against chemical weathering. Appl Surf Sci 253 (2007) 4477-4484

[76] Sassoni E., Graziani G., Franzoni E., Repair of sugaring marble by ammonium phosphate: comparison with ethyl silicate and ammonium oxalate and pilot application to historic artifact. Materials and Design 88 (2015) 1145-1157

[77] Boanini E., Gazzano M., Bigi A., Ionic substitutions in calcium phosphates synthesized at low temperature. Acta Biomater 6 (2010) 1882-1894

[78] Supova M., Substituted hydroxyapatites for biomedical applications: A review. Ceram Int 41 (2015) 9203-9231

[79] Martìnez-Martìnez J., Benavente D., Gomez-Heras M., Marco-Castaño L., Garcìa-del-Cura M.A., Non-linear decay of building stones during freeze–thaw weathering processes, Constr Build Mater 38 (2013) 443–454.

[80] Ruedrich J., Kirchner D., Siegesmund S., Physical weathering of building stones induced by freeze-thaw action: a laboratory long-term study. Environ Earth Sci 63 (2011) 1573–1586.

[81] Scherer G.W., Stress from crystallization of salt. Cem Concr Res 34 (2004) 1613–1624.

[82] Cardell C., Delalieux F., Roumpopoulos K., Moropoulou A., Auger F., Van Grieken R., Salt-induced decay in calcareous stone monuments and buildings in a marine environment in SW France. Constr Build Mater 17 (2003) 165–179.

[83] Dubelaar C.W., Dusar M., Dreesen R., Felder W.M., Nijland T.G., Maastricht limestone: A regionally significant building stone in Belgium and The Netherlands. Extremely weak, yet time-resistant, in: Proceedings of the International Conference on Heritage, Weathering and Conservation, HWC 2006, vol. 1, 2006, pp. 9–14.

[84] Sassoni E., Franzoni E., Sugaring marble in the Monumental Cemetery in Bologna (Italy): characterization of naturally and artificially weathered samples and first results of consolidation by hydroxyapatite. Appl Phys A Mater 117 (2014) 1893–1906.

[85] Franzoni E., Sassoni E., Correlation between microstructural characteristics and weight loss of natural stones exposed to simulated acid rain. Sci Total Environ 412–413 (2011) 278-285.


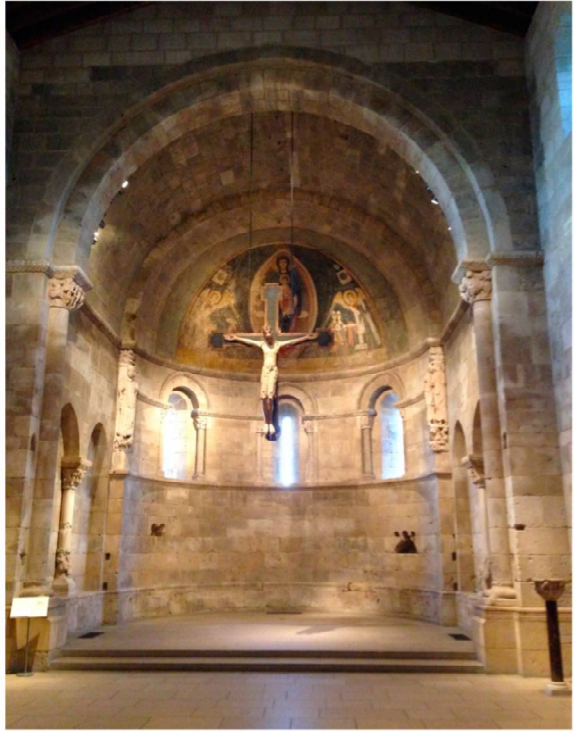
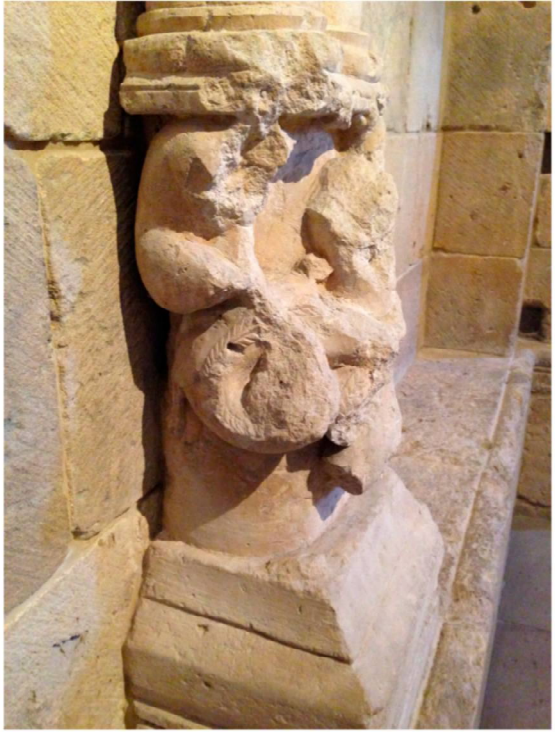

PART 1:
Limestone Consolidation







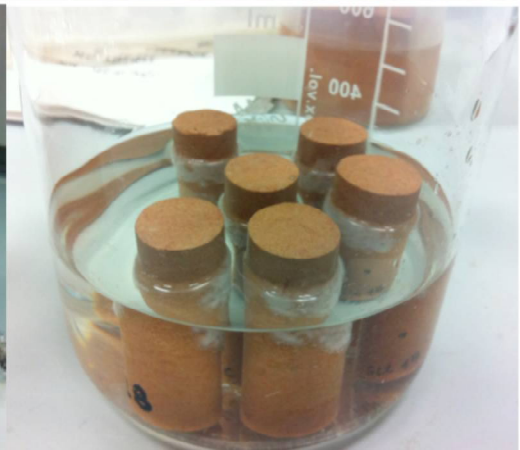

CHAPTER I: Limestone consolidation: Influence of the application method

Research aims

In the present part of the study, the most effective procedure for the application of HAP-based treatments was investigated. A 2-step treatment protocol was proposed consisting in the application of the DAP solution followed by that of a limewater poultice.

First, the attention was devoted to the determination of the most suitable method for the application of the DAP solution. In fact, application procedure determines the amount of consolidant that enters the stone and its distribution. At this step, brushing, poulticing and immersion were compared.

Then, a novel method to remove excess DAP from the stone, hence limiting chromatic alterations and DAP accumulation on the surface, while providing additional calcium ions for the HAP-formation reaction was proposed, consisting in the application of a limewater poultice.

I.1 Introduction

The efficacy of consolidation depends on several parameters, including the characteristics of the consolidant and the substrate themselves (nature and concentration of the consolidant, solvent, physical-chemical properties and microstructure of the substrate), the extent of decay and all the parameters concerning the treatment procedure [1-6]. When the substrate and the consolidant are fixed, a proper selection of the treatment parameters needs to be performed to ensure the effectiveness of the intervention. Among these, in the present research, three were identified as the most critical for HAP-based treatment and are listed below:

1. the precursor to be used and its concentration;
2. the removal of possible unreacted products that might otherwise remain in the stone;
3. the application method.

As consolidation is generally to be considered irreversible, the exact evaluation of all of these parameters is of paramount importance to avoid ineffectiveness or even worsening of the substrate decay [1,2,4,5].

1. Regarding the precursor and its concentration, HAP can be formed by a wet chemical route, by using different phosphate salts, provided that they supply the PO_4^{3-} ions necessary for the reaction [7-11]. It is also of paramount importance that the precursor does not precipitate salts or other harmful by-products during the reaction, nor involve too acidic pH or lead to the formation of hazardous compounds [12]. In view of these considerations, diammonium hydrogen phosphate (DAP, $(NH)_2HPO_4$) is the precursor most frequently chosen in literature [7-14]; together with DAP, also ammonium di-hydrogen phosphate (ADHP, $NH_4H_2PO_4$), with or without NH_3 addition to increase the solution pH, and ammonium phosphate (TAP, $(NH_4)_3PO_4$), have been proposed [14-

16]. Different concentrations have been tested for all these precursors [7,14-16]. The initial aim that pushed towards the search for alternatives to DAP was to boost the formation of PO_4^{3-}: in fact, dissociation of DAP (as well as other phosphate salts) leads to the formation of PO_4^{3-}, HPO_4^{2-} and $H_2PO_4^-$ however, only PO_4^{3-} react with calcium ions so as to form HAP [9]. Despite the initial belief that the dissociation would depend on the precursor, studies highlighted that it is irrelevant, as the pH is the driving parameter in determining the dissociation of the salt and hence the formation of a greater relevant amount of PO_4^{3-}. Moreover, DAP is the precursor that leads to the higher dissociation in PO_4^{3-} at the pH range that is relevant for the research [8,9].

As no benefit can be expected in terms of dissociation in PO_4^{3-} by using alternative salts, DAP was chosen as the most promising precursor and was the only one used in the present research, also in view of the following considerations. AP is not available in the European market, which would have made its use impractical. For the given pH range, DAP is the precursor that results in higher formation of HAP and lower formation of soluble phases, as ADPH leads to the formation of mostly brushite, which is much more soluble than HAP at the pH ranges above 4 [7,12,14,17].

Regarding the concentration, because only a limited amount of DAP dissociates into PO_4^{3-} that can react to form HAP, high concentrations are needed to achieve a good efficacy of the treatment. Consistently, previous research had highlighted that increasing DAP concentration results in greater increases in stone mechanical properties (dynamic elastic modulus and tensile strength), and enhanced formation of HAP [7,13]. For this reason, a concentration close to saturation (namely 3M, saturation being 3.7 M) was chosen in this study.

However, when high concentrations are used, high amounts of unreacted DAP remain in the stone [13], possibly resulting in unacceptable chromatic alteration and DAP accumulation on the stone surface; for this reason, removal of excess product is important. To achieve this goal, 72 hours immersion of samples in deionized water and 48 hours immersion in limewater have been tested in the literature [7,13].

In the present study, instead, a suitable procedure for removal of excess DAP was investigated. The procedure consisted in the application of a limewater poultice, with the aim of both providing additional Ca^{2+} ions to boost HAP formation reaction and to remove excess salt, by mimicking what is commonly done for salt removal on site. Limewater poultice was applied on samples after drying, so that capillary forces and not diffusion (which is much slower) could be the driving forces for calcium ion penetration inside the stone.

2. The procedure for the application of DAP solution was also investigated, by comparing different methods that are commonly used for consolidant application. The efficacy of the treatment, in fact, depends on the amount of product that enters the stone and forms HAP, on the depth that the

products reach and its even distribution in the substrate, so that it can reach the unweathered substrate and distribute uniformly, without creating a thick shallow surface-clogging layer [1,2,3]. All of these parameters depend on the application procedure [4,6].

Currently, the most used application procedures for stone conservation include total or partial immersion, brushing, poulticing, spraying and total vacuum impregnation. All of these application methods have some drawbacks that limit their effectiveness: partial immersion is easily controllable in laboratory conditions, but not on site, and it can only be used for objects of small dimensions or architectural elements that can be confined [18]. However, it can be considered as a benchmark for evaluating the efficacy of other application procedures. Poulticing is hard to control in both laboratory and on site conditions, as no control is possible before removing the poultice [18]. Spraying often results in low penetration depth and requires the use of very high amounts of product, most of which is lost due to runoff [19,20]. Brushing is normally the most used application method for stone consolidants [3,8]; however, its effect needs to be evaluated as well, as the flow of consolidant that is applied is discontinuous, and also depends on the operator. Particular concerns regarding brushing involve the amount of product to be applied, and hence the number of brush strokes needed. Technical data sheets of commercial products normally indicate application until apparent refusal; this condition, however, might require a very high number of brush strokes, especially for porous stones, and is absolutely not feasible for on-site application, where a much lower number is normally applied. Moreover, the link between increased number of applications and better consolidation results needs to be investigated, as applying a greater amount of product does not necessarily result in deeper penetration and improved mechanical properties, but might result in the formation of a superficial clogging layer, if the product accumulates close to the surface. If such a layer forms, invasion of water behind that layer could create defects, including detachment of the consolidated layer itself [1].

For this reason, in the present study, brushing and poulticing were chosen due to their applicability on site, and were compared to application by immersion, which was considered a benchmark for effectiveness testing. For brushing, two different applications were tested: one closer to the apparent refusal condition (20 applications) and the other with a reduced number of brush strokes, more feasible to apply on site (10 applications), to investigate the link between the amount of product applied and the penetration depth and efficacy of the consolidant.

I.2. Materials and methods

I.2.1 Materials

All tests were performed on Globigerina Limestone (GL), a highly porous stone from Malta. GL is an organogenic stone, essentially composed by fossils (globigerinae, that give the stone its name) and calcite crystals in a calcite matrix. Globigerina Limestone is normally divided in two varieties, the so-called "Franka" and "Soll stone" that differ in composition, microstructure and, consequently, in durability. Franka stone has a lower content of quartz and phylosilicates (2% quartz vs 3% of Soll stone and 8% phylosilicates vs 12% for Soll stone), higher porosity and generally larger pores (total open porosity about 38% vs 32% of Soll), but similar tensile strength. All these properties make Franka Stone generally more durable than Soll stone. Globigerina limestone durability, however, is a critical issue, as Malta is a severely aggressive environment, due to the combined presence of marine aerosol carrying salts, rising damp and wind that lead to phenomena such as alveolization, flaking and erosion [21-23].

The stone used in the present research (Xelini Skip Hire and High-Up Service, Malta; quarried in the area of "Ta' l-Iklin", from a depth of 3 floors below ground level), was characterized prior to the present experimentation. The results obtained are briefly summarized below:

- $CaCO_3$ content of the stone is ~ 93 wt.%, the rest being quartz and possibly clays;
- total open porosity is ~ 40%, with average pore radius of about 2 μm;
- tensile strength is ~ 3 MPa.

These results suggest that the stone can be considered belonging to "Franka" variety, even though no specific mineralogical-petrological analyses were performed.

Quarry slabs were cut into 5 cm cubes, 2 cm diameter 5 cm high cores, 7x7x1cm^3 and 7x7x2.5 cm^3 slabs (figure I.1). All samples were cut from the same slab to avoid the effects of possible heterogeneity inside the stone.

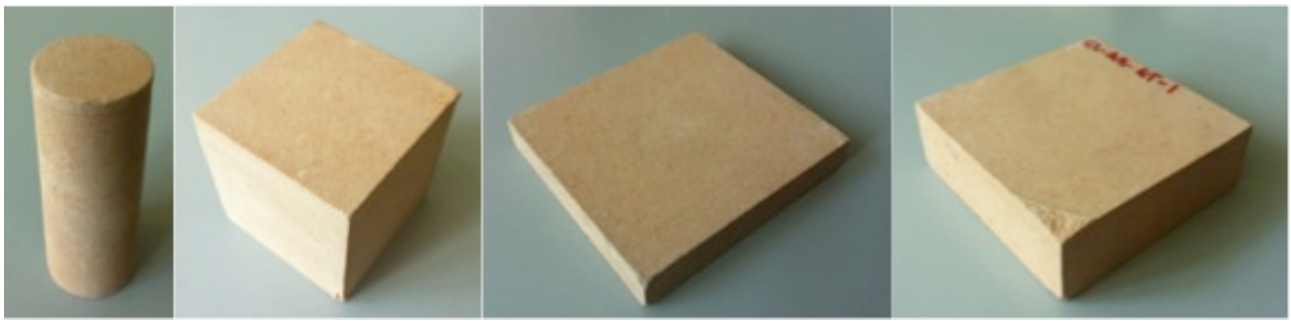

Figure I.1: Morphology of the samples used in the research

I.2.2 Artificial weathering of samples

The application of a consolidant on quarry samples is generally to be considered unrepresentative, as weathering causes considerable variations in the physical, mechanical and microstructural properties of the stone. Naturally weathered stone would be the most reliable option for testing consolidants; however, an experimental campaign on naturally weathered samples is not a realistic option, due to the scarcity of samples, especially when large dimensions are needed. Moreover, high heterogeneity in the decay level and frequent salt contamination would make the results of the tests quite hard to interpret. For this reason, either artificial stones with tailored properties that resemble those of naturally decayed ones or artificially weathered stones have been proposed for this aim [7,11,13,15]. Artificial weathering is normally to be preferred, as it is effective in reproducing grain loosening and micro-cracking that occur due to weathering.

Artificial weathering procedures include salt weathering, acid attack, mechanical pre-stress and heating. In the present study all samples were weathered by heating, according to a methodology previously reported and described below. Heating results in crack opening and grain boundary loosening, thus causing increased water absorption and decreased mechanical properties, that are characteristic of naturally weathered materials [24,25]. However, the morphology of the decay does not necessarily resemble that of naturally weathered materials, where alveolization, scaling and efflorescence occur. Salt weathering resembles more the conditions of naturally weathered samples, but it was not considered suitable for this stage of the research, because of the following consideration [1,26]:

- salt contamination might remain inside the stone despite desalinization procedures, thus possibly influencing the penetration of the consolidant and phase formation;
- a decay gradient forms, hence weathering is non-uniform in depth;
- it is hardly reproducible, as it might affect different samples to different extents, thus resulting in samples with very diverse microstructures and mechanical properties;
- samples might experience rupture during the cycles, because the extent of damage per cycle cannot be accurately predicted.

For these reasons, HAP application on salt-contaminated stone was tested in a more advanced stage of the research.

At this stage, instead, samples were artificially weathered by heating, in order to have increased porosity, water absorption and reduced mechanical properties mimicking those of naturally weathered samples, while obtaining a uniform weathering level in different samples and at different depths inside the same sample and, most importantly, no contaminants that would interact with the reaction between DAP and calcium ions.

I.2.3. Methods

I.2.3.1 Treatment procedure

HAP was obtained by reacting a 3 M solution of DAP (Sigma Aldrich, assay ≥ 98%, reagent grade) in deionized water with calcium ions deriving from millimolar dissolution of the stone.

The solution was applied by the methods described above, namely brushing, poulticing and immersion (figure I.2).

10 and 20 brush strokes (samples labeled "BR10" and "BR20") were applied in the case of brushing to evaluate the effects of increasing the amount of product that is applied. After the consolidant application by brushing, the samples were wrapped for 48 hours to allow for the HAP formation to occur without evaporation of the consolidant.

Poultice application (samples "POULT") was performed by cellulose pulp (MH300, Phase, Italy). Preliminary tests were performed to determine the ratio between dry cellulose powder and DAP solution to be used, a 1:6 weight ratio was selected. A layer of filter paper was placed between the poultice and the sample, to facilitate poultice removal. Samples were kept wrapped for 48 hours to allow samples to absorb the solution and the consolidant to cure. Then the plastic wrapping was removed and the samples were left to dry in contact with the poultice to remove excess DAP.

For samples treated with poulticing and brushing, stone cores were treated on the whole lateral surface, slabs were treated on the 7x7 cm^2 face, cubes were treated on one face perpendicular to the bedding planes, to mimick what happens on site, where the façade of the building would be perpendicular to the stone bedding planes.

Samples to be treated by partial immersion ("IMM") were first immersed into about 2 cm of solution to allow trapped air to exit the sample, so that consolidant soaking wouldn't be affected by the presence of air bubbles. Then, after all samples appeared wet, solution was added up to 1 cm from the tops of the samples. The top of the beakers containing the immersed samples were sealed with parafilm to prevent evaporation. Samples were kept immersed for 48 hours to allow curing.

The different geometry of cores and cubes/slabs made it possible to evaluate two different conditions, one where saturation of the stone is obtained, while the other where the penetration depth is lower than the thickness of the sample, so that a gradient in the mechanical properties between the treated and the untreated area is expected. Hence, cores were taken as a reference for the behavior of the consolidated material alone, while slabs and cubes reveal the transition in microstructural and mechanical properties between the treated and untreated layers.

After treatment, the samples were rinsed in deionized water and dried to constant weight at 40°C (in order not to alter the consolidant or the substrate). All samples, no matter the initial treatment conditions, were subjected to a limewater poultice, according to the procedure described below.

Limewater was prepared by mixing 1.7 g of calcium hydroxide in 1 L of deionized water. The limewater/dry poultice weight ratio was 1:6. Samples were kept wrapped for 24 hours to allow samples to absorb limewater, so that further reaction of DAP with externally supplied calcium ions could occur. Then, the plastic wrap was removed and samples were left to dry in contact with the poultice to allow excess DAP removal.

After complete drying the poultice was removed and samples were rinsed with deionized water and dried at 40°C to constant weight.

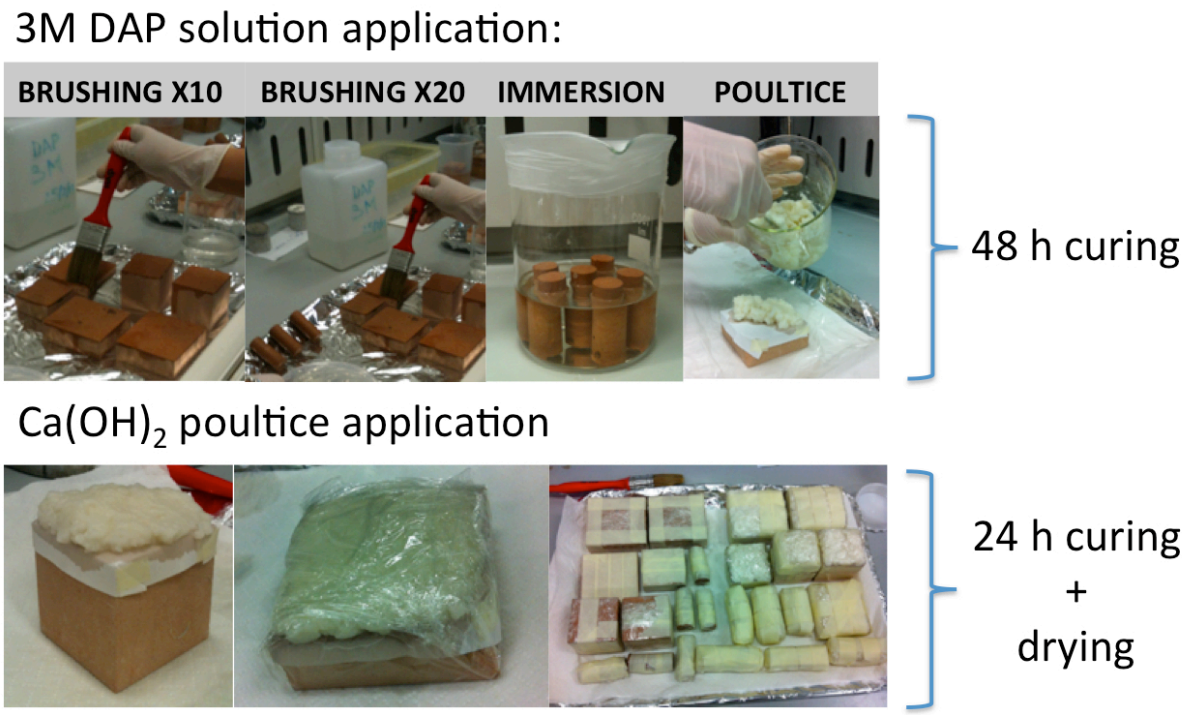

Figure I.2: Application procedures

I.2.3.2. Sample characterization

Sample characterization was performed as follows. For a better readability, all characterization techniques, the samples used for each test and the sampling points of each test are listed in Table I.1.

Parameter	**Test**	**Specimen**	**Testing position**
Dynamic elastic modulus	Ultrasonic test	cores	entire sample
Tensile strength	Tensile split test	cores	entire sample
Abrasion resistance	Modified PEI test	slabs	0, 5, 7.5 mm
Microstructure	MIP	cores	0-5 mm/5-10 mm (from treated surface)
Composition	FT-IR	cores	0-5 mm/5-10 mm (from treated surface)
Soluble phosphates content	IC	cores	0-5 mm/5-10 mm (from treated surface)
Hydrophobicity	contact angle/ absorption time	slabs	treated surface

Water transport properties	sorptivity/ absorption coefficient	cubes	entire sample, treated face up
Morphology	SEM/EDS	slabs	cross section
Color change	spectrophotometry	slabs	treated surface

Table I.1: Description of all characterization tests performed and the relevant samples and sampling points/testing positions. MIP stands for Mercury Intrusion Porosimetry test, FT-IR for Fourier Transform Infrared spectroscopy, IC for ion chromatography

Mechanical properties were evaluated in terms of dynamic elastic modulus (E_d), tensile strength (σ_T) and resistance to abrasion. These parameters were chosen because they are considered representative of the effectiveness of a consolidant. In fact, dynamic elastic modulus indicates the ability of the consolidant to distribute homogenously inside the stone and to bind cracks. Tensile strength was preferred over compressive strength as it is representative of the consolidant's ability to bind loose grains and to give cohesion to the material. E_d and σ_T were determined on 6 cores for each treatment condition and compared to that of untreated references. Dynamic elastic modulus was determined by the transmission method with a Matest instrument equipped with 55 kHz transducers; σ_T was determined by Brazilian splitting test (see scheme in figure I.3).

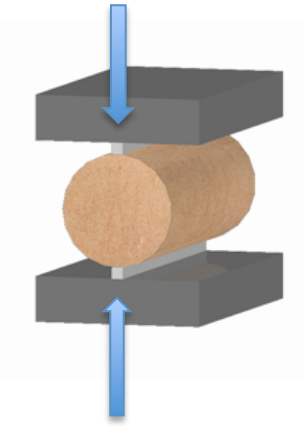

Figure I.3: Scheme of Brasilian Splitting Test

Resistance to abrasion gives a measure of the superficial resistance of the material as it is indicative of the tendency to pulverization and of stone cohesion; moreover, when it is performed at different depths inside the material, it is possible to determine whether the consolidant distributed homogeneously inside the stone or created a surface-clogging layer. By comparing resistance to abrasion at different depths it is also possible to obtain an indication of the consolidant penetration depth. Resistance to abrasion was performed by a modified version of the Porcelain Enamel Institute (PEI) test, according to a procedure previously developed and described in [8].

Sample microstructure, in terms of total open porosity and pore size distribution, was investigated by mercury intrusion porosimetry (MIP). MIP was performed at 2 different depths in the samples (stone cores, as described in Table I.1). The variability in the porosity was reduced by using samples coming from a single slab.

As susceptibility to weathering, and particularly salt weathering, depends on pore size distribution, and because a higher percentage of pores in the finer range results in a lower resistance to salt crystallization, the percentages of pores with radii $r < 0.01$ μm, 0.01 μm $< r < 0.1$ μm, 0.1μm $< r <$ 1μm and $r >$ 1μm were determined. As a result of the application of a consolidant, the microstructure of stone can be modified to different extents: if the percentage of fine pores ($r < 0.01$ μm and 0.01 μm $< r < 0.1$ μm) is increased, concerns might arise about the durability of the treated stone, no matter the effect of the consolidant on the total open porosity. The correlation between stone microstructure and resistance to weathering, together with the influence of stone consolidation on this aspect, is better elucidated in Chapter IV.

Alteration of water transport properties was investigated by the sorptivity test (EN 15801:2010-Conservation of Cultural Property – Test Methods – Determination of Water Absorption by Capillarity): water sorptivity and water absorption coefficient were determined. Contact angle and absorption time were measured by a contact angle instrument DSA30- Kruss GmbH: a 4 microliter deionized water drop was released onto dry samples and its absorption was video recorded. The measure was performed at 3 points on each sample.

Morphology of treated samples was investigated by SEM (Zeiss Evo 50 EP). EDS spectroscopy (Microprobe OXFORD INCA ENERGY 350, inserted in the SEM), was performed to evaluate the presence and distribution of reaction products (i.e. HAP or other calcium phosphates) in the substrate: in fact, as globigerina limestone does not contain phosphorus compounds, the presence of phosphorous can be considered indicative of the formation of calcium phosphates, as a result of the reaction. Phosphorous maps were collected to have an idea of the distribution of the newly formed phases in depth in the samples.

As a result of DAP application, not only HAP, but also several metastable phases might form. This is an issue for stone conservation, as these phases have a higher solubility with respect to HAP at pH above 4, which is the relevant range on site. For this reason, FT-IR (Perkin Elmer Spectrum One, KBr pellets mode) was used to determine the phases composition of the treated layer. FT-IR was performed at two different depths in the samples (see Table I.1). Given the higher solubility of these metastable phases, their presence was also investigated by ion chromatography (IC, Dionex ICS 1000), in the same sampling positions as for FT-IR measurements. Presence of phosphate ions

in IC were considered indicative of the presence of soluble phases, as HAP is expected to be insoluble.

Finally, chromatic compatibility of the treatments was evaluated by determining color parameters before and after treatment (Mercury 2000 Datacolor spectrophotometer). The color parameters used are L*, a*, b*, being L*= black-white; a*= red-green; b*= yellow-blue (CIELAB, 1976). The color change was determined according to the formula $\Delta E = (\Delta L^{*2} + \Delta a^{*2} + \Delta b^{*2})^{1/2}$.

I.3. Results

Consolidant absorption as well as the amount of consolidant retained inside the stone were evaluated for all treatment procedures, and are reported in Table I.2. To evaluate product absorption it must be considered that total saturation of samples with deionized water would correspond to 16.9 wt.% increase (results are determined on the basis of water absorption by sorptivity test at 7 days). Hence, considering the density of DAP solution (1.15 g/cm^3), this would correspond to a 19.4 wt.% gain.

		Weight Increase [wt.%]		
		After DAP treatment	After DAP treatment and drying	After limewater poultice and drying
BR 10	cylinders	17.6	4.2	0.6
	slabs	3	0.4	0.3
	cubes	1.6	0.1	0.1
BR 20	cylinders	18.1	6.6	0.1
	slabs	3.8	0.3	0.2
	cubes	1.8	0.1	0.1
IMM	cylinders	16.3	7.6	1.3
	slabs	16.9	2.1	1.1
	cubes	15.7	1.1	0.5
POULT	cylinders	18.9	2.3	1.1
	slabs	17.7	8.6	0.9
	cubes	17.4	7.1	1

Table I.2: Weight increase due to DAP uptake (after DAP treatment) and due to the formation of HAP in the samples (after DAP treatment and drying). Further weight increase after the application of limewater poultice was evaluated.

Penetration depth of the consolidant was investigated by visual inspection at the end of the treatment and is reported in figure I.4. A more detailed evaluation of consolidant penetration depth and redistribution at the end of the treatment and in the following stages will be discussed more in detail in Chapter II.

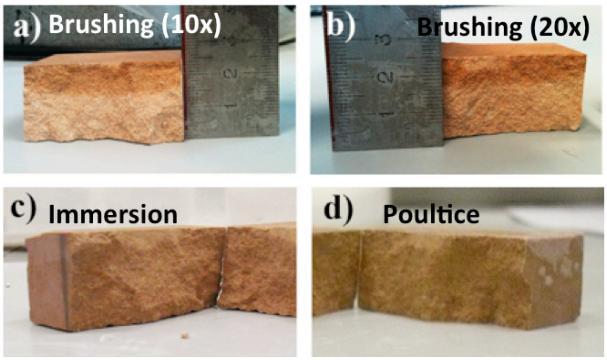

Figure I.4: Penetration depth obtained by the four different application methods as assessed immediately after treatment: the area invaded by the consolidant is wet and hence appears darker. In c) and d) the whole sample appears wet.

Mechanical properties of untreated and treated samples are reported in figure I.5. Quarry samples of globigerina limestone, tested prior to artificial weathering exhibit an average tensile strength of 3.0±0.3 MPa and a dynamic elastic modulus of 15.6±0.3 GPa. After artificial weathering, untreated globigerina limestone exhibits lower tensile strength (average σ_T = 2.70±0.3 MPa) and dynamic elastic modulus (average E_d = 11.2±0.5 GPa). The remarkable reduction in dynamic elastic modulus indicates that the heating procedure was effective for artificial weathering of the samples. After treatment, higher values ($3.23 \leq \sigma_T$ (MPa) ≤ 3.50 and $15.7 \leq E_d$ (GPa) ≤ 16.7) are achieved, depending on the application procedure.

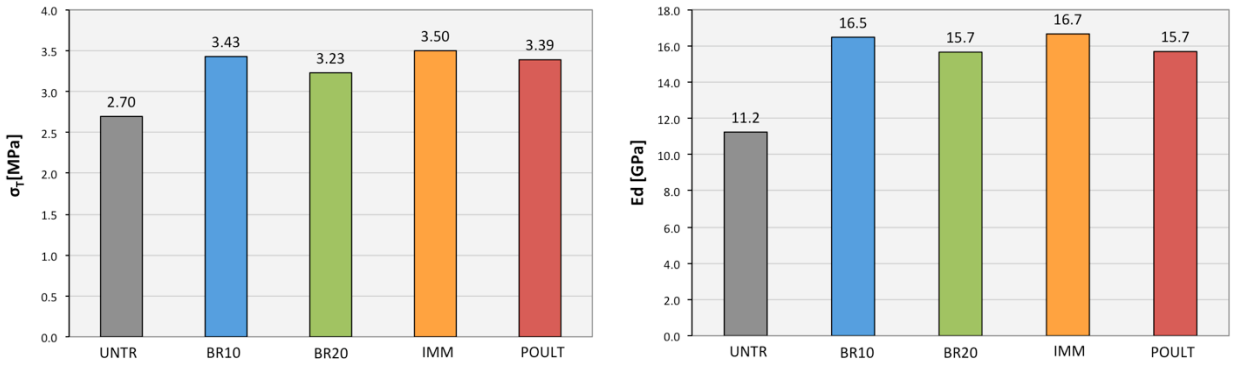

Figure I.5: Dynamic elastic modulus and tensile strength of untreated and treated samples.

Resistance to abrasion, before and after treatment, at various depths in the stone, is in reported in figure I.6.

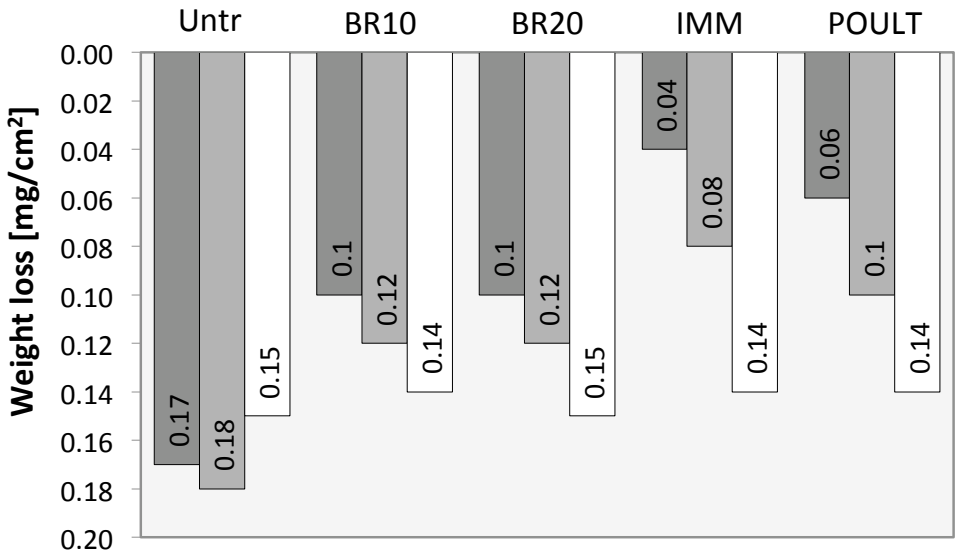

Figure I.6: Weight loss for abrasion for untreated and treated samples. The dark grey bars correspond to the superficial layer of the samples, the light grey to a 5 mm depth and the white bars to a 7.5 mm depth.

Microstructure of untreated and treated samples is reported in Table I.3 and figure I.7. MIP curves at different depths in the samples are reported, for comparison to the transition in the mechanical properties corresponding to each application procedure. In Table I.3 the alteration in porosity for each pore range is listed. Specific attention needs to be devoted to increases in the fraction of the finest pores, which may raise concerns about the samples' durability.

Sample	OP [v/v%]	Pores with $r < 0.01$ µm [v/v%]	Pores with $r < 0.01$-0.1 µm [v/v%]	Pores with $r < 0.1$-1 µm [v/v%]	Pores with $r > 1$ µm [v/v%]
untr 0-5	38.9	0.2	2.5	9.2	27
untr 5-10	37.4	0	1.8	9.9	25.7
BR10 0-5	35.1	0.4	4.9	6.8	23
BR-10 5-10	37.7	0.1	4.4	7.7	25.5
BR20 0-5	37.3	0.2	6	7.6	23.5
BR20 5-10	37.5	0.1	3.3	8.9	25.2
IMM 0-5	34.7	0.6	6.6	6.4	21.1
IMM 5-10	36.8	0.4	4.9	6.7	24.9
POULT 0-5	35.8	0.8	9.2	5.5	20.3
POULT 5-10	35.7	0.4	7.5	4.9	22.9

Table I.3: Pore size distribution in untreated and treated samples

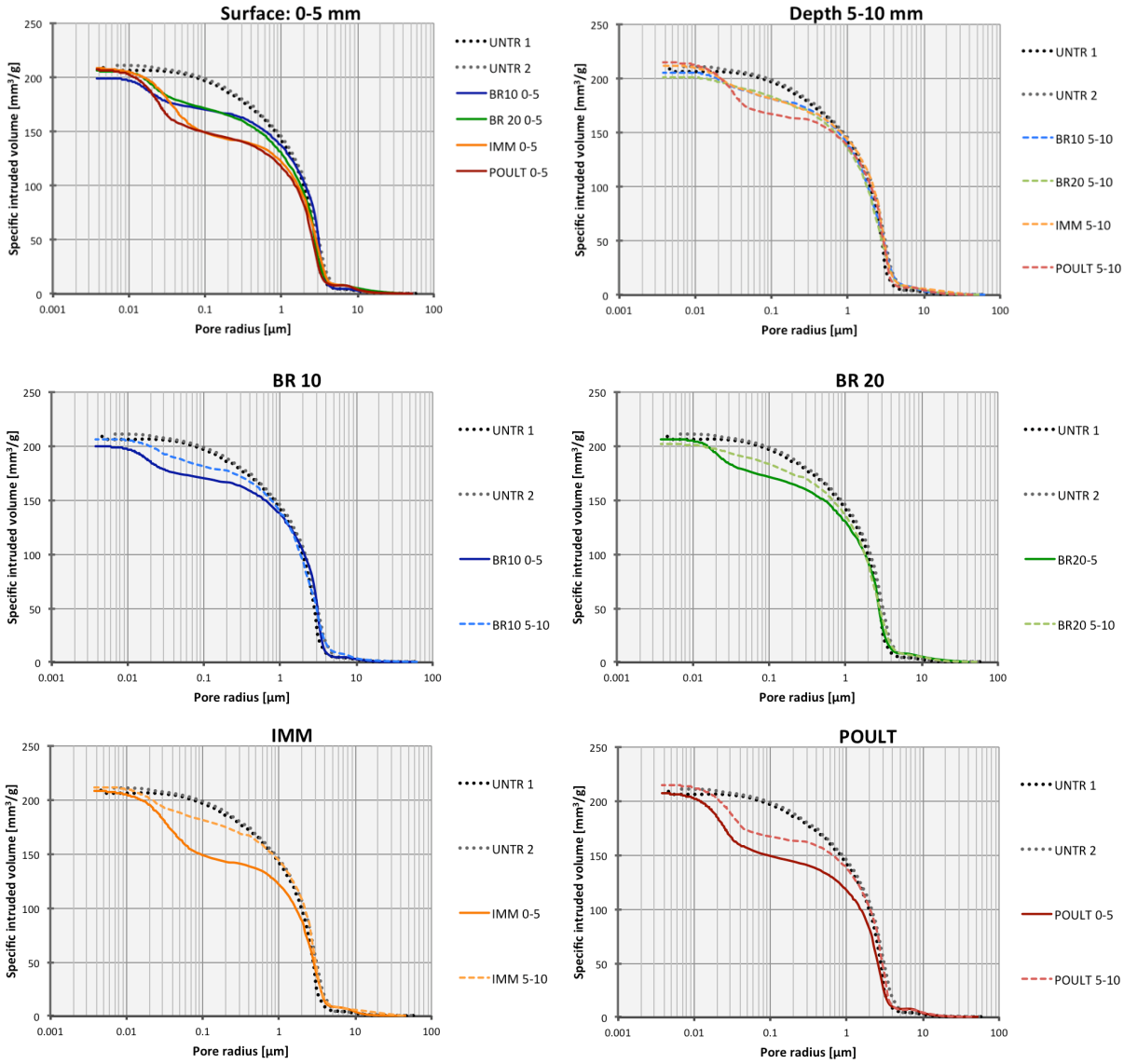

Figure I.7: Pore size distribution curves for untreated and treated cylinders at different depth.

Water transport properties before and after treatments are reported in figure I.8.

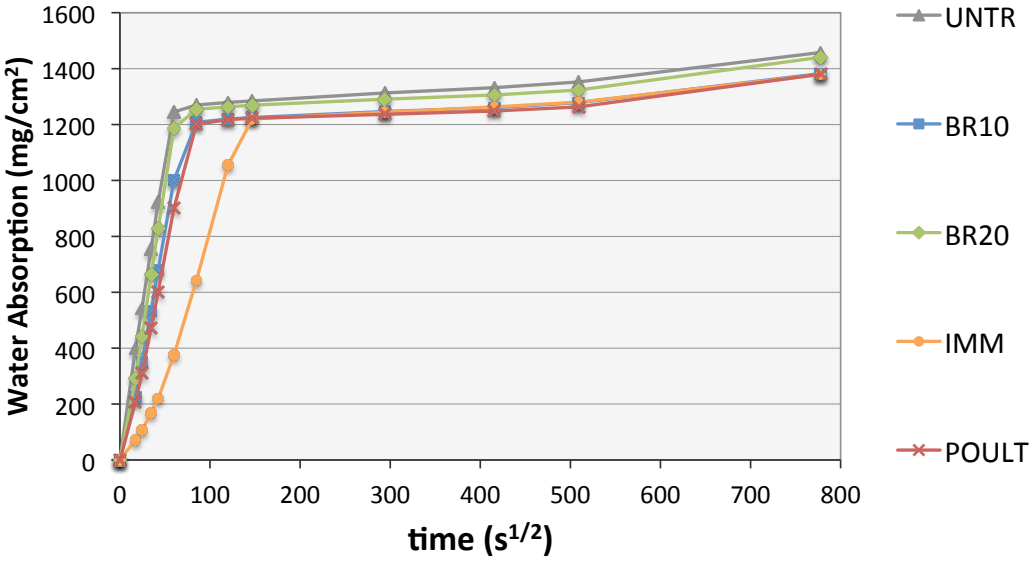

Figure I.8: Water transport properties of untreated and treated samples, as assessed by sorptivity test.

To assess whether any of the treatments would cause hydrophobicity, contact angle was determined before and after treatments, results being reported in figures I.9 and I.10. When comparing the cosines of contact angles, that are proportional to capillary suction, a decrease from 0.79 (for the untreated stone) up to 0.16 (for samples treated by poulticing) is registered. This indicates that a decrease in water sorptivity is to be expected until the liquid passes the treated layer, resulting in a slow initial penetration and then acceleration in the untreated zone.

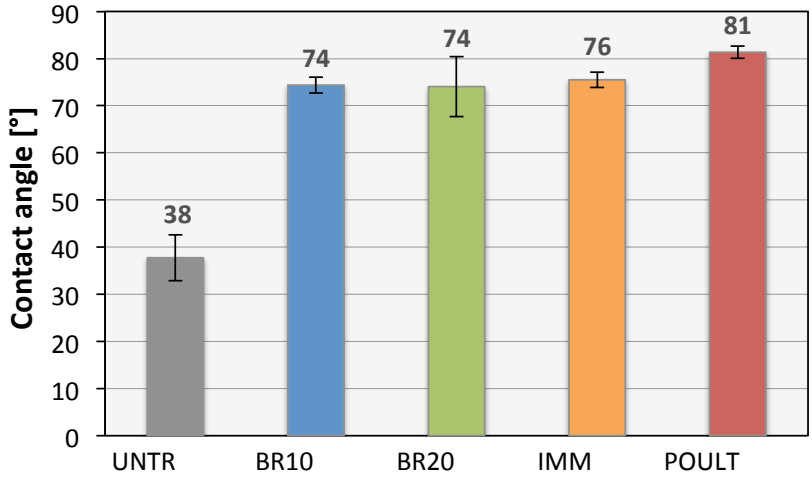

Figure I.9: Contact angle in untreated and treated samples

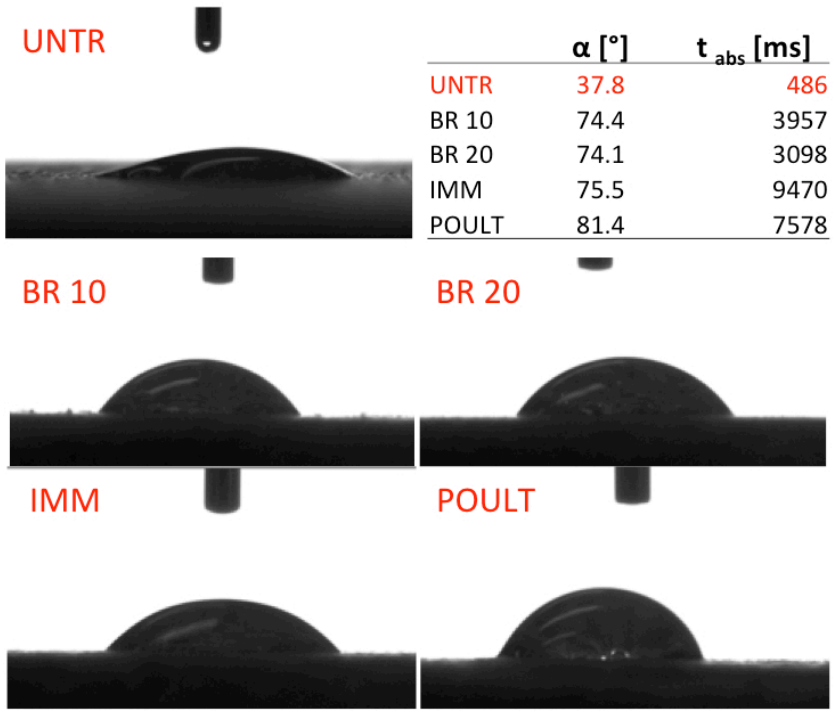

	α [°]	t_{abs} [ms]
UNTR	37.8	486
BR 10	74.4	3957
BR 20	74.1	3098
IMM	75.5	9470
POULT	81.4	7578

Figure I.10: Average contact angle and absorption time in untreated and treated samples

Color change caused by each of the treatments is reported in figures I.11 and I.12.

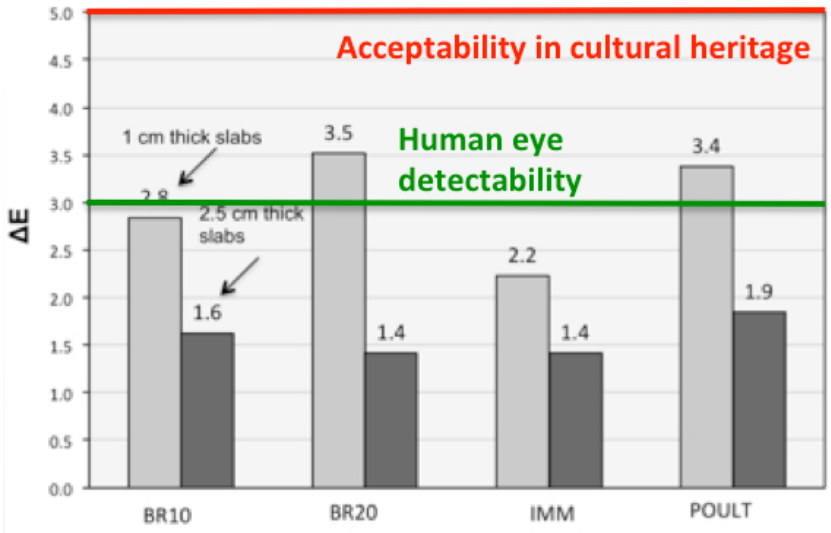

Figure I.11: Color change in treated samples with respect to untreated references and spectrophotometric analyses

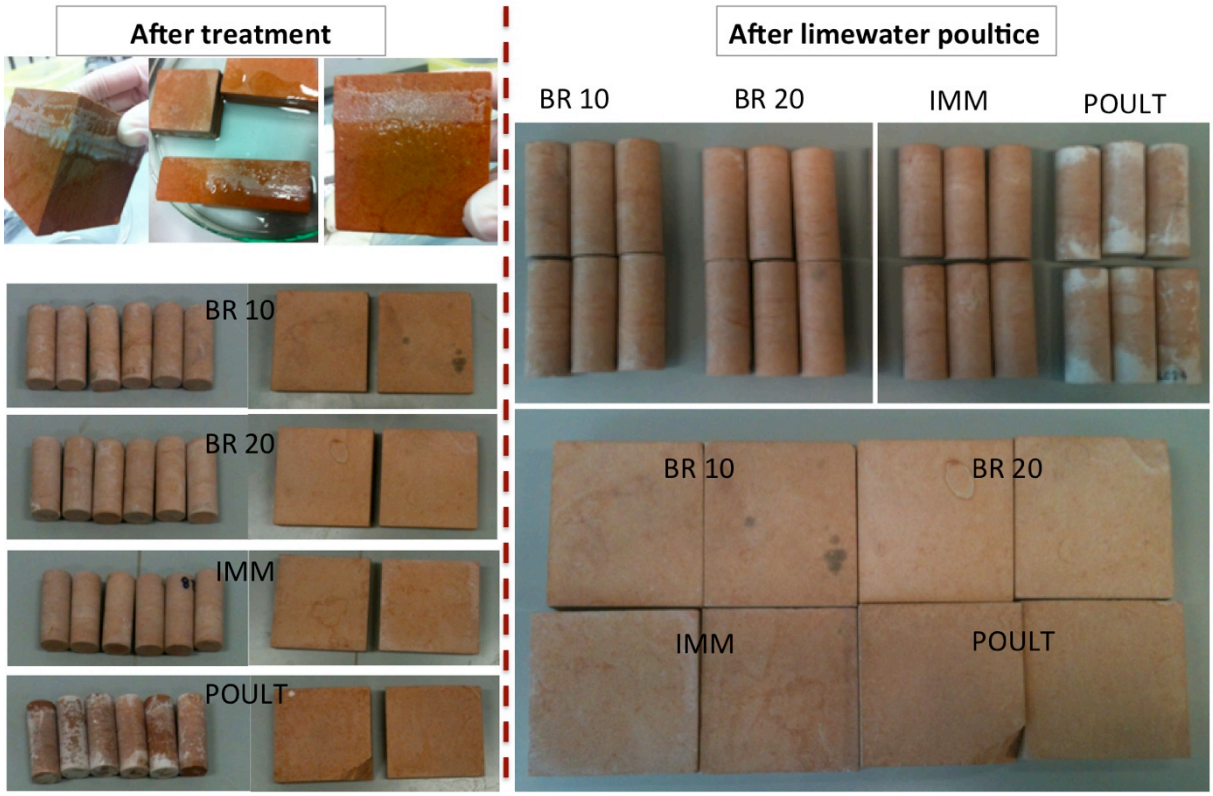

Figure 1.12: Chromatic alterations after DAP application and rinsing (left) and after the final limewater poultice application (right) as assessed by visual inspection.

The formation of calcium phosphates as a result of the treatment and their amount and distribution depending on application procedure was investigated by SEM/EDS and is reported in figure I.13. As phosphorus is not present in untreated samples, its presence has to be ascribed to phases formed as a result of DAP treatment. One image at higher magnification of sample BR 10 is reported in figure I.14, with the relevant EDS peaks, to better elucidate the sample morphology after treatment.

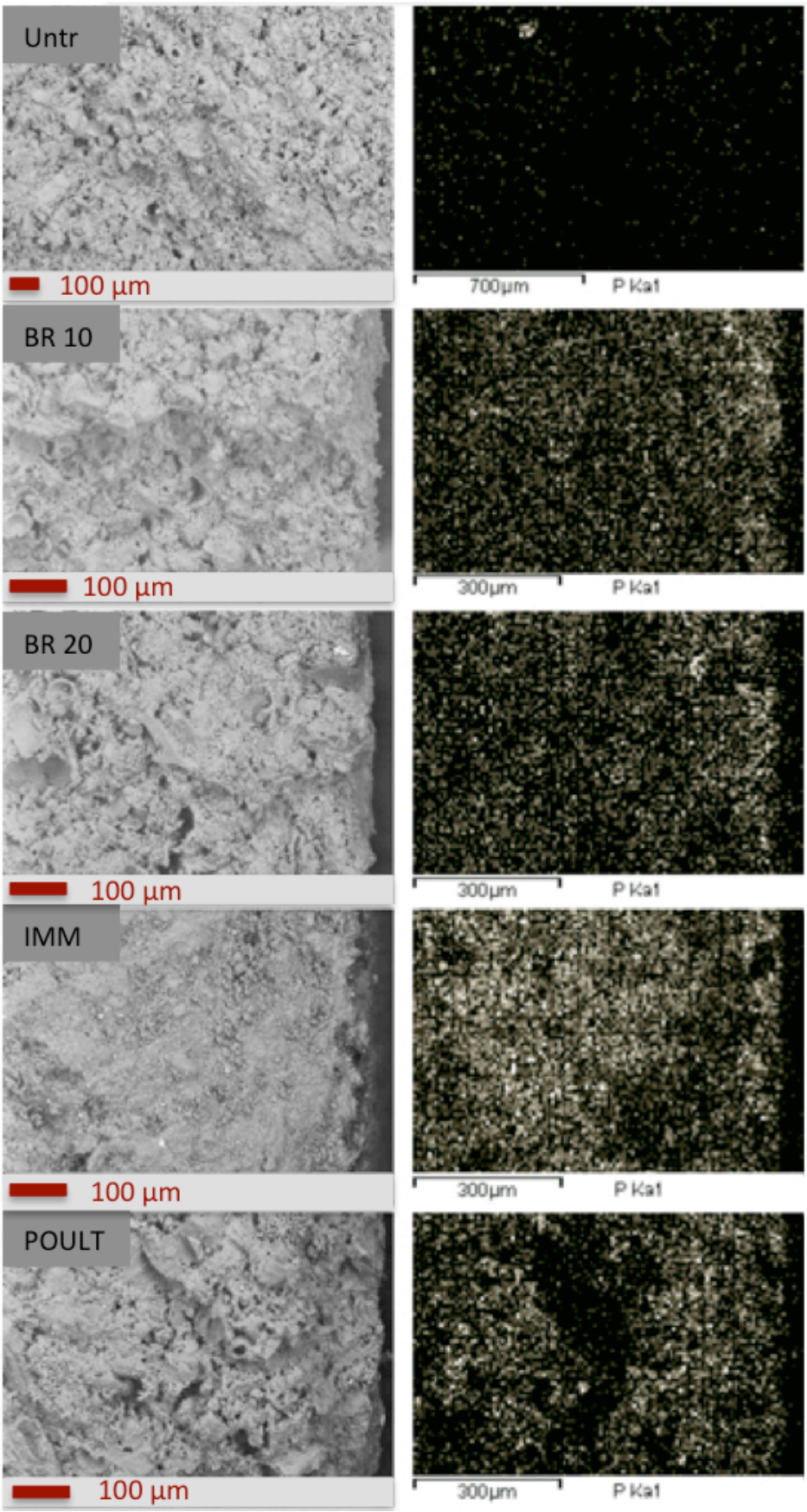

Figure I.13: SEM images (left column) and relevant phosphorous maps (right column) for untreated and treated samples.

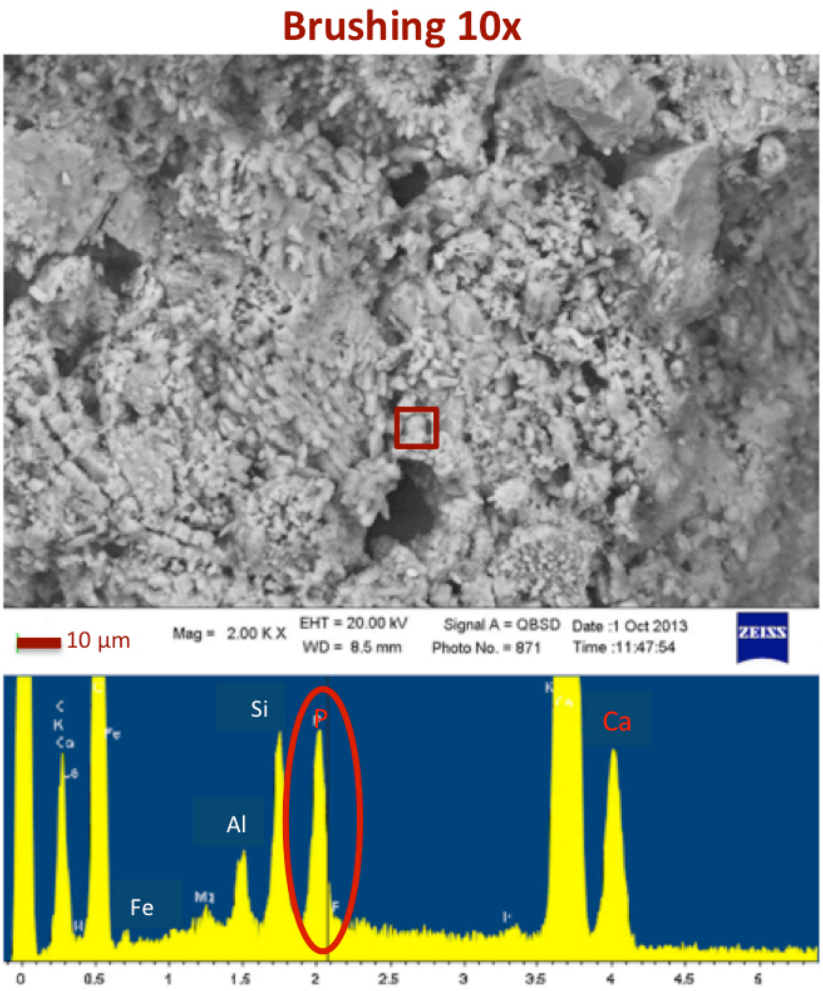

Figure I.14: SEM image and EDS map of sample BR10.

As different metastable phases may form alongside HAP as a result of the treatment, phase formation was investigated by FT-IR, results being reported in figure I.15. Because all metastable phases have a higher solubility with respect to HAP for the relevant pH range and so does unreacted DAP, their presence was also investigated by ion chromatography, results being reported in Table I.4.

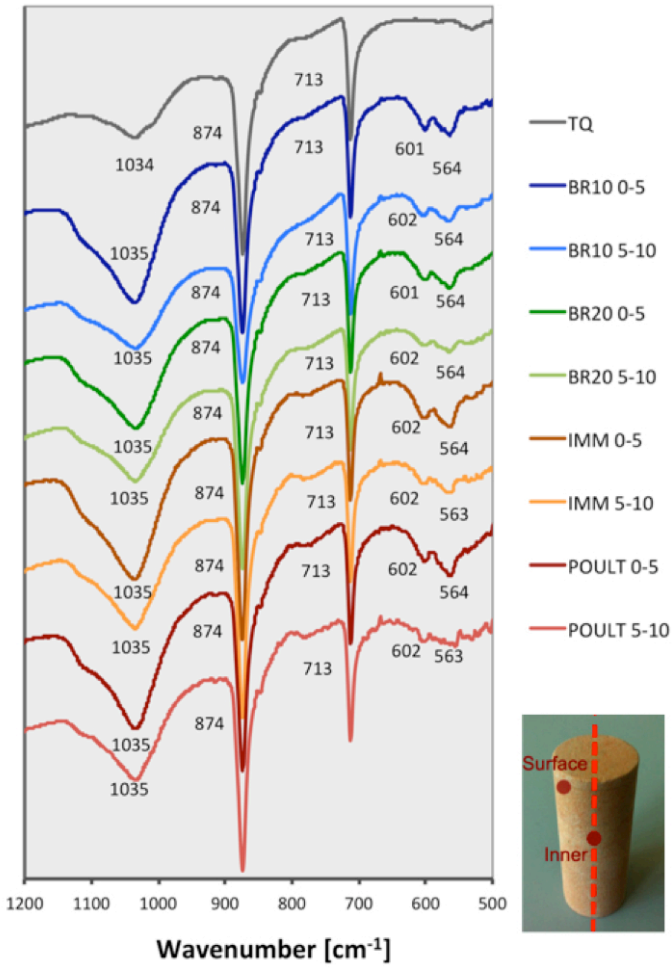

Figure I.15: Phase formation at different depths inside the stone (0-5 mm for "surface" samples and 5-10 mm for "inner" samples), assessed by FT-IR

Sample	% Cl^-	% SO_4^{2-}	% PO_4^{3-}
Untr	0.013	0.024	0
BR 10 0-5	0.021	0.019	0
BR 10 5-10	0.019	0.005	0
BR 20 0-5	0.009	0.015	0
BR 20 5-10	0.011	0.037	0
IMM 0-5	0.009	0.020	0
IMM 5-10	0.011	0.016	0
POULT 0-5	0.011	0.019	0
POULT 5-10	0.008	0.015	0

Table I.4: Anions content in treated and untreated samples, assessed by ion chromatography: presence of PO_4^{3-} would indicate the presence of unreacted DAP and/or soluble phases.

I.4. Discussion

Artificially weathered globigerina limestone, prior to the treatments, exhibits quite poor mechanical properties (figures I.5 and I.6) together with a highly porous microstructure (figure I.7) that causes remarkable water absorption (figure I.8). These parameters indicate that severe weathering was induced into the samples, whose characteristics resemble those found in naturally weathered samples.

The efficacy of consolidation was evaluated by investigating penetration depth (figure I.4) and increases in mechanical properties of treated samples with respect to untreated references (figure I.5).

All DAP treatments caused an increase in mechanical properties: significant increases were assessed in both dynamic elastic modulus and tensile strength that, notably, reach values that are slightly higher than those of unweathered quarry samples, indicating that mechanical properties were not only completely restored, but that some further mechanical benefit was obtained as a result of the treatment (figure I.5). No significant differences can be assessed in mechanical properties obtained for the 4 application procedures. This is in line with the data obtained for product uptake and consolidant retention in the stone (Table I.2). Comparing weight gain measured right at the end of the treatment (wet samples) to saturation of the samples with DAP solution, it can be noticed that, depending on the application method used, values between 16.3 wt.% and 18.9 wt.%, all very close to saturation (19.4 wt.%) are obtained for cylinders. This indicates that almost complete saturation was achieved for these samples, for all application methods. Considering that both E_d and σ_T are measured on cylinders and all cylinders being almost completely saturated, it is consistent that no remarkable differences are obtained between the samples.

In contrast, when cubes and slabs are taken into consideration, the situation is completely different: samples treated by immersion and poultice almost reach saturation, while samples treated by brushing exhibit a much lower product absorption. Consistently, when penetration depth is evaluated on 2.5 cm thick slabs, a depth of about 8-9 mm can be assessed for samples treated by brushing, while samples IMM and POULT appear fully saturated.

Penetration depth (figure I.4), as well as consolidant retention in samples BR10 and BR20 are almost identical, thus suggesting that no benefit was obtained by increasing the number of brush strokes.

When comparing weight increase after DAP application and limewater poultice, both determined on dry samples, a further decrease is registered in sample weight, indicating the removal of unreacted DAP. Weight gain at the end of the treatment can thus be attributed to HAP formation, as no other phases nor unreacted DAP were detected by FT-IR, as bands characteristic of DAP, such as 1074,

953, 895, 557, 533, 463 cm^{-1} are not detected (for DAP spectra see Chapter II, §II.3, figures II.5 and II.6).

Compatibility of the treatments was first evaluated by considering microstructural modifications (figure I.7): slight alterations can be assessed as a result of the treatments, especially in the 0.2-2 μm range; however, those alterations can be considered minor and decrease with depth in the samples, hence the treatment can be considered highly compatible in microstructural terms. Total open porosity remains unaltered for all samples, thus indicating that HAP does not reduce the dimension of pores for their entire length but only at the very surface. Regarding the difference between the treatments: modifications are higher for samples IMM and POULT, consistent with the formation of a higher amount of HAP. Water absorption (figure I.8) is substantially unaltered, and the water absorption coefficient is only slightly reduced in the case of POULT and, mostly, IMM. The fact that initially water absorption is slower, while final water uptake is identical to that of untreated stone is consistent with microstructural alterations. In fact, larger pores allow for a more rapid water absorption: in the case of IMM and POULT the fraction of larger pores is reduced, thus reducing the absorption speed. However, as total open porosity is substantially unaltered, so is final water uptake. Similar results (i.e. initial decrease in absorption speed) could be caused by hydrophobicity; however this was not the case, as all contact angles are below the hydrophobicity threshold (figures I.9 and I.10). Nevertheless, as all contact angles increase, some influence on sorptivity cannot be completely excluded. In fact, because of the remarkable increase in contact angles causes, a great retardation of absorption might be expected, at least until the water passes the treated region.

Another relevant parameter regarding microstructural alterations is the fact that they decrease with depth, thus indicating that a gradient in microstructural properties and not a surface crust is created by the treatments. Results of abrasion tests at different depths (figure I.6) confirm this result. Resistance to abrasion of the treated surface indicates significant increases with respect to untreated samples, mostly for IMM and, secondly, POULT samples. This resistance gradually decreases so that, around 7.5 mm depth, values comparable with those of the untreated samples are registered, indicating a higher HAP formation near the surface and a gradual decrease up to a depth of about 1 cm. This might seem in contrast with penetration depth values visually assessed for samples IMM and POULT, where a penetration depth of more than 2.5 cm was determined. However, a possible explanation is that redistribution of the consolidant occurs in the phases after treatment and that drying causes DAP solution to shift towards the external surfaces, where evaporation occurs. This results in the formation of more HAP in this area and hence in an improved abrasion resistance. This aspect will be better detailed in Chapter II.

Phosphorous maps (figure I.13) confirm a higher presence of phosphate near the treated surface of samples IMM and POULT. In general, phosphorous amount is higher in these samples compared to BR 10 and BR 20. No remarkable differences are assessed in the samples treated by brushing, thus further confirming that no benefit was obtained by extra brushing applications.

As phosphorous itself might not be considered sufficient to assess the formation of hydroxyapatite, as other phases might form from the reaction and/or some unreacted DAP might remain inside the stone, FT-IR was performed (figure I.15).

Bands near 1300 cm^{-1} , 600 and 560 cm^{-1}, characteristic of phosphate stretching and bending, respectively, can be detected. These bands are indicative of HAP formation. The band at 1300 cm^{-1} partially overlaps with one of globigerina limestone; however, increases in its intensity after treatment are to be ascribed to HAP formation. No evidence of soluble phases was found, nor were soluble phosphates detected by IC, indicating that HAP is the only or, at least, the predominant phase that is formed by the treatment. As for the other properties, HAP band intensity decreases with depth and this decrease is more marked for IMM and POULT samples where HAP formation near the treated surface is maximal.

Finally, a very important parameter for a treatment to be considered compatible is that it does not cause alterations in the material's appearance. Data collected with the spectrophotometer indicate that color changes after treatment are below the threshold considered acceptable for cultural heritage conservation. Samples BR10 and IMM are also below the human eye detectability. However, in the case of cylinders, where saturation is reached, some white spots can be assessed close to the sample edges in those treated by poultice. An exact determination of color change in those samples (by spectrophotometer) was made impossible by the sample geometry; however, application by poultice was considered not compatible.

By comparing sample appearance after DAP application and after limewater poultice, evidence of the poultice effectiveness in removing DAP deposits is achieved.

I.5. Conclusions

The set up and evaluation of a treatment protocol for HAP-treatment application was performed.

First, different application methods were evaluated and the most promising was chosen on the basis of efficacy and compatibility. Then, a second step consisting in the application of a limewater poultice, with the double aim of removing unreacted DAP and further promoting HAP formation was tested. The following conclusions can be derived.

DAP treatment exhibits a good efficacy and compatibility, no matter the application procedure. At the end of the treatment, all samples exhibit remarkable increases in mechanical properties, and a penetration depth >7.5 mm is achieved. HAP content, as well as mechanical and microstructural

properties, gradually decreases with depth inside the stone, so that a gradient between treated and untreated stone is created and no hard and/or impermeable crusts are formed. All treatment methods cause minor alterations in microstructure and water transport properties and cause no hydrophobicity (though a slight increase in contact angle is registered). Color change is negligible for all of the treatments: however, some residual white spots can be found on cylinders treated by poultice, hence raising some concerns about the compatibility of this application method.

The highest efficacy was obtained for samples treated by immersion, that exhibit the highest consolidant retention in the pores, penetration depth and mechanical properties, while the best compatibility was obtained for samples treated by brushing. As stated above, immersion was considered as a benchmark for evaluating the effectiveness of other application methods, as it is hardly feasible on site. As brushing exhibits comparable efficacy and higher compatibility, together with being the most widely used application method on site, it was considered as the most promising application procedure. Almost no differences were obtained by increasing the number of brush strokes, but a slightly higher color change, hence BR 10 was considered more promising than BR 20.

Limewater poultice is effective into removing unreacted DAP and soluble phases, thus enhancing treatment compatibility by reducing visual alterations. As a result, no other phases but HAP are detected at the end of the treatment.

Aknowledgements

I am thankful to Dr. Grazia Totaro for contact angle measures, Dr. Eugenia Rastelli for spectrophotometric analyses, M.D. Eufemia Papacharissis for support on stone treatment and characterization.

Chapter references

[1] Scherer G.W., Wheeler G.S., Silicate consolidants for stone. Key Eng Mat 391 (2009) 1-25

[2] Tulliani J.M., Formia A., Sangermano M., Organic-inorganic material for the consolidation of plaster. J Cult Herit 12 (2011) 364-371

[3] Ferreira Pinto A.P., Delgado Rodriguez J., Stone Consolidation: The role of treatment procedures. J Cult Herit 9 (2008) 38-53

[4] Maravelaki-Kalaitzaki P., Kallithrakas-Kontos N., Korakaki D., Agioutantis Z., Maurigiannakis S., Evaluation of silicon-based strengthening agents on porous limestones. Prog Org Coat 57 (2006) 140-148

[5] Maravelaki-Kalaitzaki P., Kallithrakas-Kontos N., Agioutantis Z., Maurigiannakis S., Korakaki D., A comparative study of porous limestones treated with silicon-based strengthening agents. Prog Org Coat 62 (2008) 49-60

[6] Ferreira Pinto A.P., Delgado Rodriguez J., Consolidation of carbonate stones: Influence of treating procedures on the strengthening action of consolidants, Journal of Cultural Heritage 13 (2012) 154-166

[7] Sassoni E., Naidu S., Scherer G.W., The use of hydroxyapatite as a new inorganic consolidant for damaged carbonate stones, J Cult Herit 12 (2011) 346-355

[8] Franzoni E., Sassoni E., Graziani G., Brushing, poultice or immersion? Role of the application technique on the performance of a novel hydroxyapatite-based consolidating treatment for limestone. J Cult Herit 16 (2015) 173-184

[9] Naidu S., Scherer G.W., Nucleation, growth and evolution of calcium phosphate films on calcite. J Colloid Interf Sci 435 (2014) 128-137

[10] Naidu S., Blair J., Scherer G.W., Acid attack mechanism on Carrara marble and efficacy of a protective hydroxyapatite film. J Am Ceram Soc (in press)

[11] Naidu S., Liu C., Scherer G.W., Hydroxyapatite based consolidants and the acceleration of hydrolysis of silicate-based consolidants. J Cult Herit 16 (2015): 94-101

[12] Naidu S., Novel Hydroxyapatite Coatings for the Conservation of Marble and Limestone, PhD Thesis.

[13] Sassoni E., Franzoni E., Scherer G.W., Naidu S., Consolidation of a porous limestone by means of a new treatment based on hydroxyapatite, Proceedings of 12th International Congress on Deterioration and Conservation of Stone, New York City (USA), 22–26 October 2012 (2014), p. 1-11

[14] Matteini M., Rescic S., Fratini F., Botticelli G., Ammonium phosphates as consolidating agents for carbonatic stone materials used in architecture and cultural heritage: preliminary research. Int J Archit Herit Conserv Anal Restor 5 (2011) 717–736

[15] Yang F.W., Liu Y., Zhu Y.C., Long S.J., Zuo G.F., Wang C.Q., Guo F., Zhang B.J., Jiang S.W., Conservation of weathered historic sandstones with biomimetic apatite. Chin Sci Bull 57 (2012) 2171–2176

[16] Yang F., Zhang B., Liu Y., Guofeng W., Zhang H., Cheng W., Xu Z., Biomimic conservation of weathered calcareous stones by apatite. New J Chem 35 (2011) 887–892

[17] Mats S., Johnsson A., Nancollas G.H., The role of Brushite and Octacalcium Phosphate in Apatite Formation. Crit Rev Oral Biol M 3 (1992) 61-82

[18] Pinna D., Salvadori B., Porcinai S., Evaluation of the application conditions of artificial protection treatments on salt-laden limestones and marble. Constr Build Mater 25 (2011) 2723-2732

[19] Wheeler G., Alkoxysilanes and the Consolidation of Stone (Research in conservation), The Getty Conservation Institute, Los Angeles, 2005

[20] Lazzarini L., Laurenzi Tabasso M., Il restauro della pietra, CEDAM, Padova (Italy), 1986 (in Italian)

[21] Cassar J., Deterioration of the Globigerina limestone of the Maltese Islands. Geol Soc. Spec Publ 205 (2002) 33–49

[22] Rothert E., Eggers T., Cassar J., Ruedrich J., Fitzner B., Siegesmund S., Stone properties and weathering induced by salt crystallization of Maltese Globigerina Limestone, in: Přikryl R., Smith B.J.

(Eds.), Building stone decay: from diagnosis to conservation. Geol Soc London Spec Publ 271 (2007) 189–198

[23] Mifsud T., Cassar J., The treatment of weathered Globigerina Limestone: the surface conversion of calcium carbonate to calcium oxalate. Proc Int Conf Herit Weather Conserv HWC, 2 (2006) 727–734

[24] Franzoni E., Sassoni E., Scherer G.W., Naidu S., Artificial weathering of stone by heating. J Cult Herit 14S (2013) e85–93.

[25] Sassoni E., Franzoni E., Influence of porosity on artificial deterioration of marble and limestone by heating. Appl Phys A-Mater 115 (2014) 809-816

[26] E. Franzoni, E. Sassoni, Comparison between different methodologies for artificial deterioration of stone aimed at consolidants testing, Proceedings of 12th International Congress on Deterioration and Conservation of Stone, New York City, USA, 22–26 October 2012 (2014), p. 1-10

CHAPTER II: Consolidant redistribution in porous substrates

II.1. Introduction

Penetration depth of consolidants is one of the key parameters that influence their efficacy, as it determines the possibility to reach the unweathered substrate. Moreover it is essential to ensure a smooth gradient in properties between the consolidated layer and the unconsolidated substrate, without creating a superficial consolidated crust that can undergo detachment [1-3].

Consolidant penetration inside the stone, however, is known to be dependent on a multitude of parameters, including the competition between capillary absorption and solvent evaporation, the pore system of the material, the characteristics of the consolidant and those of the solvent [1-7].

When penetration depth of ethyl silicate in Globigerina limestone was investigated in a previous study [3], it emerged that, when a porous stone is treated by a consolidant, the final penetration depth differs from that initially assessed right at the end of the treatment application. This fact suggests that the consolidant can further redistribute and penetrate inside the stone, thus achieving a distribution that is remarkably different from that initially assessed at the end of the application. The occurrence of redistribution after the cessation of the application was envisaged in the literature [4] also in the case of damp-proofing resins in white spirit solvent [8], that is the same solvent of the ethyl silicate based product. This is due to the fact that the migration of a liquid inside a porous material causes displacement of the fluids inside the pores, whenever these fluids are immiscible (as in the case of white spirit and water). This is also the case of air and water, as they are immiscible as well. For this reason, water is expected to displace air, thus behaving as the wetting fluid [8].

Because the HAP-based treatment is applied in water, progressive displacement of air is expected to occur and cause redistribution of the consolidant inside the pore network, hence a systematic investigation of this aspect is needed. Moreover, as discussed in the previous chapter, in the case of the HAP-based treatment, in samples treated by immersion and poulticing (i.e. by means of a continuous flux of consolidant), HAP was found to form only up to about 1 cm depth, while initially the DAP solution had reached a depth of more than 2.5 cm. HAP accumulation was found to occur in the areas close to sample surface, hence highlighting the role of evaporation in determining further redistribution of the consolidant, which moves to the surface where evaporation occurs [9]. This HAP accumulation was not detected in samples treated by brushing, thus suggesting that it might be also dependent on the consolidant application method [9].

For this reason, in the present chapter, the redistribution of the consolidant during each step of the treatment was investigated for the HAP-based treatment. This topic was considered of particular interest as the treatment with the DAP solution might involve the formation of several metastable phases [9-15], whose formation instead of HAP might be favoured by changes in pH or by

ammonia evaporation [16,17]. These circumstances might occur while the consolidant migrates inside the stone, thus making the effects of redistribution even more important. Moreover, the dynamics of penetration and distribution of the DAP solution are expected to be quite different from those of ethyl silicate, because both the active principle and the solvent are different. Ethyl silicate is applied in a volatile organic solvent, generally white spirit, while DAP is applied in water, hence the competition between solvent evaporation and capillary absorption is expected to be quite different in the two cases.

Several aspects were investigated. Firstly, it was determined whether or not DAP redistribution occurs in the phases following the application. Different application procedures, involving either continuous or discontinuous flux of consolidant, namely brushing and immersion, were examined, to test the differences in penetration depth and in HAP formation deriving from different capillary absorption mechanisms during soaking.

Then, considering that the proposed procedure consists of different steps, involving different soaking and drying phases (each possibly influencing the distribution of DAP and of reaction products), the determination of consolidant redistribution was performed at each of the treatment stages.

Finally, the actual efficacy of limewater poultice in boosting formation of HAP and removing unreacted DAP and soluble phases was systematically investigated.

As HAP-formation reaction might pass through the formation of metastable intermediate phases, particular attention was devoted to the phases obtained by the two application procedures at each step.

Experiments were carried out on Globigerina limestone, because of its high porosity and high water absorption and absorption speed, that make it particularly suitable for the study of the topic under consideration.

II.2. Materials and methods

II.2.1. Materials

Globigerina limestone was used for the tests. All tests were carried out on samples artificially weathered by heating (see Chapter I), in order to reproduce the weathering conditions that stone exhibits on site and to further increase stone porosity and water/consolidant uptake.

Tests were performed on 5x5x2.5 cm^3 prisms. One 7x7x1.5 cm^3 slab was taken for visual examination of penetration depth at different times after application by brushing. The thickness of the samples was based on the considerations of the previous chapter that highlighted that the DAP

solution fully saturates samples of this thickness when treated by immersion, while it does not saturate samples treated by brushing.

II.2.2. Methods

First, untreated Globigerina limestone microstructure and water uptake properties were evaluated by mercury intrusion porosimetry (MIP, Fisons Macropore Unit 120 and Porosimeter 2000 Carlo Erba) and sorptivity test (performed according to EN 15801).

Samples were treated on one 5x5 cm^2 surface. Half of the samples was treated by brushing, the other by partial immersion, the treatment procedure being described in the previous chapter (cfr. I.2.3.1). Briefly, a 3M DAP solution was applied and left reacting for 48h while wrapped in plastic film to prevent evaporation. Samples were rinsed and dried, then a limewater poultice was applied. Limewater poultice was kept wrapped for 24 h to prevent evaporation then left to dry in contact with the samples. Samples were rinsed to remove possible poultice residues and left to dry to constant weight.

The HAP-treatment was ideally divided into the following phases: consolidant application, consolidant curing, drying, limewater poultice application, final drying. One sample was collected for analysis after each step of the treatment, as described in detail in the following.

a) For samples treated by brushing:

- one sample was taken right after DAP application (wet), labelled BR-T0;
- one sample after 48 hours curing (samples were kept wrapped so they remained wet), labelled BR-48h;
- one sample after drying for 4 days (dry sample), labelled BR-6d;
- one sample after limewater poultice application (wet sample), labelled BR-7d;
- one sample at the end of the treatment, after drying in contact with the poultice (dry sample), labelled BR-F.

In addition, for samples treated by brushing, penetration depth was visually monitored in the steps following the treatment application, by fracturing one reference sample right after treatment, after 1 hour and 2 hours from the application. Longer times were not tested as visual evaluation of penetration depth was no longer possible as the wet area couldn't be recognised.

b) For samples treated by immersion (labelled as IMM), the same conditions as above were taken into account, except for the first step (T0) that was omitted as application itself lasts 48 hours and is not separated from the curing process. For the same reason, visual evaluation of penetration depth variation after consolidant application was not possible, as the application itself lasts 48 hours and fully saturates the sample.

The evaluation of consolidant penetration and redistribution was carried out by monitoring the presence of DAP and that of reaction products at each treatment step. To do so, all samples were cut into 5 slices, each corresponding to about 0.6 cm of thickness: the thickness was based on the final penetration depth determined in the previous chapter. In samples treated by brushing, slices are indicated by their depth with respect to the treated face (i.e. 0-6 is the slice containing the treated face, 6-12 from 6 to 12 mm from the treated face, and so on). For samples treated by immersion, the top face (0-6) is that opposite to the face immersed in the DAP solution, hence all slices are indicated in terms of their distance from this top face. For each sample, the external lateral area (1 cm) from each side was eliminated, as some leaking of the consolidant might affect the evaluation of penetration in this area, hence only the central core of the samples was kept and sliced. A scheme of the sampling areas is reported in figure II.1.

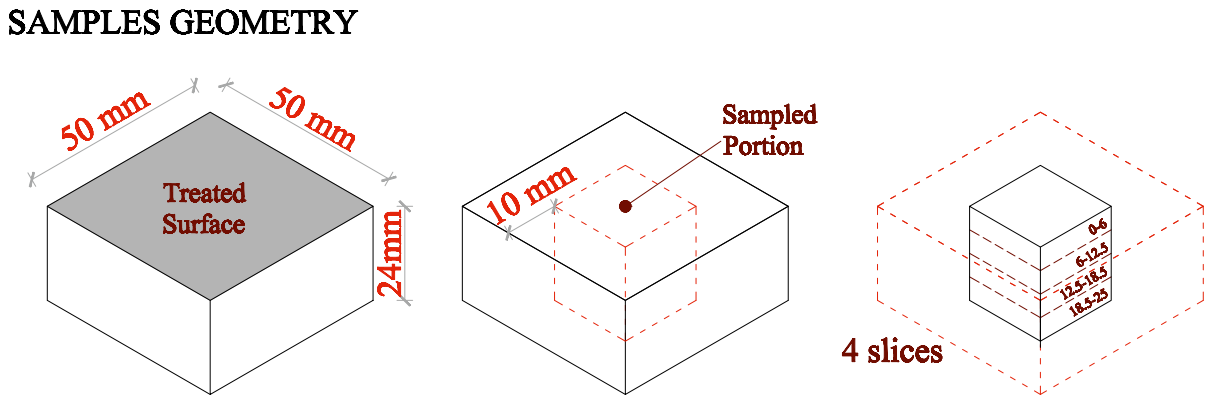

Figure II.1: Sampling positions.

To determine the penetration depth of the DAP solution right after the treatment (for samples treated by brushing) and after curing for 48 hours (for both samples treated by brushing and immersion), the content of soluble phosphate (originating from DAP dissolution in water and possibly metastable phases) was investigated. Wet samples were sliced and ground before drying, so that DAP content would not be affected by redistribution during drying. Powders were then dried to constant weight at 50°C and salt extraction was performed by boiling for 10 minutes in deionized water while stirring and final filtering. The content of soluble phosphate was then determined by ion chromatography (IC, Dionex ICS 1000). Possible reaction between globigerina limestone and DAP solution before the samples are completely dry, unfortunately, cannot be excluded. For this reason, unreacted DAP content for BR samples at time T0 could be slightly underestimated and HAP formation slightly overestimated.

Presence of soluble phosphate was also investigated in the poultice used for limewater application, after poultice removal from the samples, and in some white spots formed on the surface of samples treated by immersion, after drying.

As stated above, phosphate presence was considered indicative of unreacted DAP and, hence, of the migration of the consolidant. However, as the reaction between the DAP solution and the calcitic substrate proceeds, formation of HAP and metastable calcium phosphate phases is expected. While HAP is insoluble in the considered pH range (so that no release of soluble phosphate is expected), metastable phases are soluble (so that they are expected to contribute to the total amount of soluble phosphate detected by IC). Therefore, after consolidant application and curing (samples "48h") and after drying (samples "6d") the phase composition was determined by FT-IR (Perkin Elmer Spectrum One, KBr pellets method). This allowed to distinguish between soluble phosphate owing to DAP and metastable phases and to detect whether the treatment was effective in forming HAP or instead other phases were produced. FT-IR was also performed after limewater poultice application and drying (samples "F"), to determine whether this procedure is effective in removing unreacted DAP and boosting HAP formation.

II.3 Results

Globigerina limestone microstructure and water transport properties prior to the treatment are reported in figure II.2.

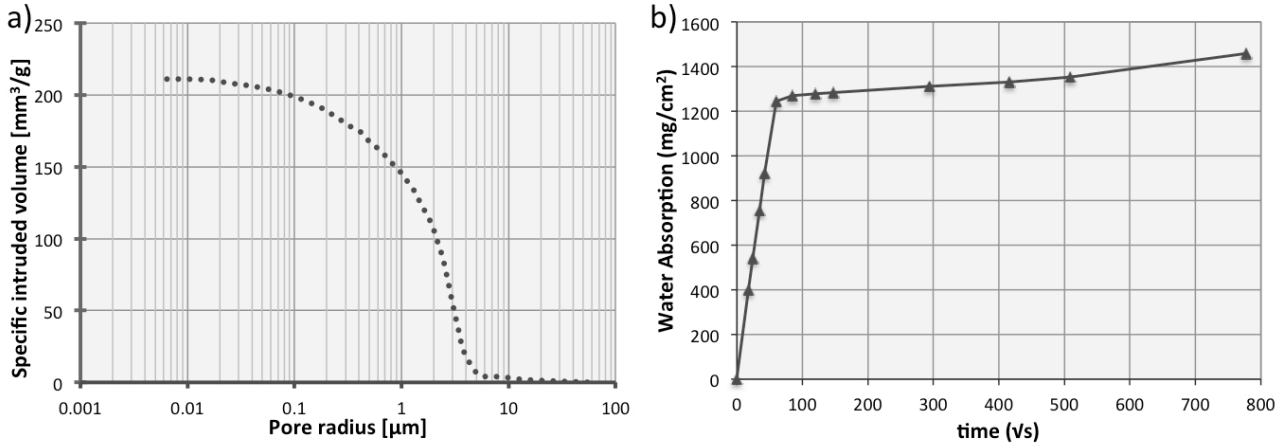

c)

Total open porosity	37.70%
Mean pore radius	2.47µm
Water Absorption at saturation	16.9 wt.%
Water Absorption coefficient	21.2 g/cm²s$^{0.5}$
DAP solution uptake	19.4 wt.%

Figure II.2: a) Pore size distribution and b) sorptivity curve of globigerina limestone. In c) relevant properties of the substrate are reported

The stone exhibits high porosity as well as high water absorption and absorption coefficient, hence a high and fast absorption of the consolidant is expected. In figure II.2c the DAP uptake was calculated by considering water uptake and DAP solution density, as described in chapter I (§I.3).
Penetration depth as visually assessed right at the end of brushing application and in the following stages is reported in figure II.3. The areas where the consolidant is present appear darker. As can be seen from the figure, a penetration depth of about 6 mm can be assessed at the end of the application. At 1h and 2h the penetration depth is remarkably increased, up to, respectively, 9 mm and 12 mm.

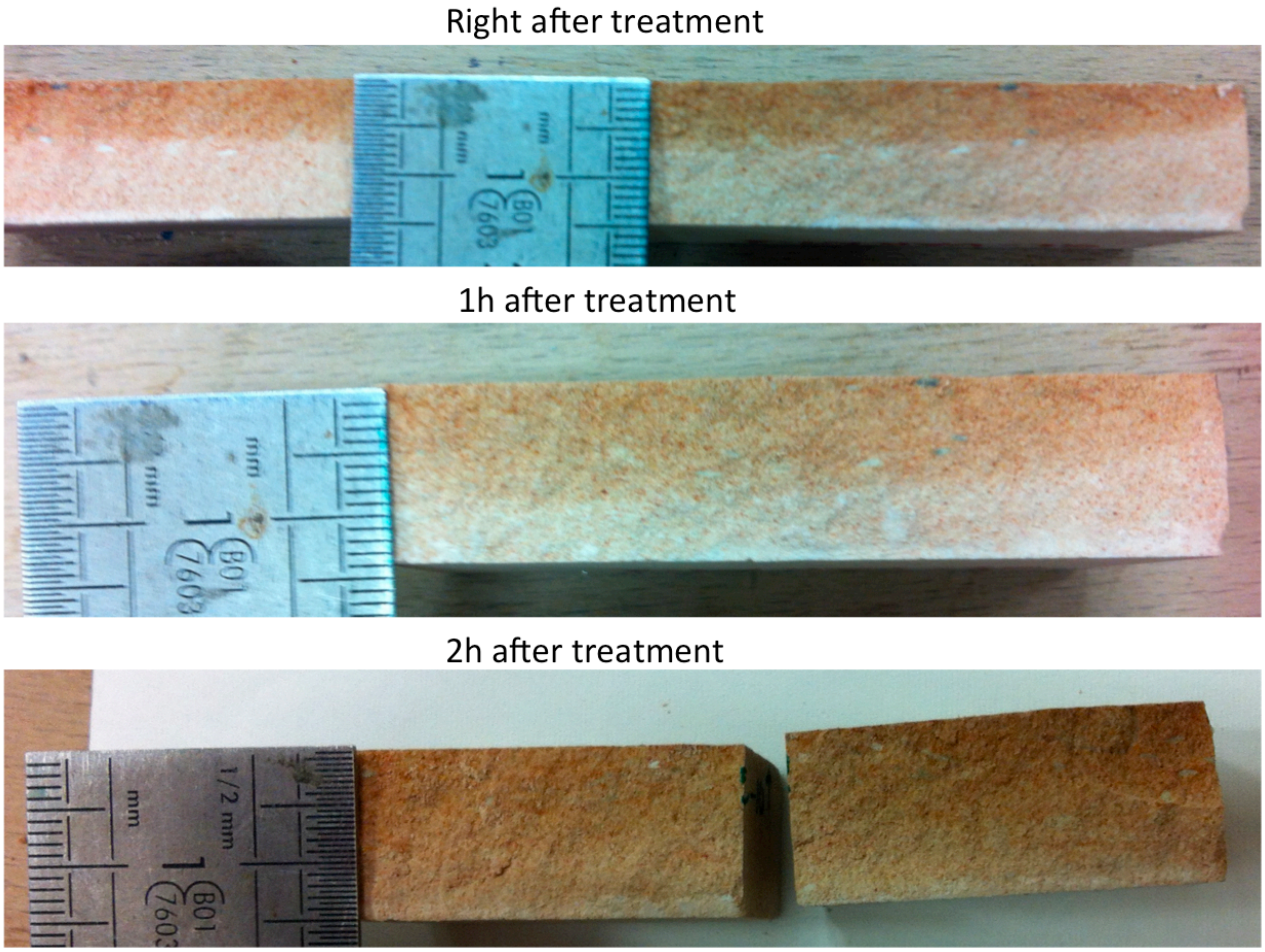

Figure II.3: Penetration depth visually assessed at different time after treatment

IC results at each treatment stage and at different depths in the samples are displayed in figure II.4.

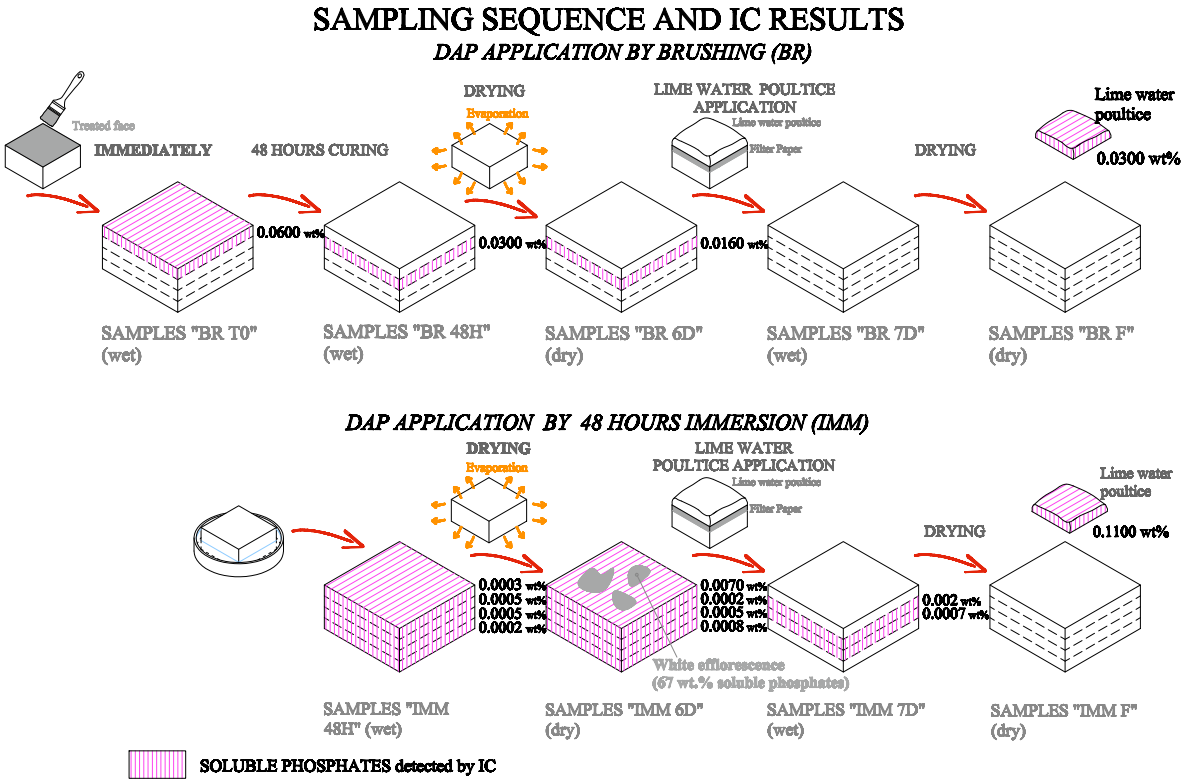

Figure II.4: Phosphate content at each treatment step and at various depths in the sample. Areas in pink indicate phosphate presence, while their exact content is reported on the side of each slice.

Phase formation at each relevant step is reported in figure II.5 for samples treated by brushing and in figure II.6 for samples treated by immersion.

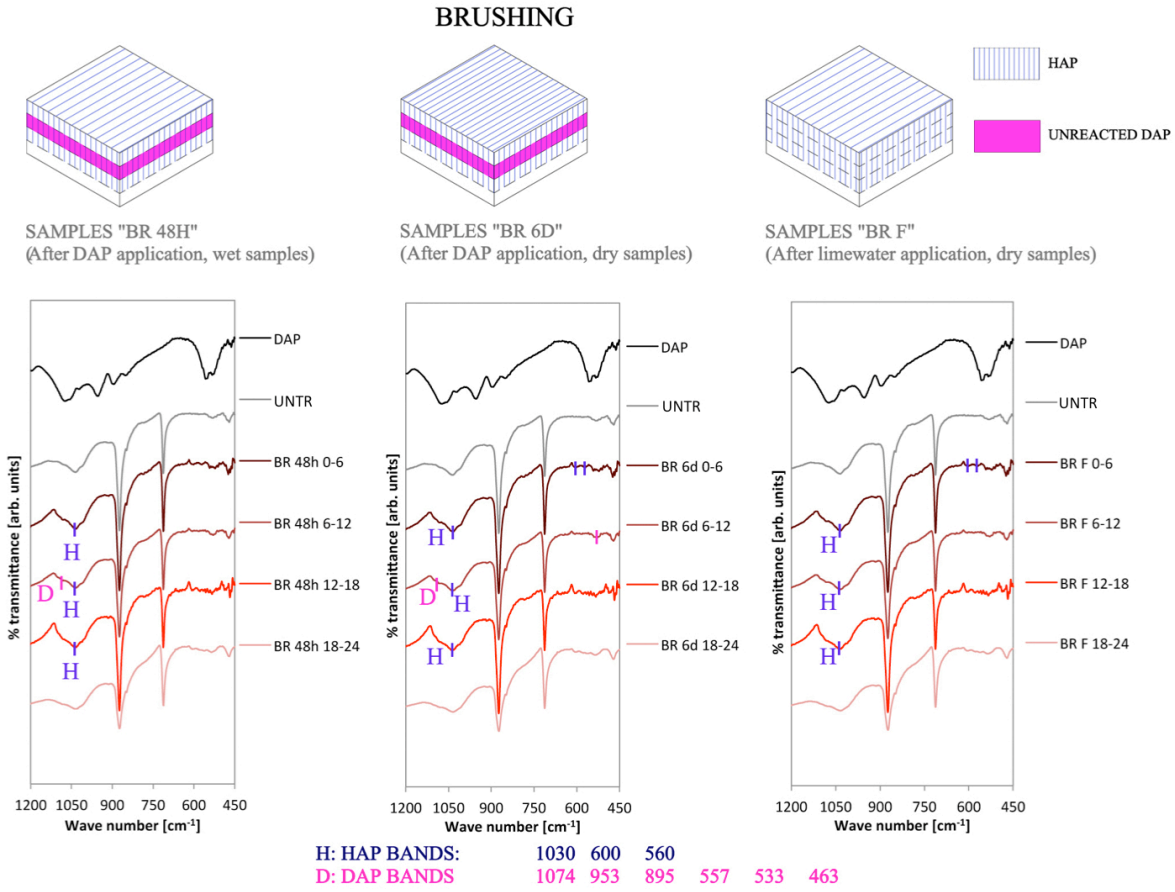

Figure II.5: FT-IR results and phase formation overview at each treatment step on samples treated by brushing.

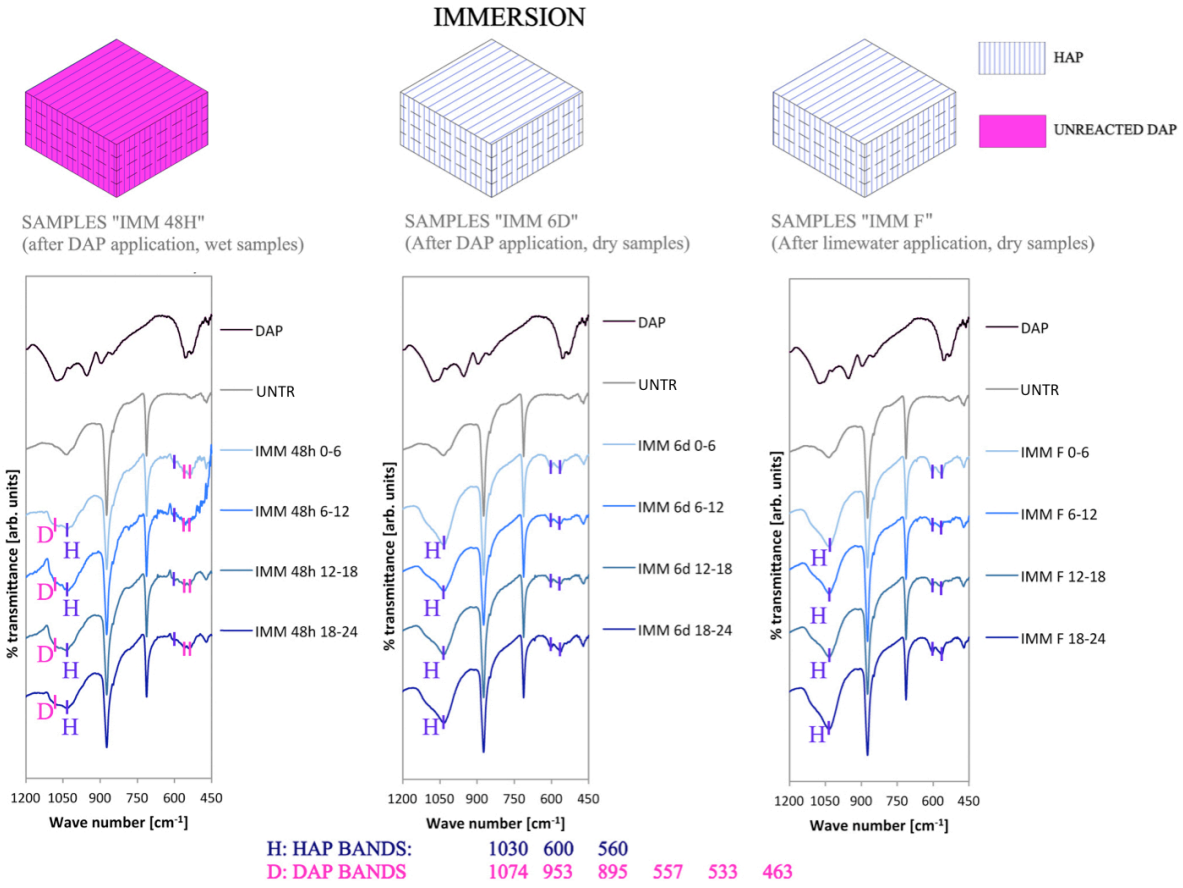

Figure II.6: FT-IR results and phase composition of samples treated by immersion

II.4 Discussion

Globigerina limestone exhibits high porosity and high water uptake and water absorption coefficient, hence being suitable for the evaluation of consolidant redistribution, especially in the case of brushing, where competition between capillary absorption and evaporation takes place due to the non-continuous flux of consolidant.

In the case of samples treated by brushing, penetration depth, as visually assessed right at the end of the treatment, is about 6 mm (figure II.3). Phosphate contents measured at this step confirm visual observation, as PO_4^{3-} (0.06 wt.%) is detected in the first slice, exactly corresponding to 6 mm thickness (figure II.4). When samples are fractured 1h and 2h after the application, an increased penetration depth is registered, corresponding to 9 mm and 12 mm, respectively. Measurement of further increases in penetration depth in the following hours has not been possible.

After curing, soluble phosphate are no longer present in the 0-6 mm slice but they are in the 6-12 mm one (see figure II.4). Total phosphate content in this zone amounts to 0.03 wt.%, sensibly lower than the initial 0.06 wt.%, suggesting that part of the DAP solution has reacted to form HAP, while another part of the DAP solution has migrated to the lower area and has not completely reacted yet.

When FT-IR is performed after curing, bands relative to HAP formation are registered down to 18 mm from the treated surface (figure II.5). The intensity of HAP bands is very low, so that bands in the bending area are barely visible, indicating that a very low amount of HAP has formed. However, the increase in the intensity of the band at 1030 cm^{-1}, although overlapping with one of Globigerina limestone, clearly indicates the formation of HAP. When examining the shape of the 1030 cm^{-1} band, a shoulder can be assessed, compatible with unreacted DAP. The relative intensity of this shoulder, compared to that of HAP band is maximal in the 6-12 mm slice, thus confirming the results of IC. The depth of formation of HAP does not match visual observation: this might be explained considering that after 2 hours the wet front corresponding to the consolidant was no longer distinguishable, thus impeding further evaluation of redistribution.
After drying, a reduction is registered in the soluble phosphate content (down to 0.016 wt.% in the 6-12 mm slice, see figure II.4), indicating that further reaction has occurred. No remarkable redistribution was assessed. In terms of phase composition (figure II.5), no alterations in bands intensity nor formation of new bands were registered. At this stage, the unreacted DAP band is no longer visible in FT-IR spectra, possibly due to too low an amount.
Limewater poultice was effective in removing possibly unreacted DAP and soluble phases, as no soluble phosphate were detected in the sample after poultice application (figure II.4). Consistently, a phosphate amount comparable to that previously present in the samples was measured in the poultice itself. The fact that the phosphate content in the poultice is slightly higher than that at the previous step might be due to the fact that phosphate evaluation was performed only in the central part of the sample, where reasonably the content is slightly lower, while the poultice is expected to have soaked salts also from the external areas of the samples. A slight increase in the intensity of the HAP band also seems to have occurred; however, due to the very low presence of HAP, variations are hard to assess.

In samples treated by immersion, after 48 hours of curing, soluble phosphate were registered in all slices, consistent with visual assessment of penetration depth (see figures II.3 and II.4). Their total content is slightly lower than that of samples treated by brushing, despite samples treated by immersion exhibiting a higher consolidant uptake (see Chapter I, §I.3). The reason for this is thought to be the formation of HAP during the 48 hours of curing, as indicated by FT-IR results (figure II.6). This suggests that, compared to application by brushing, in the case of immersion a larger part of the DAP solution has reacted with the calcitic substrate to form HAP. Bands of remarkable intensity can be detected in the 1030 cm^{-1} area, corresponding to HAP formation. As in the case of brushing, the shoulder on the left of the band is consistent with the presence of unreacted

DAP. The relative intensity of the HAP band and its shoulder indicate a significant presence of DAP in all the slices, consistent with the results of IC. Bands in the bending area (560-600 cm^{-1}) are much more confused, due to the fact that Globigerina limestone, HAP and DAP bands partially overlap in that area.

As an effect of drying, in samples treated by immersion, some white spots formed on the surface where evaporation occurs. When those spots were examined, a very high (67 wt.%) soluble phosphate content was determined, suggesting they are entirely composed by unreacted DAP (figure II.4). This suggests that the salt has migrated towards the external surface as an effect of evaporation, as hypothesized in the previous chapter.

In terms of phase composition, marked bands owing to unreacted DAP were assessed at the end of the treatment on wet samples (see figure II.6). The bands remarkably decreased after drying. This seems to be due to two possible causes. First, the majority of unreacted DAP has reached the external surface instead of remaining inside the stone pores, as suggested by unreacted DAP spots on samples external surface. Moreover, further reaction might have occurred while phosphate migrate towards the external surfaces. As a confirmation of the latter hypothesis, a remarkable increase in HAP bands intensity can be assessed in all slices after drying: at this stage also bending bands are clearly visible at 560 and 601 cm^{-1}. HAP formation is greater in the external surfaces (0-6 and 18-24), hence an accumulation has occurred in those surfaces (as found also in Chapter I). The difference between the results obtained in this chapter and in the previous one, where accumulation was detected only on the top surface, is thought to be the difference drying conditions: in this case samples were put in the oven on a grill so that evaporation took place through all external surfaces, while in the previous case the bottom surface was in contact with a petri dish, so that evaporation was impeded. However, HAP presence is maximal in the top surface, probably because of greater HAP formation during consolidant application. During the first 48 hours of reaction (when the sample is wrapped in the plastic film), PO_4^{3-} ions react with Ca^{2+}ions to form HAP. When the sample is unwrapped, redistribution of unreacted DAP takes place. When the PO_4^{3-}ions originally available (about 1%, the remaining 99% being HPO_4^{2-} ions) are consumed because they reacted to form HAP, more PO_4^{3-} ions dissociate from the still unreacted HPO_4^{2-} ions, so that HAP formation can proceed. This explain why more HAP is formed near the surface, even if uniform HAP formation through the sample is expected during the first 48 hours of reaction (when no evaporation and hence no redistribution takes place). The additional HAP formation is made possible by formation of additional PO_4^{3-} ions dissociated from the still unreacted HPO_4^{2-} ions, which are displaced during drying.

As an effect of poultice application (figure II.4), no soluble phosphate are detected in the top face (in contact with the poultice) and in the lower one, probably because of leaking of limewater from the lateral sides of the samples due to wrapping. Absence of soluble phosphate in this area is probably due to their reaction with calcium ions coming from the poultice resulting in further HAP formation. At this step, phosphate are still present in the central area of the sample, but they are removed when sample is left to dry in contact with the poultice, thus indicating efficacy in salt extraction. At the end of the treatment, as a result of the poultice application, no soluble phosphate are detected in any of the slices. Consistently, white spots on the surface have been removed. FTIR (figure II.6) indicates a slight increase in intensity of HAP bands. No bands ascribed to the presence of unreacted DAP were detected.

When comparing samples treated by brushing and by immersion (see figures II.5 and II.6, respectively), a much higher HAP formation is assessed in the latter case, which matches the higher consolidant uptake and weight increase due to the treatment assessed in the previous chapter. In samples treated by brushing, HAP forms down to a depth of about 18 mm, while it reaches 25 mm (corresponding to the whole sample thickness) in samples treated by immersion. Interestingly, this higher formation of HAP does not seem to influence much the mechanical properties (dynamic elastic modulus and tensile strength), while it does affect pore occlusion and water transport properties of the samples, as discussed in Chapter I. This is possibly due to the fact that the mechanical benefit of HAP is due to its ability to bond loose grains by nucleating at grain boundaries [15]: very low amounts of HAP are sufficient to exert this action. Much higher formation of HAP, instead, might result in precipitation in the pores thus modifying the microstructure while not increasing much the mechanical properties.

Regarding soluble phases, much more unreacted DAP can be detected in samples treated by immersion, again consistent with the higher product uptake.

In both cases, however, the limewater poultice is effective in removing unreacted DAP and soluble phases.

II.5 Conclusions

Redistribution of the consolidant was assessed after the consolidant application, thus resulting in remarkable differences in penetration depth and distribution of the reaction products. However, no formation of metastable phases occurs as an effect of redistribution.

Application method is crucial in the determination of both penetration depth and amount of HAP that forms. Also redistribution dynamics depend on the application procedure.

The drying phase is also important in determining DAP migration towards the external surface, thus influencing the amount of HAP that is formed and its distribution.

No matter the application procedure, limewater poultice is effective in removing soluble compounds, as a combined effect of limewater soaking stage, that allows for further DAP-calcium ions reactions and drying phase, and drying in contact with the sample that results in soluble product removal. Consequently, only HAP is obtained at the end of the treatment.

Chapter References

[27] Maravelaki-Kalaitzaki P., Kallithrakas-Kontos N., Korakaki D., Agioutantis Z., Maurigiannakis S., Evaluation of silicon-based strengthening agents on porous limestones. Progr Org Coat 57 (2006) 140-148

[28] Ferreira Pinto A.P., Delgado Rodriguez J., Consolidation of carbonate stones: Influence of treatment procedures on the strengthening action of consolidants. J Cult Herit13 (2012) 154-166

[29] Franzoni E., Graziani G., Sassoni E., Bacilieri G., Griffa M., Lura P. Solvent based TEOS consolidant for stone: influence of the application technique on penetration depth, efficacy and pore occlusion. Mater Struct 48 (2015) 3503-3515

[30] Scherer G.W., Wheeler G.S., Silicate consolidants for stone. Key Eng Mater 391 (2009) 1-25

[31] Tulliani J.M., Formia A., Sangermano M., Organic-inorganic material for the consolidation of plaster. J Cult Herit 12 (2011) 364-371

[32] Ferreira Pinto A.P., Delgado Rodriguez J., Stone Consolidation: The role of treatment procedures. J Cult Herit 9 (2008) 38-53

[33] Maravelaki-Kalaitzaki P., Kallithrakas-Kontos N., Agioutantis Z., Maurigiannakis S., Korakaki D., A comparative study of porous limestones treated with silicon-based strengthening agents. Progr Org Coat 62 (2008) 49-60

[34] Janson S.J., Hoff W.D., Chemical Injection remedial treatments for rising damp- I. The interaction of damp-proofing fluids with porous building materials. Build Environ 23 (1988) 171-178

[35] Franzoni E., Sassoni E., Graziani G., Brushing, poultice or immersion? Role of the application technique on the performance of a novel hydroxyapatite-based consolidating treatment for limestone. J Cult Herit16 (2015) 173–184

[36] Shanika Fernando M., De Silva R.M., Nalin de Silva K.M., Synthesis, characterization, and application of nanohydroxyapatite and nanocomposite of hydroxyapatite with granular activated carbon for the removal of Pb^{2+} from aqueous solutions. Appl Surf Sci 351 (2015): 95-103

[37] Dorozhkin S.V., Amorphous Calcium Orthophosphate: Nature, Chemistry and Biomedical Applications. Int J Mater Chem 2 (2012) 19-46

[38] Dorozhkin S.V., Biphasic, triphasic and multiphasic calcium orthophosphate. Acta Biomater 8 (2012) 963–977

[39] Dorozhkin S.V., Calcium orthophosphate coatings on magnesium and its biodegradable alloys. Acta Biomater 10 (2014) 2919–2934

[40] Dorozhkin S.V., Calcium orthophosphate, Biomatter 1:2 (2011): 121-164

[41] Sassoni E., Naidu S., Scherer G.W., The use of hydroxyapatite as a new inorganic consolidant for damaged carbonate stones, J Cult Herit 12 (2011): 346-355

[42] Graziani G., Sassoni E., Franzoni E., Scherer G.W., Hydroxyapatite coatings for marble protection: optimization of calcite covering and acid resistance. Appl Surf Sci 368 (2016): 241-257

[43] S. Naidu, G.W. Scherer, Nucleation, growth and evolution of calcium phosphate films on calcite, J Colloid Interf Sci 435 (2014) 128-137

Chapter III: Efficacy and compatibility in comparison with ethyl silicate

Research aims

All products used in stone conservation must fulfill requirements of efficacy, compatibility and durability. Each of these requirements include a multitude of parameters to be evaluated: the determination of these parameters and hence of the properties that a consolidant should confer to the substrate, as well as the desired level of modification of these properties, are debated. Differences in the properties taken into consideration to evaluate the consolidants efficacy, compatibility and durability, as well as different interpretation of the result, make data of different studies very hard to compare. For this reason, in this chapter, parameters to be used to evaluate consolidant effectiveness and compatibility are discussed.

Then, on the basis of the determined parameters, a comprehensive evaluation of the new HAP-based treatment efficacy and compatibility was carried out (evaluation of durability is in Chapter IV), in comparison with ethyl silicate, which is currently the product more commonly used for limestone consolidation. In view of the results, it will be determined whether HAP-based treatment can be considered a promising alternative for ES or, instead, whether the treatment protocol set up in Chapter I needs to be revised.

III.1 Introduction

According to conservation principles, a consolidant must fulfill a multitude of requirements, generally indicated as efficacy, compatibility, durability, reversibility and it should cause no harm to either the operator or the environment [1].

In general, to be considered effective, a consolidant must deeply and homogeneously penetrate inside the stone and reach the unweathered substrate, so that it is bonded to the consolidated area (thus enhancing cohesion) and mechanical properties are improved. By doing so, also resistance to further decay should be enhanced [2-4].

To fulfill the requirement of compatibility, the consolidant must cause no harm to the substrate [5], hence the material must not experience any alteration in its appearance, not even after long-time exposure, and the consolidant must not lead to the formation of harmful byproducts for either the stone, human health or the environment [4,6]. Evaluation of the target properties that a consolidant should confer to the substrate is debated; for example, it is generally required that physical and microstructural properties are kept as unvaried as possible, but some reduction in open porosity and water absorption might be desired according to some authors, as long as water vapor permeability is maintained [4,7]. On the other hand, too high a pore occlusion, as well as excessive reductions of water permeability might cause exfoliation or even detachment whenever a water source is present

behind the consolidated layer, due to either salt crystallization of freezing [2,3,8,9].

Compatibility includes a multitude of requirements. As for water vapor permeability, drying rate should remain unaltered [4,7], thermal behavior of the consolidated layer should match as much as possible those of the untreated material [2,4], no alterations should be caused in the stone appearance, etc. Variation in the properties should occur gradually with depth, so that no surface clogging layer is formed, which could create incompatibility and possibly detachment [2,3].

Requirement of durability, consisting in the consolidant providing resistance to weathering without suffering or causing negative alterations, will be discussed in detail in the next chapter.

Reversibility requires that the intervention could be undone at any time following its application [2,8]. Stone consolidants and protectives are generally not to be considered reversible. Some classes of thermoplastic organic resins that remain soluble in their solvent could be, but their reversibility is more theoretical than practical, as removal from the pores can rarely be performed and generally causes damage to the stone [4]. For this reason, retreatability, instead of reversibility, is normally required for consolidants, meaning that the consolidant is not required to be completely removable, but should not prevent further treatments with the same or other products [8].

Ethyl silicate (tetraethoxysilane, ES) is currently the most used among stone consolidants, because of its high efficacy on silicate materials such as quarzitic stones and bricks. ES efficacy is due to its ability to form strong Si-O-Si bonds with substrates containing –OH groups, to its low viscosity that allows for a good penetration depth, to absence of harmful by-products as a result of the reaction, to high stability and good durability [8,10]. These characteristics have made alkoxysilanes widely studied and employed in stone consolidation for several decades. ES efficacy on carbonate materials, such as marble, lime-based mortars and, to a lower extent, limestone, instead, is quite limited, hence no fully satisfactory treatments are currently available for these lithotypes. Despite the scarce efficacy, however, ethyl silicate is commonly used for limestone consolidation, essentially due to the lack of suitable alternatives [7].

In the previous chapter, efficacy of HAP as a consolidant for limestone has been highlighted, thus it is expected to be a suitable alternative to ES. In the previous part of the research, efforts have been devoted to optimization of the treatment parameters and to the development of a suitable treatment protocol for the use of this consolidant. However, no comprehensive studies have been carried out so far for the evaluation of efficacy, compatibility, and durability of the treatment. These aspects have not yet been discussed in the literature either. At this stage of the research, the evaluation of these parameters is of paramount importance, and so is the comparison with ethyl silicate, which is the main alternative to the proposed treatment. In fact, if severe issues would arise concerning any of the discussed parameters, a redefinition of the treatment would be necessary.

For this reason, the aim of this chapter is to discuss all the parameters that should be taken into account to evaluate the action of a consolidant and its desired performances. In view of these considerations, a detailed evaluation of efficacy and compatibility of the HAP-treatment was performed. The same tests were carried out on ethyl silicate-treated stone, so as to have a direct comparison between the two treatments.

These aims are quite hard to achieve, mostly because the definition of the parameters to be taken into examination for the evaluation of efficacy and compatibility is not univocally determined. Some guidelines can be drawn from RILEM Tentative Recommendations [11] and by Italian ''Istituto Centrale per il Restauro'' (Central Institute for Restoration) [4]. However, different sources indicate different parameters to be taken into account and also the level of modification that should be achieved for all the listed parameters by consolidation is debated. For example, in the literature, up to a dozen different mechanical parameters are recommended for determination of a consolidant's effectiveness, according to different authors [3,4,12], moreover, different opinions can be found about the outcome that is desired [4,7].

III.2. Materials and Methods

III.2.1 Materials

All tests were performed on globigerina limestone, that was artificially weathered prior to treatment and characterization (as recommended by [4]). Artificial weathering procedure consisted in heating the samples at 400°C for 1h, and is more fully described in Chapter I.

Cubic samples (5 cm side) and prismatic samples ($7 \times 7 \times 2.5$ cm^3) were obtained by sawing a single slab, parallel to the bedding planes; cylindrical samples (5 cm height, 2 cm diameter) were core-drilled perpendicularly to the bedding planes.

III.2.2 Methods

HAP treatment was performed according to the procedure set up in Chapter I: a 3M DAP solution was applied by brushing (10 brush strokes) and left to cure for 48 hours while wrapped in a plastic film to prevent evaporation. Samples were dried and rinsed, then a limewater poultice was applied and left to dry in contact with the samples.

Ethyl silicate treatment was performed by using a commercial product (Estel 1000, CTS, Italy), consisting of 75 wt.% ethyl silicate (40% monomers, 35% dimers/trimers, also containing 1% dibutyltin dilaurate as catalyst) and 25 wt.% solvent (white spirit).

According to previous studies performed during the PhD [13,14], application by 10 brush strokes was found to be the most effective application procedure also in the case of ethyl silicate; in fact,

this method is feasible for on site application and allows for achieving good penetration depth and increases in mechanical properties, while not dramatically altering stone microstructure.
This also made it possible to compare the performance of the two products while using the same application procedure. Ethyl silicate was left to cure for 4 weeks, as recommended by technical data sheets, before characterization.

III.2.2.1.Evaluation of the treatments effects

Efficacy

Efficacy was evaluated by analyzing weight increase, penetration depth and mechanical properties before and after treatment.
Weight increase indicates the amount of consolidant that enters and remains inside the stone. It was determined right at the end of the application and after 1 month curing, as recommended in [4]. In particular, weight increase at the end of the application gives a measure of product uptake, while measure at one month allows to determine the amount of consolidant that is retained inside the stone. Weight increase was determined on both cylindrical and cubic samples, the same that were later used for the other tests.
The assessment of penetration depth of a consolidant is a delicate task, because redistribution can occur in the phases following its application, as described in Chapter II. For this reason, many different methods have been employed in the literature for its evaluation, such as cross-section observation by SEM, coloration methods, micro-drilling resistance (MDR), X-ray radiography or tomography, just to mention some [12,14,16]. Moreover, evaluation of the stone features at different depths might allow to determine the areas reached by the consolidant: for example, FT-IR analysis, abrasion resistance, porosity, water absorption and water vapor permeability at different depths have been proposed [4,12,17]. In the present study, penetration depth was visually assessed at the end of the treatment on prismatic samples (15 mm thickness) fractured right after the end of treatment application. Then, after 1 month, the final penetration depth was evaluated by measuring the variation with depth of resistance to abrasion, microstructural properties and phase composition, determined as described in the following.
The main aim of stone consolidants is restoring stone cohesion and mechanical resistance [2,3,12,18]. However, different parameters have been evaluated by different authors, thus making results of different literature studies hard to compare. In particular, the following properties have been referred to as significant: compressive strength, tensile strength, bending strength, modulus of elasticity, ultrasonic pulse velocity, abrasion loss, surface hardness, “strength in depth” (basically corresponding to MDR), resistance to peeling [3,4,12,19]. However, the suitability of some of these

techniques to give a measure of a consolidant's ability to bind loose grains is questionable. This makes, for example, compressive strength not as representative of stone cohesion as other techniques are (for example, tensile strength).

In the present chapter, three mechanical features were selected as significant for the determination of the consolidating ability of the products under investigation, namely dynamic elastic modulus, tensile strength and resistance to abrasion.

Dynamic elastic modulus can be expressed according to the formula $E_d = \rho \times UPV^2$, where ρ is the geometric density of the stone and UPV is the ultrasonic pulse velocity. UPV, in turn, can be calculated as the ratio between the distance between the transducers (i.e. the sample thickness) and the time taken by the ultrasonic wave to cross the sample. E_d and UPV are both widely used to evaluate stone weathering and consolidation [12, 20-28] as they are obtained by non-destructive techniques [29].

In the present study E_d was determined along the axis of stone cores before and after consolidation (by a Matest instrument with 55 kHz transducers, a rubber couplant being used to ensure a good contact between the transducers and the sample), reported values being the average of 6 specimens. Being non destructive, E_d was measured on exactly the same samples before and after consolidation.

Tensile strength (σ_t) gives a measure of stone cohesion. Moreover, decay due to salt crystallization and freezing-thawing phenomena occurs when crystallization pressure exceeds stone tensile strength [8,30]. For this reason, the ability of a consolidant to increase *tensile* strength is remarkably more important than increasing its *compressive* strength; hence it is normally preferred for evaluation of consolidant efficacy, as it also gives an indication about durability [7,24,28,31]. Tensile strength was measured on the same samples used for measuring E_d. It was determined as average of 6 samples, by Brazilian splitting test (Amsler-Wolpert loading machine at a constant displacement rate of 4 mm/min).

Resistance to abrasion gives a measure of stone resistance to pulverization [2], hence it is also suitable to estimate stone cohesion. For this reason, it is particularly significant for Globigerina limestone, whose main weathering process on site is alveolization, occurring due to a combined action of salt crystallization and wind erosion, leading to significant material loss down to several centimeters from the surface. In the present study, resistance to abrasion was measured on duplicate prismatic samples, both untreated and treated, by measuring weight loss after an accelerated abrasion test, developed by modifying the PEI (Porcelain Enamel Institute) abrasion test and based on the use of steel spheres and corundum powder kept in rotatory motion over sample surface [32] . Abrasion was measured on the treated surface of the slabs and then in depth, after cutting 5 mm-

thick slices from the treated surface. In this way, it was possible to derive indirect information on the treatment penetration depth and on its distribution in depth inside the sample [3], although not in a continuous way as for instance by micro-drilling (MDR).

Compatibility

Compatibility was evaluated by analyzing alteration caused by the treatments in the following parameters: color, microstructure, contact angle, water transport properties, water vapor permeability, drying rate, thermal behavior. After the discussion on compatibility, additional requirements, such as impact on human health and environment and retreatability, were preliminarily evaluated on the basis of literature data.

The maintenance of the aesthetic aspect of stone is a key goal in cultural heritage conservation [4]. One of the most relevant parameters to evaluate aesthetic compatibility is color change (ΔE). Color parameters, namely L^*, a^*, b^* (L^* = black ÷ white; a^* = red ÷ green; b^* = yellow ÷ blue) were measured on the treated face of consolidated slabs and on untreated references by a Mercury 2000 Datacolor. Color change can be determined from color parameters by means of the formula $\Delta E = (\Delta L^{*2} + \Delta a^{*2} + \Delta b^{*2})^{1/2}$. Each value is the average of 3 measurements.

Another important factor regarding consolidants' compatibility is that they do not give rise to by-products which might be harmful for the substrate [3,4]. For this reason, phase formation as a result of the treatments was evaluated by Fourier transform infrared spectroscopy (FT-IR, Perkin Elmer Spectrum One, KBr pellets method). FT-IR analysis was performed on ground samples obtained from the cylinders used for mechanical tests at different depths from the treated surface (0–5 and 5–10 mm), so as to achieve an indication of treatment penetration depth and of the distribution of consolidant with depth inside the stone. For HAP-samples, the possible presence of soluble metastable calcium phosphate phases was investigated by salt extraction (performed as described in §I.2.2) and ion chromatography (Dionex ICS 1000).

Alterations in sample microstructure as a consequence of consolidation were evaluated by mercury intrusion porosimetry (MIP, Fisons Macropore Unit 120 and Porosimeter 2000 Carlo Erba) in terms of total open porosity and pore size distribution before and after treatment. MIP analysis was performed on samples obtained by chisel from cylinders and from cubes. As recommended in [4], MIP was performed on samples coming from different depths from the treated surface (0–5 and 5–10 mm for the cylinders, 0–5, 5–10 and 10–15 mm for the cubes), so that a further indication of treatment penetration depth and microstructure modification with depth could be derived [1,3]. One sample was taken for each condition, given the restrained variability of MIP results on GL, when coming from one same slab (*C.o.V.* = 5% [26]).

Eventual hydrophobicity as a result of the treatments was evaluated after 1 month curing (recommended by ES technical data sheets), by measuring contact angle (α) and time for absorption (t_a), both by a Contact Angle Measuring device DSA30 – Krüss GmbH. As in Chapter I, 4 µl drop of de-ionized water were dropped on the treated face of dry prismatic samples and absorption in the substrate was video-recorded. Each value is average of 3 measurements for each treatment condition.

Regarding water absorption properties, water sorptivity and absorption coefficient (AC) were measured for both untreated and treated samples (2 cubic samples for each condition) according to EN 15801 [33]. Water was allowed to penetrate inside the samples through the treated face and rise parallel to the bedding planes, to mimic the conditions on site, where stones are usually placed with the bedding planes horizontal and hence roughly parallel to wind-driven rain. Total water absorption by capillarity at 24 h (WA_{24h}) and 7 days (WA_{7d}) were evaluated.

Water vapor diffusion resistance coefficient (μ) was determined according to EN 15803 [34] on stone slabs, to measure eventual changes in water vapor permeability. Water vapor was left to flow through the treated face, that was put in contact with the cup containing the liquid.

Drying rate was evaluated by determining water evaporation rate in untreated and treated samples, according to a methodology described in [11]. Briefly, slabs were water-saturated then left to dry; weight decrease during drying was monitored over time in laboratory conditions ($T = 20 \pm 2$ °C, RH = 50 ± 5%). In order to obtain one-dimensional evaporation, water was allowed to evaporate through only a single square face of the prism by sealing the remaining part of the sample with vapor-proof tape.

Thermal behavior was evaluated on untreated and treated stone by subjecting samples to thermal cycles and measuring maximum strain (ε_{max}), residual strain (ε_{res}) and thermal expansion coefficient (α_t). Cycles were performed by a dilatometer L75/30/C/W Ceramic Instruments with computerized management system. Samples for the test ($5 \times 5 \times 25$ mm^3) were obtained in the direction perpendicular to stone bedding planes. They were subjected to a 25–80–25 °C heating–cooling cycle, temperature being increased/decreased with a rate of 1 °C/min and maximum temperature being maintained for 1 h to simulate temperature excursions comparable to those naturally occurring in the field [48]. Thermal expansion coefficient was determined as the slope of the linear part of the thermal strain/temperature curve, considering the part between 30 and 80 °C.

III.3 Results [1]

Weight increase in cubes and cylinders right after treatment with both ES and HAP are reported in Table III.1, values being indicative of the consolidant uptake and of its retention inside the stone. Results for consolidant uptake are quite different between the two products, namely HAP (0.143–0.147 g/cm^2) and ES (0.077–0.095 g/cm^2), while no significant differences are assessed between the two geometries of the samples (to evaluate differences between samples with different geometry, referral must be made to values expressed in g/cm^2).

	Consolidant uptake (wet samples)		**Consolidant retained inside the stone (dry samples)**
	[g/cm^2]	[wt.%]	[wt.%]
HAP treated cores	0.147	17.6	3.4
HAP treated cubes	0.143	1.7	5.2
ES treated cores	0.095	13.7	42.1
ES treated cubes	0.077	0.9	46.7

Table III.1: Consolidant uptake in cubes and cylinders treated by ethyl silicate and hydroxyapatite. Values for consolidant uptake were determined right at the end of the treatment application, on wet samples, while values for consolidant retained inside the substrate were determined after 28 days curing, of course on dry samples.

Penetration depth, as visually evaluated after application of the two consolidants, is reported in figure III.1: an initial value of about 7 mm was measured for both consolidants and a uniform penetration was observed.

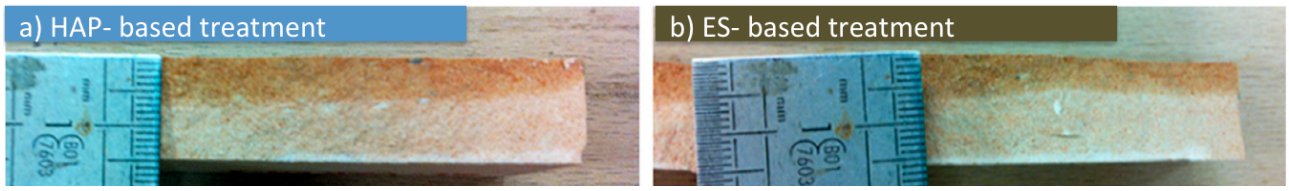

Figure III.1: Penetration depth in a) HAP treated and b) ES treated samples right at the end of the treatment application.

FT-IR analyses at different depth in the samples are reported in figure III.2. Phase formation as a result of the two treatments can be detected. In particular, bands around 1030 cm^{-1}, 600 cm^{-1} and 560^{-1}, characteristic of hydroxyapatite [35] can be observed in HAP treated samples, while bands at 1170 cm^{-1} and 1080 cm^{-1} can be seen in the case of ES treated samples, both in the superficial layer and in the underlying one. The band at 1080 cm^{-1} is owing to Si–O–Si groups of silica gel, while the band at 1170 cm^{-1} has to be ascribed to Si–O–C groups of unhydrolyzed ES [36]. In the case of HAP, as previously discussed, the phosphate stretching band at 1030 cm^{-1} partially overlaps one of

the bands of untreated globigerina limestone; however, remarkable increases in the band intensity and alteration of its shape clearly indicate the formation of HAP. FT-IR analyses were also used to have a measure of penetration depth of the two consolidants after curing. Presence of both consolidants was detected up to a depth of 1 cm from the treated surface.

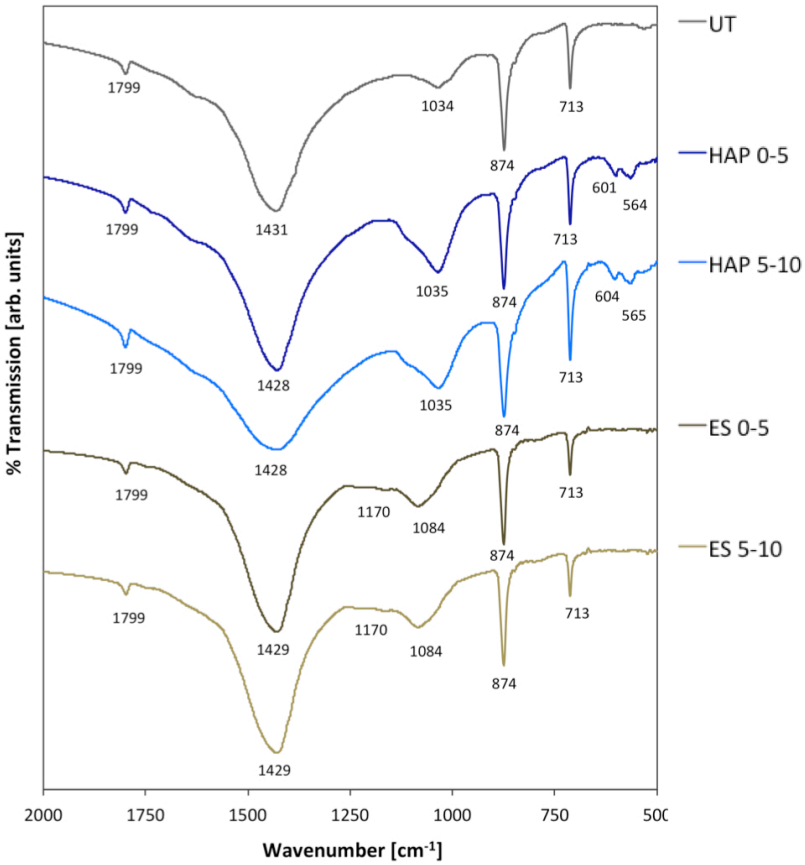

Figure III.2: FT-IR analyses performed at different depth in HAP-treated and ES-treated samples.

MIP curves for untreated and treated samples and at different depths in the samples are reported in figure III.3 (cylinders) and figure III.4 (cubes). Differential curves are also reported for comparison. As for FT-IR, microstructural modifications caused by the two consolidants were evaluated to have a measure of penetration depth. For stone cores, alterations in different pore ranges were investigated, and are reported in Table III.2.

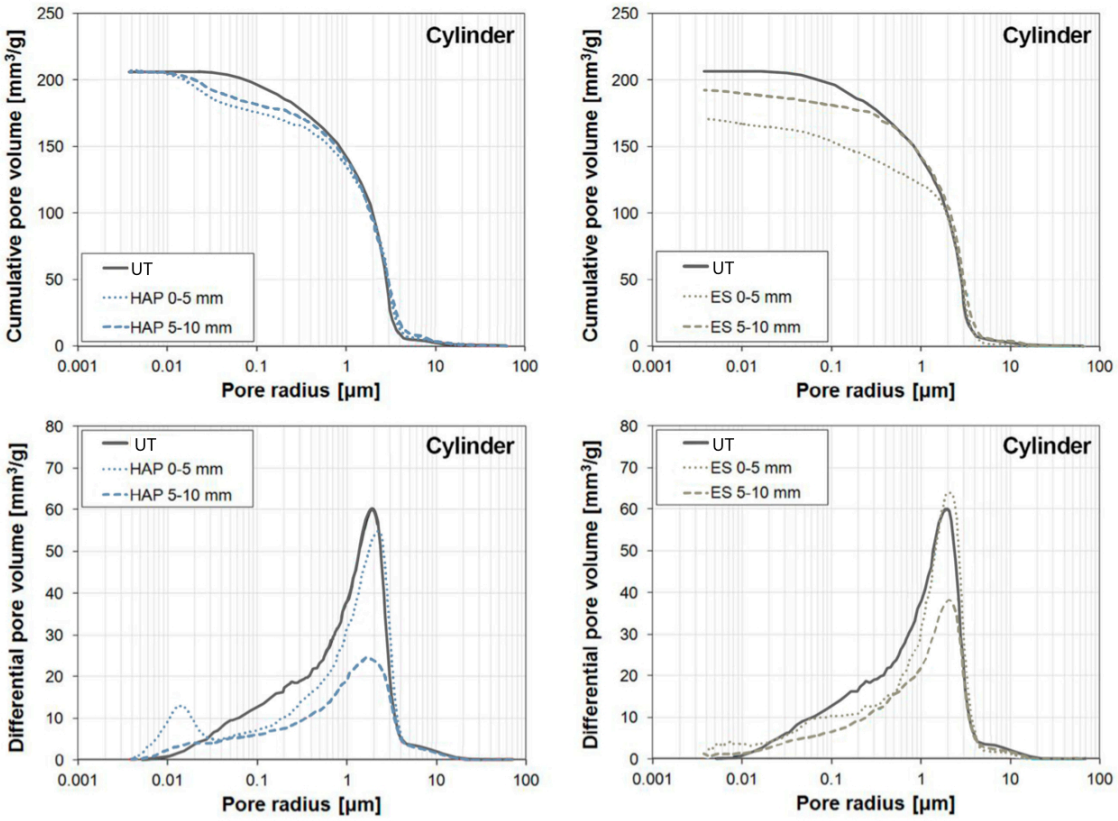

Figure III.3: MIP curves of untreated, HAP-treated and ES-treated cylinders, at different depth (0-5 mm and 5-10 mm).

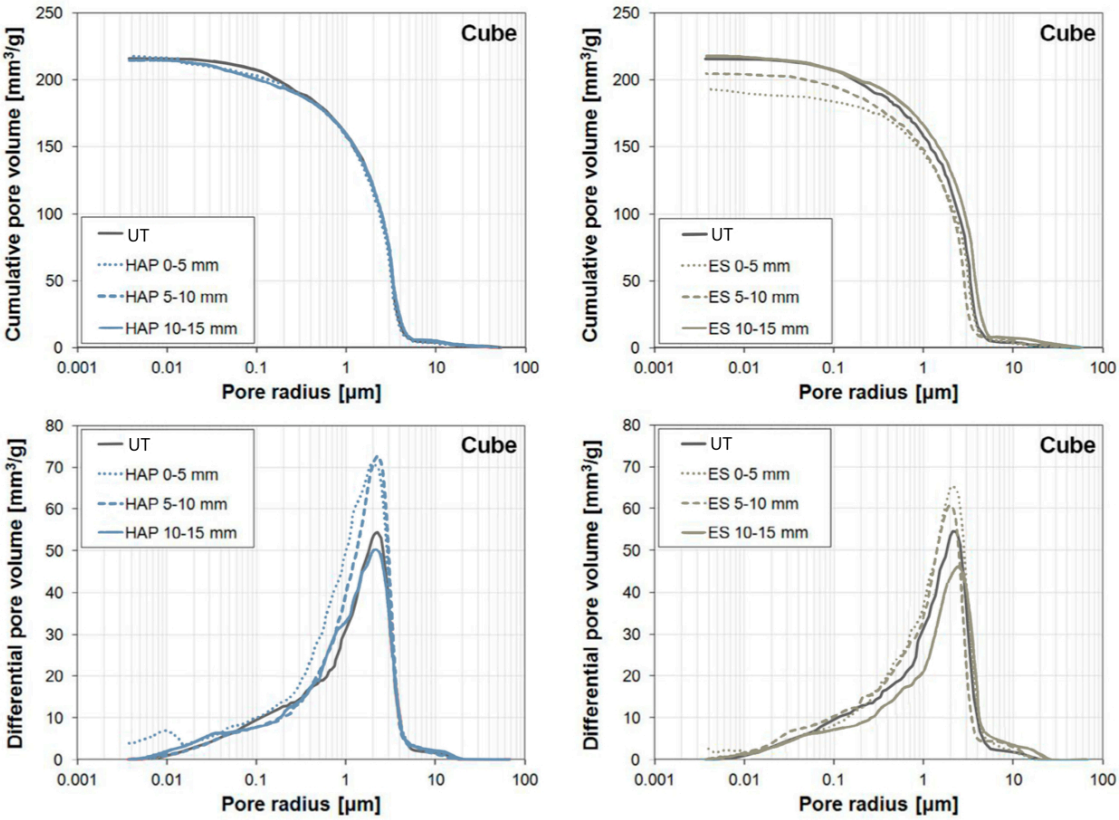

Figure III.4: MIP curves of untreated, HAP-treated and ES-treated cubes, at different depth, namely 0-5 mm, 5-10 mm, 10-15 mm.

	Pores Amount [v/v%]				Total open porosity
	< 0.01 µm	0.01÷0.1 µm	0.1÷1 µm	> 1 µm	[%]
UT	0.0	3.9	22.6	73.5	37.1
HAP	0.8	13.1	15.4	70.8	34.7
ES	2.0	5.9	15.8	76.4	32.1

Table III.2: Total open porosity and pore size distribution in untreated and treated stone cores.

Mechanical properties of untreated and treated samples are reported in Table III.3 (expressed in terms of E_d and σ_T). Increases of both dynamic elastic modulus (11.2 GPa to 16.5 GPa for HAP and to 18.1 GPa for ES) and tensile strength (from 2.7 to 3.4 MPa for HAP, from 2.7 to 4.0 MPa for ES) were observed. Results of abrasion tests on the surface and at 5 mm depth are in Table III.4.

	UW	UT	HAP	ES
E_d [GPa]	15.6 (±0.3)	11.2 (±0.5)	16.5 (±0.4)	18.1 (±0.1)
σ_T [MPa]	3.0 (±0.3)	2.7 (±0.3)	3.4 (±0.2)	4.0 (±0.2)

Table III.3: Mechanical properties of untreated and treated samples.

	UT	HAP	ES
Weight loss surface [mg/mm^2]	0.16 (±0.01)	0.10 (±0.03)	0.10 (±0.01)
Weight loss 5 mm [mg/mm^2]	0.16 (±0.01)	0.12 (±0.00)	0.11 (±0.01)

Table III.4: Weight loss due to abrasion for untreated, HAP- and ES- treated samples at 0 mm and 5mm depth from treated surface.

Chromatic alteration caused by the treatments were evaluated, results being shown in figure III.5 and Table III.5.

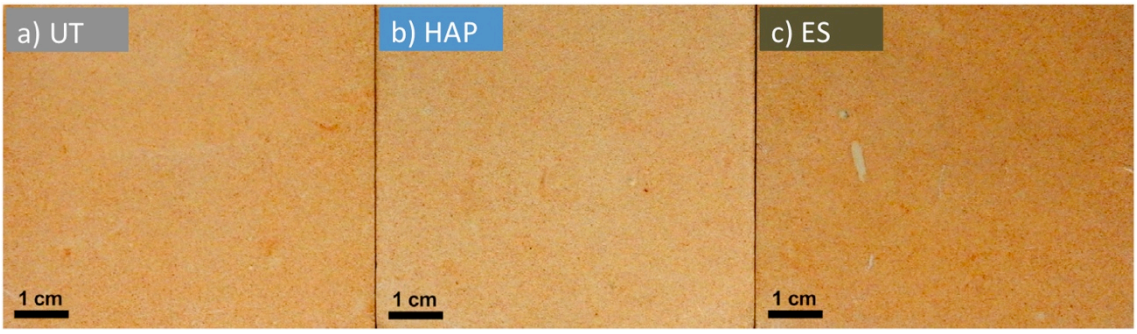

Figure III.5: Color change in samples after treatment as visually assessed

	L*	a*	b*	ΔE
UT	72.89	9.28	18.06	-
HAP	68.92	10.81	19.39	4.45
ES	72.11	9.99	18.85	1.32

Table III.5: Color parameters and final color change in untreated and treated samples, as assessed by spectrophotometer

Results of IC, performed on HAP treated samples, were not reported for brevity sake, as phosphate content was 0 wt.% for all examined samples.

Contact angle and time of absorption of treated and untreated samples are reported in figure III.6 and Table III.6.

Figure III.6: Contact angle on a) untreated, b) HAP treated and c) ES treated samples

	UT	HAP	ES
α (°)	32.3 (±12.1)	74.4 (±3.4)	114.3 (±3.8)
t_{abs} (milliseconds)	684 (±195)	3957 (±2417)	>1 h

Table III.6: contact angle values and time for absorption in untreated and treated samples.

Sorptivity curves for untreated and treated samples are reported in figure III.7, while values of total water absorption at 24 hours and 7 days, and capillary absorption coefficient are in Table III.7, together with water vapor diffusion resistance coefficient.

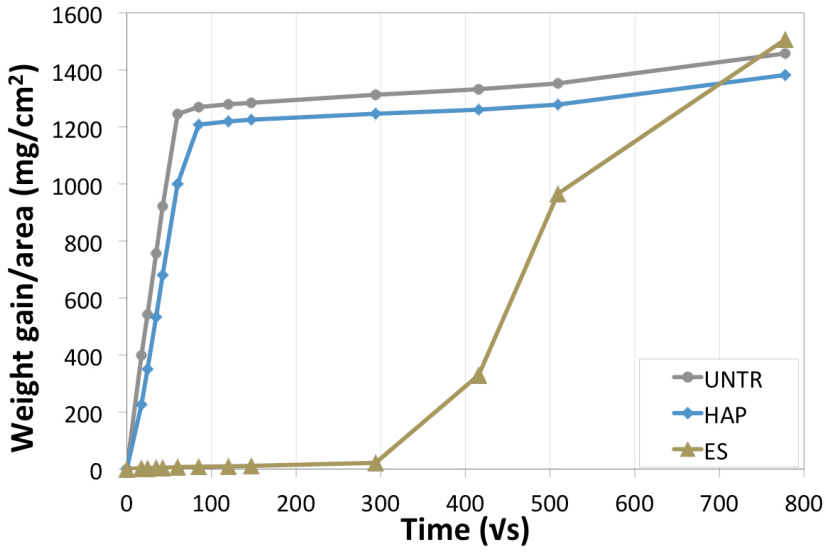

Figure III.7: Sorptivity test on untreated and treated samples.

	AC [$g/cm^2s^{0.5}$]	WA_{24h} [wt%]	WA_{7d} [wt%]	μ [-]
UNTR	21.2 ± 0.6	15.3 (±0.1)	17.1 (±0.1)	7.3
HAP	14.8 ± 2.6	15.0 (±0.1)	16.5 (±0.1)	7.8
TEOS	0.1 (±0.0)	0.3 (±0.1)	17.5 (±0.4)	7.4

Table III.7: Water uptake and capillary absorption in untreated and treated samples

Drying behavior of samples is described in figure III.8. For comparison's sake, one sample treated with ES and left to cure for only 1 week (thus still hydrophobic) before the beginning of the test was also considered.

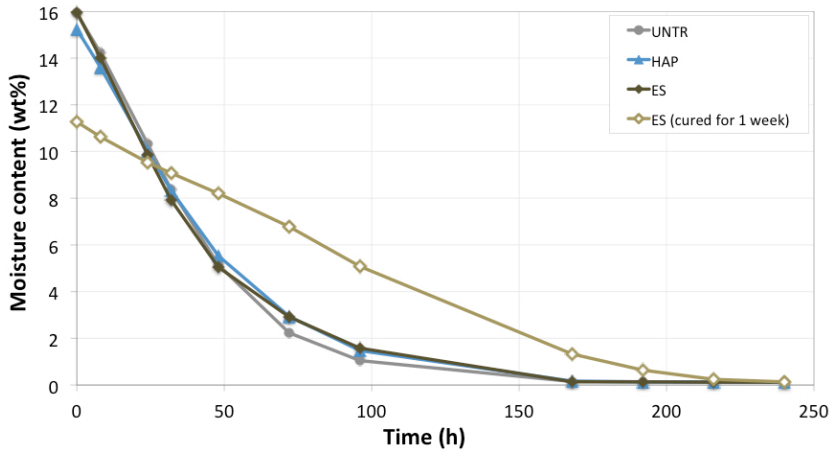

Figure III.8: Drying rate of untreated, HAP and ES treated samples. Tests were also performed on a still hydrophobic ES sample left to cure for one week only.

Thermal expansion for increasing temperature was evaluated, results being reported in figure III.9. For untreated samples, these values were registered: maximum thermal expansion ε_{max} = 0.16 mm/m, thermal expansion coefficient $\alpha_t = 3.2 \bullet 10^{-6}$ °C^{-1} and residual strain ε_{res} = -0.02 mm/m. A shrinkage was experienced after heating up to 80°C and cooling back to room temperature. This is a frequent behavior for porous limestone; for example, residual shrinkage was found when limestone was subjected to 30–80–30 °C cycles, that was attributed to vaporization of firmly adherent water molecules because of slow heating rate [37]. No significant alterations are caused by ES treatment. After HAP-treatment, lower thermal expansion coefficient ($\alpha_t = 1.6 \bullet 10^{-6}$ °C^{-1}) and higher residual strain (ε_{res} = -0.03 mm/m) are registered.

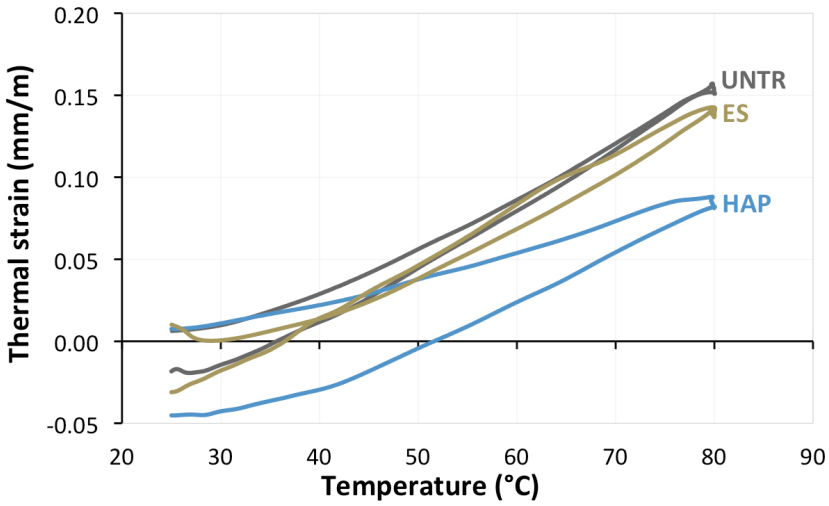

Figure III.9: Thermal behavior of untreated and treated samples

III.4 Discussion

Efficacy

Firstly, weight increase after the two treatments was evaluated (Table III.1). As detailed in [4] weight increase is generally regarded as positive, even if not necessarily indicative of a good consolidation efficacy. The differences in the initial uptake of the two consolidants have to be ascribed to the fact that consolidating solutions are very different in terms of viscosity, solvent and, mostly, density. In the case of cores, values for HAP are very close to sample saturation with water (corresponding to a weight increase of 17.1 wt.%), indicating that a condition very close to full saturation was achieved. In the case of cubes, despite values in terms of specific volume being very close to those of cores, when expressed as percentage of weight increase to weight of the sample, much lower values are obtained with respect to those of cores. This is consistent with the fact that in cubes, consolidant does not saturate the whole volume. The same trend was exhibited by ES-treated samples. This confirms what was seen in Chapter I and indicates that cores can be used to evaluate the behavior of the consolidated area of stone alone, while cubes can be used to determine consolidant distribution in depth and the transition in the properties between consolidated and unconsolidated layers, both present in cubic samples.

When dry mass increases, corresponding to the amount of consolidant retained inside the stone, is taken into exam (Table III.1), remarkable differences can be assessed between the two treatments. In particular, a much higher amount of ethyl silicate remains inside the stone pores compared to the amount of HAP that is formed. This suggests that more microstructural alterations (pore occlusion) will be assessed in ES-treated samples.

Penetration depth of a consolidant should be as high as possible, so that the unweathered part of the substrate can be reached and bonded to the more weathered superficial area, so that a gradient in the

properties of samples with depth can be achieved. Penetration depth visually assessed right at the end of the application of the treatments was about 7 mm for both consolidants (figure III.1). However, as detailed in Chapter 2, in the case of hydroxyapatite and in [13] for ES, redistribution of the consolidant occurs in the stages following its application, due to progressive migration of the consolidant, that is first absorbed into larger pores then gradually drained into finer ones. In fact, both FT-IR (figure III.2) and MIP curves (figures III.3 and III.4) indicate the presence of consolidant at a depth of at least 1 cm. This value can be considered satisfactory considering that normally the weathered layer has a depth up to about 1-2 cm [8].

Another important parameter is that a consolidant distributes uniformly inside the stone so that no crusts nor abrupt variations in stone properties are formed. This seems to be the case for both HAP and ES, as neither experiences abrupt alterations in microstructural, mechanical and physical properties.

In terms of mechanical properties, results of abrasion tests (Table III.4) indicate that comparable increases are obtained by the two treatments, both indicating a good resistance to pulverization and erosion. A gradient can be assessed between the values on the treated surface, those at 5 mm depth (being still in the consolidated layer), and those in the untreated area (values of untreated references were taken as indicative of the unconsolidated area), thus confirming that no over-consolidated crusts were formed onto the samples.

Remarkable increases of both dynamic elastic modulus (11.2 GPa to 16.5 GPa for HAP and to 18.1 GPa for ES, Table III.3) and tensile strength (2.7GPa to 3.4 MPa for HAP and 4.0 MPa for ES, Table III.3) were obtained, indicating a good consolidating efficacy of both treatments. ES exhibited more marked improvements, especially in terms of tensile strength. The evaluation of the effect that a consolidant should exert on mechanical properties of the substrate is quite debated: in fact, while Recommendation NORMAL 20/85 [4] indicates that an increase as high as possible in stone strength (in this case indicated as compressive strength) is recommended, other sources indicate that a “moderate” increase should be pursued instead. More in detail, some references indicate that increase in tensile strength should not exceed +50%, so as to prevent “over-strengthening” [7,38]. In fact, in the latter case, formation of a superficial hard crust could occur, possibly even leading to detachment of the consolidated part.

However, it must be considered that, in general, when applying a consolidant to a weathered material, it is not possible to determine the effective extent of damage that was caused by weathering on that object prior to the treatment. That is to say, it is not possible to determine whether a decrease in tensile strength higher or lower than 50% resulted from weathering, as the initial mechanical properties of the specific object are generally unknown. For this reason, another

possible criterion is that of considering the mechanical properties of the unweathered stone: in this case consolidant should provide mechanical properties as similar as possible to that of the sound stone [39].

For this reason, different considerations can be derived by following the different criteria. Both consolidants comply with the criterion of not exceeding the +50% increase threshold. If the highest increase in mechanical properties is pursued, ES performs better (see Table III.3). However, if the criterion of possibly restoring initial mechanical properties of the material is considered, strengthening caused by HAP ($\Delta\sigma_t$= +27% and ΔE_d = +47%) is closer to the original value than that caused by ES ($\Delta\sigma_t$ = +47% and ΔE_d = +61%). In fact, artificial decay resulted in decreases of 10% and 28% in tensile strength and dynamic elastic modulus, respectively. This higher strengthening caused by ethyl silicate might cause some concerns about over-strengthening and possible mismatch between unconsolidated and consolidated stone.

The fact that ethyl silicate causes an excessive increase in mechanical properties seems to be in contrast with what was discussed in the "State of the Art and Research Aims" Chapter. In fact, it was previously stated that ethyl silicate is expected to have very high efficacy on silicate stone, where OH^- groups allow for chemical bonding with the substrate, while efficacy on limestone should be quite limited. In the present case, however, due to the nature of the substrate itself, not only physical bonding occurs between ES and globigerina limestone, but some chemical bonds (though sparse) seem to occur due to the presence of quartzitic fractions in the stone [38].

Together with the characteristics of the substrate, also the product itself used in the present tests is particularly effective, due to a combination of factors: first, the formulation contains 25 wt% of organic solvent (white spirit) and partially prepolymerized TEOS (40% monomers and 35% dimmers/trimers, to reduce evaporation), both not negatively influencing penetration depth. 1% dibutyltin dilaurate added as catalyst allows for fast curing reactions. The high content of solvent also has the effect of diluting the active principle, thus limiting the silica gel layer thickness and thus its tendency to crack [8].

Regarding consolidants efficacy, another parameter to be takent into consideration is curing time, corresponding to 4 weeks in the case of ethyl silicate and about 1 week for HAP treatment (2 days are required for curing of DAP solution plus 1 day for reaction with limewater, total curing time also depending on duration of drying stages). At 4 weeks, however, when ES treated samples are examined by FT-IR, a band at 1170 cm^{-1} is detected (figure III.2), especially in the deeper zones, thus indicating the presence of Si–O–C groups of unhydrolyzed ES. This means that curing reactions are not complete after 4 weeks, which is consistent with literature data [46], indicating that up to 6-7 months may be required. Fast curing is one important advantage of HAP treatment

even though application of two treatments instead of one (as in the case of ethyl silicate) is necessary.

Compatibility

Regarding color change (see figure III.5 and Table III.5), slight modifications are assessed in ES treated samples, while more remarkable alterations are caused by HAP treatment, that tends to increase the lightness L* parameter. However, both are below the thresholds $\Delta E<5$ generally considered acceptable for stone consolidants, and $\Delta E<3$ corresponding to detectability by human eye [40]. It must be also considered that, in case of organic protectives, a threshold $\Delta E<10$ is commonly considered acceptable. Hence both consolidants can be considered compatible from this point of view.

No incompatibility derives from the mineralogical nature of the products themselves. HAP is considered a compatible material even if it is not present as a component of the stone. In fact, together with calcium oxalate, HAP is one of the minerals that constitute natural patinas, that form on carbonate stones surface over centuries [41]. These patinas were found to have a protective action towards the stone [41] and this was the consideration that pushed the research towards the study of calcium oxalate and HAP as stone protectives and consolidants. Those patinas, in contrast to pathological alterations (for example gypsum crust) are protective and do not exert any negative effect on the underlying material, hence it is required that they are maintained during restoration interventions [42]. For this reason, they can be considered compatible.

As a result of ES consolidation, instead, silica gel forms, which is similar to quartz fractions of stone, if present. In the case of globigerina limestone, where quartzitic fractions are present, it can be definitely regarded as compatible. However, quartz fractions in the stone are present in much lower amount and are dispersed in the carbonate matrix, while silica gel deposits inside stone pores, hence an effect on compatibility in terms of microstructural alterations, thermal behavior and durability, cannot be excluded and needs evaluation.

No harmful byproducts are expected to form as a result of both the reactions of HAP formation and of hydrolysis and condensation of ES. In fact, HAP reaction leads to the formation of ammonia and ES reactions to ethanol, both volatile and harmless for the stone [24]. Absence of byproducts was confirmed by FT-IR for both the consolidants. In the case of HAP, special attention was devoted to detecting eventual unreacted DAP or soluble metastable phases that might form from the reaction, but no evidence for their formation was found. Absence of metastable phases and unreacted DAP is confirmed by absence of phosphates in IC. Eventual formation of OCP, which is very hard to detect by FT-IR, cannot be excluded; however, it should not raise concerns, as, despite being more soluble

than HAP, OCP is harmless for the stone and is still much less soluble than calcite [35,43,44].

From a microstructural point of view, very different results are obtained by consolidation with HAP and ES and between cores and cubes (figures III.3 and III.4, respectively). In general, effects are more marked in cores, as they reached an almost complete saturation during consolidant application.

As seen for resistance to abrasion (Table III.4), microstructure of cubes indicates a gradual transition between the properties of the consolidated layer (both for HAP and ES) and that of untreated stone; that is to say that alterations in stone microstructure are more marked in the superficial layer (0-5 mm), lower in the underlying one (5-10 mm) and negligible in the more internal area (10-15 mm), where curves are basically identical to those of untreated reference. This also further confirms a penetration depth of about 10 mm for both treatments. The gradual transition indicates that no surface crusts were formed.

For stone cores, given the more marked microstructural alterations, and the fact that they were considered representative of the consolidated layer alone, distribution of alteration of total open porosity and of pore size distribution were evaluated to have preliminary indications about the treatment durability.

ES causes the highest reduction in total open porosity, especially in the surface layer, where total open porosity varies from 37.3% of untreated reference to 30.7%. HAP treatment leaves total open porosity substantially unaltered, but it causes some alterations in the pore range between 0.01 and 0.2 μm (modifications being more visible in surface layer).

Different opinions can be found in literature about the action that a consolidant should exert on substrate microstructure: some references indicate that a slight decrease in porosity and pore size would be recommended, as it is supposed to enhance stone durability [4,7,30]. In general, though, consolidants are required not to cause pore occlusion in order to enhance durability. In analogy with the case of mechanical properties, modifications are regarded as positive if they approach the conditions before weathering, as decay itself modifies stone microstructure, generally by increasing porosity and pore size. In the specific case, the artificial weathering procedure adopted did not substantially modify stone microstructure because cracks are expected to form at the nano-scale, thus altering stone mechanical properties but not the pore size distribution in the pore size range detectable by MIP [26], hence alterations in the MIP curves as limited as possible are considered a positive feature. From this point of view, both consolidants, bust mostly HAP, are considered compatible.

Regarding pore size distribution, alterations in the percentage of pores in the finer pore ranges were also evaluated (Table III.2) as they are crucial in the durability of stone against many deterioration

phenomena, such as salt crystallization and freeze-thaw cycles. For this reason, it is recommended [4] that increases in the fraction below 1 μm are as limited as possible. ES, despite causing higher reduction of total open porosity, does reduce the amount of pores below 1μm. This seems to indicate that ES does not penetrate smaller pores, which is in contrast with high increases obtained in dynamic elastic modulus. Further investigation of this aspect is currently in progress. HAP, instead, causes a slight increase in this fraction. However, regarding weathering caused by salt crystallization, that is the most relevant and severe degradation phenomenon for the given lithotype, it is known that crystallization pressure, that determines the extent of decay, increases as the pore radius decreases [7,30]. For this reason, attention should be focused on pores in the finest range, namely $r < 0.01$ μm that make the stone more susceptible than coarser pores: increases in this fraction need to be specifically evaluated. Both consolidants, and mostly ES, do, indeed, cause increase in this range (0.0% to 0.4% near the surface and to 0.1% at a depth of 5 mm, for HAP, from 0.0% to 0.7% near the surface and to 0.5% at a depth of 5 mm for ES): for this reason, specific evaluation of treated stone durability is needed. This topic will be discussed in detail in Chapter 4: "Treatment durability in comparison with ethyl silicate" [45].

Regarding physical properties, HAP treatment caused an increase in contact angle and absorption time (figure III.6 and Table III.6); however, samples remain hydrophilic ($\alpha<90°$). ES instead, causes hydrophobicity, as indicated by contact angle that is well above the 90° threshold and by time for absorption. Hydrophobicity of ES treated samples is caused by the presence of residual hydrophobic ethoxy groups (OC_2H_5) that are gradually converted into hydrophilic OH^- groups as hydrolysis-condensation reactions proceed. For this reason hydrophobicity caused by ES is only temporary, but might last several months because curing reaction are very slow, even when a catalyst is used, and might require up to 6-7 months to be complete (i.e. for ethoxy groups to be completely converted into OH groups) [46]. However, this temporary hydrophobicity can be removed by rinsing with water or water and ethanol solutions [13,46].

Consistently with data obtained for contact angle, the sorptivity test (figure III.7 and Table III.7) highlights a different behavior between samples treated by ES and HAP, the latter not causing significant alterations in water sorptivity and absorption. ES treated samples do not absorb water for the first 24 hours (see figure III.7), thus confirming their hydrophobicity. After 24 hours, however, a sharp increase in water absorption in registered so that final uptake is comparable to that of the untreated reference. The reason for this behavior is better detailed in [13]: briefly, conversion of ethoxy groups into hydroxyl groups occurs due to the reaction with water. Normally water for the curing comes from atmospheric moisture, thus reactions are very slow, but they might be accelerated by contact with liquid water. Of course contact with water must occur after a suitable

time, so that it does not cause consolidant displacement. For this reason, if a second sorptivity test is performed on the same samples, they exhibit hydrophilic behavior from the very start of the test.
As for microstructure, some authors suggest that reductions in water sorptivity and absorption might be desired, so that permeability to weathering agents is reduced, provided that water vapor permeability is not altered [2,4,7]. Moreover, consolidants with hydrophobic properties might be desired to combine consolidation and protection in a single treatment. However, some issues might arise connected to hydrophobicity: first, when a water source is present behind the treated layer (as in the case of the presence of condensation or rising moisture and mostly in presence of salts), moisture would be prevented from exiting the stone thus possibly leading to exfoliation. For this reason, the use of hydrophobic consolidants is discouraged in some conditions, for example in northern climates [8]. In addition, hydrophobicity makes it impossible to perform any cleaning, protective or repair treatment with water-based products after consolidation. For this reasons, many authors recommend that water transport properties remain unaltered [8,9,20].
All these limitation might be an issue for ES; moreover, it cannot be regarded as a protective, as it only provides short-term hydrophobicity, which would absolutely not be sufficient for a suitable protection of the stone. HAP, instead, keeps the stone hydrophilic, so it is more compatible. The possibility to accelerate ES curing reactions by contact with liquid water, however, was investigated during the PhD [13], as it is an important finding for consolidation by ethyl silicate allowing for faster curing and temporary hydrophobicity removal.
Both ES and HAP allowed for preserving water vapor permeability of the stone as can be seen by the fact that the water vapor diffusion resistance coefficient is maintained substantially unaltered (Table III.7). However, water vapor permeability of ES is a delicate task, as it is highly dependent on the specific product under examination: in fact, decreases of even 40% have been assessed in the literature [38].
When salt crystallization is considered, too high an evaporation rate might boost crystallization [8]. For this reason, the effective exchange of liquid moisture with the surrounding environment needs to be evaluated: this was addressed by determining drying behavior of samples (figure III.8). No significant changes in this parameter are caused by any of the treatments; however, if the test is performed after a shorter curing time of ES, much different values are obtained, hence indicating that drying behavior also depends on curing conditions of ES. This raises concerns about the behavior of ES-treated materials in the phases following the treatment, before curing is complete. For this reason, in the next chapter, devoted to investigating the durability of HAP and ES treated stone, ES-treated samples at short curing time (namely 7 days) were also evaluated.
Thermal expansion was evaluated (see figure III.9). It is generally required that consolidants do not

alter thermal expansion behavior, so that incompatibilities between untreated and treated parts of the stone are prevented, which could otherwise result into flaking and/or detachment [2,4,8]. In the present study, thermal behavior of ES samples remains substantially unaltered. In the case of HAP lower thermal expansion coefficient ($\alpha t = 1.6 \bullet 10^{-6}$ °C^{-1}) and higher residual strain (ε_{res} = -0.03 mm/m) are measured. Impact of these alterations was evaluated on the basis of literature data about thermal behavior of consolidated stone. Unfortunately no data are available for globigerina limestone, hence data concerning Carrara marble treated with ES and poly-methyl-methacrylate (PMMA) are taken into consideration [47]. Increases of 0.02 mm/m in residual strain obtained for PMMA were defined as "minor", while 0.04 mm/m obtained for ES were defined "large". Because marble is extremely susceptible to thermal weathering [48] while globigerina limestone is much less sensitive, the alterations suffered by HAP-treated globigerina limestone are expected to be less relevant than they would be on marble, hence alterations caused by HAP on GL will be considered minor.

However, further investigation of thermal behavior of treated samples will be performed due to the following considerations: a higher number of samples would probably be needed to evaluate reproducibility of the data. Tests on unheated samples (i.e. prior to artificial weathering by heating) would probably be much different, as the most significant weathering is experienced when a given temperature is reached for the first time [26,47].

Additional requirements

Ethyl silicate and hydroxyapatite, as all inorganic consolidants, are irreversible. Reversibility, despite being one of the fundamental requirements of restoration interventions, is generally never satisfied by stone consolidants and protectives, except for some acrylic resins that are expected to be removable by their solvent. Even in this case, however, removal can cause serious damage, or might be impeded by product alterations caused by interaction with the environment and hence decay. For this reason, this requirement is generally substituted by that of retreatability.

HAP and ES are both retreatable. In particular, HAP does not occlude pores, hence allowing application of subsequent treatments, with either the same or with different consolidants. In fact, double applications of the consolidant and HAP+ES treatments have been investigated, both allowing for improved efficacy [46].

ES treatment, provided that a sufficient time is allowed for temporary hydrophobicity to be lost, can be treated with other consolidants, as no complete pore occlusion is caused by the treatment.

Another important parameter to be evaluated is the impact of the products on human health and on the environment, that is to say that no harmful byproducts for either humans or the environment

should be released by stone consolidants [8,28].

DAP solution is water based, hence toxicity possibly arising because of the use of solvents is not a concern. Byproducts originating from the reaction i.e. ammonium carbonate, carbonium dioxide and water are also harmless for the operator and from an environmental point of view. According to DAP MSDS, some risks connected to the use of DAP, such as irritation to skin, eyes or breathing apparatus are to be taken into consideration. However, no exposure limitations are established for the operators as proper personal protective equipment is considered sufficient to safely handle the product.

Ethyl silicate itself has low toxicity and volatility. Both silica gel and the reaction byproduct, namely ethanol, are nontoxic and not environmentally hazardous [49]. However, in contrast to HAP, it is normally applied in a volatile organic solvent, generally white spirit, that can pose a hazard to human health and the environment. The solvent, moreover, is generally present in quite high concentration (20-25%), hence today solvent-free commercial products are available [8], that however present reduced efficacy.

For this reason, to limit the production of VOCs, consolidant in aqueous solution have to be preferred, as in the case of the HAP-treatment.

III.5 Conclusions

In this study, efficacy and compatibility of the novel HAP-based treatment were discussed, and retreatability and non-toxicity of the treatment briefly evaluated on the basis of literature data. The following conclusions can be derived.

As for *efficacy*, both treatments result in satisfactory penetration depth and uniform distribution inside the stone. Mechanical properties are highly improved, especially in the case of ethyl silicate. However, in the case of ES, final mechanical properties are much higher than those of the unweathered stone, thus raising some concerns about possible mismatches between treated and untreated area. The shorter curing time is definitely one of the advantages of HAP-based treatment even though two treatments, instead of one, are necessary.

Regarding *compatibility*, no significant aesthetic alterations were caused by any of the treatments and no byproducts were detected. Microstructural alterations were quite limited, mostly in the case of HAP. However, both treatments, mostly ES, cause slight increase in the amount of pores in the finer fractions, hence making specific evaluation of treatment durability necessary. None of the treatments causes significant decrease in water sorptivity; however, ES causes temporary hydrophobicity that can be regarded as one of the main drawbacks of the consolidant. Water vapor

permeability and drying rate are also unaltered at the end of curing. Given all these consideration it seems that HAP can be regarded as more compatible than ES.

Gradual variations in all of the measured properties indicate that no surface clogging layers were formed, but a gradient in the properties between untreated and treated layer was obtained.

Acknowledgements

Dr. Grazia Totaro (Department of Civil, Chemical, Environmental and Materials Engineering, University of Bologna, Italy) is gratefully acknowledged for collaboration on FT-IR analyses. Dr. Eugenia Rastelli and Dr. Paolo Malavasi (Centro Ceramico, Bologna, Italy) are gratefully acknowledged for spectrophotometric and dilatometric analyses. M.Eng. Eufemia Papacharissis is gratefully acknowledged for collaboration on stone characterization.

Chapter references

[1] Sassoni E., Graziani G., Franzoni E., An innovative phosphate-based consolidant for limestone. Part 1: Effectiveness and compatibility in comparison with ethyl silicate. Constr Build Mater 102 (2016) 918-930

[2] Amoroso G., Fassina V., Stone decay and conservation. New York: Elsevier; 1983.

[3] Lazzarini L., Laurenzi Tabasso M., Il restauro della pietra. Padua: CEDAM; 1986.

[4] Italian Recommendation NORMAL 20/85. Conservazione dei materiali lapidei: Manutenzione ordinaria e straordinaria, Istituto Centrale per il Restauro (ICR), Rome; 1985.

[5] Van Balen K., Papayanni I., Van Hees R., Binda L., Waldum A., Introduction to requirements for and functions and properties of repair mortars. Mater Struct 38 (2005) 781–5.

[6] Cnudde V., Cnudde J.P., Dupuis C., Jacobs PJS., X-ray micro-CT for the localization of water repellents and consolidants inside natural building stones. Mater Charact 53 (2004) 259-71.

[7] Maravelaki-Kalaitzaki P., Kallithrakas-Kontos N., Korakaki D., Agioutantis Z., Maurigiannakis S., Evaluation of silicon-based strengthening agents on porous limestones. Prog Org Coat 57 (2006) 140–8.

[8] Scherer G.W., Wheeler G., Silicate consolidants for stone. Key Eng Mater 391 (2009) 1–25.

[9] Baglioni P., Chelazzi D., Giorgi R., Carretti E., Toccafondi N., Jaidar Y., Commercial $Ca(OH)_2$ nanoparticles for the consolidation of immovable works of art. Appl Phys A 114 (2004) 723–32

[10] Wheeler G., Alkoxysilanes and the consolidation of stone. Los Angeles: The Getty Conservation Institute; 2005.

[11] Commission 25-PEM Protection et Erosion des Monuments. Recommended tests to measure the deterioration of stone and to assess the effectiveness of treatment methods. Mater Struct 13 (1980) 175–253.

[12] Ferreira Pinto A.P., Delgado Rodrigues J., Consolidation of carbonate stones: influence of treatment procedures on the strengthening action of consolidants. J Cult Herit 13 (2012) 154–66.

[13] Franzoni E., Graziani G., Sassoni E., TEOS-based treatments for stone consolidation: acceleration of hydrolysis-condensation reactions by poulticing, J Sol-Gel Sci Tech 74 (2015) 398-405

[14] Franzoni E., Graziani G., Sassoni E., Bacilieri G., Griffa M., Lura P., Solvent-based ES consolidant

for stone: influence of the application technique on penetration depth, efficacy and pore occlusion. Mater Struct 48 (2015): 3503-3515

[15] Ferreira Pinto A.P., Delgado Rodriguez J., Stone consolidation: the role oftreatment procedures. J Cult Herit 9 (2008) 38–53.

[16] Leroux L., Vergès-Belmin V., Costa D., Delgado Rodrigues J., Tiano P., Snethlage R., Singer B., Massey S., De Wi E., Measuring the penetration depth of consolidating products: Comparison of six methods. Proceedings of the IX International Congress on the Deterioration and Conservation of Stone, Venice, vol. 2, June 19–24; 2000, 361–370.

[17] Zendri E., Biscontin G., Nardini I., Riato S., Characterization and reactivity of silicatic consolidants. Constr Build Mater 21 (2007) 1098–106.

[18] Delgado Rodrigues J., Grossi A., Indicators and ratings for the compatibility assessment of conservation actions. J Cult Herit 8 (2007) 32–43.

[19] Drdàcky´ M., Lesàk J., Rescic S., Slìzˇkovà Z., Tiano P., Valach J., Standardization of peeling tests for assessing the cohesion and consolidation characteristics of historic stone surfaces. Mater Struct 45 (2012) 505–52.

[20] Sassoni E., Franzoni E., Pigino B., Scherer G.W., Naidu S., Consolidation of calcareous and siliceous sandstones by hydroxyapatite: comparison with a ES based consolidant. J Cult Herit 14S (2013) e103–8.

[21] Luque A., Ruiz-Agudo E., Cultrone G., Sebastiàn E., Siegesmund S., Direct observation of microcrack development in marble caused by thermal weathering. Environ Earth Sci 62 (2011) 1375–86.

[22] Weiss T., Rasolofosaon PNJ, Siegesmund S., Ultrasonic wave velocities as a diagnostic tool for the quality assessment of marble. In: Siegesmund S., Weiss T., Vollbrecht A., editors. Natural stone, weathering phenomena, conservation strategies and case studies, Geological Society, London, Special Publications, 205 (2002) 149–164.

[23] Malaga-Starzec K., Åkesson U., Lindqvist J.E., Schouenborg B., Microscopic and macroscopic characterization of the porosity of marble as a function of temperature and impregnation. Constr Build Mater 20 (2006) 939–47.

[24] Sassoni E., Naidu S., Scherer G.W., The use of hydroxyapatite as a new inorganic consolidant for damaged carbonate stones. J Cult Herit 12 (2011) 346–55.

[25] Skoulikidis T., Vassiliou P., Tsakona K., Surface consolidation of pentelic marble – criteria for the selection of methods and materials – the acropolis case. Environ Sci Pollut Res 12(2005) 28–33.

[26] Sassoni E, Franzoni E. Influence of porosity on artificial deterioration of marble and limestone by heating. Appl Phys A Mater 115 (2014) 809–16.

[27] Moropoulou A., Kouloumbi N., Haralampopoulos G., Konstanti A., Michailidis P., Criteria and methodology for the evaluation of conservation interventions on treated porous stone susceptible to salt decay. Prog Org Coat 48 (2003) 259–70.

[28] Miliani C., Velo-Simpson M.L., Scherer G.W., Particle-modified consolidants: a study on the effect

of particles on sol–gel properties and consolidation effectiveness. J Cult Herit 8 (2007) 1–6.

[29] Lòpez-Arce P., Gomez-Villalba L.S., Pinho L., Fernàndez-Valle M.E., Álvarez de Buergo M., Fort R., Influence of porosity and relative humidityon consolidation of dolostone with calcium hydroxide nanoparticles: effectiveness assessment with non-destructive techniques. Mater Charact 61 (2010) 168–84.

[30] Scherer G.W., Stress from crystallization of salt. Cem Concr Res 34 (2004) 1613–24.

[31] Franzoni E, Sassoni E, Scherer GW, Naidu S. Artificial weathering of stone by heating. J Cult Herit 14S (2013) e85–93.

[32] Sandrolini F., Franzoni E., Cuppini G., Predictive diagnostics for decayed ashlars substitution in architectural restoration in Malta. Mater Eng 11 (2000) 323–37.

[33] European Standard EN 15801. Conservation of cultural property – test methods – determination of water absorption by capillarity; 2010.

[34] European Standard EN 15803. Conservation of cultural property – test methods – determination of water vapor permeability (dp); 2010.

[35] Koutsopoulos S., Synthesis and characterization of hydroxyapatite crystals: a review study on the analytical methods. J Biomed Mater Res 62 (2002) 600–12.

[36] Rubio F., Rubio J., Oteo J.L., A FT-IR study of the hydrolysis of tetraethylortosilicate [ES]. Spectrosc Lett 3 (1998) 199–219.

[37] Gräf V., Jamek M., Rohatsch A., Tschegg E., Effects of thermal-heating cycle treatment on thermal expansion behavior of different building stones. Int J Rock Mech Min Sci 64 (2013) 228–35.

[38] Maravelaki-Kalaitzaki P, Kallithrakas-Kontos N, Agioutantis Z, Maurigiannakis S, Korakaki D. A comparative study of porous limestones treated with silicon-based strengthening agents. Prog Org Coat 62 (2008) 49–60.

[39] Lubelli B, van Hees RPJ, Nijland TG, Bolhuis J. A new method for making artificially weathered stone specimens for testing of conservation treatments, J Cult Herit; 205. doi: 10.1016/j.culher.2015.01.002.

[40] Franzoni E., Sassoni E., Graziani G., Brushing, poultice or immersion? Role of the application technique on the performance of a novel hydroxyapatite-based consolidating treatment for limestone. J Cult Herit 16 (2015) 173–84.

[41] Maravelaki-Kalaitzaki P., Black crusts and patinas on Pentelic marble from the Parthenon and Erecteum (Acropolis, Athens): characterization and origin. Anal Chim Acta 532 (2005) 187–98.

[42] Giusti A., La competenza umanistica. In: Tiano P., Pardini C., editors. Le patine – Genesi, significato, conservazione, Proceedings of the Workshop ‘‘Le patine – Genesi, significato, conservazione’’, 4–5 May 2004, Florence, Italy, Nardini Editore, Florence; 2005, p. 77–82.

[43] Dorozhkin SV. Calcium orthophosphates. Biomatter 11 (2011) 121–64.

[44] Naidu S., Scherer G.W., Nucleation, growth and evolution of calcium phosphate films on calcite. J Colloidal Interface Sci 435 (2014) 128–37.

[45] Sassoni E., Graziani G., Franzoni E., An innovative phosphate-based consolidant for limestone. Part 2. Durability in comparison with ethyl silicate. Constr Build Mater 102 (2016) 931-42

[46] Naidu S., Liu C., Scherer G.W., New techniques in limestone consolidation: Hydroxyapatite based consolidant and the acceleration of hydrolysis of silicate-based consolidants, J Cult Herit 16 (2015) 94-101

[47] Ruedrich J., Weiss T., Siegesmund S., Thermal behavior of weathered and consolidated marbles. In: Siegesmund S., Weiss T., Vollbrecht A., editors. Natural stone, weathering phenomena, conservation strategies and case studies, Geological Society, London, Special Publications 205 (2002) 255–271.

[48] Siegesmund S., Ullemeyer K., Weiss T., Tschegg E.K., Physical weathering of marbles caused by anisotropic thermal expansion. Int J Earth Sci 89 (2000) 170–82.

[49] Moropoulou A., Kouloumbi N., Haralampopoulos G., Konstanti A., Michailidis P., Criteria and methodology for the evaluation of conservation interventions on treated porous stone susceptible to salt decay. Prog Org Coat 48 (2003) 259–70.

Chapter IV: HAP treatment durability, in comparison with ethyl silicate

In this chapter, durability of the novel HAP-based treatment was systematically evaluated and compared to that of an ethyl silicate-based treatment. Prior to the evaluation, the most severe weathering actions for the stone were determined and the criteria for the evaluation of the durability of a consolidant were discussed.

IV.1. Introduction

In the previous chapter, efficacy and compatibility of HAP based treatment were discussed and evaluated, in comparison with those of an ethyl silicate based treatment [1]. Preliminary literature investigation of retreatability and non toxicity were also carried out.

Results indicated that HAP treatment exhibits remarkable efficacy and compatibility, and it is able to overcome some of the most relevant drawbacks of ethyl silicate, namely long time needed for curing and temporary hydrophobicity, thus possibly being an even more promising option for limestone consolidation.

However, when evaluating the performance of a consolidant, durability is also a key requirement to be evaluated [2]. Durability consists in the consolidant capability of not losing efficacy and not suffering nor causing alterations that could cause harm to the stone, as a result of interactions with the environment and hence decay [3]. That is to say the consolidant itself should not experience damage nor should it cause it to the treated substrate nor enhance its susceptibility to decay. Durability is also linked to the other requirements: for example, efficacy in enhancing stone mechanical properties might enhance resistance to weathering, while lack of compatibility between the treated and untreated part of the stone would be extremely critical for durability. The requirement of durability is made even more important by the fact that consolidation has to be considered a non-reversible operation [4], thus possible issues arising from poor durability would generally not be reversible either. For this reason, retreatability is of paramount importance [5,6].

The evaluation of durability is particularly complicated because of the following conditions:

- weathering depends on exposure and on environmental conditions in which the substrate is placed [2];
- weathering phenomena, morphology and extent also strongly depend on the substrate. In fact, different substrates exhibit completely different susceptibility to the same weathering agents as well as different weathering types. For example, dissolution in acidic rain and thermal weathering are the most relevant actions that cause decay in marble [7,8], while they are much less relevant for other lithotypes, including porous limestone. On the other hand, freeze-thaw cycles and salt crystallization

are the most relevant decay phenomena that cause decay in porous limestone [9-13], while their effect is much less relevant in marble. Again, hygric dilatation and wet/dry cycles might be a severe issue for clay bearing stones [14] as they might cause swelling of clays, while it is obviously not in the case of stones that do not contain clays;

- given a specific lithotype, the level of weathering also depends on the characteristic of the specific stone under exam, namely microstructure, mechanical properties, specific composition. These characteristics, in turn, can be modified to various extents by decay. Each weathering condition is influenced to a higher or lower extent by each of the stone characteristics; for example, decay due to salt crystallization is sensibly affected by stone tensile strength and microstructure [6,11,15].

First, the weathering phenomena potentially critical for limestone durability were examined: freezing-thawing, salt crystallization and wetting-drying cycles were selected. Wetting-drying cycles, in the case of HAP-treatment, also allowed to evaluate the behavior of possible soluble phases originating from the treatment [16]. In the previous chapters no soluble phases were detected by dedicate analyses; however, the exact discrimination between different calcium phosphate phases is complicated as spectra (both XRD and FT-IR) of different CaP phases can be very similar, and a strong signal coming from the substrate might overlap and hide some relevant bands or peaks, thus making some phases non identifiable. Moreover, formation of metastable phases of low solubility, such as OCP, though being less favorable than formation of HAP, would not necessarily hamper treatment success [1,17,18]. Dissolution, instead, would be indicative of formation of highly soluble metastable phases.

After the definition of the relevant weathering actions, the procedure to be followed for artificial weathering of the samples, as well as the parameters to take into account to evaluate their effects were identified.

Different national and international standards are available to perform and evaluate artificial weathering: among the others, European EN 12371 [19] and Italian UNI 11186 [20] for freezing–thawing test, European EN 12370 [21], RILEM MS-A.1 [22] and RILEM MS-A.2 [23] for salt weathering test. Moreover, several tests have been proposed in the literature for the same goal, as the procedures indicated by the standards are generally considered not completely satisfactory [24].

Briefly, the different procedures generally differ for either experimental conditions (regarding specimen type, immersion and drying conditions, temperature and duration of each part of the cycles, duration of the cycles, salt type and saline solution concentration if used) and evaluation of the weathering [25]. For the latter, visual inspection, measurement of weight, dynamic elastic modulus, tensile strength and evaluation of microstructure are proposed [25]. Experimental conditions are particularly relevant as they determine the extent of decay that is caused and hence

the representativeness of the results [25].

After selection of weathering actions and of the procedures to be followed for performing the cycles and evaluating their effects, durability of HAP-treated samples was systematically evaluated, in comparison with untreated and ES-treated globigerina limestone.

IV.2. Materials and Methods

IV.2.1. Materials

All tests were carried out on Globigerina Limestone, as in the previous chapters.

Cylindrical samples (5 cm height, 2 cm diameter), cubic samples (5 cm side) and prismatic samples (7 x 7 x 2.5 cm^3) were obtained from one same slab so as to mitigate possible heterogeneity of the stone. All samples were artificially weathered by heating prior to the tests, as recommended by Italian Recommendation NORMAL 20/85 for testing of consolidants [4] and by the literature when concerning evaluation of durability of consolidants to salt crystallization [25].

IV.2.2. Methods

Treatments were performed as described in the previous chapters. Stone cores were treated on the whole surface, so as to evaluate the behavior of the consolidated layer alone, while cubic and prismatic samples were treated on one face to investigate the interface between consolidated and unconsolidated parts and incompatibilities that might arise from their coupling [1,26].

HAP-based treatment consisted in two steps: application by brushing of a 3M DAP solution (10 brush strokes) followed by application of a limewater poultice (as in figure IV.1).

In the case of ES, one commercial product (Estel 1000, CTS, Italy) was applied by brushing (10 brush strokes, as for HAP). Samples were left to cure for 4 weeks in laboratory conditions (T = 20 ± 2 °C, RH = 50 ± 5%) as recommended by technical data sheets. As detailed in Chapter III, after 4 weeks curing, ES-treated samples still exhibit marked hydrophobicity, that persists until curing reactions are complete (which might require 6-7 months) [1,6,27,28]. Hydrophobic behavior completely alters or even impedes water, as well as saline solution, uptake, thus making it impossible to evaluate the effects of artificial weathering cycles for comparison with HAP. For this reason, after curing, hydrophobicity was removed by a methodology purposely developed during the PhD thesis [28]. This method consists in applying a water poultice (water: dry poultice weight ratio 5:1) that is left reacting for 4 days while wrapped (figure IV.1). Application time was set on the basis of sorptivity curves registered for ES cured samples: a time suitable for completely removing hydrophobicity was chosen. The aim is that of providing liquid water that can react with ethoxy groups so as to allow hydrolysis and their conversion in hydroxyl groups. The efficacy of

the proposed methodology was evaluated in detail, results being reported in [28]. Of course samples were dried before being subjected to the cycles. This way it was possible to simulate the behavior of hydrophilic ES treated samples after long time curing.

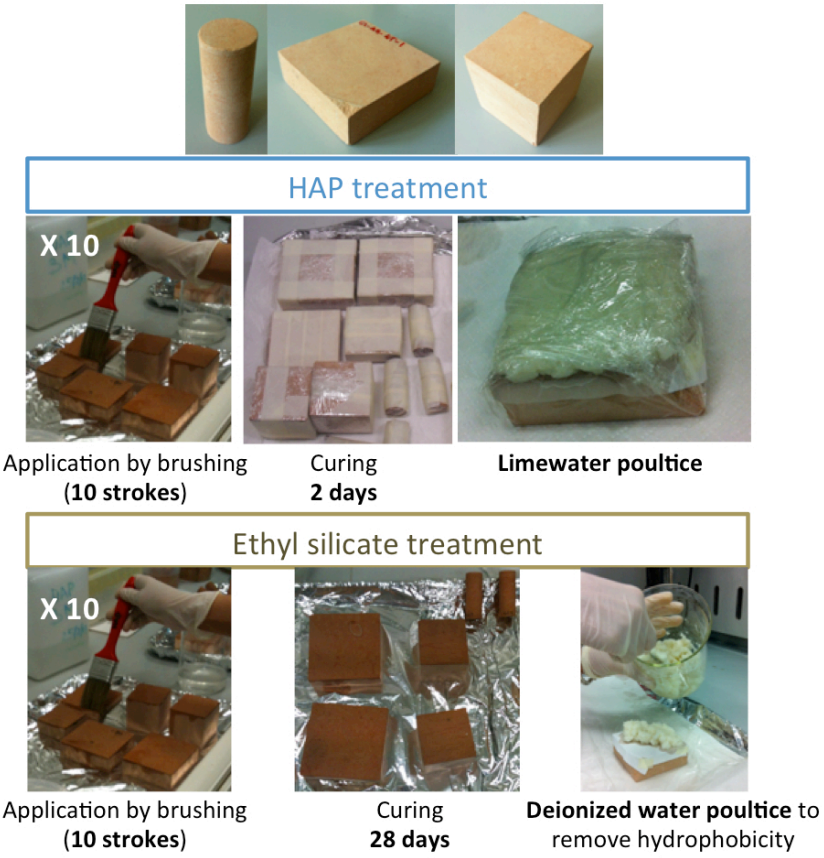

Figure IV.1: Treating procedures scheme

Temporary hydrophobicity, however, might cause severe issues in terms of durability [6,29,30]: for this reason short time curing was also taken into consideration and a set of ES treated samples were subjected to the cycles after only 7 days curing.

IV.2.3. Accelerated weathering cycles

All treatment and weathering conditions as well as relevant labeling are summarized in Table IV.1.

Treatments	**Weathering conditions**			
	Unweathered (UW)	Wetting-drying cycles	Freezing-thawing cycles	Salt weathering cycles
Untreated	UT-UW	UT-WD	UT-FT	UT-SW
HAP-treated	HAP-UW	HAP-WD	HAP-FT	HAP-SW
ES-treated	ES-UW	ES-WD	ES-FT	WS-SW

Table IV.1: Treating and weathering conditions overview and labeling of relevant samples.

For each condition 6 cores and 2 prisms were tested. For salt weathering cycles, 8 cores were examined because more tests were performed.

The methodology used for the cycles and the characterization techniques for assessment of damage are described in the following:

Seven *wetting-drying cycles (WD)* were performed, consisting in 3 phases:

- partial immersion (about 5 mm) in deionized water until the wet fringe reaches the top of the samples (1h);
- complete submersion in water. Total time from immersion start 24h;
- oven-drying at 50°C for 24 h.

Samples were characterized by visual inspection of the damage and by measuring weight change and dynamic elastic modulus at each cycle. For HAP treated samples, IC was performed on water used at each cycle to detect possible presence of soluble phosphates, indicating dissolution of soluble phases. Tensile strength was measured at the end of the cycles.

Seventy *Freezing–thawing (FT)* cycles were performed, following a procedure adapted from a combination of Italian Standard UNI 11186 [20] and European Standard EN 12371 [19]. The number of cycles was chosen as it was sufficient to highlight significant differences between the 2 consolidants. Standards recommend ‘‘all-directional freezing” that simulates the condition usually suffered by freestanding objects and statues, but in the case of buildings ‘‘one-directional freezing” generally occurs. However, the procedure suggested by the standards was followed for simplicity.

Samples were saturated in deionized water (as for wet/dry cycles, by partial immersion in 5 mm deionized water until the wet-fringe reaches the top of the samples then by total immersion for 72h after the beginning of immersion), then cycles were performed, consisting in:

- 2h freezing in air at -20± 2°C
- 2h thawing in water at 20 ± 2° C.

Three cycles per day were performed, interruption of the cycles (overnight) was always during thawing phase in water.

Every 10 cycles, samples were oven-dried so that visual inspection, weight and dynamic elastic modulus determination could be performed. As for wetting-drying cycles, tensile strength was measured at the end of the tests.

Salt weathering cycles (SW) were performed by using a sodium sulfate solution. This salt was chosen as it causes the most severe decay among those relevant for weathering of building materials and hence is widely used for accelerated weathering tests [25,31,32].

The severe action of sodium sulfate is due to the transition between the anhydrous phase (thenardite, Na_2SO_4) and the decahydrate phase (mirabilite $Na_2SO_4 \bullet 10H_2O$), that occurs with a volume expansion of 314% [32]. Concentration of the solution was 14 wt.% in deionized water.

The testing scheme is described in figure IV.2.

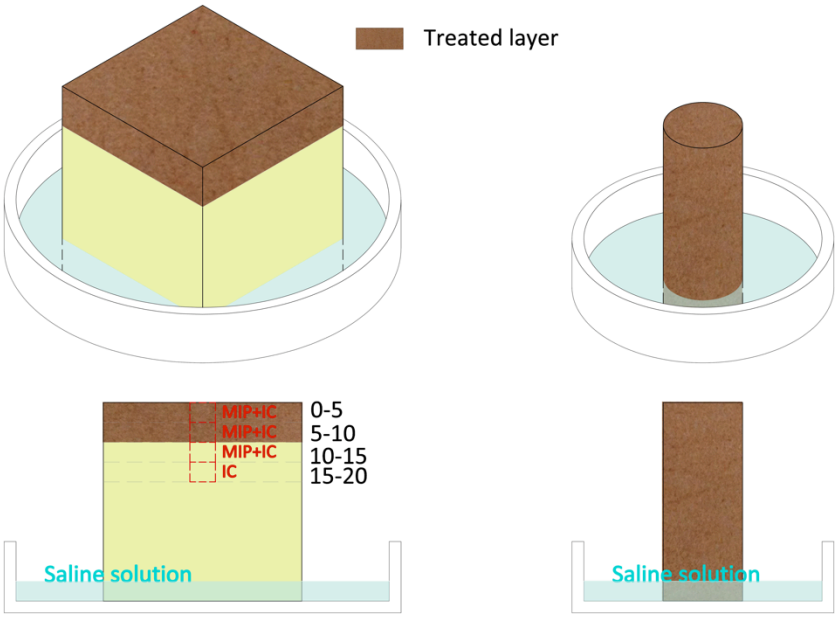

Figure IV.2: Testing setup scheme. The sampling position for IC and MIP were also indicated for cubic samples.

A procedure for artificial weathering by salt crystallization is described in the European Standard EN 12370 [21]; however, differently from the standard, partial immersion (in about 5 mm solution) was preferred to complete immersion as suggested in [24]. In fact, partial immersion prevents formation of air bubbles, hence resulting in a higher saturation of the samples, so the test is more severe, and is closer to the real conditions on site. To resemble conditions in the field, solution was left to penetrate the samples through the face opposite to the treated one and evaporate through the treated one, as would occur on site for a consolidated wall, where saline solution enters the stone from behind the consolidated facade and leaves through consolidated face (either as liquid or vapor) [25].

SW cycles were performed as follows:

- 24h partial immersion in saline solution;
- 22h drying at 50°C;
- 2h cooling at room temperature.

After each cycle, samples were visually inspected and weight change and dynamic elastic modulus were measured.

In the case of stone cores, after 5 cycles, half of the samples (4) were subjected to the following tests: one sample was used for mercury intrusion porosimetry without removing salts, while the other 3 were desalinated to evaluate dynamic elastic modulus and weight change without the pore-clogging effect of salts, that might be misleading. Then, tensile strength was determined on desalinated samples and their microstructure was evaluated by MIP so as to detect formation of

micro-cracks due to the action of salts.

Five cycles were chosen so as to cause significant decay without causing rupture or too severe surface deterioration that would impede mechanical characterization.

Desalination was performed by gently brushing the surface to remove efflorescence and subsequently applying a deionized water poultice that was kept wrapped for 24 h to allow for salt solubilization, then left to dry in contact with the samples. The effectiveness of water poultice in removing salts was evaluated by IC, by comparing salt amount (mainly sulfates, i.e. those intentionally added by the cycles) in desalinated and non-desalinated samples.

For both desalinated and non-desalinated samples, MIP was performed on specimens taken from the top of the sample. In the case of non-desalinated samples, the area affected by efflorescence was excluded.

The rest of the non-desalinated samples were subjected to 5 additional SW cycles (so that total number of samples was 10). As for the first 5 cycles, weight and dynamic elastic modulus were monitored at each cycle. Additional cycles were performed to cause more severe damage and hence better highlight the differences between the treatments. Measurement of tensile strength at the end of the 10 cycles was impossible as weathering was too severe and had compromised the surface integrity of samples.

As for cubic samples, specimens were collected after the 5th cycle at different depths from the treated surface, and subjected to MIP and IC, see figure IV.2. The aim of the tests was to determine whether salt accumulation would occur behind the treated surface. MIP was performed on two samples for each depth, obtained by chisel, one of which was desalinated according to the procedure described above. Sampling positions for IC were the same as for MIP but, of course, only one non-desalinated sample was examined.

As mentioned before, for ES also a “highly hydrophobic” short time curing condition (7 days) was taken into consideration: this condition was tested on prismatic specimens, without performing any accelerated curing procedure. Those samples were subjected to SW cycles performed exactly as for the cubes. By letting saline solution penetrate the samples from the face opposite to the treated one, durability issues connected to the impossibility of saline solution escapjng through the treated layer could be assessed. To better understand this phenomenon, lateral faces of the sample were sealed with water- and water vapor-proof tape.

IV.2.4. Evaluation of the effects of accelerated weathering cycles

The effects of all accelerated weathering cycles were evaluated as described below.

In particular visual assessment of the damage, measurement of weight change and dynamic elastic

modulus were carried out at each cycle, as recommended, among the others, in [9,30,31].

Weight change should provide an indication of detachment and/or pulverization of material, as well as dissolution of soluble phases. Its interpretation, however, can be complicated in the case of SW cycles, where weight decrease due to loss of parts of the samples is partially counterbalanced by salt accumulation [25], thus making it necessary to perform desalinization to analyze the contributions of the two phenomena.

Dynamic elastic modulus is a very useful tool as it can be measured by a non-destructive test [33] and it can be performed on the same samples at different cycles. Moreover, it allows for an accurate indication of micro-cracks even when samples appear undamaged [9,10,15,31]. However, also in this case, accumulation of salts in the pores can make the results hard to interpret, as their effect is that of clogging the pores, hence possibly increasing dynamic elastic modulus and counterbalancing the effect of salt weathering [25]. For this reason, desalination is advisable so as to evaluate the effect of both salt accumulation and damage caused by salt crystallization. As in the previous chapters, dynamic elastic modulus was measured on cylindrical samples using a Matest instrument with 55 kHz transducers [1].

Tensile strength reveals the effects of micro-cracks (FT and SW cycles) as well as dissolution of soluble fractions (WD cycles). This is a key parameter because it allows for an exact determination of the damage cause by the cycles, and also because weathering due to FT and SW cycles occurs when crystallization pressure exceeds tensile strength of the material; hence residual tensile strength gives a measure of residual resistance to these stresses [6,11]. It was measured by Brazilian splitting test, using an Amsler-Wolpert loading machine (constant displacement rate 4 mm/min). In contrast to E_d, tensile strength is measured by means of a destructive test, so its determination was possible only at the end of the cycles.

Mercury intrusion porosimetry was performed after FT and SW cycles. In the case of SW tests, both non-desalinated and desalinated samples were tested, so as to evaluate both the pore clogging effect of salts and the decay that they cause (opening of micro-cracks). MIP was performed by a Fisons Macropore Unit 120 and a Porosimeter 2000 Carlo Erba instruments. In the tests on salt-contamined samples, a mercury-sample contact angle of 141.3° was assumed, thus neglecting the possible differences in contact angle that may arise when the sample is contaminated with salts [34]. The variation in contact angle in presence of salts might be worth further investigating.

As for WD cycles, dissolution of possible soluble phases was investigated by analyzing the water of the cycles by IC (Dionex ICS 1000 ion chromatographer). The same technique was used for determination of sulfate content prior to and after desalination in the relevant tests. In this case, prior to IC, salt extraction was performed on ground samples by boiling in deionized water and

filtering.

IV.3 Results [2]

IV.3.1. Sample characterization prior to artificial weathering

The effects of the two consolidating treatments were evaluated in terms of mechanical properties (Table IV.2) and alterations in stone microstructure (figure IV.3).

Treatments	**Weathering conditions**			
	Unweathered (UW)	Wetting-drying cycles (WD)	Freezing-thawing cycles (FT)	Salt weathering cycles (SW)
Dynamic elastic modulus Ed [GPA]				
Untreated	12.5 (±0.7)	12.1 (±0.9)	11.8 (±1.0)	11.1 (±0.7)
HAP-treated	16.4 (±0.3)	16.0 (±0.2)	15.5 (±0.3)	17.2 (±0.2)
ES-treated	18.9 (±0.4)	17.6 (±0.6)	14.4 (±0.4)	16.3 (±0.5)
Tensile strength σ_T [MPa]				
Untreated	2.53 (±0.12)	2.53 (±0.31)	2.66 (±0.09)	-
HAP-treated	3.48 (±0.32)	3.79 (±0.37)	3.27 (±0.44)	2.94 (±0.31)
ES-treated	5.56 (±0.16)	4.92 (±0.48)	4.59 (±0.26)	3.23 (±0.34)

Table IV.2: Dynamic elastic modulus and tensile strength in untreated and treated samples, before and after accelerated weathering. In Table, values for salt crystallization cycles refer to samples tested after 5 cycles and desalinated. Tensile strength values for untreated sample after SW cycles are not available, as the test could not be performed due to excessive surface damage

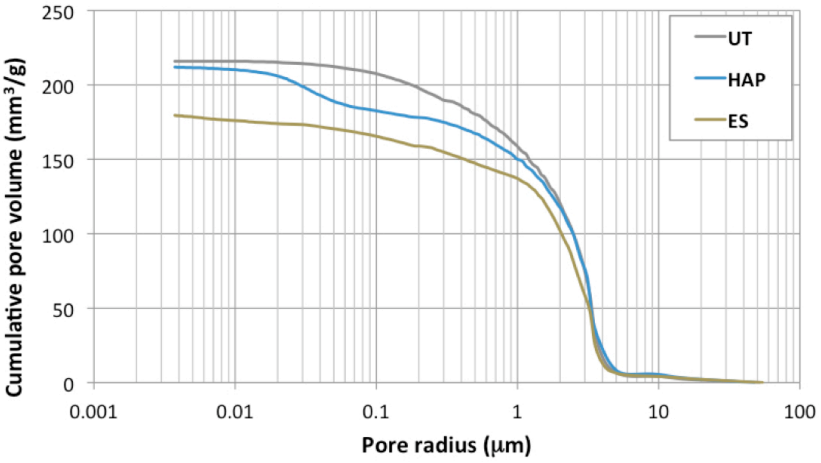

	Pores distribution[%]			
	< 0,01 µm	0,01÷0,1 µm	0,1÷1 µm	> 1 µm
UT	0.0	3.9	22.6	73.5
HAP	0.8	13.1	15.4	70.8
ES	2.0	5.9	15.8	76.4

Figure IV.3: Microstructural modifications as a result of ES and HAP treatments, for UW samples

Stone physical properties before and after treatment are reported in figure IV.4. In figure, ES treated samples had been subjected to accelerated curing by water poultice so as to remove hydrophobicity.

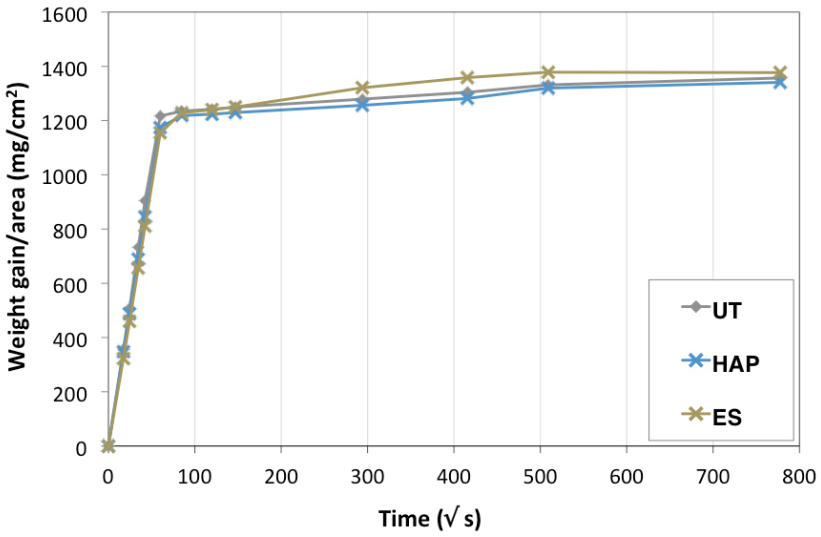

Figure IV.4: Water transport properties of untreated and treated samples (unweathered)

IV.3.1 Wet/dry cycles

Alterations in samples weight and dynamic elastic modulus as a result of WD cycles are illustrated in figure IV.5, while tensile strength after 7 WD cycles is reported in Table IV.2.

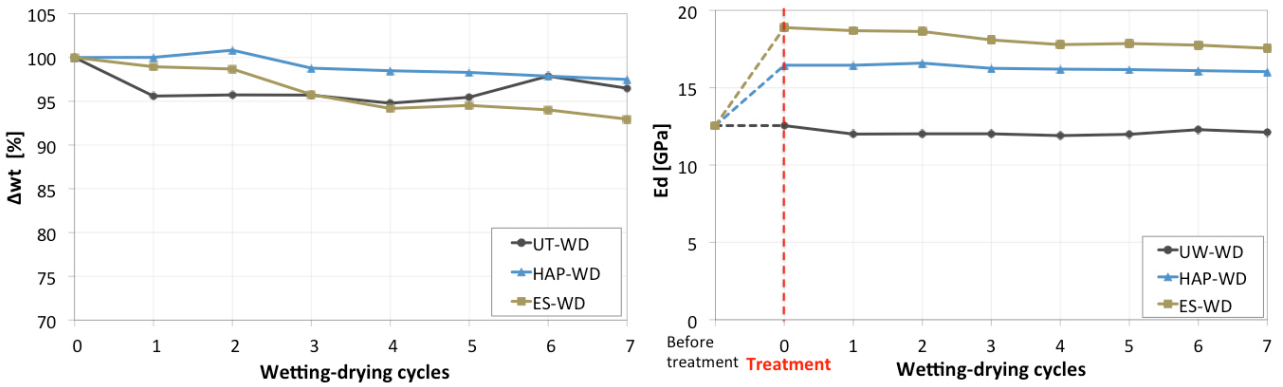

Figure IV.5: Weight change and dynamic elastic modulus at each wet/dry cycle. Results were obtained on cylindrical samples.

Untreated samples do not experience major alterations in dynamic elastic modulus. Slight modifications registered can be attributed to experimental variability; in fact final values are very close to those before weathering (E_d decrease 4%). Correspondingly, tensile strength remains unaltered.

Also HAP-treated samples exhibit negligible alterations in all the parameters investigated: actually a slight increase is registered in tensile strength ($\Delta\sigma_t$ = +8%), that falls within natural stone

variability, as suggested by σ_t standard deviations. Results of IC on the water used for the cycles indicate negligible amounts of soluble phosphates (≈3 ppm, lower than the 4 ppm amount of sulfates present in the substrate prior to any weathering cycle, extracted by using the same amount of sample and water).

ES-treated samples, instead, suffer a decrease in both weight and dynamic elastic value and a final $\Delta\sigma_t$ of 11%.

IV.3.2 Freeze-thaw cycles

Behavior of the consolidated layer, as evaluated in stone cores, is reported in the following. Sample weight and dynamic elastic modulus at each cycle are reported in figure IV.6 and Table IV.2, while tensile strength at the end of the cycles is in Table IV.2.

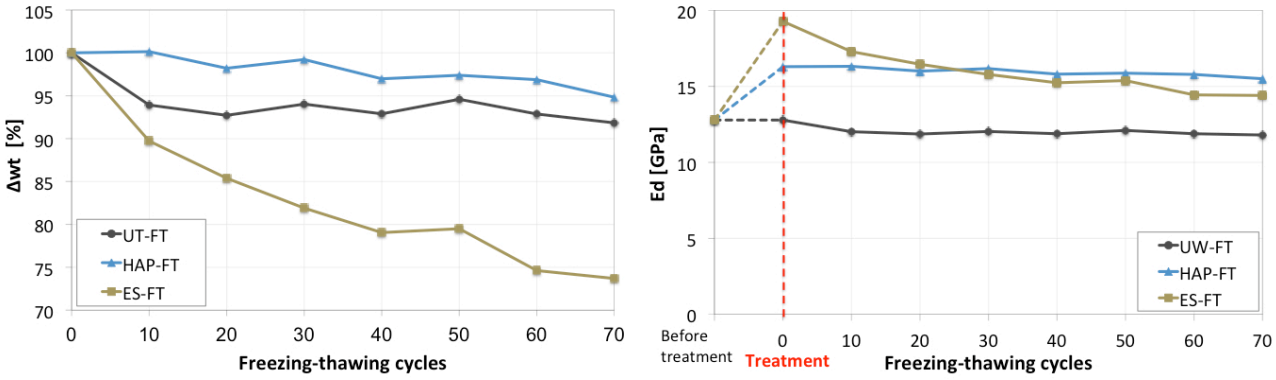

Figure IV.6: Weight change and dynamic elastic modulus at each FT cycle.

Untreated samples are not dramatically affected by the cycles, as a final $\Delta\sigma_t$ = +5% was registered, which can again be ascribed to the natural stone variability.

After 47 cycles, one ES sample experienced rupture and one sample adjacent to the fracture was taken for MIP (results in Figure IV.7).

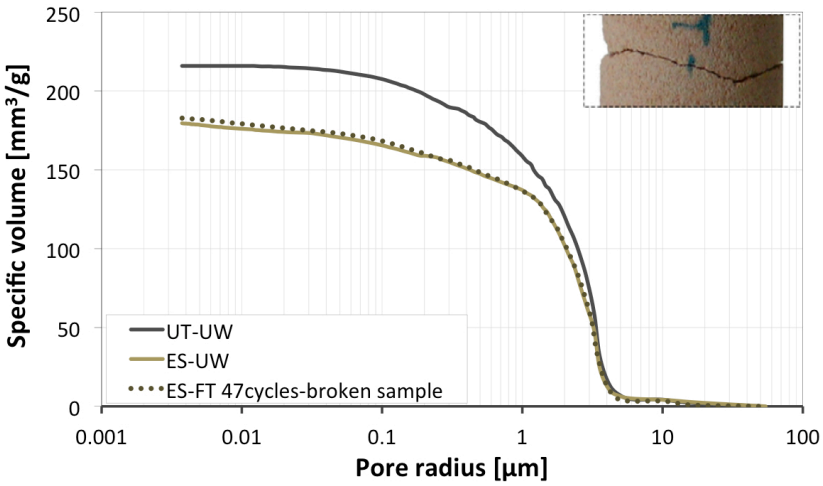

Figure IV.7: Pore size distribution in the sample taken close to the fracture line from the specimen that has broken during 47th FT cycle, in comparison with untreated and ethyl silicate treated samples, both unweathered.

HAP-treated samples do not suffer remarkable alterations as a result of the cycles, the final changes being ΔE_d = -5% and $\Delta \sigma_t$ = -6%. ES-treated samples are those to exhibit the most significant susceptibility to weathering, final $\Delta \sigma_t$ =-17%.

IV.3.3 Salt crystallization cycles

The behavior of consolidated stone in terms of weight variations and dynamic elastic modulus is reported in figure IV.8 for stone cores.

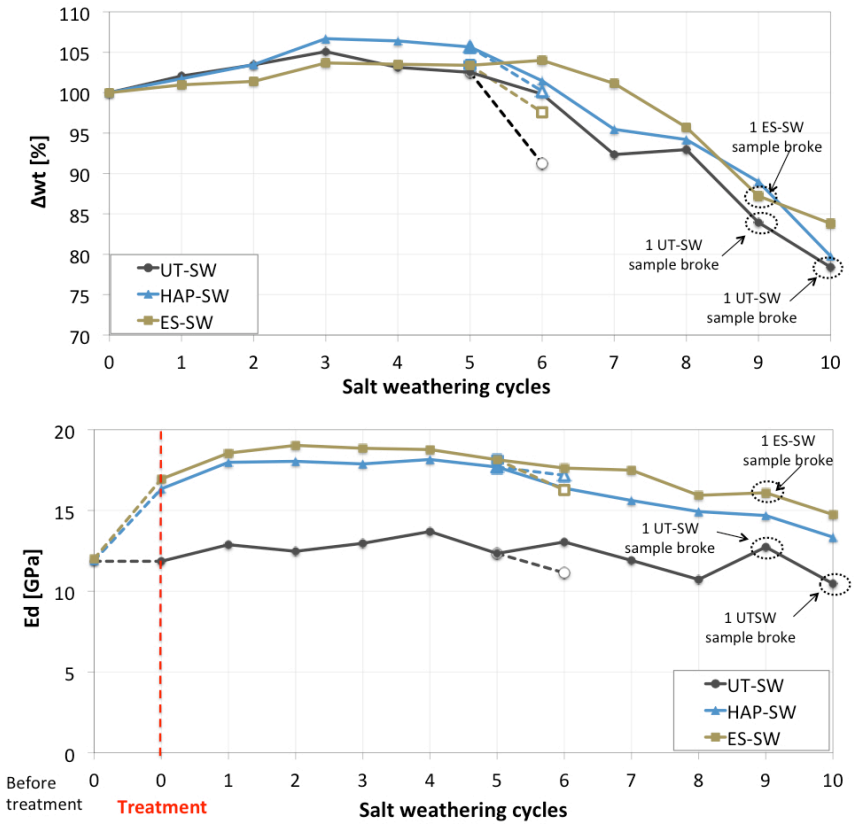

Figure IV.8: Variations in weight and dynamic elastic modulus of stone cores at each SW cycle. Dashed lined and open symbols indicate samples desalinated after the 5th cycle.

After cycle 5, half of the samples were desalinated. Desalination was very effective as it led to decreases in sulfate content from 9.8 to 0.1 wt.% in untreated samples, from 2.9 to 0.4 wt.% in HAP samples, from 6.4 to 0.3 wt.% in ES samples. Samples were visually inspected after desalination (figure IV.9).

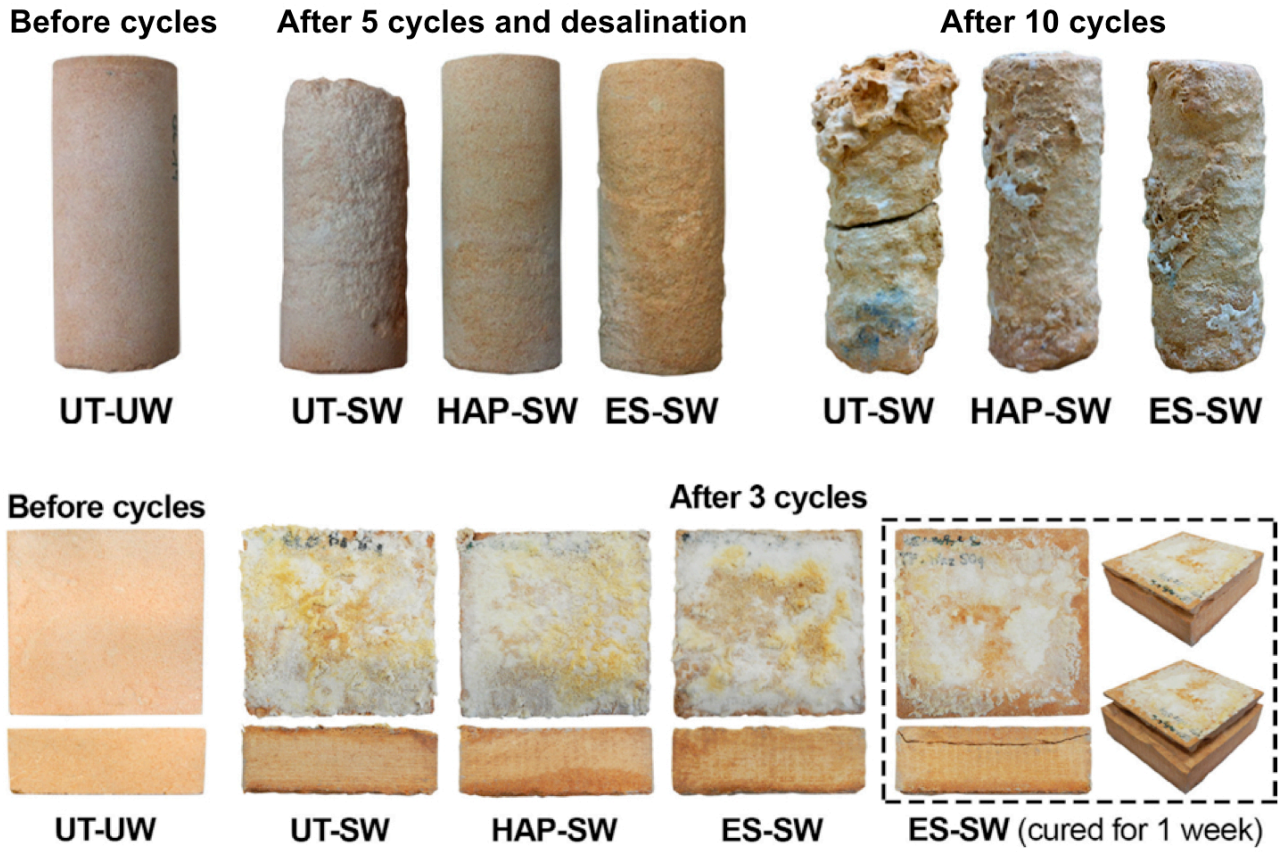

Figure IV.9: Samples after salt weathering cycles and after SW cycles and desalination. For cylinders, samples after 5 cycles had undergone desalination prior to visual inspection, while samples at 10 cycles did not. Prisms have not been desalinated prior to visual inspection either.

In terms of weight change and dynamic elastic modulus, after 5 SW cycles and desalination (figure IV.8) HAP samples exhibited the lowest deterioration: $\Delta wt = +0.2\%$ is registered for HAP samples, vs. $\Delta wt = -8.8\%$ for UT and $\Delta wt = -2.4\%$ for ES samples; $\Delta E_d = +5\%$ is measured for HAP, vs. $\Delta E_d = -6\%$ for UT and $\Delta E_d = -4\%$ for ES samples).

Results in terms of tensile strength are in Table IV.2. ES samples underwent a much higher decrease compared to the initial situation ($\Delta\sigma_t = -42\%$), with respect to HAP samples ($\Delta\sigma_t = -15\%$); tests could not be performed on UT samples due to excessive decay.

Pore size distribution before and after SW cycles is in figure IV.10.

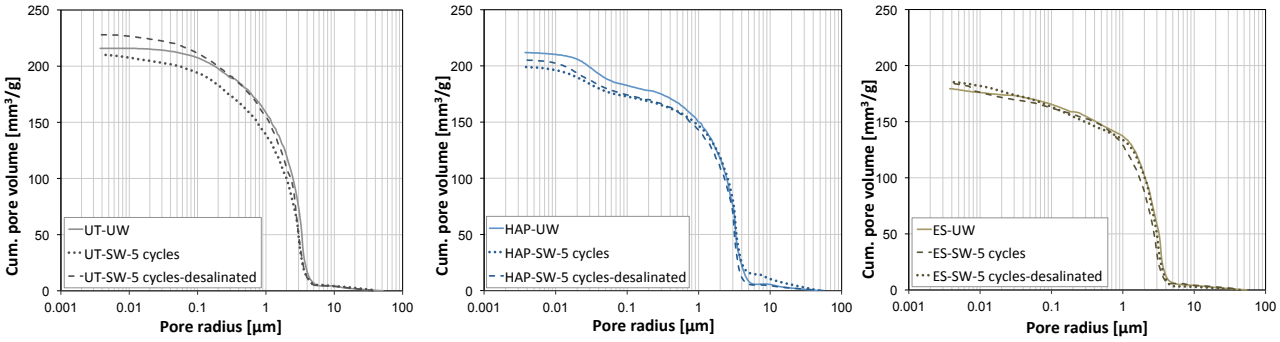

Figure IV.10: Pore size distribution before and after SW cycles and after desalination.

When cores are subjected to 5 additional SW cycles, 2 UT samples, 1 ES sample and no HAP samples broke down. Weight decrease and dynamic elastic modulus alterations were assessed and are reported in figure IV.8. Due to excessive weathering, tensile strength could not be determined at the end of the cycles.

Pore size distribution at different depth in the samples was also evaluated on cubes used for the tests, results being in figure IV.11.

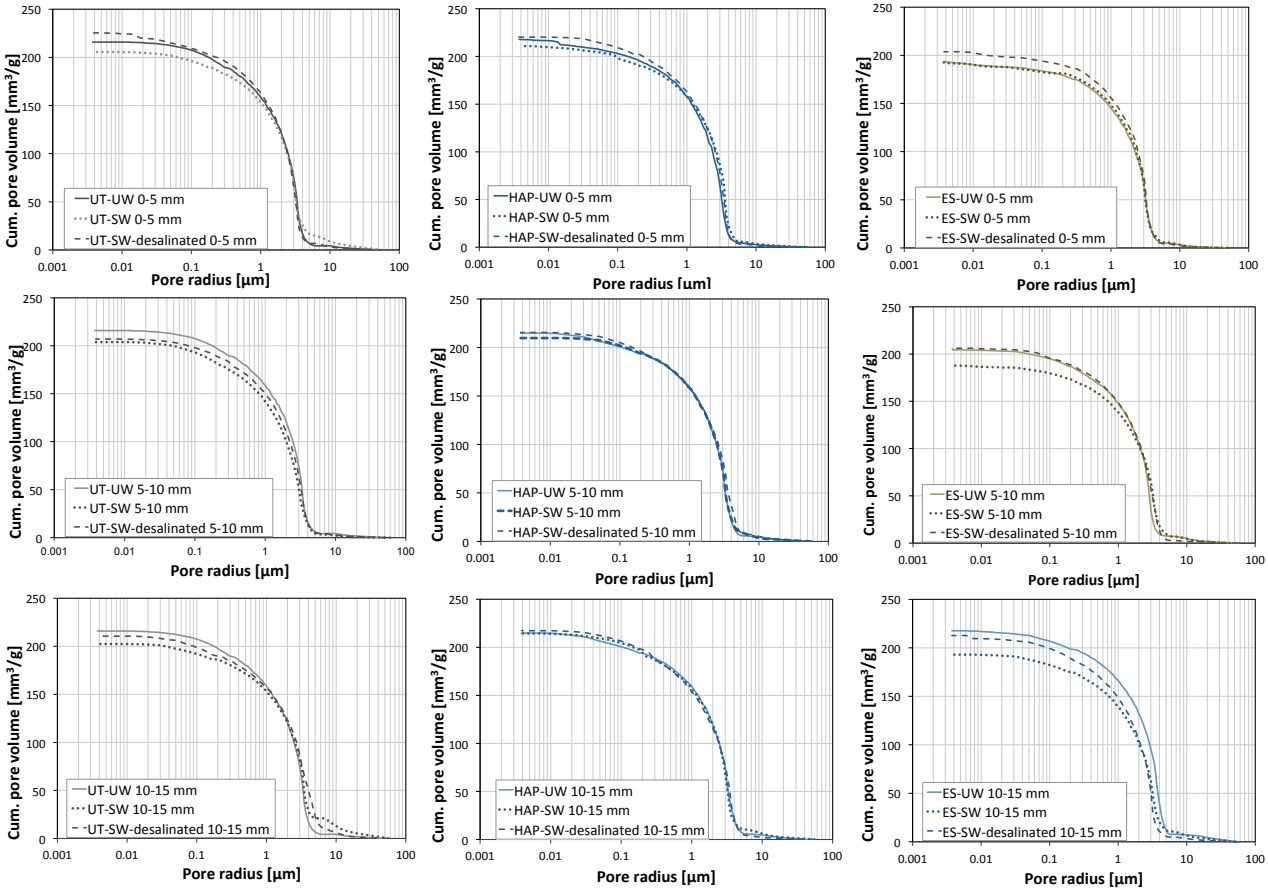

Figure IV.11: Pore size distribution on treated and untreated cubes before and after artificial weathering

IC at different depth from the treated surface is reported in figure IV.12.

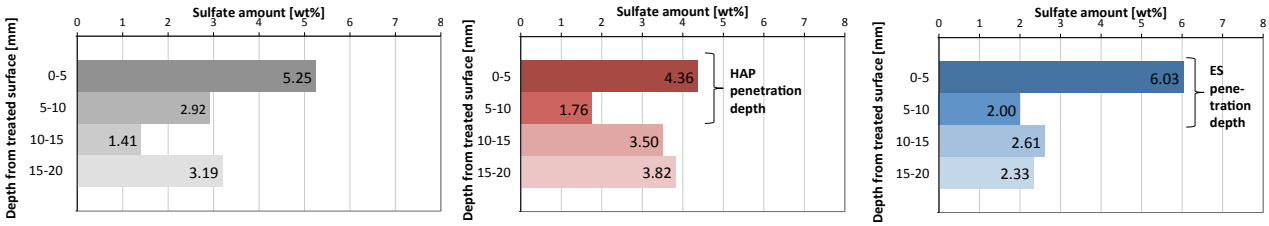

Figure IV.12: Salts content at different depth in untreated and treated samples

Visual observation of prisms including the still hydrophobic ES sample left to cure for 1 week, is reported in figure IV.9.

IV.4 Discussion

Results obtained by mechanical, physical and microstructural investigations (shown in Table IV.2, figure IV.4 and figure IV.3, respectively) after HAP and ES treatments are in line with those obtained in the previous chapter and indicate marked increases in mechanical properties after both treatments and not-excessive modifications in physical and microstructural alterations, the latter being more pronounced in ES treated samples. The behavior of the interface between treated and untreated parts of the sample was investigated on stone cubes and prisms. Microstructural alterations caused by both consolidants were decreasing with depth in the samples, hence no water trapping behind consolidated layer, possibly leading to flaking or detachment, is to be expected.

Alterations in physical properties are negligible also in the case of ES treatment, thus confirming that the proposed accelerated curing procedure was effective in removing temporary hydrophobicity.

The evaluation of the effects of each accelerated weathering procedure is described in the following.

IV.4.1 Wet/dry cycles.

Wet/dry cycles cause no significant variations in weight nor in dynamic elastic modulus of untreated samples (figure IV.5). Some alternate variations are registered, but those are probably owing to experimental variability. In fact, the final value is very close to that prior to the cycles, thus indicating that, as expected, globigerina limestone is not much susceptible to this weathering phenomenon. Consistently, negligible alterations were assessed in untreated samples tensile strength (Table IV.2).

Values obtained for HAP treated samples indicate negligible variations in tensile strength and dynamic elastic modulus (Table IV.2), that can be ascribed to stone variability, as suggested by

standard deviations of untreated samples. Consistently, negligible phosphate content was detected in water after cycles (< 3 ppm, thus being lower than that of sulfates dissolving in untreated samples), as displayed in figure IV.12. This confirms the absence of soluble phases found in the previous chapters.

ES-treated samples, instead, suffer a limited but constant reduction in both weight and dynamic elastic modulus and a final $\Delta\sigma_t$ = -11% (Table IV.2). These decreases are not very marked but indicate a trend that is consistent with literature for clay-bearing stones treated with ES when subjected to wet/dry cycles or prolonged immersion in water [29,35]. In fact, ES treatment was found to accelerate weathering due to swelling of clays in particular by reducing the number of cycles necessary for weathering to occur, with respect to untreated references [35]. No clays were detected by XRD in globigerina limestone used for this study [26]; however, their presence was reported in the literature [36], hence it cannot be excluded that some fractions, in an amount below instrument detectability threshold, are present. Swelling of clays hence seems to be the reason behind weathering of ES samples. However, this is debatable, since no damage at all occurred to the untreated sample. Expansion tests on untreated and treated samples are currently in progress to better evaluate if swelling of clays occurred.

IV.4.2. Freezing-thawing cycles

The behavior of the treated layer with respect to FT cycles was investigated by using cylindrical samples. Untreated samples experience a slight decrease in weight and dynamic elastic modulus after 10 cycles, even though no damage was visible (figure IV.6). Tensile strength remains substantially unmodified as alterations in its value ($\Delta\sigma_t$ =+5%) are within the stone variability (see Table IV.2).

This indicates that Globigerina limestone, despite having quite low tensile strength and high porosity, is not much affected by FT cycles. This might be due to the porosity distribution that is characteristic of the stone: in fact, most of the pores are coarse (73% of the total having radius r > 1 l μm) hence crystallization pressure are quite low [15]. Moreover, pore size distribution is quite narrow around the average value (2 μm) hence, when water freezes in these pores, only a small amount of water, that could serve as a source of for further growth of crystals in coarse pores, remains unfrozen in thinner pores [10,31].

ES treated samples, instead, suffer a remarkable, gradual decrease in both Ed and weight with cycles (figure IV.6). In fact, fissures running parallel to the bedding planes originate between cycle 35 and 60, which confirms that FT cycles activate pre-existing irregularities [10]. This fact is also important because it indicates the need for performing a very high number of cycles to see the

effects of FT cycles (at least 50, as reported in the literature [9,10]), despite standards suggesting a much lower number [20].

One ES-treated sample broke during cycles: microstructure of the samples taken in proximity of the fracture does not reveal significant alteration in pore size distribution, indicating that the development of the crack had not affected the surrounding stone (figure IV.7).

Tensile strength at the end of the cycles has experienced a 17% reduction, however remaining higher than that of untreated references, even though they had not suffered reductions (Table IV.2).

Marked susceptibility of ES treated samples to FT cycles might be due to several reasons. First, ES increases the amount of pores in the finer fraction (<0.01 μm) thus raising crystallization pressures [37]. Moreover, a mismatch in thermal expansion coefficient between calcite crystals of the stone and silica gel might have arisen, thus generating further stress [37]. In fact, thermal expansion coefficient of stone is tipically 5-12 $\bullet 10^{-6}$ $°C^{-1}$, while that of silica gel deriving from ES curing is 10–40 $\bullet 10^{-6}$ $°C^{-1}$ up to 140 $\bullet 10^{-6}$ $°C^{-1}$ [38,39]. Even though this mismatch should be mitigated because Young's modulus of elasticity of silica gel is quite low and so should be thermal stress [38], still a contribution to generation of stress is possible. Finally, additional stresses might be caused by the fact that ES affects contact angle between crystals and pore walls (for values below 90° no tensile stress and hence damage would arise [37]). The investigation of the latter aspect, however, is still in progress.

HAP-treated samples, instead, did not experience significant decrease in weight and dynamic elastic modulus as a result of the cycles (figure IV.6). As a result, after 30 cycles the initial benefit of ES with respect to HAP was already lost in terms of E_d. As for E_d, tensile strength remains substantially unaltered; however, the final value for ES samples is still slightly higher than that of HAP samples, both being higher than untreated references. The lower susceptibility of HAP to FT decay with respect to ES might be due to different reasons: HAP causes a smaller increase in pores in the finer fraction and it has a better thermal compatibility with calcite (values in literature indicating α_t =12-16 $\bullet 10^{-6}$ $°C^{-1}$ [40]). The effect of HAP on contact angle between ice crystal and material pore walls is yet to be determined.

IV.4.3. Salt crystallization cycles

When subjected to SW cycles all stone cores exhibit the same trend in terms of weight change (figure VI.8): first weight increases as a result of accumulation of salts in the pores, then weight variations are registered due to opposite action of further salt accumulation and material detachment, finally weight drops gradually as the contribution of material loss becomes predominant over salt accumulation. This behavior is in line with data found in the literature [41].

Correspondingly, also in terms of E_d, different phases can be highlighted: first an increase due to pore clogging, followed by a progressive decrease due to the competing action of weathering and salt accumulation and, finally, a decrease due to predominant action of opening of micro-cracks [31].

As pore clogging due to salt accumulation partially counterbalances the effects of weathering caused by salt crystallization, desalination was performed on half of the samples, after cycle 5.

After desalination UT samples have suffered the highest weathering, leading to pulverization and rounding of the samples edges (figure IV.9). Pulverization is actually the form of weathering that is caused by salt crystallization on site, hence artificial weathering was effective in reproducing conditions experienced in the field [25]. HAP-treated samples suffered the least alterations, visual appearance being very close to that before cycles. ES-treated samples exhibit some pulverization, though less than that of untreated samples.

Results in terms of weight change and dynamic elastic modulus after 5 cycles and desalination match visual observation: untreated samples experience the most decrease, followed by ES, while that of HAP-treated samples is negligible. However, it must be noted that values for HAP might be slightly overestimated, as samples were those with the highest residual presence of salts after desalination, hence salts still inside the stone might slightly mitigate the effects of weathering.

After just 5 cycles of salt crystallization, the initial advantage of ES with respect to HAP is lost, at least in terms of E_d (Table IV.2). As for freeze-thawing cycles, ES samples experience a much higher decrease in σ_t with respect to HAP, though the final value is still slightly higher (Table IV.2). Also in this case, initial benefit of ES treatment is almost completely lost due to limited durability.

From MIP on desalinated and non-desalinated cylinders (figure IV.10) it can be highlighted that: prior to salt removal (dotted curves) some alterations can be assessed in total open porosity and pore size distribution, mostly in HAP and UT samples, but these alteration are less than expected on the basis of visual inspection; after desalination (dashed curves) significant modifications are detected in UT sample, while those of ES and HAP are much less pronounced. These results are in line with literature studies [34]. The behavior exhibited by the samples can be explained considering that when MIP is performed, thenardite and not mirabilite (which occupies a volume about 3 times higher) is expected to be the phase inside the pores (as it is the one to be stable at temperature $T < 32.4$ °C and relative humidity $RH < 71\%$, and hence in laboratory conditions) [32,42,43]; moreover, after salt removal, stresses are released and some micro-cracks can close down [34].

The following observations can be made:

- as expected, for all samples, salts exert pore clogging effect as total open porosity increases after salt

removal;

- UT samples and, to a lower extent, ES are those to suffer the most alterations, as porosity is increased after salt weathering and removal, suggesting that micro-cracks have opened;
- in HAP samples, porosity after cycles is slightly lower with respect to that before cycles. This might be partially due to the higher salt content after desalination: a reduction in porosity does not seem likely to have occurred, however, it indicates that no relevant micro-crack opening occurred, thus these samples are less sensitive than both ES and UT.

To better compare residual salt content after desalination and pore size distribution curves, IC tests were repeated on samples adjacent to those used for MIP, exactly as for testing efficacy of the desalination procedure: 0.7 wt% sulfates was detected for HAP samples and 0.4–0.5 wt% for UT and ES samples, in fair agreement with results obtained when measuring the efficacy of the desalinization procedure. Residual salt content in HAP sample is very low compared to that prior to desalination (up to 6–7 wt%, Fig. 6), so their pore clogging action should be very limited: for this reason it is confirmed that no relevant crack opening must have occurred in HAP treated samples.

When stone cores are subjected to further salt crystallization cycles, they experience further decreases in terms of weight and dynamic elastic modulus (figure IV.8). At cycle 9, UT and ES samples undergo fractures along bedding planes, which are frequently described in the literature as a typical decay pattern for salt crystallization [31]. Dynamic elastic modulus of consolidated samples remains higher than that of UT samples (see Table IV.2). It is relevant to notice that HAP samples were the only ones not to undergo rupture during cycles, though of course suffering powdering and material loss. As in the case of freezing-thawing, this behavior of HAP samples might be due to lower increases in the finer fractions of pores with respect to ES. Also in this case possible alterations in contact angle between pore surface and salt crystal might occur after consolidation, further influencing susceptibility to weathering.

Results obtained for microstructural analyses on cubes (figure IV.11) match those obtained for the cores, alterations in desalinated UT and ES samples being more significant than those on HAP. Beneficial effect of HAP hence is not dependent on specimen shape and dimensions.

Cubes and prismatic samples were also used to investigate the behavior of the interface between the treated and untreated areas of the samples.

As a result of MIP at different depths from the treated surface, some considerations can be derived: microstructural alteration caused by HAP and ES treatments (prior to weathering) in cubes are much less pronounced than in stone cores, consistent with lower saturation. Moreover, they decrease with depth, so that they become negligible at 10-15 mm from treated surface.

After salt weathering, no dramatic pore occlusion is found in non-desalinated samples (dotted lines in figure IV.11), not even in the 10-15 mm layer, which is the one below the consolidated area of

the samples. This is very important because it indicates that consolidants still allow salt diffusion through the substrate and do not cause salt accumulation and crystallization behind the treated surface. The most relevant salt accumulation was registered for ES samples, while HAP porosity is barely modified.

Regarding desalinated samples (dashed lines in figure IV.11), some opening of micro-cracks is detected in the top layer, where crystallization occurs, while curves for other layers basically match those of unweathered samples.

IC results confirmed that the consolidated layer does not act as a barrier for salt diffusion: in fact, the amount of sulfates is maximal in the top layer for all samples (consistent with higher evaporation in this area), including HAP and ES (results in figure IV.12). No relevant accumulation is found in the area underlying the consolidated layer.

Visual observation of UT, HAP and ES prisms (cured for 28 days) show marked efflorescence formation on the top of the samples, matching previously discussed results, while limited alteration could be assessed in the lateral area (see figure IV.9). When still hydrophobic ES samples (cured for 1 week) are examined (figure IV.9), instead, efflorescence is less relevant and a distinct fracture between the consolidated and the non-consolidated parts is noticed, that caused the complete detachment of the treated layer. This is due to the fact that hydrophobic layer impeded salt migration towards the external surface, thus causing salts to crystallize at the interface and resulting in high crystallization stresses.

IV.5 Conclusions

Durability of HAP-treatment with respect to wetting-drying, freeze-thaw and salt crystallization cycles was evaluated, in comparison with that of ethyl silicate. The following conclusions can be derived.

Globigerina limestone is not much affected by wetting drying and freeze-thaw cycles, while it is highly susceptible to weathering due to salt crystallization.

HAP treatment exhibits remarkable resistance towards all of the tested parameters. No soluble phase dissolution occurs due to wet-dry cycles, hence mechanical properties remain basically unaltered. As for wetting-drying, HAP-treated samples do not experience severe decay as a result of freezing-thawing cycles. SW is the mechanism that affects HAP-treated sample the most; however, no severe alterations are experienced in either microstructure or mechanical properties, indicating that resistance to salt weathering is much higher than that of untreated samples. HAP treatment does not cause incompatibility between the treated and untreated layer as it does not prevent salts from diffusing towards the external surface.

Ethyl silicate, despite resulting in enhanced efficacy compared to HAP prior to weathering, tends to

lose its advantage as an effect of lower durability. In particular, all of the three phenomena tested caused reduction in ES samples' mechanical properties. Wetting-drying possibly causes swelling of clays, thus affecting ES-treated samples but not untreated and HAP-treated sample. However, ES-treated samples suffer much more severe decay as a result of both freeze-thaw and salt weathering cycles. In particular, ES treated samples are the most sensitive to FT cycles, possibly due to microstructural alterations and, mostly, increases in the finer pores fractions, caused by the treatment. After both SW and FT cycles, ES treated samples exhibit lower dynamic elastic modulus than HAP while tensile strength remains higher, though suffering a more dramatic decrease. The difference in the behavior of HAP and ES seems due to different modifications caused by the two consolidants in stone microstructure (and in particular to different impact in the finer pore range), different thermal behavior, and possibly alterations in contact angle between the pore and the forming crystals.

All these considerations are valid for samples subjected to accelerated curing procedure, specifically developed for the purpose, but are expected to be reached in the field after about 6-7 months curing. When ES samples are examined while still hydrophobic, instead, the risk of detachment due to salt weathering exists: this is very relevant as ES hydrophobicity, though temporary, might last several months, during which time treated samples are prone to dramatic weathering. This also indicated that the newly developed accelerated curing procedure is particularly promising for use in the field so as to mitigate this drawback of ES.

Summarizing the results of this chapter and the previous one, both HAP and ES have shown good efficacy and compatibility for consolidation of limestone. In particular, ES is more effective and HAP more compatible. Moreover, HAP has shown remarkable durability, much higher than that of ethyl silicate. In view of this higher durability, while mechanical benefit of ES is rapidly lost after a few weathering cycles, HAP properties are maintained, thus HAP seems to be a more promising option with respect to ES for porous limestone consolidation.

Acknowledgments

M.Eng. Francesco Sagripanti, M.Eng. Matteo Glorioso, Claudia Castelli and Paolo Carta (DICAM, University of Bologna) are gratefully acknowledged for collaboration on stone characterization.

Chapter References

[1] Sassoni E., Graziani G., Franzoni E., An innovative phosphate-based consolidant for limestone. Part 1: Effectiveness and compatibility in comparison with ethyl silicate. Constr Build Mater 102 (2016) 918-930

[2] Sassoni E., Graziani G., Franzoni E., An innovative phosphate-based consolidant for limestone. Part

2. Durability in comparison with ethyl silicate. Constr Build Mater 102 (2016) 931-942

[3] Lazzarini L., Laurenzi Tabasso M., Il restauro della pietra, CEDAM, Padua, 1986.

[4] Italian Recommendation NORMAL 20/85, Conservazione dei materiali lapidei: Manutenzione ordinaria e straordinaria, Istituto Centrale per il Restauro (ICR), Rome, 1985.

[5] Amoroso G.G., Fassina V., Stone Decay and Conservation, Elsevier, New York, 1983.

[6] Scherer G.W., Wheeler G.S., Silicate consolidants for stone, Key Eng Mater 391 (2009) 1–25.

[7] E. Sassoni, E. Franzoni, Sugaring marble in the Monumental Cemetery in Bologna (Italy): characterization of naturally and artificially weathered samples and first results of consolidation by hydroxyapatite. Appl Phys A Mater 117 (2014) 1893–1906.

[8] Franzoni E., Sassoni E., Correlation between microstructural characteristics and weight loss of natural stones exposed to simulated acid rain. Sci. Total Environ 412–413 (2011) 278–285.

[9] Martìnez-Martìnez J., Benavente D., Gomez-Heras M., Marco-Castaño L., Garcìa-del-Cura M.A., Non-linear decay of building stones during freeze–thaw weathering processes. Constr Build Mater 38 (2013) 443–454.

[10] Ruedrich J., Kirchner D., Siegesmund S., Physical weathering of building stones induced by freeze-thaw action: a laboratory long-term study. Environ Earth Sci 63 (2011) 1573–1586.

[11] Scherer G.W., Stress from crystallization of salt. Cem Concr Res 34 (2004) 1613–1624.

[12] Cardell C., Delalieux F., Roumpopoulos K., Moropoulou A., Auger F., Van Grieken R., Salt-induced decay in calcareous stone monuments and buildings in a marine environment in SW France. Constr Build Mater 17 (2003) 165–179.

[13] Dubelaar C.W., Dusar M., Dreesen R., Felder W.M., Nijland T.G., Maastricht limestone: A regionally significant building stone in Belgium and The Netherlands. Extremely weak, yet time-resistant in: Proceedings of the International Conference on Heritage, Weathering and Conservation, HWC 2006, vol. 1, 2006, pp. 9–14.

[14] Wangler T., Scherer G.W., Clay swelling mechanism in clay-bearing sandstones. Environ Geol 56 (2008) 529–534.

[15] Lòpez-Arce P., Gomez-Villalba L.S., Pinho L., Fernàndez-Valle M.E., Álvarez de Buergo M., Fort R., Influence of porosity and relative humidity on consolidation of dolostone with calcium hydroxide nanoparticles: effectiveness assessment with non-destructive techniques. Mater Charact 61 (2010) 168–184.

[16] E. Sassoni, S. Naidu, G.W. Scherer, The use of hydroxyapatite as a new inorganicconsolidant for damaged carbonate stones, J. Cult. Herit. 12 (2011) 346–355.

[17] Dorozhkin SV., Calcium orthophosphates. Biomatter 1(201) 121–64.

[18] Naidu S., Scherer G.W., Nucleation, growth and evolution of calcium phosphate films on calcite. J Colloid Interf Sci 435 (2014) 128–37.

[19] European Standard EN 12371, Natural stone test methods – Determination of frost resistance, 2010.

[20] Italian Standard UNI 11186, Cultural heritage – Natural and artificial stones – Methodology for exposure to freeze-thawing cycles, 2008.

[21] EN 12370 – Natural stone test methods – Determination of resistance to salt crystallization, 1999.

[22] RILEM Recommendation MS-A1 Determination of the resistance of wallettes against sulfates and chlorides, Mater. Struct. 31 (1998) 2–19.

[23] RILEM Recommendation MS-A2, Unidirectional salt crystallization test for masonry units, Mater. Struct. 31 (1998) 10–11.

[24] Benavente D., García Del Cura M.A., Bernabéu A., Ordóñez S., Quantification of salt weathering in porous stones using an experimental continuous partial immersion method, Eng Geol 59 (2001) 313–325.

[25] Lubelli B., van Hees R.P.J., Nijland T.G., Salt weathering damage: how realistic are existing ageing tests?, in: H. De Clercq (Ed.), Proceedings of SWBSS2014, 3rd International Conference on Salt Weathering of Buildings and Stone sculptures, 14–16 October 2014, pp. 259–273.

[26] Franzoni E., Sassoni E., Graziani G., Brushing, poultice or immersion? Role of the application technique on the performance of a novel hydroxyapatite-based consolidating treatment for limestone. J Cult Herit 16 (2015) 173–84.

[27] Sassoni E., Franzoni E., Pigino B., Scherer G.W., Naidu S., Consolidation of calcareous and siliceous sandstones by hydroxyapatite: comparison with a ES based consolidant. J Cult Herit 14S (2013) e103–e108.

[28] Franzoni E., Graziani G., Sassoni E., TEOS-based treatments for stone consolidation: acceleration of hydrolysis-condensation reactions by poulticing. J Sol-Gel Sci Technol 74 (2015) 398–405.

[29] Wheeler G., Alkoxysilanes and the Consolidation of Stone. The Getty Conservation Institute, Los Angeles, 2005.

[30] Sandrolini F., Franzoni E., Sassoni E., Diotallevi PP. The contribution of urban-scale environmental monitoring to materials diagnostics: a study on the Cathedral of Modena (Italy). J Cult Herit 12 (2011) 441–450

[31] Ruedrich J., Siegesmund S., Salt and ice crystallisation in porous sandstones, Environ Geol 52 (2007) 225–249.

[32] Tsui N., Flatt R.J.,. Scherer G.W., Crystallization damage by sodium sulfate. J Cult Herit 4 (2003) 109–115.

[33] Ruedrich J., Weiss T., Siegesmund S., Thermal behavior of weathered and consolidated marbles. In: Siegesmund S., Weiss T., Vollbrecht A., editors. Natural stone, weathering phenomena, conservation strategies and case studies, Geological Society, London, Special Publications 205 (2002) 255–271.

[34] Angeli M., Benavente D., Bigas J.P., Menéndez B., Hébert R., David C., Modification of the porous network by salt crystallization in experimentally weathered sedimentary stones. Mater Struct 41 (2008) 1091–1108.

[35] Jimenez Gonzalez I, Scherer G.W., Effect of swelling inhibitors on the swelling and stress relaxation of clay bearing stones. Environ Geol 46 (2004) 364–377.

[36] Cassar J., Deterioration of the Globigerina Limestone of the Maltese Islands. Geol Soc London, Spec Publ 205 (2002) 33–49.

[37] Scherer G.W., Crystallization in pores, Cem Concr Res 29 (1999) 1347–1358.

[38] Miliani C., Velo-Simpson M.L., Scherer G.W., Particle-modified consolidants: a study on the effect of particles on sol–gel properties and consolidation effectiveness. J Cult Herit 8 (2007) 1–6.

[39] Moropoulou A., Kouloumbi N., Haralampopoulos G., Konstanti A., Michailidis P., Criteria and methodology for the evaluation of conservation interventions on treated porous stone susceptible to salt decay. Prog Org Coat 48 (2003) 259–270.

[40] Hoepfner T.P., Case E.D., An estimate of the critical grain size for microcracks induced in hydroxyapatite by thermal expansion anisotropy. Mater Lett 58 (2004) 489–492.

[41] Angeli M., Bigas J.P., Benavente D., Menéndez B., Hébert R., David C., Salt crystallization in pores: quantification and estimation of damage. Environ Geol 52 (2007) 205–213.

[42] Rodriguez-Navarro C., Doehne E., Sebastian E., How does sodium sulfate crystallize? Implications for the decay and testing of building materials. Cem Concr Res 30 (2000) 1527–1534.

[43] Flatt R.J., Salt damage in porous materials: how high supersaturations are generated. J Cryst Growth 242 (2002) 435–454.


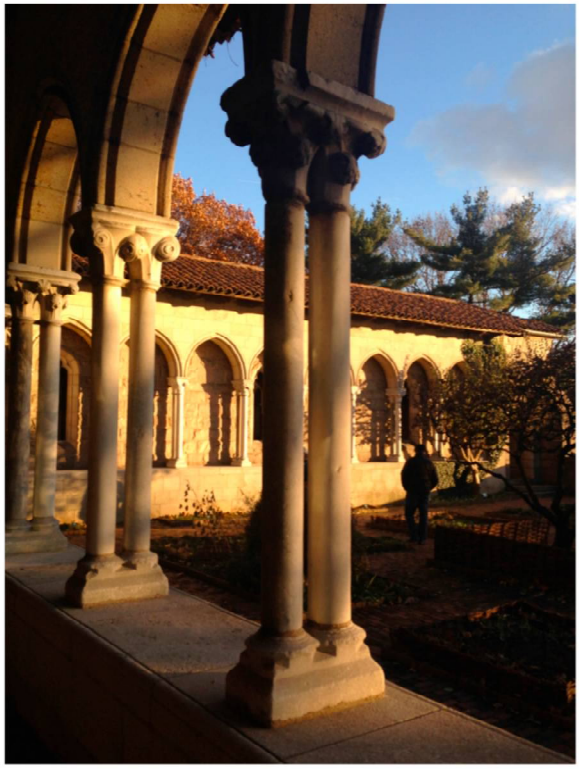


PART 2:
Marble Consolidation







Chapter V: Consolidation of marble: experiments on laboratory specimens

Research aims

Despite marble being one of the most widespread materials in cultural heritage for both architectural elements and sculptures, no fully satisfactory products are currently available for its consolidation. This is a critical issue as marble is prone to severe decay phenomena that cause significant material loss. They are caused by the susceptibility of its main constituent, namely calcite, to weathering, due to some of its intrinsic characteristics.

Among others, sugaring, i.e. loss of cohesion between the grains and subsequent pulverization that occur due to anisotropic deformation of calcite grain, is particularly widespread and severe.

In this Chapter and in Chapter VI, consolidation of sugaring marble by means of the novel HAP-based treatment is investigated. First, a treating protocol was developed by investigating different parameters such as solution concentration, possible additions of calcium ions and application of limewater poultice. In the first step of the research (Chapter V) tests were carried out in laboratory on artificially weathered samples. For reproducing decay conditions of naturally weathered samples by means of an accelerated procedure, one real marble fragment affected by severe sugaring was analyzed, so as to investigate its morphology, microstructure and mechanical properties. Then, different artificial weathering procedures were tested for reproducing as closely as possible the conditions of the real specimen.

The most promising treating conditions were chosen on the basis of an evaluation of efficacy and compatibility with the substrate, then a comparison was carried out between the HAP-treatment and treatments by ethyl silicate and ammonium oxalate, currently the most used stone-consolidant for stone and protective for marble, respectively.

Particular attention was devoted to the exact determination of the phases that form as a result of the HAP-treatment.

V.1. Introduction

Marble artifacts, widely diffused in cultural heritage, suffer severe decay phenomena such as bowing, black crusts, dissolution in acidic rain etc. Among the others, the so-called “sugaring” is particularly relevant. Sugaring consists in the pulverization and detachment of calcite grains that is triggered by their anisotropic deformation [1]. In fact, as a result of temperature increase, calcite suffers an expansion parallel to the c-axis and a shrinkage perpendicular to the same axis that causes micro-cracks opening at grain boundaries [2]. Temperature variations are very frequent on site as they might result from day-night excursions and from different exposure to solar radiation

[2]. As a consequence, crumbling of grains and pulverization of the material frequently occur especially in thin carved areas and/or near the edges of architectural elements [1].

Despite the relevance of this phenomenon, no fully satisfactory treatments for sugaring marble are available at present: in general traditional inorganic treatments lack efficacy, while organics lack compatibility and/or durability [1,3,4]. As mentioned in the previous chapter, ethyl silicate is the most widely used stone consolidant: when applied to marble, that is essentially composed by calcite, it can provide immobilization of calcite grains as a result of silica gel formation, but of course no chemical bonding can occur due to absence of silicate fractions in the stone. Lack of chemical bonding, in turn, causes scarce improvements in mechanical properties and long-term efficacy [5,6]. Ammonium oxalate has been recently proposed for consolidation and protection of marble, mimicking well-adherent calcium oxalate patinas that are found on historic marble elements [7,8]. However, limited penetration depth and incomplete coverage of the support [8] are significant drawbacks of this treatment at present. Nano-limes have also been proposed, but they also lack penetration depth and grain bonding ability [3,4].

For these reasons, in this chapter, marble consolidation by HAP is proposed. HAP, as described in the previous chapters, is not introduced in the stone in the form of particles (not even at the nano-scale) but is formed directly inside the micro-cracks that form due to weathering, by reaction between DAP solution and calcium ions [1, 9-13]. HAP treatment has also been proposed for marble protection, discussed in literature [14,15] and investigated in Chapter VIII and IX.

As for limestone, testing HAP consolidation on quarry slabs was considered not representative of real efficacy on site (also considering that unweathered marble presents minor porosity and water uptake) and leading a systematic testing campaign on naturally weathered samples was considered infeasible [16-19]. Moreover, as for limestone, non-contaminated and uniformly weathered samples were preferred at the early stages of research, to better evaluate the effects of HAP treatment. For this reason, one real historic slab affected by severe sugaring was examined and its morphology, microstructure and mechanical properties were evaluated. Then, an artificial weathering procedure was set up so as to reproduce these weathering conditions as closely as possible.

Different formulations were tested for the DAP treatment, so as to select the most promising [20]. Solutions with and without calcium ions additions were investigated, the aim of external addition of calcium being that of suppressing substrate dissolution, even though millimolar. The efficacy and compatibility of the proposed treatments were investigated in laboratory conditions, on the artificially weathered samples, in comparison with ethyl silicate and ammonium oxalate. Special attention was devoted to analysis of phase formation as a result of each treatment. Then, in the

following step of the research (Chapter VI) the very same slab used for characterization of weathering was used for testing the efficacy of HAP based treatment on real historic artifacts [20].

V.2. Materials and Methods

V.2.1. Materials

For characterizing weathering of a real sugaring marble artifacts, one slab (~12x3x9 cm^3) was taken from a fractured historic gravestone dating back to 1848 and located in the Monumental Cemetery in Bologna (Italy, XIX century) (figure V.1). The slab had spontaneously detached from the rear wall and was collected after approval by the Superintendence for Architectural Heritage and Landscape of Bologna, Modena and Reggio Emilia. The surface facing the exterior was covered by a black crust and severely affected by sugaring. The side opposite to that of the crust, instead, did not seem significantly affected by weathering.

Provenance of gravestone marble was investigated: no data regarding the specific tomb were available, but an analysis of the materials used in Certosa Cemetery indicates that the large majority of marble used in coeval gravestones was quarried in Carrara area (Italy), hence it seems likely that the selected sample has the same provenance. For this reason, for laboratory tests, freshly quarried slabs of "Marmo Bianco di Carrara" (White Carrara marble, supplied by Imbellone Michelangelo s.a.s., Italy) were selected, all macroscopically similar to the gravestone slab in terms of color, veins and texture.

V.2.2. Methods

V.2.2.1. Characterization of historic slab

Presence of gypsum was investigated by XRD so as to confirm that the superficial dark deposit on the slab surface is a black crust.

Then, prior to further tests, the superficial crust was gently cleaned by brushing. Neutral soap in low concentration and deionized water were used as cleaning agents. Both the use of soap and mechanical action might not always be recommended for marble cleaning, but, in the present case no carving, nor decoration were present on the surface, hence allowing for this cleaning procedure. More delicate procedures, such as deionized water applied by agar and/or laser cleaning, are recommended for more delicate objects: experiments on cleaning by means of these methods with and without preconsolidation by HAP are currently in progress.

When the black crust was removed, the underlying substrate appeared affected by sugaring, mostly in the proximity of the sample edges (see figure V.1, BC and CD). Grain disaggregation was better examined by means of optical microscopy (stereo-optical microscope Olympus SZX10) and electronic microscopy (SEM Zeiss EVO 50EP).

As previously mentioned, the opposite side of the slab (not exposed to external atmosphere) seemed not affected by weathering, so it was referred to as "sound".

To evaluate the difference in the decay level of the two parts, mercury intrusion porosimetry (Fisons Macropore Unit 120 and Porosimeter 2000 Carlo Erba) was performed on fractured samples, taken by chisel from the sugaring and the sound part, so as to detect presence of micro-cracks.

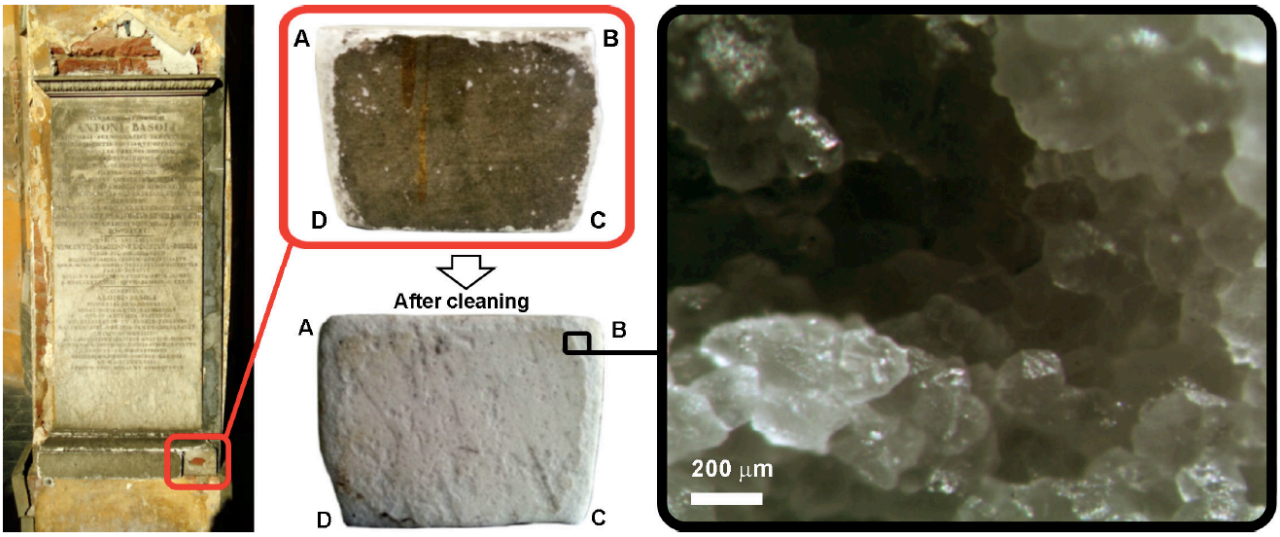

Figure V.1: Initial position and surface appearance of the detached slab taken for characterization of weathering. The slab when cleaned and examined by SOM [69].

V.2.2.2. Artificial weathering of laboratory samples

In the previous part of this thesis (Chapter I), a procedure for artificial weathering of limestone was proposed, consisting in heating samples for 1h at 400°C. In the case of limestone, the procedure allowed to obtain uncontaminated, uniformly weathered samples with reduced mechanical properties and increased porosity and water uptake that resemble properties of naturally weathered samples. However, the origin and the morphology of so-produced decay does not resemble that found in real conditions on site, normally caused by freezing-thawing and salt weathering cycles [9,16,17]. Instead, in the case of marble, artificial weathering by heating not only allows to obtain samples with uniform and reproducible characteristics, as in the case of limestone, but also to reproduce in an accelerated way conditions very similar to those occurring on site, such as micro-crack formation, porosity increase, reduction of mechanical properties etc.. This is because sugaring of marble occurs precisely because of repeated thermal stress cycles [1,17].

Different methods were tested for artificial weathering, such as different heating temperatures and times on both dry and water-saturated samples. However, none of the tested procedures resulted in improved efficacy with respect to heating at 400°C for 1 hour, hence results will not be reported for

brevity's sake.

Three slabs with different microstructural and mechanical characteristics were purchased from the vendor; artificial weathering was tested on all three. After weathering, MIP and SEM observation were performed to choose the slab that more closely resembling weathering conditions of the real historic slab.

The selected slab was then cut into (65x65x20 mm^3) prisms that were artificially weathered as described above.

V.2.2.3 Treatments

The possibility to form HAP by reaction of DAP with calcium ions deriving from the substrate itself was discussed in the previous chapters. However, some aspects can be critical for its successful application on marble and are described below. In view of the discussed parameters, several solutions and testing procedures for the formation of HAP were tested:

- dissociation of DAP does not only produce PO_4^{3-} that react to form HAP, but the majority dissociates into HPO_4^{2-} and $H_2PO_4^-$ [15]. For this reason, high concentrations of DAP are required to produce a suitable amount of PO_4^{3-} for HAP production, but most of the salt that is introduced in the stone does not react;
- substitutions can occur in HAP, the most common being partial replacement of OH^- groups by carbonate, resulting in formation of carbonated HAP [21] that has increased solubility with respect to stoichiometric HAP [15];
- together with HAP, many metastable phases can form, also depending on treating parameters (supersaturation, temperature, pH, foreign ions presence etc.) [9][22]. At the relevant pH range, all those metastable phases are more soluble than HAP, hence their formation is undesirable;
- calcium ions necessary for the reaction derive from dissolution of the substrate. Though millimolar, this dissolution might not be considered desirable when carved or polished surfaces are treated [23].

For these reasons, 4 treating procedures were taken into exam [20]:

- treatment "H0": application of a 3M DAP solution. This concentration is very close to that of saturation of DAP in deionized water and was chosen to provide a high amount of PO_4^{3-} ions for the reaction. Solution was applied by brushing until apparent refusal (i.e. the condition when marble surface remained wet for 1 minute after application [24,33]), corresponding to 15 brush strokes. Samples were left to cure for 48 hours, while wrapped to prevent evaporation, then rinsed and dried at room temperature up to constant weight;
- treatment "H1": application of 3M DAP solution followed by that of a limewater poultice. Treatment was performed exactly as for globigerina limestone, but DAP solution was brushed until apparent refusal;

- treatment “H2”: application of a 3M DAP solution, with addition of 1 mM $CaCl_2$ so as to prevent dissolution of the substrate, followed by application of a limewater poultice. $CaCl_2$ concentration was selected on the basis of [15], where addition in this amount to 1M DAP solution was proven to be sufficient to suppress calcite dissolution. Prior to treatments, it was verified that no precipitation in the solution would occur because of $CaCl_2$ addition. Treatment was performed exactly as “H1”;
- treatment “H3” application of a 3M DAP solution, with addition of 3 mM $CaCl_2$ so as to prevent dissolution of the substrate, followed by limewater poultice application. Paper [15] was still taken as a reference for determining $CaCl_2$ concentration to be used, but in this case the ratio of $CaCl_2$ to DAP was kept constant instead of the concentration of $CaCl_2$ itself. Again, absence of precipitation in the solution was verified. Treating procedure was exactly the same as for “H1” and “H2”.

The four different treating procedures were compared in terms of morphology, elemental and mineralogical composition of the treated layer.

Morphology was investigated by observing the treated face of prisms (by an SEM Zeiss EPEVO 50; samples were made conductive by using gold) and their elemental composition was assessed by energy dispersive spectrometry (EDS, Oxford Instruments INCA ENERGY 350) incorporated in SEM. EDS allows to detect phosphorous peaks, which are absent in untreated marble and hence are indicative of calcium phosphate formation as a result of the treatments, but does not allow to discriminate between the different phases. For that purpose micro-Raman and Raman spectrometry were performed using a Renishaw Raman Invia spectrometer, linked to both a retractable probe inside the SEM (which allows to acquire SEM images, EDS and Raman spectra on the same zone with micrometric precision) and to a Leica DMLM optical microscope (OM). For each treatment, at least three spectra were acquired in different positions.

Another option for phase identification would have been that of investigating the Ca/P ratio (that is different for different CaP phases) by semi-quantitative EDS; however the so determined Ca content may be overestimated because of the influence of the calcitic substrate underneath the calcium phosphate layer, hence this method was dismissed.

On the basis of the above listed techniques, the two most promising treatments were selected and compared with AmOx and ES in terms of efficacy and compatibility.

V.2.2.4 Evaluation of most promising treatments efficacy and compatibility in comparison with ethyl silicate and ammonium oxalate

H1 and H2 treatments were selected as most promising (cfr. §V.3.1) and their efficacy and compatibility were evaluated and compared to ethyl silicate based treatment (ES) and ammonium oxalate based treatment (AmOx).

Application of the latter was performed as described in the following:

- ES treatment consisted in the application of the commercial product "Estel 1000" (CTS s.r.l. Italy) by brushing until apparent refusal. Samples were then left to cure in laboratory conditions (T=20±2 °C, RH=50±5%) for 1 month, as recommended in the product technical data sheets, then an accelerated curing procedure was performed by applying a deionized water poultice (as described in Chapter IV and [26]) so as to accelerate curing reactions and remove temporary hydrophobicity;
- "AmOx" treatment was performed by applying a 5 wt.% solution of ammonium oxalate (Sigma-Aldrich, reagent grade) in de-ionized water as recommended in [27,28]. Samples were treated by brushing to apparent refusal and left reacting while wrapped in a plastic film for 48 hours prior to rinsing and drying to constant weight.

First, phase formation as a result of the treatments was evaluated by SEM/EDS on the treated surface and on cross sections, so as to evaluate morphology of the treated layer and consolidant penetration in micro-cracks, respectively. For observation of cross sections, samples were included in epoxy resin, then sawn and lapped: samples were made conductive using graphite.

The efficacy of the treatments was determined by evaluating increases in ultrasonic pulse velocity (UPV) and resistance to abrasion, both measured on duplicate samples. UPV and resistance to abrasion were selected as the relevant mechanical parameters because: UPV is determined by a completely non destructive tests (hence it can be evaluated on the very same samples before and after consolidation), moreover, it is widely indicated as a very accurate parameter for evaluating marble cohesion, as it is very sensitive to the presence/formation of micro-cracks and hence to their eventual repair [29-31]. Moreover, a classification of marble weathering based on UPV has been proposed in the literature (see Table V.1) [29,32]. One of the drawbacks of this measure might be its high sensitivity to marble anisotropy, but in the present tests, all samples were taken from one same slab and tested in the same direction, so the effects of anisotropy can be neglected.

Damage class	UPV [Km/s]	Condition
0	> 5	Fresh
I	3.0-5.0	Increasing porosity
II	2.0-3.0	Granular disgregation
III	1.5-2.0	Fragile
IV	<1.5	Crumbling rock

Table V.1 Damage classes as a function of UPV, as reported in [29]

Resistance to abrasion was evaluated because it is sensitive to stone tendency to pulverization [33] which, of course is representative of marble sugaring. It was measured by a modified version of the PEI (Porcelain Enamel Institute) abrasion test, as seen in §I.2.2. Weight loss due to abrasion was measured, for each sample, on the treated surface and then, after cutting a 4 mm-thick slice, at a depth of 4 mm from the treated surface, so that treatment presence at this depth could also be evaluated.

Compatibility of the treatments was evaluated in terms of chromatic alterations, measured by spectrophotometer (Mercury 2000 Datacolor) and microstructural alterations, measured by MIP. ΔE values reported are average for 3 measures. MIP was performed on duplicate samples taken by chisel from the 4 mm slices sawn for abrasion test (of course, parts non affected by the test were chosen). Determination of water transport properties was neglected, as the stone is scarcely porous and the consolidants are not expected to cause marked pore clogging.

V.3. Results [20]

V.3.1. Historic slab characterization and artificial weathering of the samples

Results of MIP on samples taken from the external surface of the slab ("sugaring", solid black line) and from internal surface ("sound", dashed black line) are reported in figure V.2. Porosity curves of unweathered ("Unheated" sample, dashed red line) and artificially weathered ("Heated" sample solid red line) marble taken from the quarry slab are reported for a direct comparison. Curves relative to Carrara marble slabs not chosen for the tests are not reported for clarity's sake.

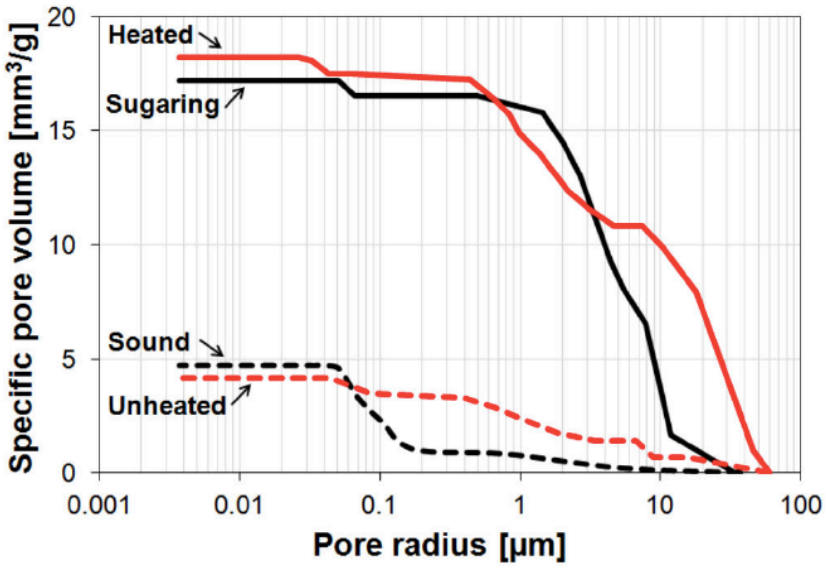

Figure V.2: Pore size distribution of external and internal surface of historic marble slab and of quarry samples, before and after artificial weathering by heating [20].

Morphology of marble samples before and after heating is in figure V.3.

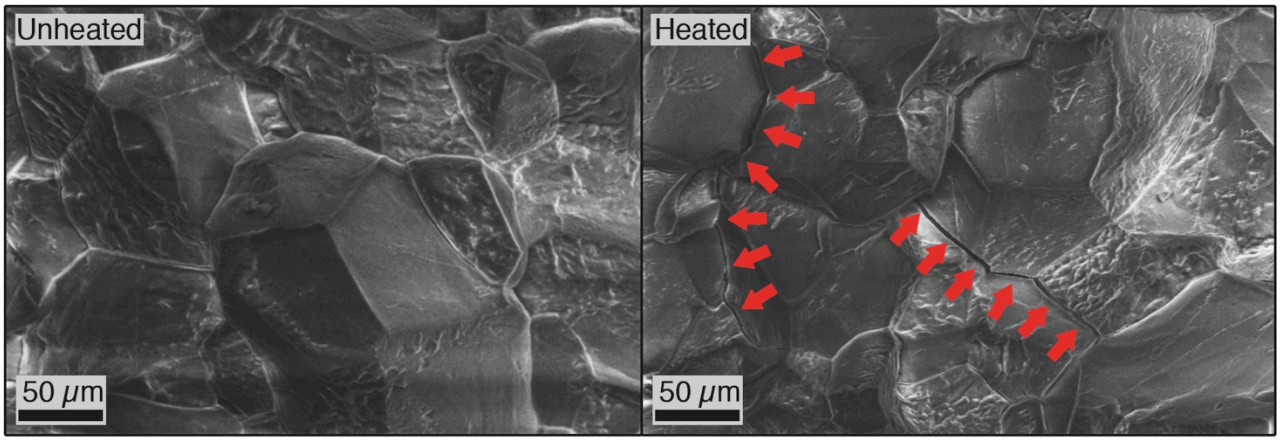

Figure V.3: Cracks opening as a result of heating (left) with respect to unheated reference (right).

V.3.2 Evaluation of the alternative consolidation procedures

Selection of the most promising HAP treating procedure was carried out by analyzing the composition and morphology of the phases that form as a result of the treatment. Morphology of the phases as assessed by SEM is displayed in figure V.4, while relevant Raman spectra are in figure V.5.

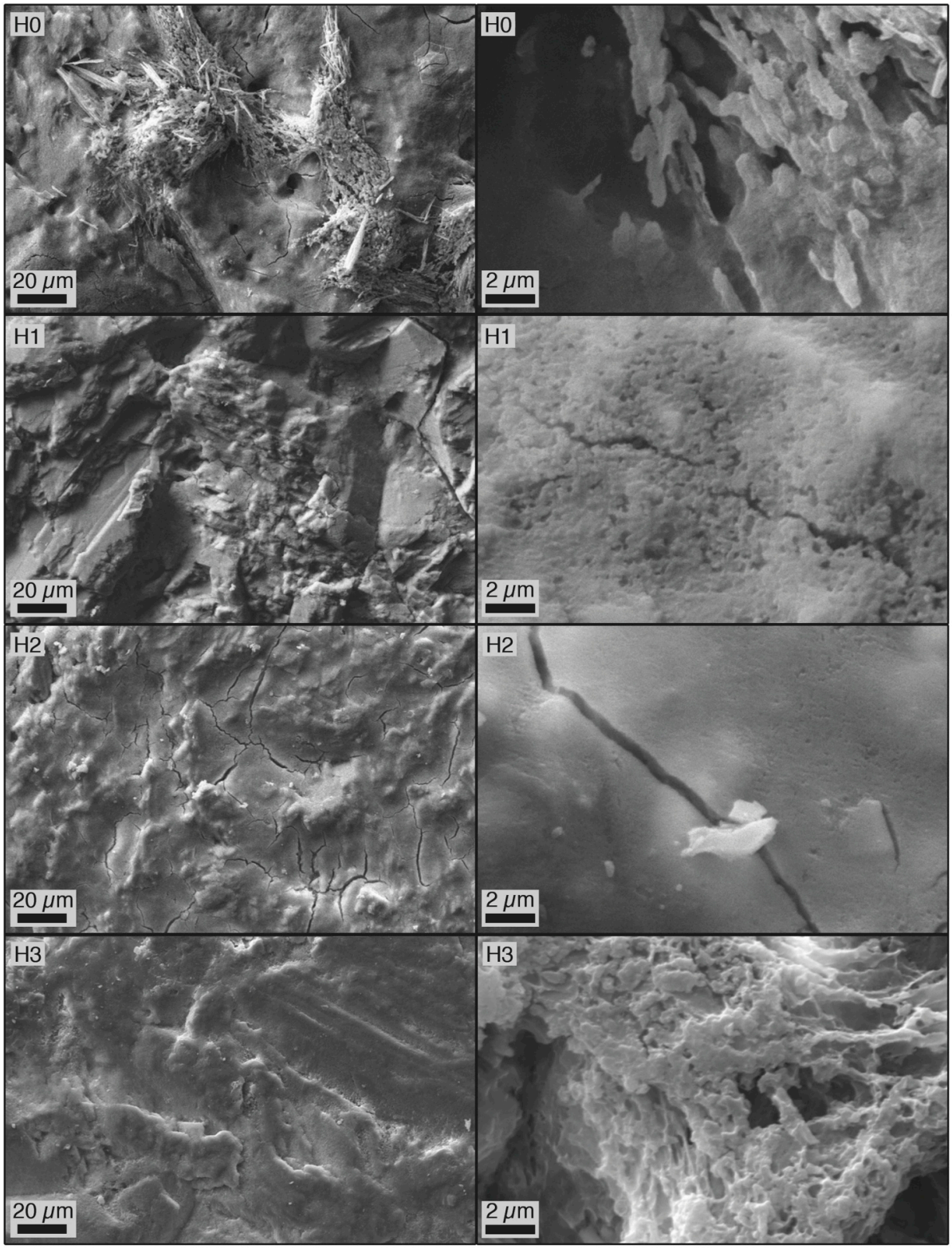

Figure V.4: SEM observation of treated surface of the specimens.

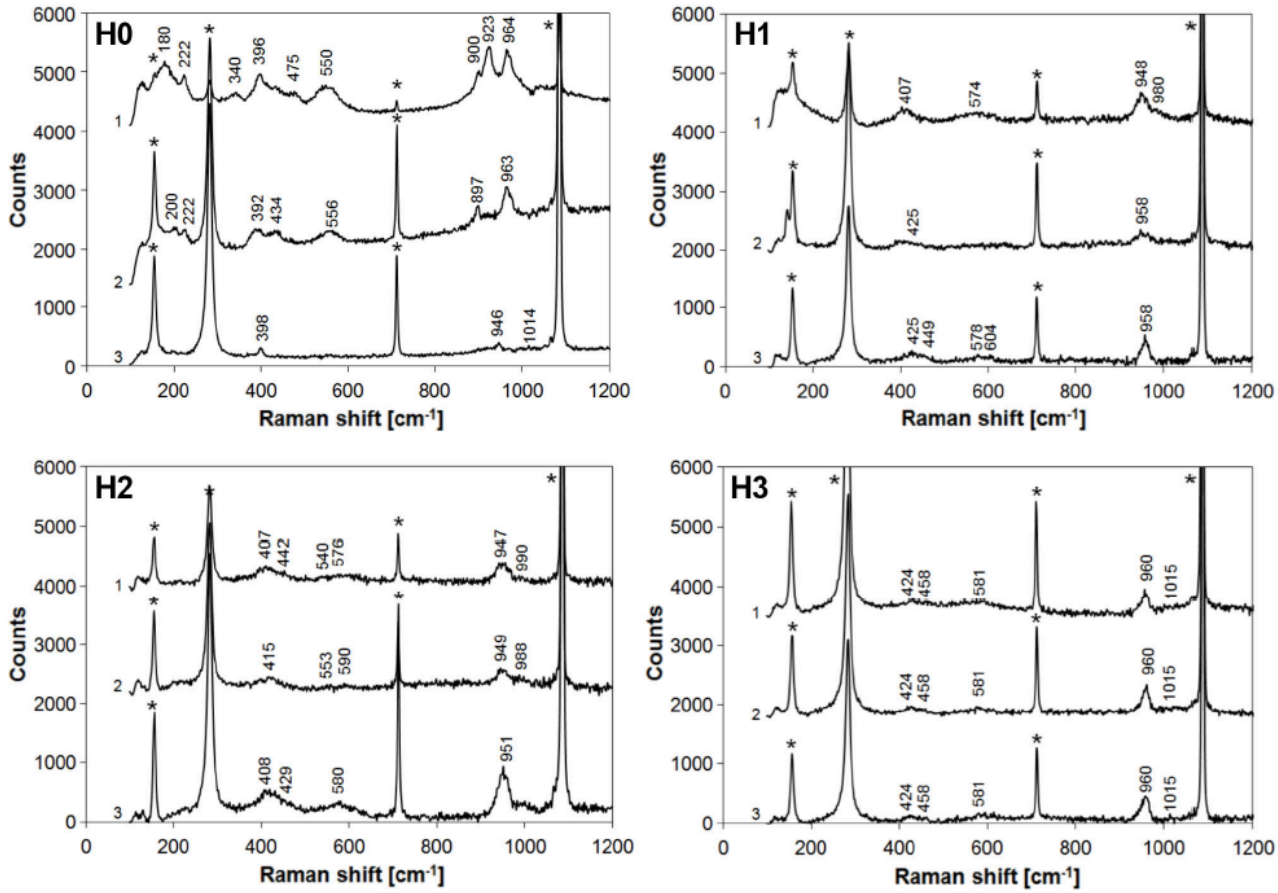

Figure V.5: Raman spectra of treated samples. In each figure, 3 spectra are reported for each treating conditions, in different positions in the samples [20].

For reasons detailed in section V.4.2, H1 and H2 treatments were chosen as the most promising and further characterized, in comparison with ES and AmOx.

V.3.3 Comparison with alternative treatments

Comparison between the chosen HAP based treatments, ES and AmOx was carried out both in terms of efficacy and compatibility of the treatments.

Regarding efficacy: morphology of treated samples' surface and of cross-sections is in figure V.6. Elemental composition maps (for relevant elements i.e. P for HAP treatments and Si for ES, both absent in the untreated substrate) are also reported. By SEM observations and EDS maps it was also possible to determine the penetration depth of the treatments.

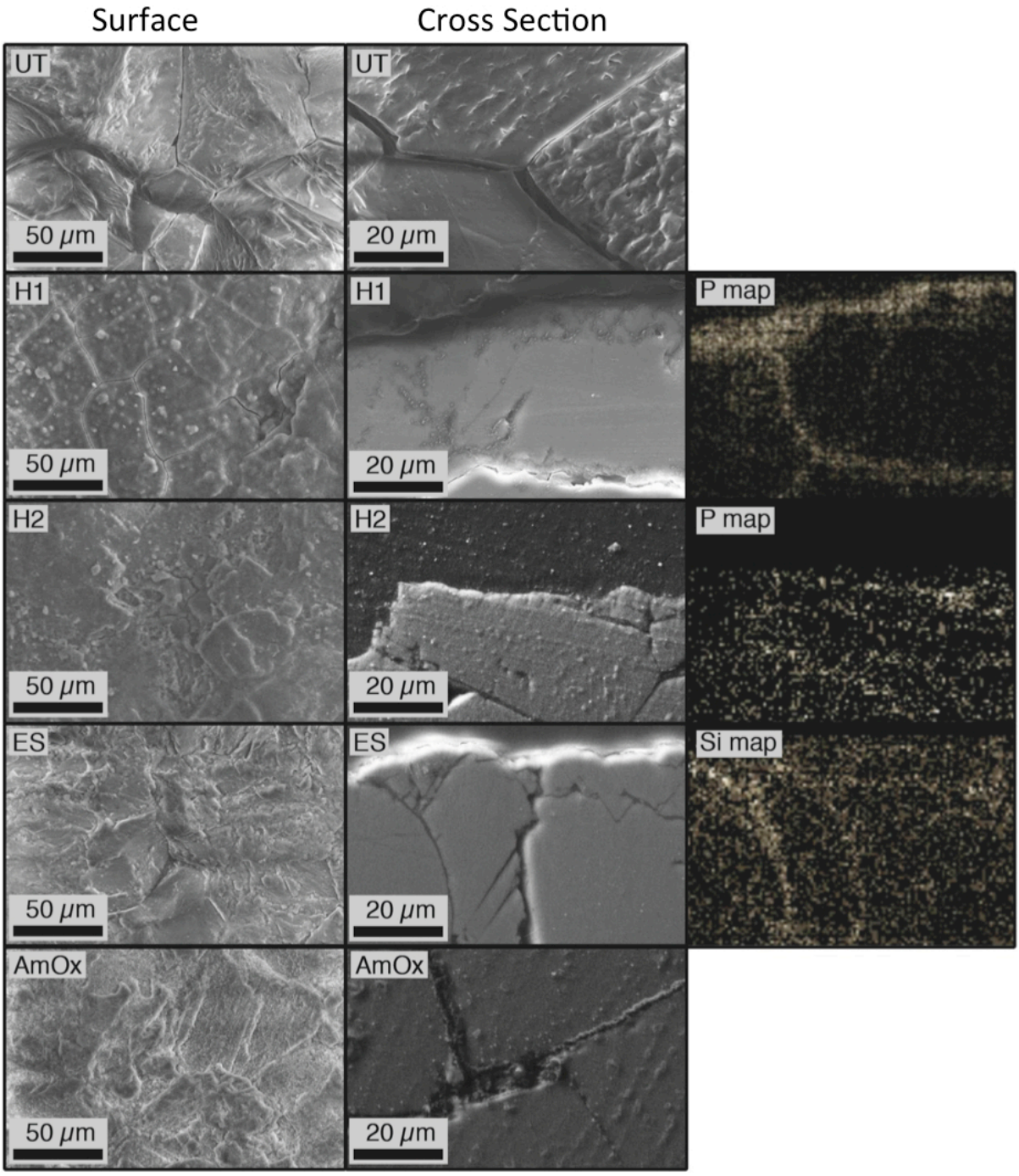

Figure V.6: Phase formation on specimens surface and in cross sections. Maps are referred to the adjacent cross section.

Mechanical properties in terms of UPV and resistance to pulverization, assessed by resistance to abrasion on H1, H2, ES and AmOx treated samples are reported in Table V.2.

		UT	H1	H2	ES	AmOx
UPV	[km/s]	0.8 (±0.0)	4.0 (±0.3)	4.3 (±0.2)	2.1 (±0.4)	1.4 (±0.1)
Δw-surface	[mg/cm^2]	14.2 (±1.5)	1.3 (±0.2)	2.0 (±0.6)	5.6 (±0.0)	2.1 (±0.2)
Δw-4 mm	[mg/cm^2]	10.4 (±0.3)	3.4 (±1.2)	4.4 (±1.0)	5.1 (±1.2)	-

Table V.2: Mechanical properties of untreated and treated samples, in terms of ultrasonic pulse velocity (UPV) and weight loss due to abrasion (Δw) on samples surface and at 4 mm depth [20].

Compatibility of the treatments was evaluated and compared. Microstructural alterations caused by each of the treatments is reported in figure V.7.

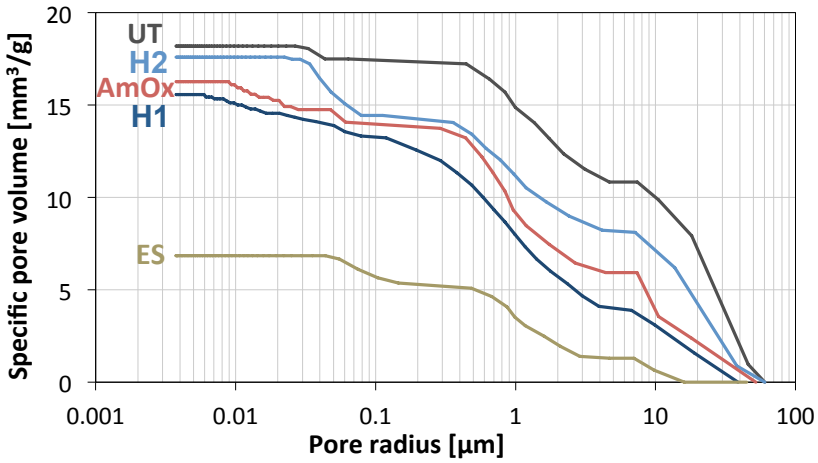

Figure V.7: Microstructural alterations as a result of each treating condition

Color alterations are listed in Table V.3. H1, H2 and AmOx cause alterations lower than human eye detectability threshold, **Δ**E being 1.9, 1.5 and 2.5, respectively, while ES, results in a dramatic darkening of the stone, **Δ**E being 12.2.

	L*	a*	b*	ΔE
UT	92.17	0.15	2.51	-
H1	90.30	0.02	2.09	1.9
H2	90.76	-0.30	1.90	1.6
ES	80.02	-0.14	2.63	12.2
AmOx	90.61	0.24	4.49	2.5

Table V.3: Color change in treated samples [20].

V.4. Discussion

V.4.1 Historic slab characterization and artificial weathering of the samples

In the historic slab, visual observation of different decay extent between the external and internal parts were confirmed by MIP analysis: “sound sample” exhibits low porosity and an average pore radius of about ~0.1 µm, while "sugaring" sample has a much higher total open porosity and generally coarser pores (average pore radius ~8 µm). Both increase in porosity and coarsening of pores indicate weathering due to repeated thermic cycles, that cause micro-crack formation between the grains [1,2].

A quarry slab of Carrara marble, prior to artificial weathering, exhibited microstructural features

similar to those of the “sound sample” (both in terms of total open porosity and pore size distribution), while after artificial weathering (see “heated” curve in figure V.2) it showed increased porosity and mean pore radius that closely resembles “sugaring” sample. These modifications are due to thermal stress causing anisotropic deformation of calcite and subsequent micro-cracks formation (figure V.3).

As a result, remarkable decreases are experienced in UPV, that switches from the condition of "progressive granular disintegration", to that of "complete structural damage" [32].

Based on the above described evaluations, the proposed procedure was considered effective for artificial weathering of samples and representative of real decay conditions on site.

V.4.2 Evaluation of the alternative consolidation procedures

Regarding morphology and nature of the newly formed phases (figures V.4 and V.5), evidence of CaP phases formation was obtained by Raman spectra. However, an indisputable identification was not possible in most of the cases, as no perfect match was obtained with bands of pure CaP references (references for Raman spectra of CaP phases were taken from literature data [34-42]). This problem could be mitigated by analyzing pure standards for each CaP phases in the same conditions and with the same instrument used for the tests; however, this was not possible at the present stage of the research, also considering the multitude of existing CaP phases and of substitutions that can be incorporated in their lattice (among the others, carbonate groups). In fact, impurities and substitutions can alter crystalline structure of CaPs, that though might differ from stoichiometric standards [43,44]. However, some considerations can be derived.

H0 sample surface is characterized by the presence of small and dispersed crystals over a coating characterized by porosity and presence of cracks (figure V.4). Bands assessed by Raman indicate presence of both CaP phases and unreacted DAP (see figure V.5): HAP formation is suggested by bands at 963-964 cm^{-1}, but the absence of other bands (such as that at 1049 cm^{-1}) make a conclusive identification not possible. Similarly, bands compatible with ACP and MCPA were detected, but their certain identification was not possible either.

In the case of H1 sample, no small crystals are detected over the Ca-P coating (Figure V.4) that is more uniform than in the case of H0 but still cracked and non continuous. Based on Raman spectra (Figure V.5), the phases formed after the treatment were identified as presumably TCP (spectrum 1, bands at 948 and 980 cm^{-1}) and OCP (spectra 2 and 3, bands at 958 cm^{-1}), even if OCP band at 1010 cm^{-1} could not be observed.

Sample H2 is covered by a thicker, more continuous and less porous coating. Even in this case cracks are detected (Figure V.4). From Raman spectrometry, the same phases as in sample H1 were

identified, i.e. TCP and OCP (Figure V.5).

In sample H3, a more continuous and less cracked Ca-P coating was obtained (Figure V.4). As revealed by Raman spectrometry, the main phase formed after this treatment seems to be OCP (Figure V.5).

The fact that all the examined layers are cracked might be ascribed to excessive thickness of the treated layer caused by very high concentration of the DAP solution, that makes it prone to drying cracks. Further studies aimed at reducing the concentration of the starting solution so as to reduce cracking, without affecting consolidant efficacy, are currently in progress. However, it must be borne in mind that the consequences of cracks in the consolidant layer are not as dramatic as they would be in case of a protective layer, where they would allow decay of the underlying substrate.

In light of the above described observations, H1 and H2 were selected as more promising and tested for the prosecution of the study because: (i) they lead to the formation of TCP and OCP, which are more soluble than HAP, but still much less soluble than calcite, hence they are not expected to dramatically affect consolidation efficacy; (ii) treatment H3 caused formation of an apparently continuous and non-cracked OCP coating over marble surface, but the relatively high concentration of $CaCl_2$ added to the DAP solution might possibly induce some competition between CaP phase formation on the marble surface and in solution, which might inhibit DAP solution absorption deep into marble micro-cracks (further studies are in progress to ascertain the kinetics of CaP phases formation).

V.4.3 Comparison with alternative treatments

Results on phase formation on the surface and in cross-sections after treatments H1 and H2 are reported in figure V.6.

Both treatments led to the formation of CaP phases on samples surface, treated layer being more cracked in case of H1. Both treatments result in a satisfactory penetration depth (about 20 mm, corresponding to the entire thickness of the samples) as denoted by the presence of phosphorous up to this depth (see EDS maps, figure V.6).

ES treatment causes the formation of a layer of silica gel on samples surface. Penetration depth (determined by EDS and visual observation) is 20 mm, as in the case of H1 and H2.

For both HAP and ES treatments, penetration depth visually assessed during treatment was confirmed by reaction products detection by SEM/EDS.

Instead, in AmOx samples, a penetration depth around 10-15 mm (anyhow lower than the thickness of the samples) was assessed by visual observation after application, while SEM highlighted the presence of newly formed crystals only on the treated surface and in its proximity (EDS could not

be performed as elemental composition of calcium oxalate is the same of calcite). This suggests that penetration depth of the product is very scarce. This might be due to the fact that AmOx reacts very quickly with the substrate and hence only water reached the penetration depth that was visually assessed.

In terms of UPV (see Table V.2), artificially weathered marble exhibits UPV = 0.8 km/s, corresponding to the state of "complete structural damage" according to [32]. Treatments H1 and H2 lead to increases up to 4.0 and 4.3 km/s, respectively (corresponding to an "increasing porosity" conservation state [32]), hence even enhancing the original “Sound” condition (UPV = 2.5 km/s).

ES and AmOx exhibited less remarkable efficacy, leading to increases in UPV, up to 2.1 km/s ("progressive granular disintegration" condition [32]) and 1.4 km/s ("complete structural damage" [32]), respectively.

The abrasion test (Table V.2) confirmed the superior efficacy of H1 and H2 with respect to ES and AmOx (weight loss by abrasion was reduced by ~10 and ~7 times as a result of H1 and H2 treatments, respectively, while a reduction by ~2 times was caused by ES). Results obtained by UPV and abrasion test indicate that ES was able to deposit silica-gel into cracks between the grains, but no chemical bonding was formed [45].

AmOx was as effective as H2 in improving abrasion resistance, despite its lower effect on UPV. However, due to excessive tendency to pulverization of the sample, it was impossible to cut a slice and repeat the test at 4 mm. This is consistent with the fact that calcium oxalate is formed only close to the treated surface and penetration depth is very limited, as assessed by SEM and found in the literature [46,47]. Except for AmOx, all treatments were capable of enhancing resistance to abrasion also at 4 mm depth (Table V.2). In samples treated by HAP (both H1 and H2), resistance gradually decreases with depth, hence indicating that no crusts were formed as a result of the treatments. Because the consolidant had fully saturated samples during application by brushing, this gradient also indicates that redistribution has occurred after treatment, leading to higher formation of CaP phases close to the evaporation surface, as in the case of globigerina limestone. A comparison study of redistribution in marble and globigerina limestone due to their different porosity is currently in progress.

Regarding compatibility, both HAP treatments, as well as AmOx, cause no substantial microstructural modifications in terms of total open porosity and pore size distribution (figure V.7), thus suggesting that no negative alterations should be expected in stone durability. ES, instead, causes a marked, even though not complete, pore occlusion because of its deposition in micro-cracks. For this reason, stone susceptibility to weathering might be increased.

Both HAP treatments and AmOx can be regarded as highly compatible, much more than ES.

However, the fact that AmOx results in very low microstructural alterations is also due to the fact that a very low penetration depth is achieved.

H1 and H2 also resulted in the lowest chromatic alterations, (**Δ**E being1.9 and 1.5, respectively, see Table V.3). All values but those of ES are below the threshold considered acceptable for cultural heritage conservation (**Δ**E = 5) and that of human eye detectability (**Δ**E = 3) [48]. ES, instead, causes a **Δ**E=12.3 alteration, mostly due to dramatic darkening of the stone, that is absolutely not to be considered compatible.

In view of all these considerations, H1 and H2 are more compatible than AmOx and, especially, ES. No substantial benefit was obtained by H2 with respect to H1, despite less cracking. Moreover, due to severe pulverization of the sample, leading to loss of a significant amounts of grains, it seems that millimolar dissolution of calcium ions can be regarded as negligible. For these reasons, despite H2 presenting some advantages, H1 was chosen as the most promising among the tested treatments.

V.5. Conclusions

In this chapter, different HAP-based treatments were compared to select the most promising treatment to be used in the following steps of the research. Efficacy and compatibility of the most promising formulations were evaluated in comparison with those of ES and AmOx treatments.

The following conclusions can be derived:

- The application of a 3M DAP solution followed by a limewater poultice, previously proposed for consolidation of porous limestone, allows to obtain low solubility CaP phases (TCP and OCP);
- Addition of millimolar amounts of $CaCl_2$ allows for reductions in cracking and porosity of the treated layer, but no relevant changes are assessed in its composition (TCP and OCP are obtained for 1 mM $CaCl_2$ addition, OCP for 3 mM $CaCl_2$ addition);
- When compared to ethyl silicate, both HAP based treatments exhibit better efficacy and, mostly, compatibility. In fact, ES causes remarkable microstructural alterations and incompatible color change;
- When compared to AmOx, both HAP treatments exhibit a much improved efficacy, especially in terms of penetration depth, that is insufficient in the case of AmOx, and slightly enhanced compatibility;
- Despite some decrease in cracks, $CaCl_2$ additions do not cause substantial benefits.

In view of these considerations, treatment H1 was selected as the most promising and used in the following stages of the research.

Acknowledgements

Dr. Francesca Ospitali (Dept. Industrial Chemistry “Toso Montanari", University of Bologna) is gratefully acknowledged for precious collaboration in Raman analyses. Elisa Scozia is acknowledged for collaboration in physical-mechanical tests.

"Museo Civico del Risorgimento di Bologna" (Museum of Italian Unification of the City of Bologna, encompassing the Monumental Cemetery), in particular Dr. Otello Sangiorgi and Dr. Roberto Martorelli, and the Superintendence for Architectural Heritage and Landscape of Bologna, Modena and Reggio Emilia (Arch. Leonardo Marinelli), are acknowledged for valuable collaboration.

Chapter references

[50] Sassoni E., Franzoni E., Sugaring marble in the Monumental Cemetery in Bologna (Italy): characterization of naturally and artificially weathered samples and first results of consolidation by hydroxyapatite. Appl Phys A Mater 117 (2014) 1893-1906

[51] Siegesmund S., Ullemeyer K., Weiss T., Tschegg E.K., Physical weathering of marbles caused by anisotropic thermal expansion. Int J Earth Sci 89 (2000) 170-182

[52] Skoulikidis T., Vassiliou P., Tsakona K., Surface consolidation of Pentelic marble – Criteria for the selection of methods and materials - The Acropolis case. Environ Sci & Pollut Res 12 (2005) 28-33

[53] Hansen E., Dohene E., Fidler J., Larson J., Martin B., Matteini M., Rodrìguez-Navarro C., Pardo E.S., Price C., de Tagle A., Teutonico J. M., Weiss N., A review of selected inorganic consolidants and protective treatments for porous calcareous materials. Reviews in conservation 4 (2003) 13-25

[54] Wheeler G.S., Alkoxysilanes and the Consolidation of Stone (Research in conservation), The Getty Conservation Institute, Los Angeles, 2005

[55] Verges-Belmin V., Orial G., Garnier D., Bouineau A., Coignard R., Impregnation of badly decayed Carrara marble by consolidating agents: Comparison of seven treatments, In: La conservation des monuments dans le bassin metiterraneen: Actes du 2° symposium international, Geneve, 19-21/11/1991, 1992, 421-437

[56] Matteini M., Inorganic treatments for the consolidation and protection of stone artefacts. Conserv Sci Cult Herit 8 (2008) 13-27

[57] Charola A.E., Centeno S.A., Normandin K., The New York Public Library: Protective treatment for sugaring marble. Journal of Architectural Conservation 16 (2010) 29-44

[58] Sassoni E., Naidu S., Scherer G.W., The use of hydroxyapatite as a new inorganic consolidant for damaged carbonate stones. J Cult Herit 12 (2011) 346-355

[59] Sassoni E., Franzoni E., Pigino B., Scherer G.W., Naidu S., Consolidation of calcareous and siliceous sandstones by hydroxyapatite: comparison with a TEOS-based consolidant. J Cult Herit 14S (2013) e103-e108

[60] Naidu S., Liu C., Scherer G.W., New techniques in limestone consolidation: Hydroxyapatite based consolidant and the acceleration of hydrolysis of silicate-based consolidants. Journal of Cultural Heritage 16 (2015) 94-101

[61] Sassoni E., Graziani G., Franzoni E., An innovative phosphate-based consolidant for limestone. Part 1: Effectiveness and compatibility in comparison with ethyl silicate. Constr Build Mater 102 (2016) 918-930

[62] Sassoni E., Graziani G., Franzoni E., An innovative phosphate-based consolidant for limestone. Part 2: Durability in comparison with ethyl silicate. Constr Build Mater 102 (2016) 931-942

[63] Naidu S., Scherer G.W., Development of hydroxyapatite films to reduce the dissolution rate of marble, In: Proceedings of 12th International Congress on Deterioration and Conservation of Stone, New York City (USA), 22-26 October 2012, p. 1-9, http://iscs.icomos.org/pdffiles/NewYorkConf/naidsche.pdf

[64] Naidu S., Scherer G.W., Nucleation, growth and evolution of calcium phosphate films on calcite. J Colloid Interf Sci 435 (2014) 128-137

[65] Franzoni E., Sassoni E., Scherer G.W., Naidu S., Artificial weathering of stone by heating. J Cult Herit 14S (2013) e85-e93

[66] Sassoni E., Franzoni E., Influence of porosity on artificial deterioration of marble and limestone by heating. Appl Phys A-Mater 115 (2014) 809–816

[67] Wheeler G.S., Fleming S.A., Ebersole S., Evaluation of some current treatments for marble, In: La conservation des monuments dans le bassin mediterraneen: Actes du 2° symposium international, Geneve, 19-21/11/1991, 1992, 439-443

[68] Sassoni E., Franzoni E., Consolidation of Carrara marble by hydroxyapatite and behavior after thermal ageing, In: Toniolo L. et al. (Eds), Built Heritage: Monitoring Conservation Management, Research for Development, Springer International Publishing, 2015, p. 379-389, DOI: 10.1007/978-3-319-08533-3_32

[69] Sassoni E., Graziani G., Franzoni E., Repair of sugaring marble by ammonium phosphate: comparison with ethyl silicate and ammonium oxalate and pilot application to historic artifact. Materials and Design 88 (2015) 1145-1157

[70] Kamiya M., Hatta J., Shimida E., Ikuma Y., Yoshimura M., Monma H., AFM analysis of initial stage of reaction between calcite and phosphate. Mater Sci Eng B 111 (2004) 226-231

[71] Dorozhkin S.V., Calcium orthophosphates - Occurrence, properties, biomineralization, pathological calcifications and biomimetic applications. Biomatter 1 (2011) 121-164

[72] Naidu S., Sassoni E., Scherer G.W., New treatment for corrosion-resistant coatings for marble and consolidation of limestone, in Stefanaggi M., Vergès-Belmin V. (Eds), "Jardins de Pierres– Conservation of stone in Parks, Gardens and Cemeteries", Paris (F) 22-24 June 2011, p.289-294

[73] Ferreira Pinto A.P., Delgado Rodrigues J., Stone consolidation: The role of treatment procedures. J Cult Herit 9 (2008) 38-53

[74] Sassoni E., Franzoni E., Scherer G.W., Naidu S., Consolidation of a porous limestone by means of a new treatment based on hydroxyapatite, 12th International Congress on Deterioration and Conservation of

Stone, Columbia University, New York City (USA), 22-26 October 2012, p. 1-11, http://iscs.icomos.org/pdf-files/NewYorkConf/sassetal.pdf

[75] Franzoni E., Graziani G., Sassoni E., TEOS-based treatments for stone consolidation: acceleration of hydrolysis-condensation reactions by poulticing. J Sol-Gel Sci Tech 74 (2015) 398-405

[76] Mudronja D., Vanmeert F., Hellemans H., Fazinic S., Janssens K., Tibljas D., Rogosic M., Jakovljevic S., Efficiency of applying ammonium oxalate for protection of monumental limestone by poultice, immersion and brushing methods. Appl Phys A- Mater 111 (2013) 109-119

[77] Doherty B., Pamplona M., Selvaggi R., Miliani C., Matteini M., Sgamellotti A., Brunetti B., Efficiency and resistance of the artificial oxalate protection treatment on marble against chemical weathering. Appl Surf Sci 253 (2007): 4477-4484

[78] Weiss T., Rasolofosaon P.N.J., Siegesmund S., Ultrasonic wave velocities as a diagnostic tool for the quality assessment of marble, In: Siegesmund S., Weiss T., Vollbrecht A., Natural stone, weathering phenomena, conservation strategies and case studies, Geological Society, London, Special Publications, 205 (2002) 149-164

[79] Luque A., E. Ruiz-Agudo, G. Cultrone, E. Sebastiàn, S. Siegesmund, Direct observation of microcrack development in marble caused by thermal weathering. Environ Earth Sci 62 (2011) 1375-1386

[80] Malaga-Starzec K., Åkesson U., Lindqvist J.E., Schouenborg B., Microscopic and macroscopic characterization of the porosity of marble as a function of temperature and impregnation. Constr Build Mater 20 (2006) 939-947

[81] Pamplona M., Simon S., Ultrasonic pulse velocity - A tool for the condition assessment of outdoor marble sculptures, Proceedings of 12th International Congress on Deterioration and Conservation of Stone, New York City (USA), 22-26 October 2012, p. 1-13, http://iscs.icomos.org/pdf-files/NewYorkConf/pampsimo.pdf

[82] Yavuz H., Ugur I., Demirdag S., Abrasion resistance of carbonate rocks used in dimension stone industry and correlations between abrasion and rock properties. Int J Rock Mech Min Sci 45 (2008) 260–267

[83] Koutsopoulos S., Synthesis and characterization of hydroxyapatite crystals: A review study on the analytical methods. J Biomed Mater Res 15 (2002) 600-612

[84] Yamini D., Devanand Venkatasubbu G., Kumar J., Ramakrishan V., Raman scattering studies on PEG funcionalized hydroxyapatite nanoparticles. Spectrochim Acta A 117 (2014) 299-303

[85] Kodati V.R., Tomasi G.E., Turumin J.L., Tu A.T., Raman spectroscopic identification of phosphate-type kidney stones. Appl Spectrosc 45 (1991) 581-583

[86] Saber-Samandaria S., Alamarab K., Saber-Samandaric S., Calcium phosphate coatings: Morphology, micro-structure and mechanical properties. Ceram Int 40 (2014) 563–572

[87] Karampas I.A., Kontoyannis C.G., Characterization of calcium phosphates mixtures. Vib Spectrosc 64 (2013) 126– 133

[88] Xu J., Gilson D.F.R., Butler I.S., FT-Raman and high pressure FT-infrared spectroscopic investigation of monocalcium phosphate monohydrate $Ca(H_2PO_4)2{\cdot}H_2O$. Spectrochim Acta A 54 (1998) 1869-1878

[89] http://rruff.info/

[90] Sun J., Wu Z., Cheng H., Zhang Z., Frost R.L., A Raman spectroscopic comparison of calcite and dolomite. Spectrochim Acta A 117 (2014) 158-162

[91] Kloprogge J.T., Frost R.L., Raman microscopy at 77 K of natural gypsum CaSO4·2H2O. J Mater Sci Lett 19 (2000) 229-231

[92] Boanini E., Gazzano M., Bigi A., Ionic substitutions in calcium phosphates synthesized at low temperature. Acta Biomater 6 (2010) 1882-1894

[93] Supova M., Substituted hydroxyapatites for biomedical applications: A review. Ceram Int 41 (2015) 9203-9231

[94] Scherer G.W., Wheeler G.S., Silicate consolidants for stone. Key Eng Mater 391 (2009) 1-25

[95] Conti C., Colombo C., Matteini M., Reailini M., Zerbi Z., Micro-Raman mapping on polished cross sections: a tool to define the penetration depth of conservation treatment on cultural heritage. J Raman Spectrosc 41 (2010) 1254-1260

[96] Conti C., Colombo C., Dellasega D., Matteini M., Reailini M., Zerbi Z., Ammonium oxalate treatment: Evaluation by μ-Raman mapping of the penetration depth in different plasters. J Cult Herit 12 (2011) 372-379

[97] Franzoni E., Sassoni E., Graziani G., Brushing, poultice or immersion? Role of the application technique on the performance of a novel hydroxyapatite-based consolidating treatment for limestone. J Cultl Herit16 (2015) 173–184

Chapter VI: Consolidation of marble: experiments on real marble artworks

Research Aims

In the previous chapter, a procedure was set up for consolidation of sugaring marble in laboratory conditions. However, application of a consolidant on real artworks is much more complicated, as samples might exhibit unknown weathering level. Moreover, contaminants might be present, possibly interacting with the reaction of the consolidant.

For this reason, application was tested on a real historic slab. The slab was initially located in Certosa Cemetery in Bologna, a monumental cemetery built at the beginning of the XIX century, where several marble tombs of great historic and artistic relevance are present, many of which in a dramatic weathering condition that often leads to rupture and detachment of entire slabs. Due to the lack of suitable alternatives for their consolidation, many of the historic fragments are stored in storage rooms.

VI.1 Introduction

Sugaring is a very relevant phenomenon affecting marble artworks on site [1,2]. In the previous chapter HAP treatment has shown good efficacy and compatibility for consolidation of sugaring marble on artificial weathered samples. The outcome of consolidant application on real historic artifacts, however, is much more uncertain than it is in laboratory samples, as contaminants might be in the stone, and they might interact with penetration and reaction of the consolidant. This is a critical issue, considering that consolidating treatments are generally irreversible [3-6].

The presence of contaminants is particularly relevant in the case of HAP treatment because of two main reasons: first, HAP easily absorbs foreign ions [7,8], to such an extent that it has recently been proposed for purification of water. Foreign ions can either be adsorbed onto the crystal surface or incorporated into its lattice and generally affect HAP crystallinity, crystal size and solubility [9,10]. Second, other soluble calcium phosphates phases might form instead of HAP from reaction of DAP with calcium ions [11,12]: formation of these phases instead of HAP can be favored by alteration of treating parameters and mostly of pH, starting solution supersaturation, temperature, presence of foreign ions etc. [13-15].

Historic artifacts in the great majority of the cases are affected by the presence of crusts, salts and deposits, that generally cannot be completely removed prior to consolidation and make the control of phase formation as a result of the HAP treatment even more critical [15].

In light of these considerations, testing HAP efficacy on laboratory samples might not be sufficient to predict the outcome of consolidation on real historic artifacts. For this reason, in view of HAP application on site, application on naturally weathered samples was carried out. The same slab

previously characterized to investigate weathering conditions of marble on site was now used for the application of DAP solution. Special attention was devoted to the correct identification of the phases that form as a result of the treatment and the morphology of the treated layer.

VI.2. Materials and Methods

VI.2.1. Materials

All tests were performed onto the historic slab previously characterized. For a detailed characterization of the slab and its weathering conditions see chapter V (§V.3.1). The detached slab used in this study was available thanks to a collaboration between the DICAM Department of the University of Bologna, the Museum of Italian Unification of the City of Bologna (encompassing the Monumental Cemetery) and the Superintendence for Architectural Heritage and Landscape of Bologna, Modena and Reggio Emilia.

VI.2.2. Methods

To evaluate the treatment efficacy and compatibility, comparison with an untreated reference was needed: for this reason, only two-thirds of the slab were treated while the other part was left untreated, as described in figure VI.1.

The most promising treating procedure identified in the previous chapter (namely "H1") was applied on the surface that was previously covered by the black crust and now affected by severe sugaring.

The evaluation of HAP-treatment was performed partially by repeating the same tests used for artificially weathered samples and by additional tests.

The slab had already been characterized in terms of morphology and microstructure, prior to the tests. However, a mechanical characterization was also performed to evaluate the effectiveness of the treatment: UPV was evaluated across the slab, before and after consolidation, in two orthogonal directions: 3 cm thickness and 9 cm height (see figure VI.1). Several measuring points were taken, so as to obtain a sort of tomographic representation of UPV.

Resistance to abrasion was neglected because non-destructive tests were necessary. Evaluation of sugaring extent before and after treatment was hence evaluated by non-destructive scotch tape test (STT), that is largely diffused in the conservation practice for assessing consolidant effectiveness, also in situ, even though it is not included in international standards [16]. It was performed as described in figure VI.1 on both treated and untreated area, by means of a commercial tape (about 6 cm^2 area). Pieces were peeled off with a rapid and constant action three minutes after application by means of steel pincers, maintaining a peel angle of about 90°. The amount of removed material was then expressed as weight loss per unit area, weight loss being determined by weighing scotch pieces

before and after the test, with a resolution of 0.01 mg. In both untreated and treated parts, three tests were carried out in the same position, as this is the minimum number of tests required for assessing a consolidant efficacy [16].

Microstructural alterations caused by the treatment were assessed by MIP on small fragments taken by chisel (pore size distribution before treatment was discussed in the previous chapter §V.3).

Morphology and composition of the phases were assessed by SEM/EDS as in §V.2.2. In this case it was possible to introduce the whole slab in the SEM chamber (areas previously subjected to STT were avoided). Observations were made in low vacuum mode so that the samples did not need to be made conductive. The newly formed CaP phases were analyzed by Raman spectrometry, performed in combination with both SEM and OM (cf. § 3.1.2). Identification of Raman bands was performed based on literature data [17-25].

VI.3. Results [1]

Results of UPV are in Figure VI.1, expressed in terms of percentage amount of the maximum UPV value in each direction, so as to better show the parts that are more affected by weathering. Maximum UPV values were 4.1 km/s in the perpendicular direction (condition of "increasing porosity" according to [26]) and 5.8 km/s in the parallel direction ("unweathered" condition according to [26]). Lowest values, instead, were measured in the most external parts, namely 3.0 km/s (condition of "progressive granular disintegration" [26]).

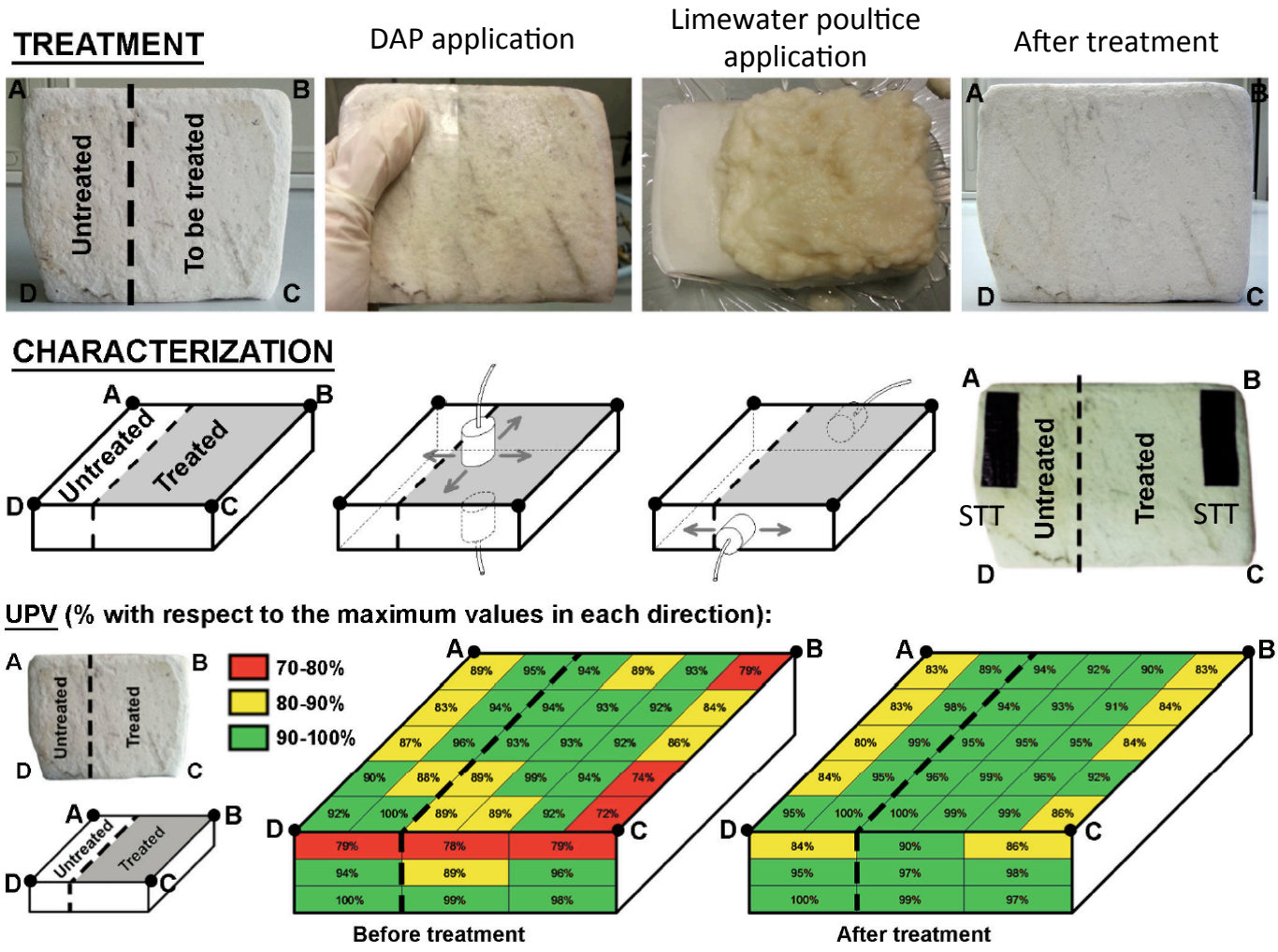

Figure VI.1: Treating and testing scheme in the historic slab. UPV distribution in the marble slab, before and after consolidation is also reported.

As weathering conditions of the slab were quite nonuniform, the part less severely affected by weathering was chosen to be left untreated.

UPV values after treatment are in figure VI.1. UPV in treated parts is highly improved so that “red areas”, corresponding to the most severe weathering conditions, are no longer present in any part of the slab. Some increase in UPV was also registered in the untreated areas in proximity of the part where consolidant was applied, presumably because of some spreading of the consolidant inside

cracks.

STT results before and after treatment are in figure VI.2.

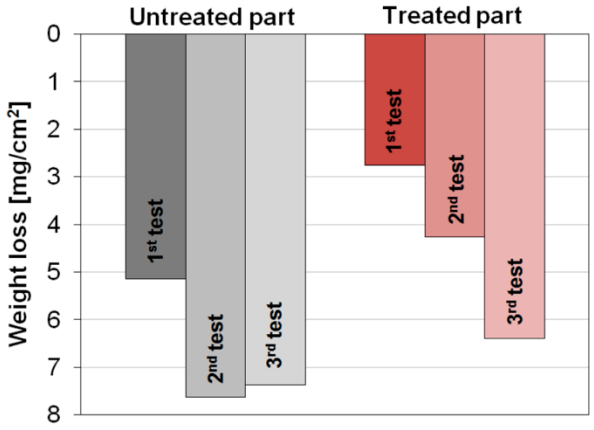

Figure VI.2: STT results before and after treatment. For both untreated and treated area, three consecutive tests were performed in the same positions.

Microstructure and morphology of the stone slab before treatment are discussed in the previous chapter (§). Pore size distribution in the treated and untreated area is in figure VI.3.

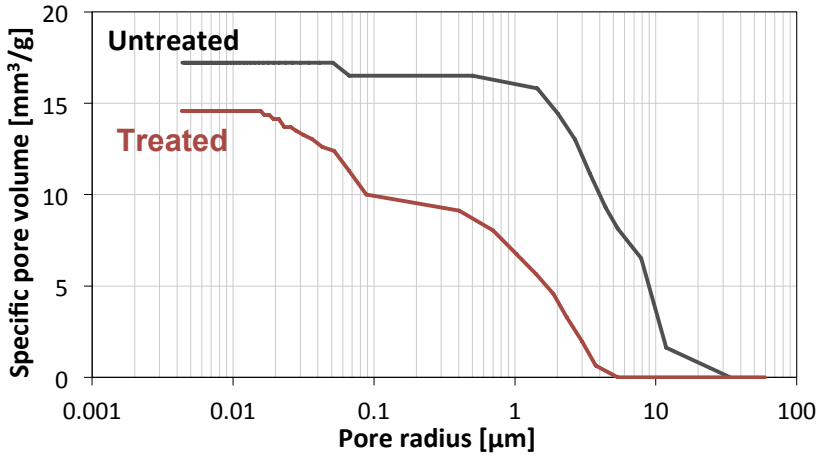

Figure VI.3: Pore size distribution in untreated and treated areas of the slab

Color change was measured: a $\Delta E = 2.7$ value was registered after treatment. Color parameters before and after treatment are in Table VI.1.

	L*	a*	b*	ΔE
Untreated	85.95	-0.19	6.46	-
Treated	88.02	-0.28	4.71	2.7

Table VI.1 Color change after treatment

Morphology and phase composition of the treated layer, as assessed by SEM and Raman spectrometry, respectively, are reported in figure VI.4 and VI.5. The treated layer is largely cracked and composed by big crystals. Bands at 960-963 cm^{-1} and 1050-1051 cm^{-1} were detected by Micro-Raman spectrometry, indicating formation of HAP.

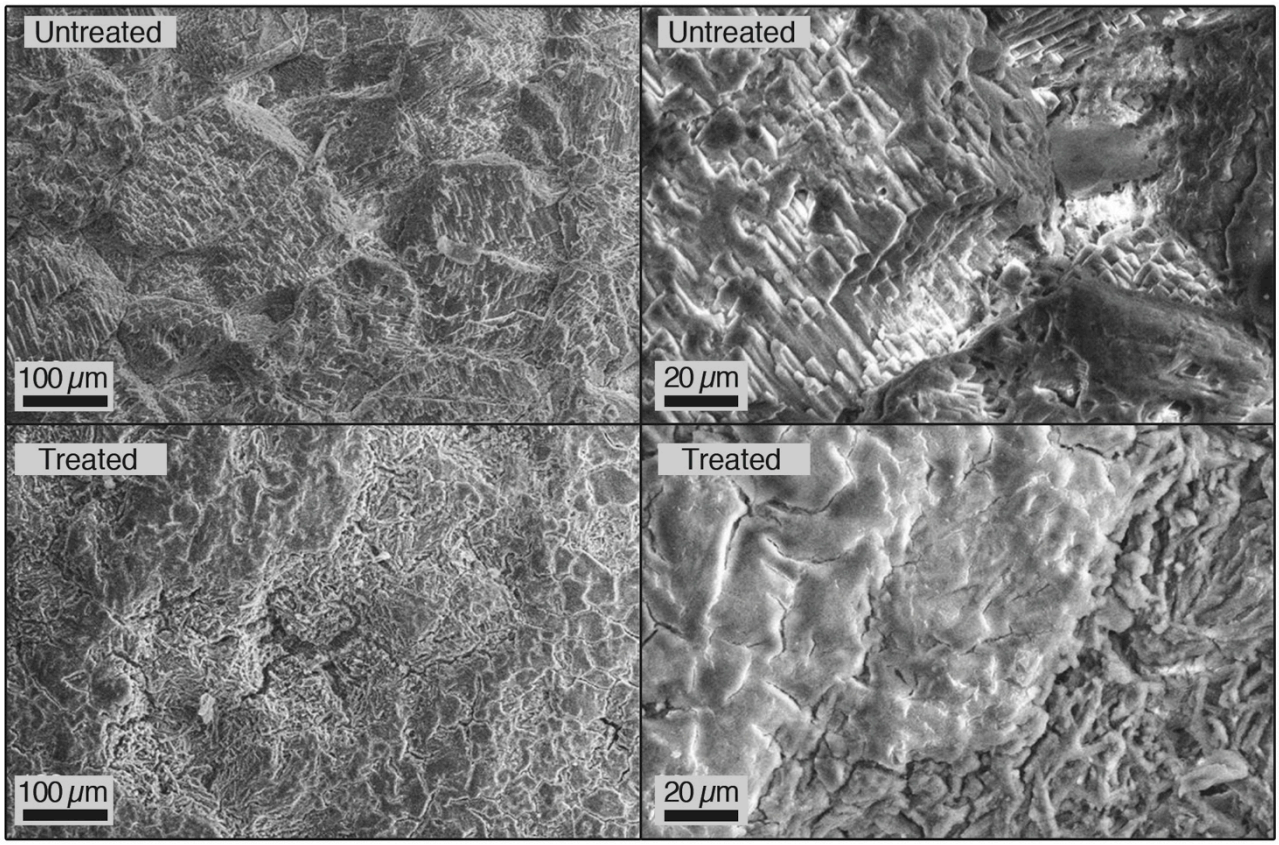

Figure VI.4: Morphology of marble slab surface before and after treatment

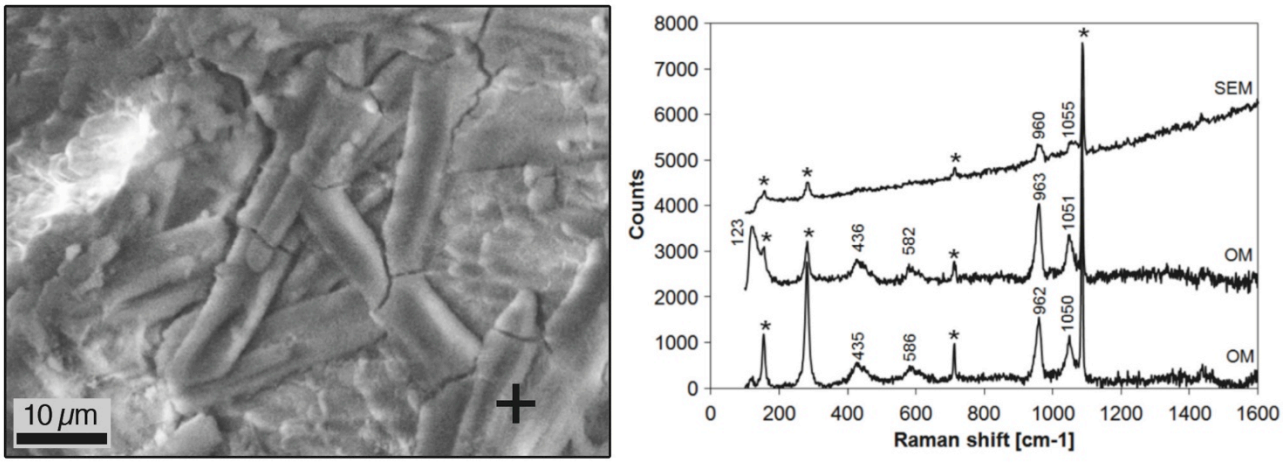

Figure VI.5: Phase composition of the treated samples

VI.4. Discussion

Prior to the treatment, higher UPV values (corresponding to less severe weathering conditions) were registered in the areas that were originally more distant from the slab edges (figure V.1). In fact in the edges, more exposed to thermal weathering, UPV values were minimum and a condition of "progressive granular disintegration" [26] was assessed.

A difference in UPV in the two perpendicular directions was registered: this might be due to both anisotropy of marble and to the fact that measurements perpendicular to the slab thickness are more affected by severe disaggregation of the superficial layer.

After treatment, remarkable increases were registered in UPV (figure VI.1), the most significant increases being assessed in the areas that were previously more affected by weathering. It is noteworthy that almost all areas of the slab exhibited UPV corresponding to “unweathered” condition, including those that were previously more weathered. UPV increase was also measured in the areas of the slab that were not directly treated but located in the proximity of the consolidated area: this is due to DAP migration towards this area as a consequence of its penetration in the cracks.

STT (figure VI.2) confirms the good efficacy of the treatment: in the first test, materials loss by peeling is almost doubled in the untreated part, indicating that HAP treatment is effective in bonding loose grains.

When test was repeated in the untreated area, slightly higher material loss was registered, possibly due to some weakening caused by the first test [16]. In the treated area, the material removed from repeating the test on the same zone progressively increased as well, though remaining lower than that of the untreated area. This might raise concerns about consolidant distribution in depth; however, this is not expected to be an issue, as previous abrasion tests were carried out and indicated a good penetration depth of the consolidant [15].

The remarkable increase in mechanical properties is made even more relevant by the fact that the untreated part was initially less weathered than that left untreated (figure VI.1): in fact, slab edges exhibited remarkably different decay levels, hence all results concerning treatment efficacy are underestimated.

Regarding microstructural alterations (figure VI.3), no significant changes in pore size distribution were registered after treatment, total open porosity being only slightly diminished (from 5.0% to 3.8%).

Chromatic alterations caused by HAP treatment were below the acceptability threshold (table VI.1). ΔE value, however, was higher than that assessed on laboratory samples, possibly due to darker color of the original material (HAP tends to increase lightness parameter): however, the treatment

can be definitely regarded as compatible.
In light of these results, efficacy and compatibility assessed on artificially weathered samples were confirmed by data on the real historic artifact.
Instead, morphology of the treated layer (figure VI.4) and composition of the newly formed phases (figure VI.5), are remarkably different from those assessed in laboratory samples (cfr. figure V.4, figure V.5). A thick, largely cracked coating was obtained, characterized by formation of large crystals. Raman spectrometry indicated that these crystals are composed of HAP. HAP, in particular, was the only phase detected by SEM-Raman and OM-Raman: no OCP nor TCP, that were the phases formed by the very same treatment on laboratory specimens, were detected.
This difference is ascribed essentially to two different reasons: some gypsum crystals were detected by Raman also after cleaning of the slab: gypsum is highly soluble compared to calcite and might have acted as an additional Ca^{2+} source, thus mimicking $CaCl_2$ additions. Moreover, the slab is characterized by high roughness. Previous studies of calcium phosphate nucleation on calcite indicate that surface roughness and presence of defects highly influence HAP growth [27].
In the previous chapter Ca^{2+} addition alone did not favor HAP formation, but only reduced cracking: this indicates that it was the combination of these two conditions, and not one of the two factors alone, to favor HAP formation.

VI.5 Conclusions

In this chapter, consolidation of marble by means of an HAP-based treatment, previously set up, was tested on a real historic artifact, naturally weathered and exhibiting sugaring and by the presence of a black crust.
It was demonstrated that efficacy and compatibility of the treatment, previously assessed on artificially weathered samples, are confirmed, even though slight differences can be found in the treatment performance, in terms of chromatic alterations.
However, phases that originate from the treatment, as well as the morphology of the treated layer are remarkably different from those obtained on artificially weathered, non-contaminated, samples. In particular, it seems that the combination of higher surface roughness together with presence of gypsum that acts as a Ca^{2+} ions source might favor HAP formation instead of soluble phases.

Acknowledgements

I would like to thank the "Museo Civico del Risorgimento di Bologna" (Museum of Italian Unification of the City of Bologna, encompassing the Monumental Cemetery), in particular Dr. Otello Sangiorgi and Dr. Roberto Martorelli, and the Superintendence for Architectural Heritage and Landscape of Bologna, Modena and Reggio Emilia (Arch. Leonardo Marinelli), for valuable

collaboration.
Dr. Francesca Ospitali (Dept. Industrial Chemistry “Toso Montanari", University of Bologna) is gratefully acknowledged for precious collaboration in Raman analyses.
M.Eng. Elisa Scozia is acknowledged for collaboration in physical-mechanical tests.

Chapter references

[1] Sassoni E., Franzoni E., Sugaring marble in the Monumental Cemetery in Bologna (Italy): characterization of naturally and artificially weathered samples and first results of consolidation by hydroxyapatite. Appl Phys A-Mater 117(2014) 1893-1906

[2] Siegesmund S., Ullemeyer K., Weiss T., Tschegg E.K., Physical weathering of marbles caused by anisotropic thermal expansion. Int J Earth Sci, 89 (2000) 170-182

[3] Scherer G.W., Wheeler G.S., Silicate consolidants for stone. Key Eng Mater 391 (2009) 1-25

[4] Tulliani J.M., Formia A., Sangermano M., Organic-inorganic material for the consolidation of plaster. J Cult Herit 12 (2011) 364-371

[5] Maravelaki-Kalaitzaki P., Kallithrakas-Kontos N., Korakaki D., Agioutantis Z., Maurigiannakis S., Evaluation of silicon-based strengthening agents on porous limestones. Progr Org Coat 57 (2006) 140-148

[6] Maravelaki-Kalaitzaki P., Kallithrakas-Kontos N., Agioutantis Z., Maurigiannakis S., Korakaki D., A comparative study of porous limestones treated with silicon-based strengthening agents. Progr Org Coat 62 (2008) 49-60

[7] Kanno C.M., Sanders R.L., Flynn S.M., Lessard G., Myneni S.C.B., Novel apatite-based sorbent for defluoridation: synthesis and sorption characteristics of nano-micro-crystalline hydroxyapatite-coated limestone. Envir Sci Tec 48 (2014) 5798-5807

[8] Shanika Fernando M., De Silva R.M., Nalin de Silva K.M., Synthesis, characterization, and application of nano hydroxyapatite and nanocomposite of hydroxyapatite with granular activated carbon for the removal of Pb^{2+} from aqueous solutions. Appl Surf Sci 351 (2015) 95-103

[9] Boanini E., Gazzano M., Bigi A., Ionic substitutions in calcium phosphates synthesized at low temperature, Acta Biomater 6 (2010) 1882-1894

[10] Supova M., Substituted hydroxyapatites for biomedical applications: A review, Ceram Int 41 (2015) 9203-9231

[11] Sassoni E., Naidu S., Scherer G.W., The use of hydroxyapatite as a new inorganic consolidant for damaged carbonate stones. J Cult Herit 12 (2011) 346-355

[12] Dorozhkin S.V., Calcium orthophosphates - Occurrence, properties, biomineralization, pathological calcifications and biomimetic applications. Biomatter 1 (2011) 121-164

[13] Naidu S., Liu C., Scherer G.W., New techniques in limestone consolidation: Hydroxyapatite based consolidant and the acceleration of hydrolysis of silicate-based consolidants. J Cult Herit 16 (2015) 94-101

[14] Sassoni E., Graziani G., Franzoni E., An innovative phosphate-based consolidant for limestone. Part 1: Effectiveness and compatibility in comparison with ethyl silicate. Constr Build Mater 102 (2016) 918-930

[15] Sassoni E., Graziani G., Franzoni E., Repair of sugaring marble by ammonium phosphate:

comparison with ethyl silicate and ammonium oxalate and pilot application to historic artifact. Materials and Design 88 (2015) 1145-1157

[16] Drdcký M., J. Lesàk, S. Rescic, Z. Sl.žkov., P. Tiano, J. Valach, Standardization of peeling tests for assessing the cohesion and consolidation characteristics of historic stone surfaces. Mater and Struct 45 (2012) 505-520

[17] Koutsopoulos S., Synthesis and characterization of hydroxyapatite crystals: A review study on the analytical methods. J Biomed Mater Res 15 (2002) 600-612

[18] Yamini D., Devanand Venkatasubbu G., Kumar J., Ramakrishan V., Raman scattering studies on PEG funcionalized hydroxyapatite nanoparticles. Spectrochim Acta A 117 (2014) 299-303

[19] Kodati V.R., Tomasi G.E., Turumin J.L., Tu A.T., Raman spectroscopic identification of phosphate-type kidney stones. Appl Spectrosc 45 (1991) 581-583

[20] S. Saber-Samandaria, K. Alamarab, S. Saber-Samandaric Calcium phosphate coatings: Morphology, micro-structure and mechanical properties. Ceram Int 40 (2014) 563–572

[21] Karampas I.A., Kontoyannis C.G., Characterization of calcium phosphates mixtures. Vibrational Spectroscopy 64 (2013) 126– 133

[22] Xu J., Gilson D.F.R., Butler I.S., FT-Raman and high pressure FT-infrared spectroscopic investigation of monocalcium phosphate monohydrate $Ca(H_2PO_4)_2{\cdot}H_2O$. Spectrochim Acta A 54 (1998) 1869-1878

[23] http://rruff.info/

[24] J. Sun, Z. Wu, H. Cheng, Z. Zhang, R.L. Frost, A Raman spectroscopic comparison of calcite and dolomite. Spectrochim Acta A 117 (2014) 158-162

[25] Kloprogge J.T., Frost R.L., Raman microscopy at 77 K of natural gypsum $CaSO_4{\cdot}2H_2O$. J Mater Scie Lett 19 (2000) 229-231

[26] M. Pamplona, S. Simon, Ultrasonic pulse velocity - A tool for the condition assessment of outdoor marble sculptures, Proceedings of 12th International Congress on Deterioration and Conservation of Stone, New York City (USA), 22-26 October 2012, p. 1-13, http://iscs.icomos.org/pdf-files/NewYorkConf/pampsimo.pdf

[27] Naidu S., Scherer G.W., Nucleation, growth and evolution of calcium phosphate films on calcite. J Colloid Interf Sci 435 (2014) 128-137

Chapter VII: Consolidation of marble: on site testing on Rolandino de' Passeggeri Tomb (Bologna, Italy)

Research Aims

Application of a consolidant on site is a very delicate task; for this reason, prior to application on site, several tests were carried out both on laboratory and real historic specimens, so as to determine all the parameters regarding efficacy, compatibility and durability of the novel HAP-based treatment, all being described in the previous chapters.

Then, application of the HAP-based treatment was tested on site, on Rolandino de' Passeggeri's tomb (Bologna, Italy), as a part of a restoration intervention that was undergoing on the roof of the Tomb. Characterization of stone weathering and consolidant efficacy and compatibility was conducted by means of non-destructive tests.

VII.1 Introduction

As detailed in the previous chapters, consolidation treatments are irreversible operations [1-4], hence adequate selection of all the parameters of the treating procedure is of primary importance for the treatment to be effective and for avoiding occurrence of defects. The success of a consolidation treatment or its failure are determined by several factors including product characteristics (chemical composition of the active principle and the solvent, concentration, etc.), substrate properties (chemical-mineralogical composition, porosity, transport properties), morphology and extent of decay affecting the stone [1,3,4,6,7]. When passing from the application on artificially weathered samples to real samples taken on site, presence of contaminants, different morphological features and non-uniform decay conditions even inside one single artifact can alter the results of consolidation [8]. For example, in the previous chapter, it was demonstrated that, when HAP treatment is applied to a real historic slab instead of artificially weathered samples, different results are obtained in terms of color change and mostly, morphology and phase composition of the treated layer [9]. In fact, reaction between DAP and calcium ions does not necessarily lead to the formation of HAP, but can produce different calcium phosphate phases, phase formation being strongly dependent on several parameters, such as solution pH, presence of foreign ions, supersaturation, temperature etc. [9-13]. All of these parameters, in turn, might depend on environmental conditions, on presence of contaminants, on weathering level of the stone and on its composition. As seen in the case of Globigerina Limestone consolidation by ethyl silicate, in fact, the presence of very small percentages of a component in the stone (in that case silicate fractions) can completely alter the efficacy of the consolidant on that specific lithotype [13-15].

Transition from application in laboratory to application on site is challenging, due to several reasons [8,16]. First, environmental conditions can surely be evaluated, but it is impossible to select the external parameters (for example temperature and humidity) which, in turn, affect evaporation conditions and hence absorption and redistribution of the consolidant. Furthermore, unpredictable events, such as rain or sudden increase or decrease in temperature cannot be prevented. Another concern regards possible presence of moisture in the stone pores, that may prevent consolidant from entering the stone or lead to incompatibility after consolidation [1]. Contaminants can also be present, thus possibly interacting with consolidant curing reactions.

All of these parameters are hard to evaluate, as it is often impossible to take any samples from the artifact and hence to fully characterize the substrate composition, microstructure, mechanical and transport properties, presence of contaminants, weathering level and hence predict the uptake and distribution of the consolidant and hence its effectiveness. For this reason, despite HAP-based treatment having been fully evaluated in the previous chapters, its application on site, that, to the author's best knowledge is yet to be tested, is still challenging.

In this chapter, application of HAP-based treatment on site was performed on Rolandino de' Passeggeri tomb in Bologna. The tomb was undergoing interventions in the roof. As no samples could be taken from the monument, weathering conditions of the artifact as well as efficacy and compatibility of the treatment were evaluated only by means of non-destructive tests.

VII.2 Materials and Methods

VII.2.1.Materials

Tests were performed on Rolandino de' Passeggeri Tomb in Bologna (figure VII.1) that dates back to about 1215-1300 A.D. [17]. The monument was severely damaged during WWII when a bomb hit piazza San Domenico, where the monument is located, on July 24th 1943: the columns, the roof and the sarcophagus containing the remains of the Jurist were completely destroyed and were rebuilt in a restoration performed between 1948 and 1950, re-collocating the collapsed elements, when possible. The tomb was originally constituted by Istria stone, but during restoration, due to unavailability of the stone, all the parts that were rebuilt were composed by a compact variety of marble, the so-called "Biancone di Verona", aesthetically quite similar to the original stone [18,19].

Figure VII.1: Rolandino De' Passeggeri Tomb, piazza San Domenico, Bologna

Two different parts were chosen for application of the consolidant: the base of one of the external columns and one lateral slab (see figure VII.2), differing in exposure and weathering.

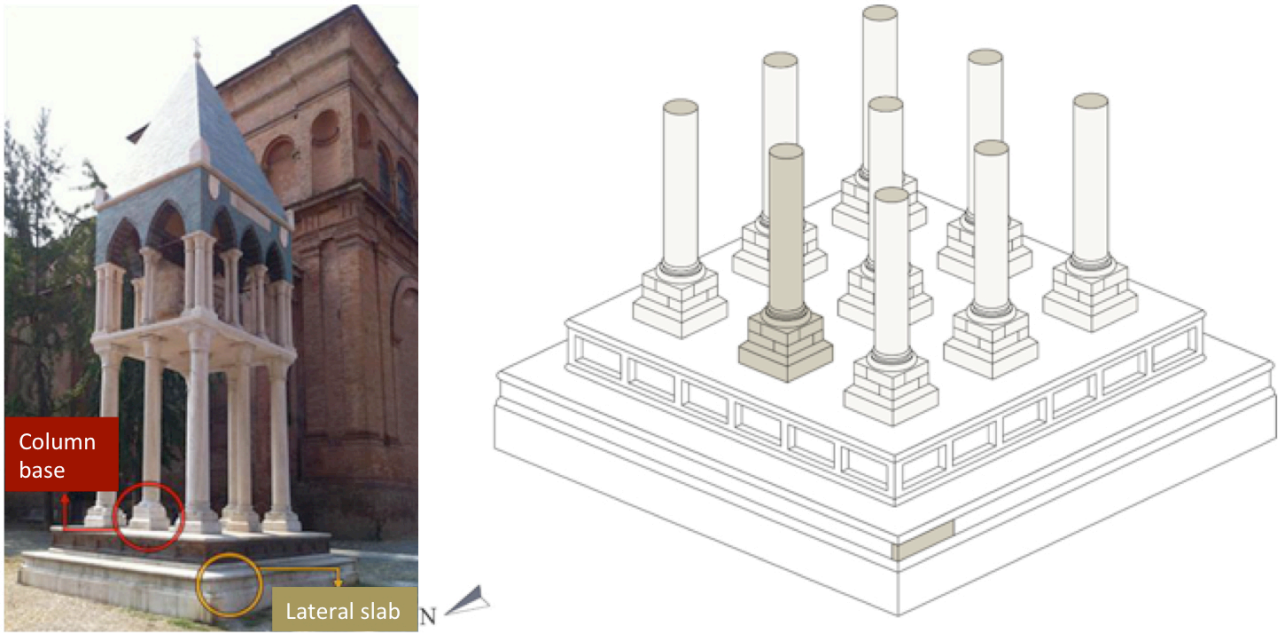

Figure VII.2: Areas selected for the treatment

The column base has one side facing the square, while the others are facing the interior, covered area of the monument. This made it possible to evaluate both sheltered and unsheltered areas with different orientations. The column base is made by superimposed layers of ashlars, that exhibit

different extents of weathering: the first layer, in contact with the basement of the monument seems much more severely affected by cracks, while the upper part presents rounding and some material loss in the edges but seems less weathered. The basement of the column bears the inscription "1950" thus suggesting that it was rebuilt during the restoration intervention. Though no specific mineralogical-petrological analyses were possible, it is presumable that its constituent might be "Biancone di Verona" marble.

The lateral slab is facing the square but is sheltered by a protruding element that mitigates the action of environmental agents: in fact, all protruding parts of the tomb base are more severely weathered than that slab taken into consideration. By choosing this slab and the column base it was possible to evaluate effectiveness and compatibility of the treatment for artifacts exhibiting very different weathering conditions.

VII.2.2 Methods

Characterization of the weathering conditions of the tomb as well as treatment application and after treatment characterization were carried out between June and July 2015.

Evaluation of weathering conditions of the tomb as well as the efficacy and compatibility of HAP treatment were performed by non-destructive tests, as no samples (not even small fragments or powders) could be taken from the Tomb.

The weathering conditions of the column base and of the lateral slab were evaluated by a tomographic representation of ultrasonic pulse velocity [9]. In the column base, UPV was measured at two different heights corresponding to two layers of ashlars with macroscopically different decay conditions. At each height, several measuring points were taken, according to the scheme reported in figure VII.3. 3 points were selected in the lower layer and 2 in the first layer of ashlars. External points are at 2 cm from the basement edges because transducers (3.8 cm diameter) were kept tangent to the edge, while the third measure was taken in the center point of each side. UPV (Matest instrument, 55 kHz transducers) was then mapped so as to obtain ultrasonic tomography at each height, as in the case of the real historic slab (§VI.2.2) [9]. To do so, one of the transducers was kept fixed in one measuring point, while the other was moved to each one of the other points so as to determine time taken by the ultrasonic pulse. Then, the first transducer was moved to the second measuring point and the same procedure was replicated. This was repeated for all measuring points, as described in figure VII.3. A view of all UPV measuring directions is in figure VII.4. In total, 82 measurements were collected.

The measuring scheme used for the lateral slab is in figure VII.5: in this case, given the smaller dimensions, only 4 measuring points were considered, all taken at half of the height of the slab.

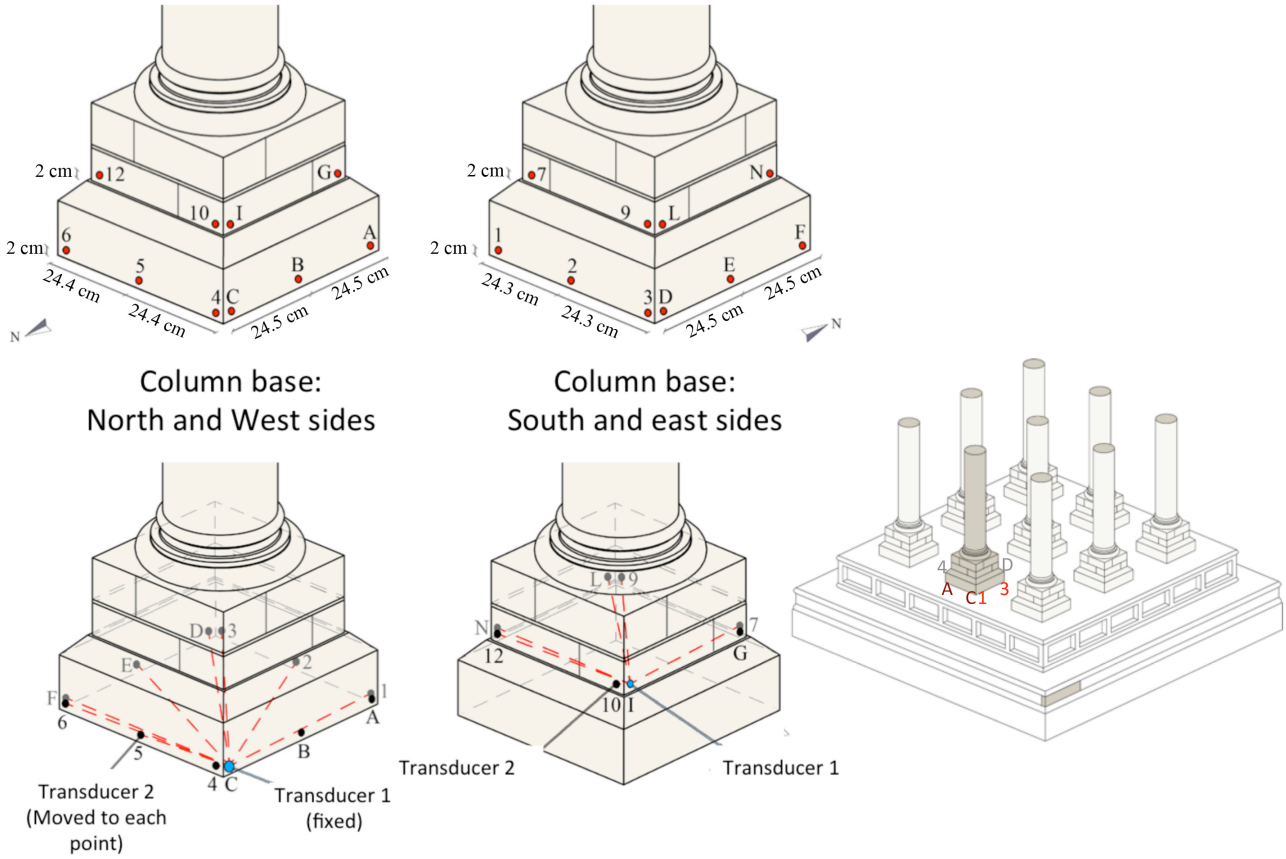

Figure VII.3: Schematic view of measuring points and procedure. For UPV measuring, one of the transducers was kept fixed in each one of the selected points and while the other was moved to all other positions at the same height.

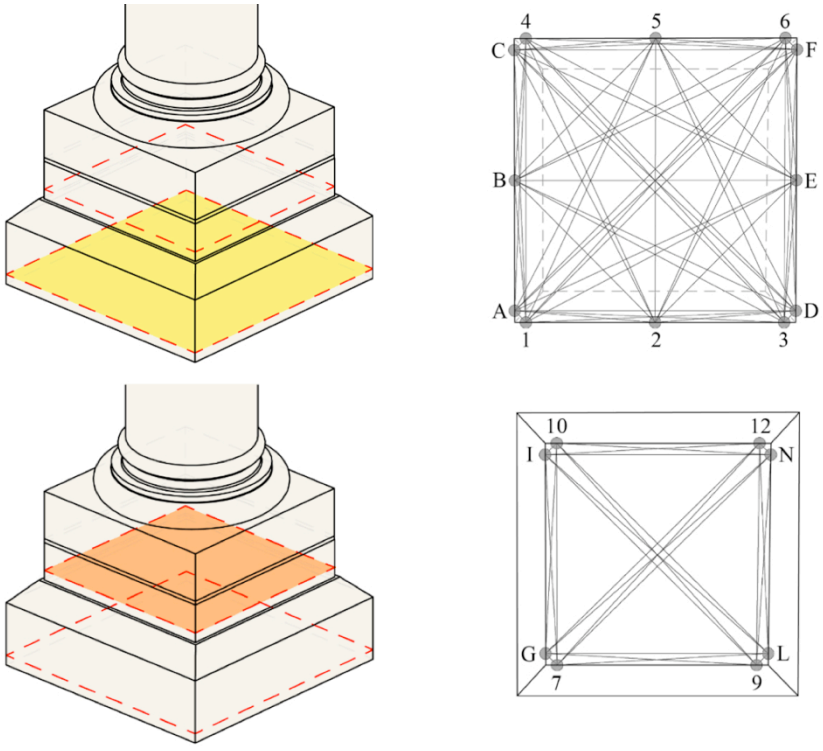

Figure VII.4: Overview of all directions used for measuring UPV.

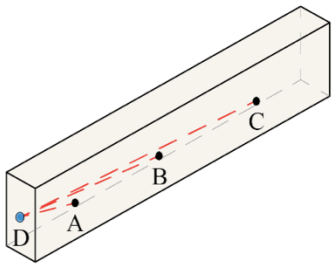

Figure VII.5: Measuring scheme for lateral slab

Data obtained were compared to a classification for marble weathering reported in literature and also used in Chapter 6 for evaluating marble decay (§ Table V.1) [9,20]. In the classification, 5 classes of decay are listed, depending on ultrasonic pulse velocity. Of course, in this case not enough information is available about the substrate material to evaluate its compliance to the classification, hence the comparison is meant to be just qualitative; however, as the tests allow for measuring UPV in exactly the same points before and after treatment, some conclusions can be drawn about the treatment efficacy.

Prior to treating, aesthetic appearance of the stone was evaluated by determining color parameters, as described in the following.

The HAP-treatment was performed following the procedure set up in the previous chapters [13-15]. A 3M DAP solution in deionized water was applied by brushing until apparent refusal (3 brush strokes). Then the treated surfaces were sealed by a plastic film for 72 hours, so as to prevent evaporation during curing (figure VII.6). This procedure was particularly delicate, especially for the lateral slab that is not confinable. A slightly longer curing time was selected with respect to that determined as sufficient in laboratory conditions (72 hours instead of 48 hours).

The treated surfaces were rinsed and gently brushed, then left to dry. Of course it was not possible to measure the exact content of moisture in the stone; however, given the low porosity of the stone and the high external temperature, one week was considered sufficient for complete drying.

Figure VII.6. Application of 3M DAP solution. White spots owing to unreacted DAP are visible after DAP application.

A saturated limewater solution was applied by poultice: differently from laboratory tests, this time a mixture of cellulose pulp and sepiolite (ratio between the components being 1:2) was used to provide better support, because the surfaces to be treated were vertical. This also slightly changed the solution to dry pulp ratio that was adjusted to provide the best workability possible (new ratio being about 1:0.4 in weight). Japanese paper was put between the stone and the poultice, so as to favor its removal. Limewater poultice was kept sealed for 48 hours (as in the case of consolidant curing, a longer time was chosen with respect to that used in laboratory) then left to dry in contact with the stone (figure VII.7).

Figure VII.7: Sequence of the phases in the limewater poultice application

After drying, part of the poultice spontaneously detached from the substrate, and the remaining was removed. The stone was then rinsed with nebulized water, gently brushed and left to dry (figure VII.8).

Figure VII.8: Poultice removal and final rinsing

The efficacy of consolidation was evaluated by determining UPV exactly as described above and comparing values before and after treatment.

The compatibility was assessed in terms of chromatic alterations. These were measured at three different heights in the column basement: one in the column basis, and two in the higher layers of ashlars, each at half of the height of each layer. For one of the sides, more values were taken, to obtain a better evaluation of the heterogeneity of the stone (figure VII.9). Measuring points taken in the lateral slab are the same as for UPV determination. In total 23 points were chosen for the basement and 4 in the lateral slab due to the high heterogeneity of the stone.

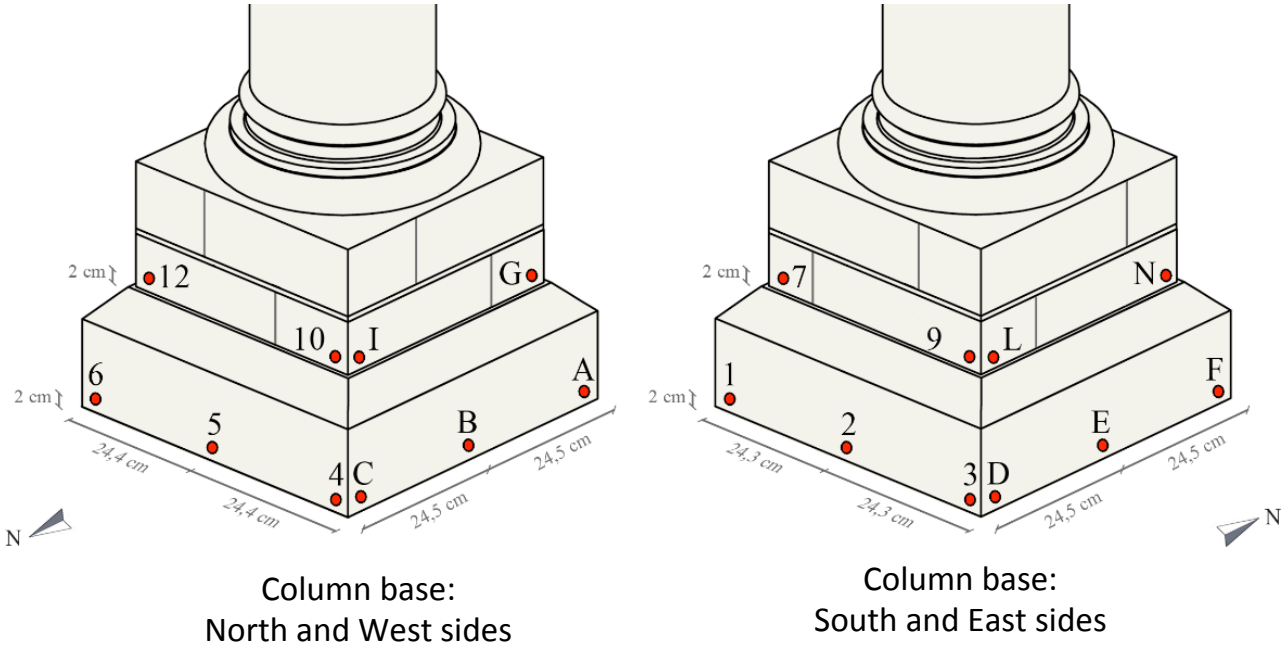

Figure VII.9: Measuring points for color change evaluation. Measuring points for lateral slab are the same as for Ed.

Values before and after treatment were compared, so as to determine ΔE. Each value is average of 6 measurements.

Prior to application of the consolidant, a light cleaning had been performed on the stone so as not to incorporate dust and deposits coming from the restoration previously performed on the roof of the monument, in the treated layer. Color change was also measured before and after cleaning, exactly as described below. Color change as a result of cleaning was negligible, hence results will not be reported for brevity's sake.

VII.3. Results

First, a visual evaluation of weathering was performed before HAP application. Before the treatment (figure VII.10), in the column basement, several cracks were detected on the surface and some loss of material in the edges. However, no signs of loss of cohesion, pulverization or flaking were noticed.

Figure VII.10: Column basement prior to consolidation

Values of ultrasonic pulse velocity for each measuring line are in Table VII.1, VII.2 and VII.3, for the first and second layer of column base, respectively, and for the lateral slab. For a better readability, in figure VII.11, UPV was divided in classes following the classification given in [20] for Carrara marble, one color was assigned to each class and UPV was graphically represented according to the color. Color transition from yellow to darker shades of red indicates gradually more severe weathering status.

The UPV map before treatment, according to the same color scheme, is also reported in figure VII.11. In order to have a continuous representation of UPV, for each area delimited by UPV lines, the average of all UPV values of the lines that surround the area was calculated. These values were graphically represented by means of a color scale gradually switching from yellow to dark red for increasing weathering. As the average is only relevant where several UPV lines cross, this procedure was followed only for the basement borders, that are also more representative of consolidant action.

	POSITION	UPV [km/s] BEFORE treatment	UPV [km/s] AFTER treatment	Δ UPV [km/s]
	1 4	1.5	1.7	**0.2**
	1 B	2.6	3.3	**0.7**
SIDE AC	1 C	1.4	1.8	**0.4**
	4 A	2.2	2.2	**0.0**
	4 B	2.6	2.7	**0.1**
	1 D	4.4	4.4	**0.0**
	2 A	6.0	5.8	**-0.2**
SIDE AD	2 D	5.8	6.1	**0.3**
	3 A	4.2	4.2	**0.0**
	A D	6.0	6.1	**0.1**
	3 6	2.4	1.8	**-0.6**
	3 E	2.5	2.2	**-0.3**
SIDE DF	3 F	1.5	2.3	**0.8**
	6 D	2.4	2.4	**0.0**
	6 E	2.7	2.7	**0.0**
	4 F	4.0	4.2	**0.2**
	5 C	5.4	5.6	**0.2**
SIDE CF	5 F	5.4	5.4	**0.0**
	6 C	4.4	4.6	**0.2**
	C F	5.7	5.7	**0.0**
	1 A	6.3	8.0	**1.7**
	3 D	3.3	3.8	**0.4**
CORNERS	4 C	6.7	7.5	**0.8**
	6 F	7.1	8.8	**1.7**
CENTER	2 5	3.1	3.1	**0.0**
LINES	B E	3.0	3.0	**0.1**
	1 6	2.5	2.5	**0.0**
	1 F	2.6	3.0	**0.4**
	6 A	2.6	2.6	**0.0**
	A F	2.8	3.3	**0.5**
	3 4	2.1	1.8	**-0.3**
DIAGONALS	3 C	2.3	2.3	**0.0**
	4 D	2.3	2.3	**0.0**
	C D	2.8	2.8	**0.0**
	2 B	2.8	3.2	**0.4**
	2 E	3.2	2.6	**-0.6**

	5 B	4.0	4.1	**0.1**
	5 E	2.7	2.7	**0.0**
	2 C	1.8	2.2	**0.3**
	2 4	2.3	2.0	**-0.3**
	2 6	2.0	2.0	**0.0**
	2 F	1.9	2.2	**0.3**
	5 1	2.0	2.2	**0.2**
	5 A	2.3	3.0	**0.7**
	5 3	2.2	2.0	**-0.3**
	5 D	2.8	2.0	**-0.8**
	B 6	3.0	3.6	**0.6**
	B F	3.3	3.3	**0.0**
	B 3	3.0	3.0	**0.0**
	B D	3.3	3.5	**0.2**
	E 4	1.9	2.3	**0.3**
	E C	2.8	2.6	**-0.2**
	E 1	2.7	2.7	**0.0**
	E A	3.2	3.3	**0.1**

Table VII.1: UPV values and ΔUPV before and after treatment in the lower layer of the basement

		UPV [km/s]		**Δ UPV [km/s]**
		BEFORE treatment	AFTER treatment	
SIDE GI	10 G	5.7	5.7	**0.0**
	7 I	5.5	5.7	**0.2**
	7 10	5.8	5.8	**0.0**
SIDE GL	G L	6.1	6.1	**0.0**
	9 G	4.2	5.8	**1.7**
	7 L	5.7	5.9	**0.2**
SIDE IN	I N	6.2	6.2	**0.1**
	12 I	5.8	6.1	**0.2**
	10 N	4.4	5.8	**1.5**
SIDE LN	12 L	5.6	5.7	**0.2**
	9 N	4.3	5.6	**1.4**
	9 12	6.0	6.0	**0.0**
CORNERS	7 G	6.5	7.0	**0.5**
	10 I	9.3	12.0	**2.8**
	9 L	4.7	8.9	**4.2**
	12 N	6.8	7.6	**0.8**
DIAGONALS	G N	5.6	5.7	**0.1**
	12 G	5.7	5.8	**0.1**

	7 N	3.6	4.9	**1.3**
	7 12	5.6	5.6	**0.0**
	I L	5.8	5.9	**0.1**
	9 I	5.6	5.8	**0.2**
	10 L	5.6	5.8	**0.2**
	9 10	5.7	3.8	**-1.9**

Table VII.2: UPV values and ΔUPV before and after treatment in the upper layer of the basement

		UPV [km/s]		**Δ UPV [km/s]**
		BEFORE treatment	AFTER treatment	
D	A	6.5	6.3	**-0.2**
	B	6.0	6.2	**0.1**
	C	5.9	5.9	**-0.1**

Table VII.3: UPV values and ΔUPV before and after treatment in the lateral slab

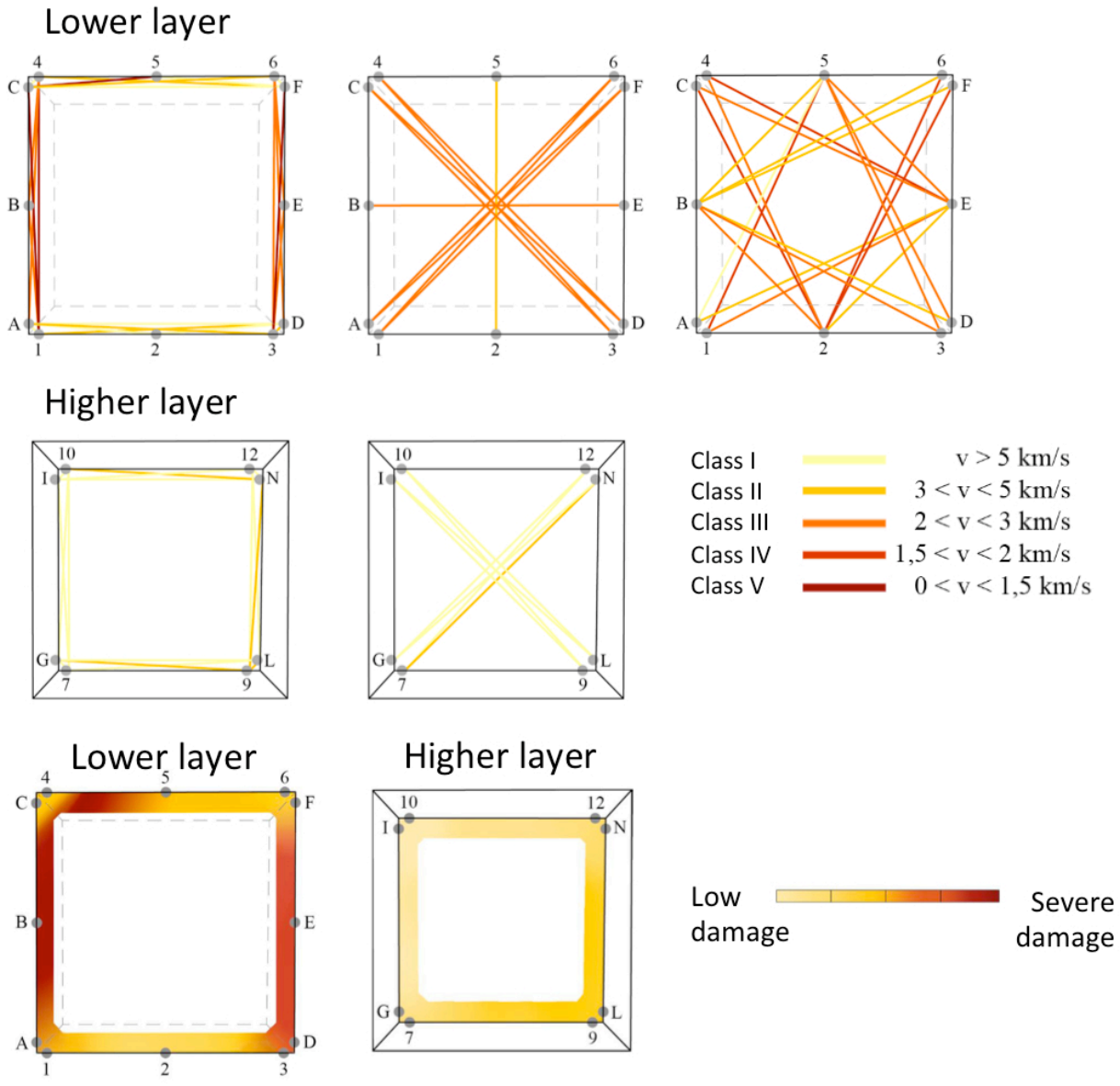

Figure VII.11: Basement: ultrasonic pulse velocity before treatment.

Values after consolidation are reported in table VII.1, VII.2 and VII.3. Graphical representation of UPV, obtained exactly as in the situation before treatment, is in figure VII.12.

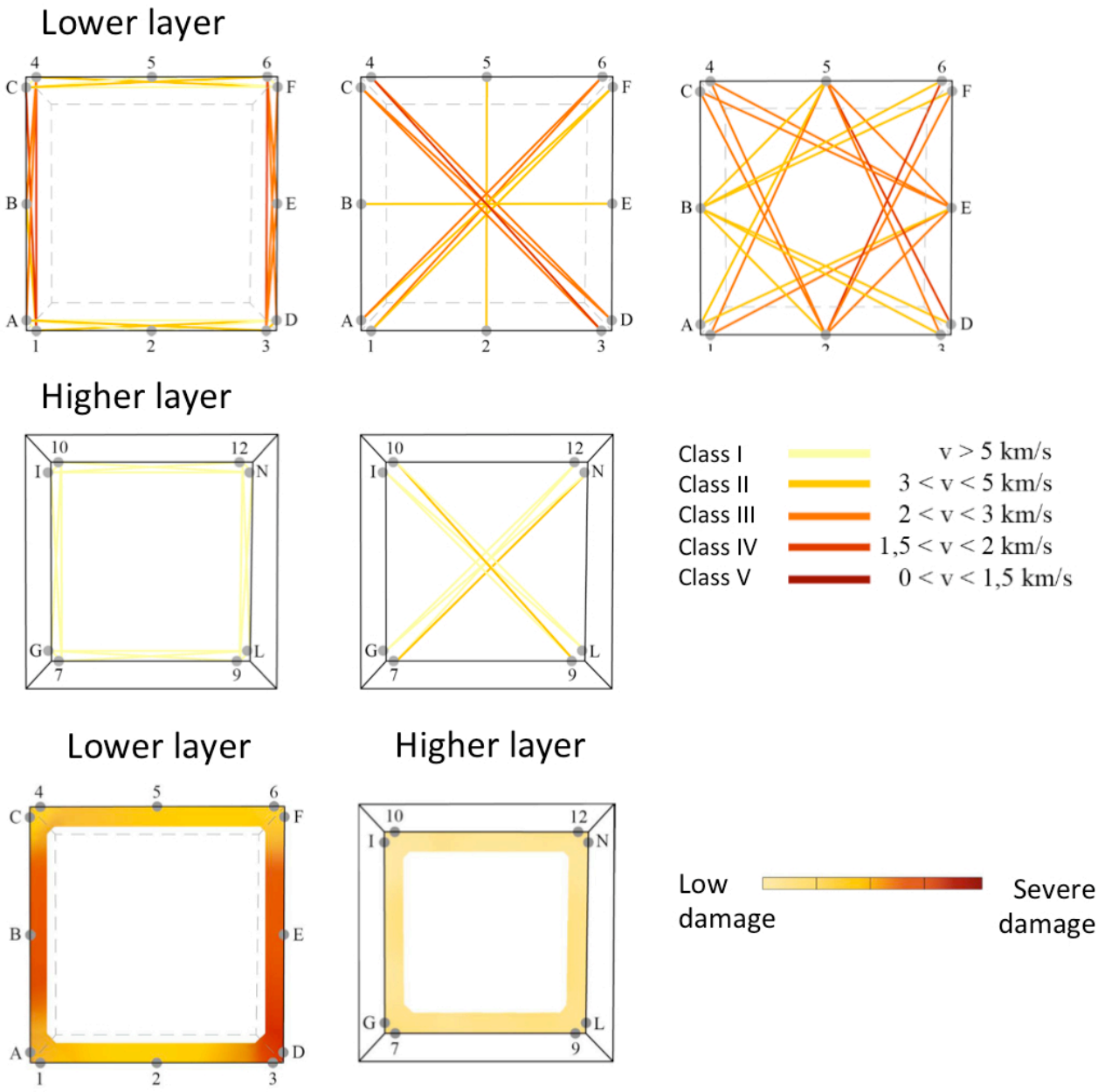

Figure VII.12: Basement: Ultrasonic pulse velocity after treatment. Notably, no values are in the most severe damage class.

For clarity's sake, a direct comparison between the situation before and after treatment is also reported, see figure VII.13. In figure VII.13 changes in UPV, corresponding to values indicated as "ΔUPV" in Table VII.1 and VII.2, are graphically represented. Green indicates improved values, red worse values and grey unaltered values. The thickness of the lines indicates the extent of improvement. Briefly, increases or decreases below ±0.2 km/s are neglected as very close to

instrument error. Increases between ±0.2 and ±0.7 km/s are regarded as moderate and indicated with thin lines, alteration of more than ±0.7 km/s are considered major and indicated by a thick line. By calculating the average UPV value for each area comprised between UPV lines, a complete map of UPV alterations was also obtained and is reported in figure VII.13.

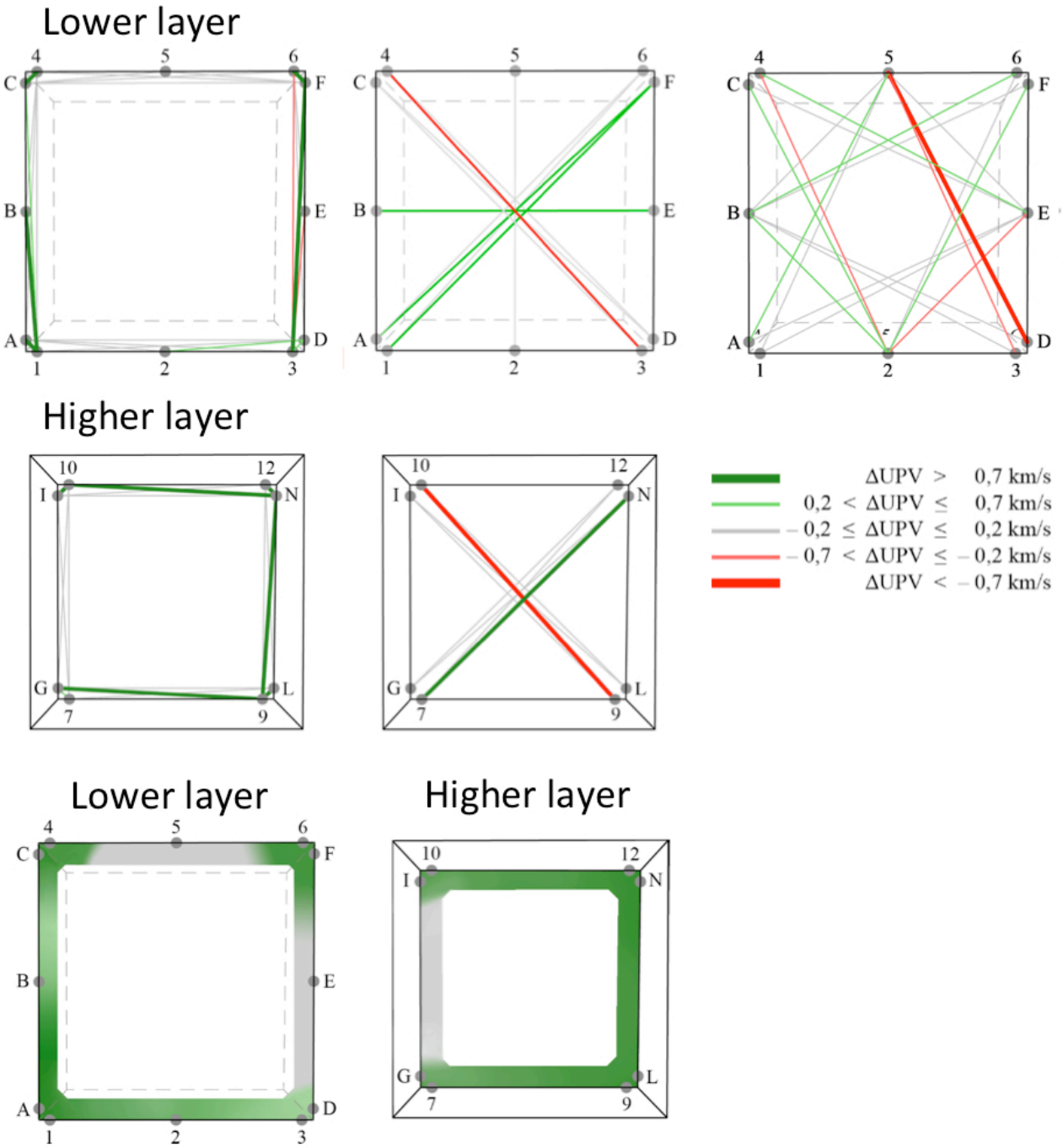

Figure VII.13: Basement: Alterations in UPV before and after treatment.

Aesthetic alterations were visually evaluated at each step of the treatment, results at the end of the treatment being in figure VII.14. After DAP application, some white spots were assed (figure

VII.6), especially in the lateral slab, that also seemed less weathered. Those spots are no longer visible after limewater poultice application (figure VII.14). Moreover, after consolidation, superficial cracks seem filled (figure VII.15).

Figure VII.14: Basement before (top) and after (bottom) the consolidant application.

Figure VII.15: After DAP application, cracks of smaller dimensions seem healed by the consolidant.

Chromatic alterations after treatments were measured by spectrophotometer, results being in figure VII.16 and VII.17. In figure VII.18, an evaluation of the initial heterogeneity of the stone is reported.

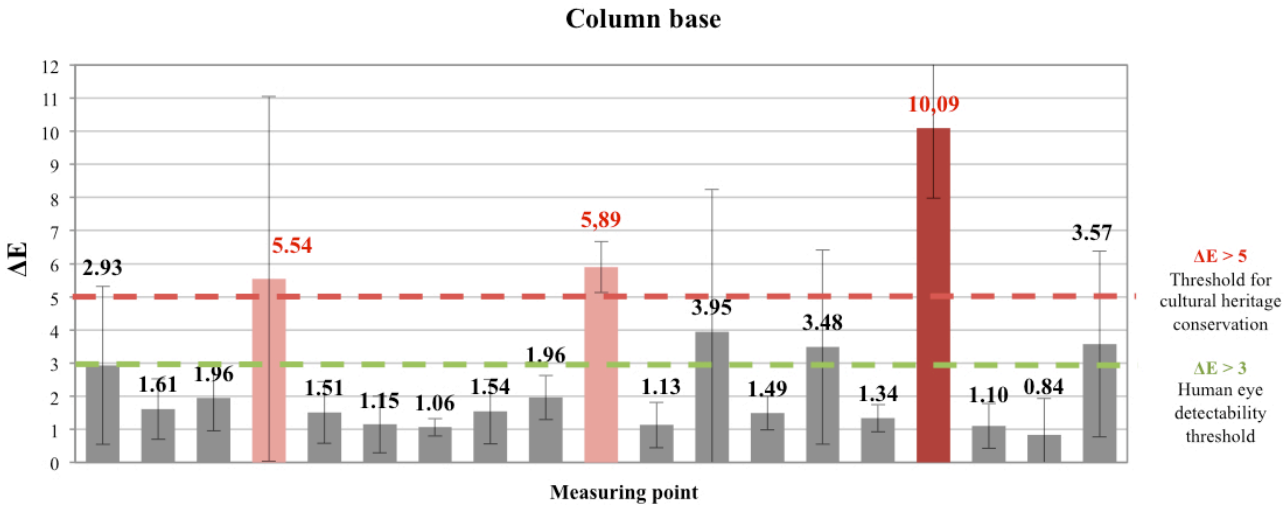

Figure VII.16: Color change after treatment in the column basement

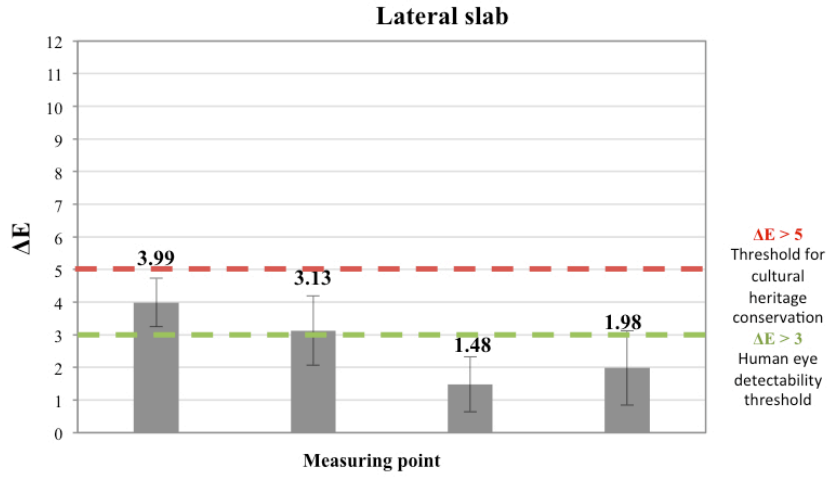

Figure VII.17: Color change in the lateral slab as an effect on HAP treatment

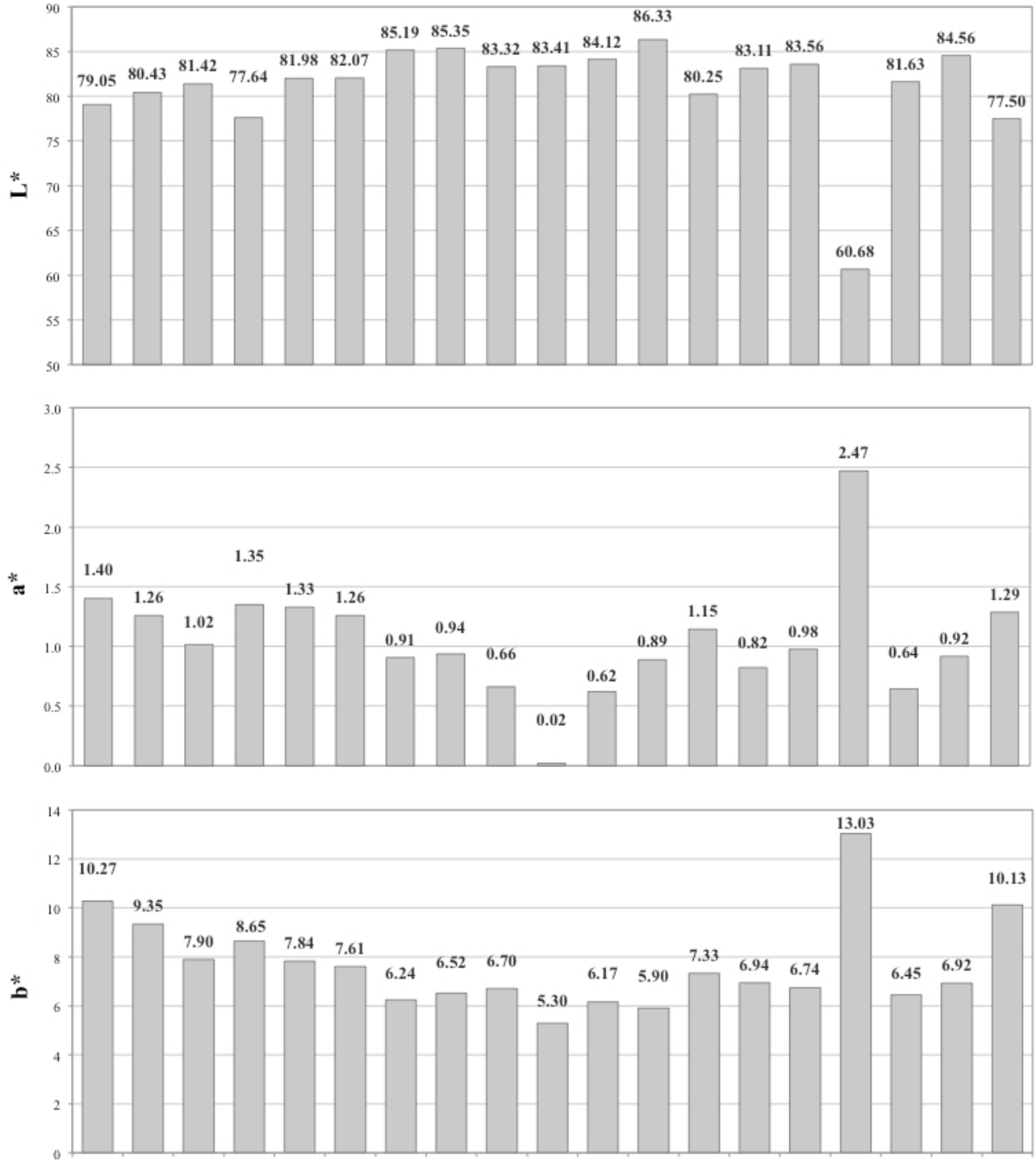

Figure VII.18: Color parameters of untreated stone in different measuring points

VII.4 Discussion

UPV values before treatment (Tables VII.1, VII.2, VII.3 and figure VII.11) indicate remarkably different weathering conditions between the two parts that were taken into consideration, namely the basement and the lateral slab, and in the two superimposed layers of the basement. In fact, the lower layer presents quite severe weathering condition, despite the quite sound appearance of the stone, with several areas exhibiting values below 3 km/s, corresponding to weathering classes II, III and IV [20].

As expected, the least weathered area is that located in the most sheltered part of the tomb. The most severe decay conditions, however, are registered in layers AC and DF, where UPV values are about half of those registered in the other edges. AC and DF are not directly exposed to the exterior; however, their severe weathering might be due to the fact that the roof of the tomb had not undergone restoration yet and leakage of water occurred onto the lower parts.

Instead, the higher ashlars layer is not remarkably weathered, UPV values being above 5 km/s for almost all the area investigated. This is consistent with the fact that it is less exposed to environmental agents as it is less protruded.

In the lateral slab, all values are between 4.9 and 12 km/s (table VII.3), only one point being 3.8 km/s (thus lower than 5 km/s, corresponding to “unweathered” class).

However, it must be borne in mind that the classification was developed for Carrara Marble and that an exact determination of mechanical properties of the stone when unweathered, that would allow to determine the fitting between the classification and the stone, was not possible. In particular, the fact that values as high as 12 km/s are recorded, clearly indicates that mechanical properties of this stone are higher than those of marble, hence weathering indications given by the classification employed are likely to underestimate weathering conditions of the substrate. Still, an internal comparison between the different areas of the monument and between the situation before and after treatment is possible.

UPV was measured in several directions so as to obtain a sort of tomographic representation of UPV inside the column base. However, when evaluating weathering and the effectiveness of the consolidants, some further aspects need to be taken into consideration:

- first, because of the characteristics of the tomographic evaluation itself, values are more precise where more UPV lines are present, because that makes possible to divide the part in smaller areas and calculate averages of more values, and this occurs close to the borders;
- given the heterogeneity of the UPV in the central area of the base, it seems that values are highly affected by slight changes in the transducers positions, possibly due to the presence of cracks inside

the basement. This makes the evaluation of effects of consolidants impossible to assess in these parts;

- weathering normally affects the first 1-2 centimeters from the stone surface [1], while the basement has much bigger dimensions (about 50x50 cm^2) hence UPV values, except for those on the base edges (that remain in the 2 cm layer) are more affected by structural cracks in the internal part of the basement than by material weathering. These cracks have typically big dimensions and are not healed by the action of consolidants. Moreover, mortar joints are present between the different ashlars that compose the basement that can also affect UPV measurements;
- given the dimensions of the base and the expected penetration depth of the consolidant of a few centimeters (a penetration depth of up to 3 cm was registered in the previous chapters, but, considering UPV values, it is likely that "Biancone di Verona" marble is more compact than weathered Carrara Marble, thus penetration depth might be significantly lower), it seems that only UPV values measured in the external layer and mostly those in the corners can reflect the action of the consolidant.

For these reasons, only changes in UPV in the external area of the column base are considered reliable for evaluation of HAP based treatment efficacy.

After treatment, no significant changes are assessed in UPV in the lateral slab, probably due to the fact that no significant weathering affected the stone even before consolidation. For this reason, evaluation of compatibility in the slab is very important as application of the consolidant on a part that is barely weathered might result in reduced penetration depth and more significant aesthetical alterations. A general increase in UPV, instead, is present both in the higher and in the lower layer of the column base, where weathering was more severe. Several areas experienced increases above ±0.7 km/s, regarded as major. Moreover, higher increases in UPV were achieved in the more weathered areas, so that, notably, after treatment none of the values measured are in the most severe damage class.

These values confirm the good efficacy of HAP-based treatment.

As for the aesthetic appearance of the stone, a great heterogeneity is assessed prior to the treatment (figure VII.18).

After DAP application, some white spots were detected (figure VII.6), probably owing to unreacted DAP; however, they are no longer visible after limewater poultice application (figure VII.14).

No changes could be highlighted by visual observation at the end of the treatment (figure VII.14).

Regarding color change as measured by spectrophotometer, most of the values are below the threshold of human eye detectability $\Delta E<3$ (figures VII.16 and VII.17). In the column base, only three values out of 19 are above the acceptable threshold for cultural heritage conservation $\Delta E<5$.

For values above the threshold, standard deviation is very high. This might be ascribed to very high heterogeneity in stone color due to the presence of veins, that make slight movements in the position of the instrument result in remarkable color differences.
In the case of the lateral slab (figure VII.17), all measured values are below the acceptability threshold.
For this reason it can be stated that promising results were obtained for HAP application on site both in terms of efficacy and compatibility. Further tests are currently in progress to monitor HAP effects after long time exposure.

VII.5 Conclusions

The first tests of HAP application on site gave promising results both in terms of efficacy and compatibility, both evaluated by non-destructive tests. HAP treatment allowed obtaining good improvements in UPV in all tested areas, without dramatically affecting the aesthetic appearance of stone.
Further tests for characterization of long-term performance of the consolidant will start in June 2016, i.e. at 1 year from the treatment application.

Acknowledgments

M.Eng. Matteo Glorioso is gratefully acknowledged for the graphical representation of the data and for support to characterization, M.D. Adele Galetti for application of the treatment and cleaning of stone prior to testing. M.D. Rossana Gabrielli and Leonardo Restauri S.r.L (Bologna, Italy) are gratefully acknowledged for collaboration on the project.

Chapter references

[1] Scherer G.W., Wheeler G.S., Silicate consolidants for stone. Key Eng Mater 391 (2009) 1-25

[2] Tulliani J.M., Formia A., Sangermano M., Organic-inorganic material for the consolidation of plaster. J Cult Herit 12 (2011) 364-371

[3] Maravelaki-Kalaitzaki P., Kallithrakas-Kontos N., Korakaki D., Agioutantis Z., Maurigiannakis S., Evaluation of silicon-based strengthening agents on porous limestones. Prog Org Coat 57 (2006) 140-148

[4] Maravelaki-Kalaitzaki P., Kallithrakas-Kontos N., Agioutantis Z., Maurigiannakis S., Korakaki D., A comparative study of porous limestones treated with silicon-based strengthening agents. Prog Org Coat 62 (2008) 49-60

[5] E. Franzoni, G. Graziani, E. Sassoni, TEOS-based treatments for stone consolidation: acceleration of hydrolysis-condensation reactions by poulticing. J Sol-Gel Sci Tech 74 (2015) 398-405

[6] Ferreira Pinto A.P., Delgado Rodriguez J., Stone Consolidation: The role of treatment procedures. J Cult Herit 9 (2008) 38-53

[7] Ferreira Pinto A.P., Delgado Rodriguez J., Consolidation of carbonate stones: Influence of treating procedures on the strengthening action of consolidants. J Cult Herit 13 (2012) 154-166

[8] Franzoni E., Pigino B., The role of moisture in sandstone decay in the monumental cemetery of Bologna (Italy). In: Stefanaggi M., Verges-Belmin V. (eds), Proceeding of Jardins de Pierres, conservation of stone in parks, gardens and cemeteries Conference, Paris, France. XL Print Saint-Etienne, 22-24 June 2011, pp 377

[9] Sassoni E., Graziani G., Franzoni E., Repair of sugaring marble by ammonium phosphate: comparison with ethyl silicate and ammonium oxalate and pilot application to historic artifact. Materials and Design 88 (2015) 1145-1157

[10] Sassoni E., Naidu S., Scherer G.W., The use of hydroxyapatite as a new inorganic consolidant for damaged carbonate stones. J Cult Herit 12 (2011) 346-355

[11] Dorozhkin S.V., Calcium orthophosphates - Occurrence, properties, biomineralization, pathological calcifications and biomimetic applications. Biomatter 1 (2011) 121-164

[12] Naidu S., Liu C., Scherer G.W., New techniques in limestone consolidation: Hydroxyapatite based consolidant and the acceleration of hydrolysis of silicate-based consolidants. J Cult Heritage 16 (2015) 94-101

[13] Sassoni E., Graziani G., Franzoni E., An innovative phosphate-based consolidant for limestone. Part 1: Effectiveness and compatibility in comparison with ethyl silicate. Constr Build Mater 102 (2016) 918-930

[14] Sassoni E., Graziani G., Franzoni E., An innovative phosphate-based consolidant for limestone. Part 2: Durability in comparison with ethyl silicate. Constr Build Mater 102 (2016) 931-942

[15] Franzoni E., Sassoni E., Graziani G., Brushing, poultice or immersion? Role of the application technique on the performance of a novel hydroxyapatite-based consolidating treatment for limestone. J Cult Herit 16 (2015) 173–184

[16] Wheeler G., Alkoxysilanes and the Consolidation of Stone (Research in conservation), The Getty Conservation Institute, Los Angeles, 2005

[17] Solmi F., Dezzi Bardeschi M., A. Rubbiani: I veri e i falsi storici, Grafis, Casalecchio di Reno, Bologna

[18] Direzione generale delle antichità e delle belle arti, La ricostruzione del patrimonio artistico italiano, La Libreria dello Stato, Roma, 1950, 13-107

[19] Barbacci A., Monumenti di Bologna. Distruzioni e restauri, Bologna, Cappelli, 1977, 44-45

[20] Pamplona M., Simon S., Ultrasonic pulse velocity - A tool for the condition assessment of outdoor marble sculptures, Proceedings of 12th International Congress on Deterioration and Conservation of Stone, New York City (USA), 22-26 October 2012, p. 1-13

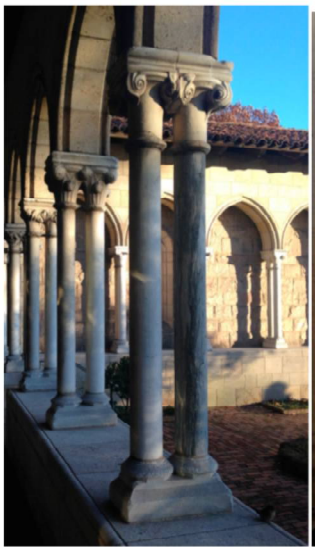

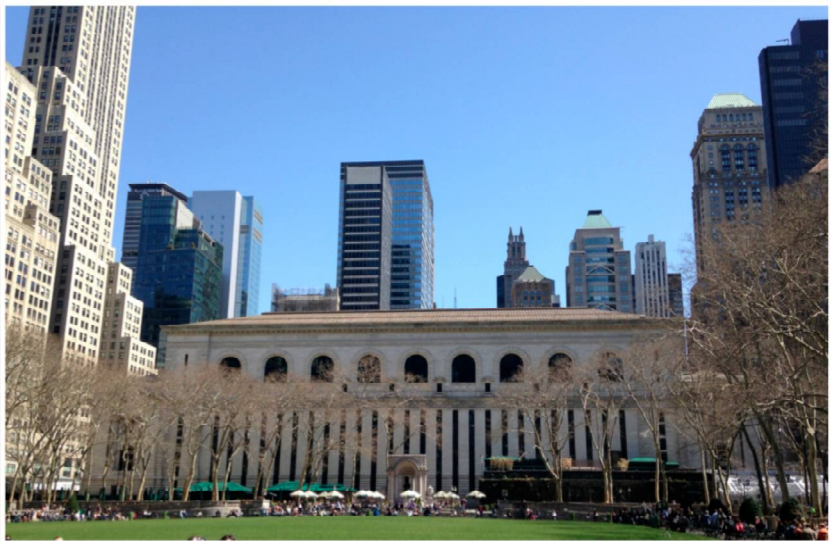

PART 3:
Marble Protection

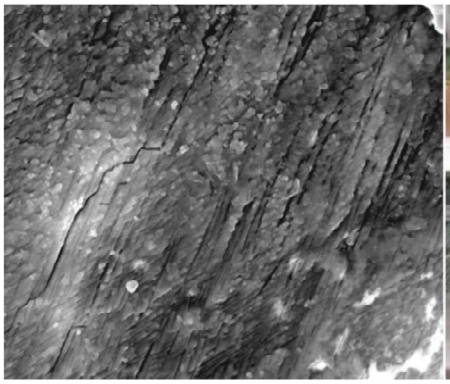
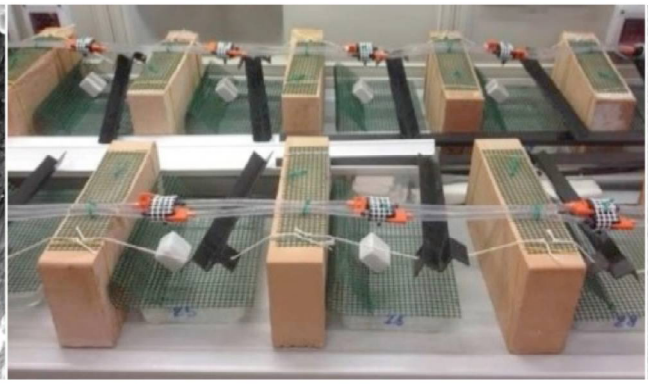
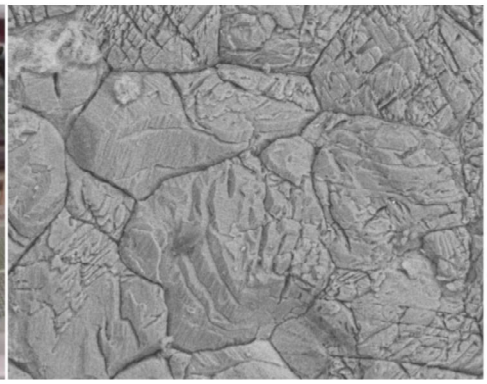


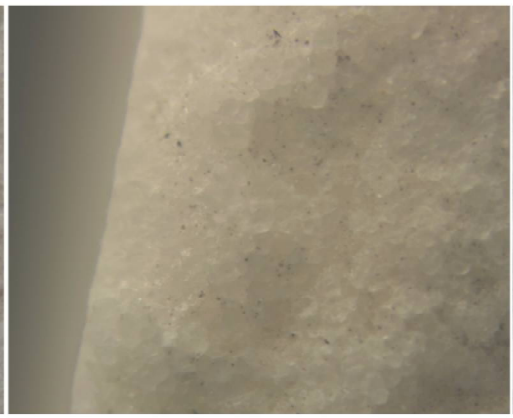


Chapter VIII- Marble protection against acidic rain corrosion [1]

Research aims

Hydroxyapatite (HAP) has a much lower dissolution rate and solubility than calcite, especially in an acidic environment, so it has been proposed for the protection of marble against acidic rain corrosion. Promising results were obtained, but further optimization is necessary as the treated layer is often incomplete, cracked and/or porous.

In this Chapter, several parameters were investigated to obtain a coherent, uncracked layer, and to avoid the formation of metastable, soluble phases instead of HAP: the role of the pH of the starting solution; the effect of organic and inorganic additions, and in particular that of ethanol, as it is reported to adsorb on calcite, hence possibly favoring the growth of the HAP layer. Finally, a double application of the treatment was tested. Results were compared to those obtained with ammonium oxalate treatment, widely investigated for marble protection.

Results indicate that adding small amounts of ethanol to the formulation remarkably increases the acid resistance of treated samples, and yields better coverage of the surface without crack formation. The effectiveness of the treatment is further enhanced when a second treatment is applied. The efficacy of ethanol-doped DAP mixtures was found to be remarkably higher than that of ammonium oxalate based treatments.

VIII.1 Introduction

Conservation of marble artifacts is one of the main goals in the field of cultural heritage. Marble is widely used both in architecture and sculpture, and it is affected by severe decay phenomena, such as sugaring, bowing and dissolution. Among all the weathering phenomena that may affect marble in situ, one of the most relevant is that linked to the solubility of its main constituent, namely the mineral calcite, in acidic environments [1-8]. Rain has a pH that can vary from 5.6 in normal conditions [6] (where the acidity results from ambient CO_2), to levels as low as 4.5 in areas polluted by SO_2 and NO_x. As the pH decreases, the dissolution rate of calcite increases. Degradation of carbonate stones may occur due to three different processes, all leading to chemical dissolution and surface recession [6]: degradation due to “pure” rain in equilibrium with CO_2 at pH 5.6, decay due to acid rain (containing nitric and sulfuric acid), and dry deposition of SO_2 and NO_x. The first mechanism is the main cause of limestone and marble surface recession (causing 50 to 90% of stone dissolution in European climates [6]), and its relevance is expected to increase in the next 100 years, due to the expected increase in CO_2 and temperature. On the other hand, the contribution of the other 2 phenomena is expected to become less relevant, as they are both linked to the

concentration of SO_2 and NO_x in the atmosphere, which is expected to decrease due to pollution regulation policies [5,6].

Despite protection of marble surfaces from dissolution due to acid rain having been widely studied, no completely satisfactory treatment is available so far, as they all exhibit drawbacks that limit their success [9]. Traditionally, protection was performed by organic coatings, meant to protect the surfaces by making them water repellent [4]. These treatments, however, exhibit poor durability [4, 9-13] and water drainage [10], limited chemical compatibility with the substrate [14] and can significantly alter the water transport properties of the material [14]. The improvement of organic protective coatings is currently being studied to overcome these limitations [10,12]. Inorganic coatings, on the other hand, are meant to act as "passivating treatments" [4], i.e. to enhance surface resistance by creating a uniform layer much less soluble than the starting material, that can prevent or at least slow down the dissolution.

Among the inorganic treatments, ammonium oxalate (AmOx) has been proposed [9, 15-17], with the aim of reacting with the calcite of the substrate to create a calcium oxalate patina over the marble surface. The AmOx treatment is rather effective in slowing down marble decay; however, its efficacy is limited by the relatively high solubility of calcium oxalate (whewellite, $CaC_2O_4 \cdot H_2O$), not remarkably higher than that of calcite [18].

As an alternative to calcium oxalate, hydroxyapatite (HAP), successfully proposed and employed for limestone consolidation [18,19], has also been investigated, as it is expected to provide protection against acid dissolution, because it has much lower solubility and dissolution rate than calcite [18] or calcium oxalate [18]. HAP is formed by reaction of aqueous solutions of a phosphatic salt (diammonium hydrogen phosphate, DAP) with calcium ions, which can come from the partial dissolution of the substrate (only millimolar quantities are required) or be externally added [2,18,20].

Previous studies on HAP for marble protection have given very promising results [2,20,21]. The protection, however, is still much lower than that expected on the basis of HAP solubility and dissolution rate, and this is ascribed to layer porosity, incomplete coverage and/or to the presence of cracks. Film cracking is thought to be linked to the excessive thickness of the HAP layer, leading to high capillary forces that cause cracking during drying. To reduce the thickness of the film, a lower concentration of DAP might be employed; however, the film is required to cover the whole substrate, because uncovered marble spots would become preferential sites for acid attack. Film porosity is expected to be controllable by incorporating additions to the film, that could alter its morphology. As HAP easily adsorbs foreign ions [22,23], inorganic additions have been tested to improve the features of the treated layer [20], but they have not shown promising results (because

of low film coverage, reduction of reaction speed, or failure in incorporating the additions into the lattice).

Some of the approaches found in the literature to control HAP layer morphology and acid resistance (given that crystallinity, morphology and structure of HAP influence its properties [24]), cannot be considered for cultural heritage protection, such as decreasing solution pH [22], increasing reaction temperature, or adding toxic compounds such as zinc [25-27]. For this reason, the present paper was aimed at improving the acid resistance of HAP-treated marble and optimizing the treating procedure with the goals of:

- obtaining a uniform coverage of the support;
- creating a crack-free HAP film;
- investigating the alterations in morphology, composition and acid resistance of the HAP layer obtained by altering the treatment procedure.

To achieve these goals, several process modifications were investigated, that seem to offer the best likelihood of improved performance: raise of the pH to increase the concentration of PO_4^{3-} ions, incorporation of other cations into the HAP lattice, use of organic additives to improve the coverage of HAP on calcite, and multiple treatments to reduce porosity.

The pH plays a fundamental role in the dissolution of DAP. Previous studies have shown that at high pH (around 11), the dissolution of DAP produces more PO_4^{3-} ions, with respect to HPO_4^{2-} [20]. As only PO_4^{3-} reacts to produce HAP, high concentrations of DAP are required to get enough PO_4^{3-} to cover a marble substrate. By raising the pH, it should be possible to obtain a higher ratio of PO_4^{3-} to HPO_4^{2-} and hence reduce the concentration of the precursor. This would have benefits in terms of layer thickness and treatment compatibility, together with economical advantages.

In the present work, inorganic ions (magnesium, strontium) were added to the solution at high pH, with the aim of reducing the specific surface area of the film and, hence, the susceptibility to acid attack. These additions have already been tested at low pH [20], so in the present work they were only tested at high pH. The influence of aluminum additions, often used in biomedical application, was also evaluated. In this case, tests were performed at both low and high pH, as no previous tests had been carried out on low pH formulations.

Calcite growth modifying compounds often include -OH as functional groups [28]. Ethanol was found to adsorb on calcite as it binds to it through –OH groups [28], and to have a stronger affinity for $CaCO_3$ surface than water does. For this reason, ethanol might successfully bind to the substrate and enhance its coverage. Ethanol has also been recently found to enhance HAP crystallization and to adsorb on HAP [24] as well as on calcite. Therefore, different concentrations of DAP and ethanol were tested to determine the combination that would allow for a complete coverage of the support without increasing the layer thickness too much (which would make it more prone to cracking).

The use of a double application was tested with the aim of creating a more uniform layer. Excessive increase in DAP concentration is expected to increase the layer thickness, making it more prone to cracking during drying; however, a second treatment at low concentration would create two overlying layers of reduced thickness, thus possibly reducing the drying stresses while improving coverage of the surface. Combinations of treatments were also tested with the aim of creating a uniform first layer that could successfully cover the substrate and a second less soluble one to grow on the first, to guarantee the protection of the substrate.

As HAP easily adsorbs foreign ions and because many metastable phases might form from the reaction of DAP and calcium [23, 29-32], special attention was devoted to the analysis of the composition of the treated layers formed by changing the treating precursors or parameters. The results of the tests were compared to those obtained with ammonium oxalate, which is currently the most used material for marble protection [33,34]. Combinations of ammonium oxalate and HAP were tested as well, to try to combine the ability of AmOx to uniformly cover the substrate, with the much lower solubility of HAP.

VIII.2. Materials and Methods

VIII.2.1 Materials

All tests were performed on calcite powders to speed up the dissolution process and hence better understand the mechanism of acid attack on treated and untreated powders, reducing the relevance of other mechanisms that might take place aside from dissolution (e.g., ion exchange, …). The use of powders also made it possible to investigate the link between acid resistance and sample specific surface and to verify the treatment effects on a very high number of grains, with different crystallographic orientations and, possibly, impurities, which otherwise would have required dozens of massive samples.

The behavior of calcite powders is expected to be representative of that of coarse samples. Therefore, preliminary tests on Carrara marble cubes were performed for the most promising formulations, to assess the representativeness of tests on powders.

To select the most suitable fraction for the tests, calcite powders (30-50 White, Imerys) were sieved and specific surface was determined by BET. The particle size has to be large enough to allow many nucleation sites on each particle, but small enough to provide a high specific surface area for dissolution tests. The fraction between 30 and 35 mesh (500 – 595 μm) was selected.

In addition, cubes (1 cm side) were cut from Carrara Marble quarry slabs [BasketweaveMosaics.com, 538 Huyler St, South Hackensack, NJ 07606 USA], to run preliminary tests of the most promising formulations on coarse samples.

Diammonium hydrogen phosphate (DAP, > 99%, Sigma Aldrich), calcium chloride ($CaCl_2.2H_2O$, assay > 99.0%, Sigma Aldrich), magnesium chloride ($MgCl_2 \cdot 6H_2O$, ACS reagent > 99.0%, EMD Millipore), strontium chloride ($SrCl_2 \cdot 6H_2O$, ACS reagent ⩾ 99.0%, Sigma Aldrich), aluminum nitrate ($Al(NO_3)_3 \cdot 9H_2O$, ≥ 98%, Sigma Aldrich), ethanol (Fisher-Scientific) and ammonium oxalate ($(NH_4)_2C_2O_4 \cdot H_2O$, ≥ 99.99%, Sigma Aldrich) were used for treating calcite powders and marble cubes, as described in § VIII.2.2.2. Sodium hydroxide (NaOH, ACS reagent grade > 97%, ACROS) was used to increase solution pH.

Pure hydroxyapatite (reagent grade, Sigma Aldrich) and pure brushite (Calcium phosphate dibasic dihydrate, ≥ 98%, Sigma Aldrich) powders were examined as references.

VIII.2.2 Methods

VIII.2.2.1 Characterization of the starting calcite powders

Untreated marble powders were analyzed to determine their crystal phase and composition (Rigaku MiniFlex XRD/X-Ray Diffractometer; FT-IR Nicolet 6700 FTIR Spectrometer, ATR mode, 16 scans, resolution of $1cm^{-1}$; EDS probe Oxford spectrometer incorporated in FEI Quanta 200 FEG Environmental-SEM, spectrometer controlled by Oxford INCA software), morphology (SEM, FEI Quanta 200 FEG Environmental-SEM, low vacuum mode) and specific surface area (BET, Micromeritics ASAP 2020). All samples were coated with carbon to render them conductive for SEM observation. Different marble powders were examined, and those with the most suitable specific surface (grains coarse enough to allow the HAP layer to grow) were selected.

All powders and cubic samples were rinsed with water and ethanol prior to treating and characterization, so that possible surface impurities could be removed, and left to dry overnight.

VIII.2.2.2 Treatments

Hydroxyapatite was formed by mixing aqueous solutions at various concentrations of DAP with calcium chloride and making them react with marble powders. Calcium chloride was added to all the formulations, so that the calcium ions necessary for the reaction could be provided without dissolution of the calcitic substrate ($CaCl_2$: DAP = 1:1000).

First, a 0.1 M DAP + 0.1 mM $CaCl_2$ solution was taken into consideration (from now on indicated as “D8”). The concentration was chosen on the basis of previous experiments to avoid too high a thickness of the treated layer that would lead to drying cracks. The solution was modified to study the influence of pH, cationic additions, ethanol additions, and double treatments. Results were also compared with those of ammonium oxalate treatment. Description and labeling of the tested formulations are reported in Table VIII.1.

Effect of pH. Two pH values were tested: pH 8, which is the pH of DAP solution without additions (as assessed by a Oakton pH-meter pH 1100 series and as found in the literature) and one at pH 11, selected to increase the amount of PO_4^{3-}. Duplicate samples at pH 11 were left reacting for 72 hours ("D11-72") to see if possible metastable phases would convert into HAP at longer reaction times [35]. Reaction times over 72 h were not tested as they would not be feasible on site.

Effect of cationic additions. Magnesium and strontium additions were tested to increase the performance of solutions at high pH. The precursors, magnesium chloride and strontium chloride, were chosen to provide maximal solubility in water and minimal toxicity. Zinc was also investigated as a precursor, but was excluded because of its toxicity. All the additions were added at the highest concentration possible, while avoiding precipitation; a second test was then performed on solutions at a lower concentration, to test their effectiveness. Concentrations of 0.1 mM and 0.2 mM $MgCl_2{\cdot}6H_2O$ were used for magnesium chloride, 0.5 mM and 1 mM $SrCl_2{\cdot}6H_2O$ for strontium chloride. The most promising formulations (i.e., those causing the lowest increase in specific surface area) were selected and subjected to further characterization to determine whether the additions would enhance the behavior of pH 11-treated samples.

Aluminum nitrate was selected as a precursor for aluminum additions: 0.010 mM and 0.025 mM concentrations were examined at pH 8 and 11, 0.025 mM being the highest concentration that would allow the solution not to precipitate. Samples treated with $Ca(NO)_3$ additions were also examined to detect possible negative effects connected to adding nitrates to the formulation. The best concentration to be used was chosen on the basis of BET results, as in the case of Mg and Sr additions.

Effect of ethanol addition. Ethanol was added to solutions indicated in Table VIII.1 as "E". Concentrations of 0.1, 0.5, 5 and 20 wt% in water were tested. The effect of the most promising ethanol concentration (0.5 wt%) was also tested on solutions with higher DAP content (1 M DAP + 1 mM $CaCl_2$), to test the ability of ethanol to reduce drying cracks.

Comparison with ammonium oxalate (AmOx). Ammonium oxalate treatment was tested as a benchmark: a 5 wt% ammonium oxalate solution was reacted with the powders for 24 hours, as suggested in ref. [33] to form calcium oxalate. The procedure was the same used for HAP treated powders. Samples treated with ammonium oxalate were tested exactly as DAP-treated ones; no EDS was performed, as the elemental composition of calcium oxalate is the same as calcite. Combined treatments of ammonium oxalate and HAP were also tested, with the aim of creating an acid resistant HAP layer on the top of a first, uniform layer of calcium oxalate. Ethanol was added to calcium oxalate in double treatments, to determine whether it would adsorb and enhance acid resistance.

Effect of double treatments. Samples treated with combined treatments were characterized to determine the most effective combination. Different formulations were tested, using DAP with and without ethanol additions and AmOx. The best formulation was selected, and additional tests were performed, as described in Table VIII.1.

At least 2 samples were prepared for each treatment condition listed in Table VIII.1. Samples were treated by immersion. Five grams of marble powder were taken for each sample and put into a 1-liter cylinder containing 250 mL of solution. Plastic containers were used for all samples to avoid silica contamination at high pH. Containers were sealed and kept rotating for 24 h at 3 rpm to ensure uniform reaction of the powders. Samples with Sr^{2+} addition were left reacting for 48 hours, as $SrCl_2$ had been found to slow down the reaction rate [20]. Two samples at pH 11 were left reacting for 72 hours to determine the effects of a longer reaction time on the ratio between HAP and metastable phases formed by the reaction (octacalcium phosphate and brushite, for example, have been found to be possible precursors for HAP formation [35]). At the end of the treatment time, the powders were washed with water and ethanol, filtered and left to dry overnight.

After drying, some of the powders were subjected to a second treatment, either using the same solution as the first treatment, or a different one, according to Table VIII.1. Second treatments were performed exactly as the first ones, but on pre-treated powders.

	Sample name	Treating condition	Treating time	Characterization tests
	Untr	Untreated marble powder	/	acid attack test, acid attack test pH 3.5, SEM/EDS before and after acid attack test, XRD, FT-IR 16 scans, FT-IR 320 scans, BET before and after acid attack test
	HAP	Pure hydroxyapatite powder	/	Acid attack test (repeated 2 times), BET
	Brushite	Pure brushite powder	/	Acid attack test
pH effect	D8	0.1 M DAP + 0.1 mM CaCl2 pH 8	24h	acid attack test, acid attack test pH 3.5, SEM/EDS before acid attack test, FT-IR 16 scans, BET
	D11	0.1 M DAP + 0.1 mM $CaCl_2$ pH 11	24h	acid attack test, acid attack test pH 3.5, SEM/EDS before and after acid attack test, FT-IR 16 scans, FT-IR 320 scans, BET
Cationic Additions	M11	0.1 M DAP + 0.1 mM $CaCl_2$+ 0.1 mM $MgCl_2 \cdot 6H_2O$ pH 11	24h	acid attack test pH 3.5, BET, SEM/EDS, FT-IR16 scans
	M11-H	0.1 M DAP + 0.1 mM $CaCl_2$+ 0.2 mM $MgCl_2 \cdot 6H_2O$ pH 11	24h	BET
	S11	0.1 M DAP + 0.1 mM $CaCl_2$+ 0.5 mM $SrCl_2 \cdot 6H_2O$ pH 11	48h	acid attack test pH 3.5, BET, SEM/EDS, FT-IR16 scans
	S11-H	0.1 M DAP + 0.1 mM $CaCl_2$+ 1 mM $SrCl_2 \cdot 6H_2O$ pH 11	24h	BET
	A8	0.1 M DAP + 0.1 mM $CaCl_2$+ 0.020 mM $Al(NO_3)_3 \cdot 9H_2O$ pH 8	24h	acid attack test pH 3.5, BET, SEM/EDS, FT-IR16 scans
	A11	0.1 M DAP + 0.1 mM $CaCl_2$+ 0.020 mM $Al(NO_3)_3 \cdot 9H_2O$ pH 11	24h	acid attack test pH 3.5, BET, SEM/EDS, FT-IR16 scans
Ethanol Addition	D8E	0.1 M DAP + 0.1 mM CaCl2 + 0.5 wt.% ethanol	24h	acid attack test, acid attack test pH 3.5, SEM/EDS before and after acid attack test

	D1ME	1 M DAP + 1 mM $CaCl_2$+ 0.5 wt.% ethanol	24h	acid attack test, SEM/EDS before and after acid attack test
	D1ME+1M	first treatment: 1 M DAP + 1 mM $CaCl_2$+ 0.5 wt.% ethanol second treatment: 1 M DAP + 1 mM $CaCl_2$	24h-drying-24h	acid attack test, SEM/EDS before and after acid attack test, FT-IR 16 scans
AmOx	AmOx	5 wt% Ammonium Oxalate	24h	acid attack test, acid attack test pH 3.5, SEM/EDS before and after acid attack test
Double Treatments	AmOx+D8	first treatment: 5 wt% Ammonium Oxalate second treatment 0.1 M DAP + 0.1 mM $CaCl_2$ pH 8	24h-drying-24h	acid attack test, acid attack test pH 3.5, SEM/EDS before and after acid attack test
	AmOxE+D8	first treatment: 5 wt% Ammonium Oxalate + 5 wt.% ethanol second treatment 0.1 M DAP + 0.1 mM $CaCl_2$ pH 8	24h-drying-24h	acid attack test
	AmOx+D8E	first treatment: 5 wt% Ammonium Oxalate second treatment: 0.1 M DAP + 0.1 mM CaCl2 + 0.5 wt.% ethanol	24h-drying-24h	acid attack test
	D8+11	first treatment 0.1 M DAP + 0.1 mM CaCl2 pH 8 second treatment: 0.1 M DAP + 0.1 mM CaCl2 pH 11	24h-drying-24h	acid attack test, acid attack test pH 3.5, SEM/EDS
	D11+8	first treatment: 0.1 M DAP + 0.1 mM CaCl2 pH 11 second treatment 0.1 M DAP + 0.1 mM CaCl2 pH 8	24h-drying-24h	acid attack test, acid attack test pH 3.5, SEM/EDS, FT-IR 16 scans
	D8+8	first treatment 0.1 M DAP + 0.1 mM CaCl2 pH 8 second treatment 0.1 M DAP + 0.1 mM CaCl2 pH 8	24h-drying-24h	acid attack test, SEM/EDS
	D8E+8	first treatment: 0.1 M DAP + 0.1 mM CaCl2 + 0.5 wt.% ethanol second treatment 0.1 M DAP + 0.1 mM CaCl2 pH 8	24h-drying-24h	acid attack test (repeated 2 times), 15 h acid attack test, acid attack test pH 3.5, SEM/EDS before and after acid attack test, FT-IR 16 scans, FT-IR 320 scans, BET before and after acid attack test, acid attack test on solid samples
	D8E+8E	first treatment: 0.1 M DAP + 0.1 mM CaCl2 + 0.5 wt.% ethanol second treatment: 0.1 M DAP + 0.1 mM CaCl2 + 0.5 wt.% ethanol	24h-drying-24h	acid attack test
	D11E+8	first treatment: 0.1 M DAP + 0.1 mM CaCl2 pH11 + 0.5 wt.% ethanol second treatment 0.1 M DAP + 0.1 mM CaCl2 pH 8	24h-drying-24h	acid attack test

Table VIII.1: Samples labelling and description:

Description and labelling of all the formulations used for the treatments and corresponding reaction time. The HAP treatment that was taken as a benchmark and then modified according to the formulations listed in the table is 0.1 M DAP + 0.1 mM $CaCl_2$ solution (sample D8).

It must be noticed that, in the labelling: "D" stands for DAP-treated, "AmOx" for ammonium oxalate treatments, the number (8 or 11) indicates the pH of the starting solution, letter "E" indicates the addition of ethanol to the solution, "1M" indicates the concentration of DAP solution. Where not specified the DAP concentration is always 0.1 M and the pH is the one of the solution without any NaOH addition.

VIII.2.2.3 Characterization of treated samples

All treated powders were subjected to acid attack tests to determine the efficacy of each treatment. Morphology and composition of the treated layer were assessed by SEM/EDS, using the same microscope described above and an EDS probe. SEM observations were also repeated after acid attack.

The actual formation of HAP as a result of the reaction was verified for relevant samples (see Table VIII.1) by FT-IR (Nicolet 6700 FTIR Spectrometer, ATR mode) by performing 16 scans with a resolution of 1 cm^{-1}. To determine the capability of FT-IR test to detect possible soluble phases

present in the powders, mixtures of pure HAP and pure brushite at varying percentage (1 to 20 wt%) were prepared and analyzed in exactly the same way as for the powders. Acid attack tests were also performed on the mixtures of pure HAP and pure brushite, to determine the influence of varying percentage of soluble phases on acid resistance of hydroxyapatite-based coatings.

More detailed FT-IR tests were performed for the most promising formulation (D8E+8), and for samples treated at pH11, as results obtained for D11 mixture were controversial, to determine possible presence of metastable phases. FT-IR on the selected formulations were performed using a time resolved Fourier Transform infrared spectrometer Bruker IFS 66 V/S, diamond crystal, performing 320 scans instead of 16. Curves were shifted to zero at 1600 cm^{-1} and peak heights were matched at 873 cm^{-1} so that curves could be compared.

Specific surface determination (BET) was performed on relevant samples (see Table VIII.1), before and after acid attack by nitrogen adsorption (Micromeritics ASAP 2010).

Acid attack tests were repeated on Carrara marble cubes, untreated and treated with the most promising formulations.

VIII.2.2.3.1. Acid attack test

Duplicate samples for each treatment were subjected to acid attack test. Acid attack tests were performed at pH 5, due to the following considerations:

- The main mechanism that leads to marble surface recession on site was found in literature to be the dissolution in CO_2-saturated water at pH 5.6, while the contribution of acid rain attack is lower, and is expected to decrease in the next century [6].
- Rain pH in Europe is generally spanning from 5 to 7 [6], hence pH 5 can be considered as the most severe condition that can be experienced on site, while still being more severe than natural (pH 5.6) conditions.

Lower pH values could have been selected, thus reproducing more severe conditions, but these would have not necessarily been representative of the behavior of marble samples. In fact, according to ref. [36], dissolution kinetics of calcite vary in 3 different pH regimes (acid solutions, neutral and alkaline solution, and transitional regime). In each regime the dependence of dissolution rate on H^+ concentration and the presence of Ca^{2+} in solution varies, and hence the dissolution rate can be chemically controlled, transport-controlled, or determined by mixed kinetics. The pH range of rain is in the transitional regime, which is substantially between pH 4 and pH 5.5; for this reason, no significant variations are expected by lowering the pH inside that range, while a further decrease would result in switching to a more acidic regime, controlled by different kinetics. Moreover, HAP is known to be the most stable calcium phosphate in a pH range spanning from 4 to 4.5 [35], while, for example, DCPD is more stable than HAP below pH 4. For this reason, in case soluble phases

were formed from the reaction, the behavior of samples at too low a pH (below 4) would not be representative of their behavior at pH above 4. The mechanisms of dissolution of HAP-treated and untreated Carrara marble are elucidated more in detail in ref. [21].

Together with tests for reproducing acid rain, performed at pH 5, tests at pH 3.5 (chosen to be in the reaction-controlled regime below pH 4) were run for samples D8, D11, D8E and for the best double treatments formulations (D8E+8 and D11+8), to better understand the behavior of samples treated in both transitional and acidic solutions. Results were compared to those obtained for AmOx samples.

Prior to each test, the pH-meter was calibrated in pH 4, 7 and 10 buffer solutions. Nitric acid (HNO_3) was used to adjust the solution pH to 5; HNO_3, was chosen over HCl, as it causes the lowest ion exchange with HAP [37]. The HNO_3 solution was left stirring to allow equilibration with atmospheric CO_2 prior to the tests. pH variations as a function of time were recorded (Oakton pHmeter, pH 1100 series). Results were expressed as pH versus time graphs.

Tests were kept running until a stable pH value was attained (150 minutes). Longer tests were performed on bare marble and marble treated with the most promising formulation (D8E+8), to better determine the mechanisms of acid attack. Longer acid attack tests were performed exactly as described above, but lasted 72 hours.

Second acid attack tests were performed on D8E+8 powders after the first acid attack test, to determine whether soluble phases, possibly present on the sample surface, would dissolve during the first test, hence leaving only insoluble HAP. The same procedure was performed on marble powder to detect the possible presence of soluble phases in the starting material. HAP powder was subjected to double acid attack test, for comparison's sake. The purity of commercial HAP powders was verified by submerging them for 12 hours in acid at pH 3.5, then re-running tests at pH5.

VIII.2.2.4. Preliminary tests on Carrara Marble Cubes

The most promising treatments were also performed on Carrara marble cubes, according to the same procedure described above, to compare results obtained on cubes with those of powders. The rotational speed of the container was adjusted so that samples could rotate inside the cylindrical containers and the whole external surface could be in contact with the solution. Six cubes were tested in total: 2 marble cubes were treated with D8 and D8E+8 formulations, and 2 were left untreated as a reference.

Acid attack tests on coarse samples were performed exactly as for the powders, but a longer exposure time (72 h) was used, to let the pH reach a stable value.

Before performing acid attack on coarse Carrara marble samples, the dependence of acid attack resistance on material composition was investigated, by manually grinding both Carrara marble cubes and powders and performing acid attack test. To assess whether the samples could be considered comparable after manually grinding, their specific surface was assessed by nitrogen sorption BET. Manually ground samples were also used to determine the effects of specific surface increase on acid resistance of samples.

VIII.3. Results

VIII.3.1. Characterization of the starting calcite powder

The composition of marble powders used for the tests was found to be magnesium-calcium carbonate. The specific surface area of the powders is reported in Table VIII.2. Acid attack resistance of bare marble is reported in Figure VIII.1, and its morphology before and after acid attack is available in Figure VIII.2 and Figure VIII.3.

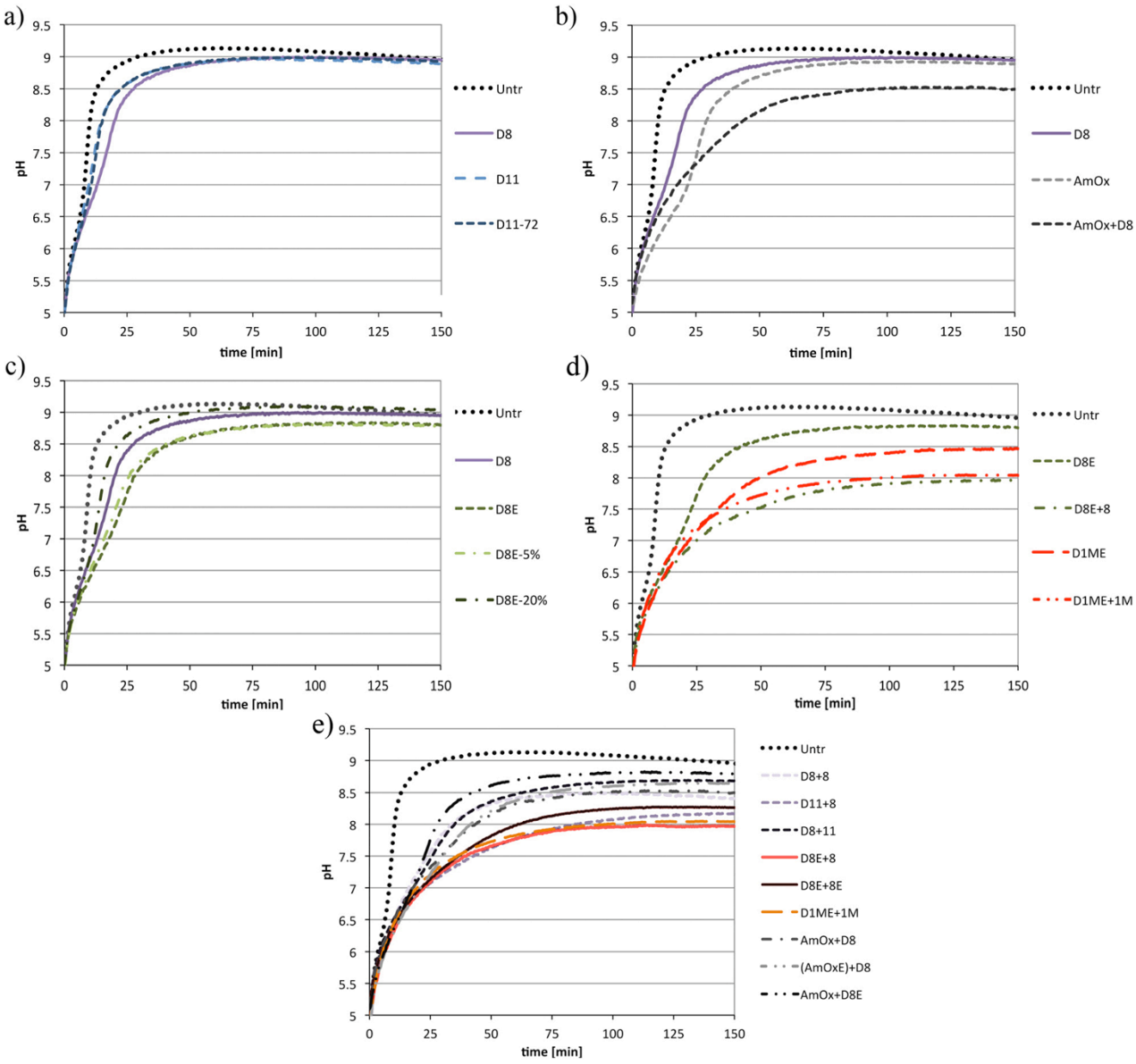

Figure VIII.1: Acid attack test results (pH vs time) for samples treated with a) solutions at different pH, b) hydroxyapatite and ammonium oxalate, alone and mixed, c) ethanol additions at different concentrations, d) ethanol and variable concentration of DAP, e) double treatments.

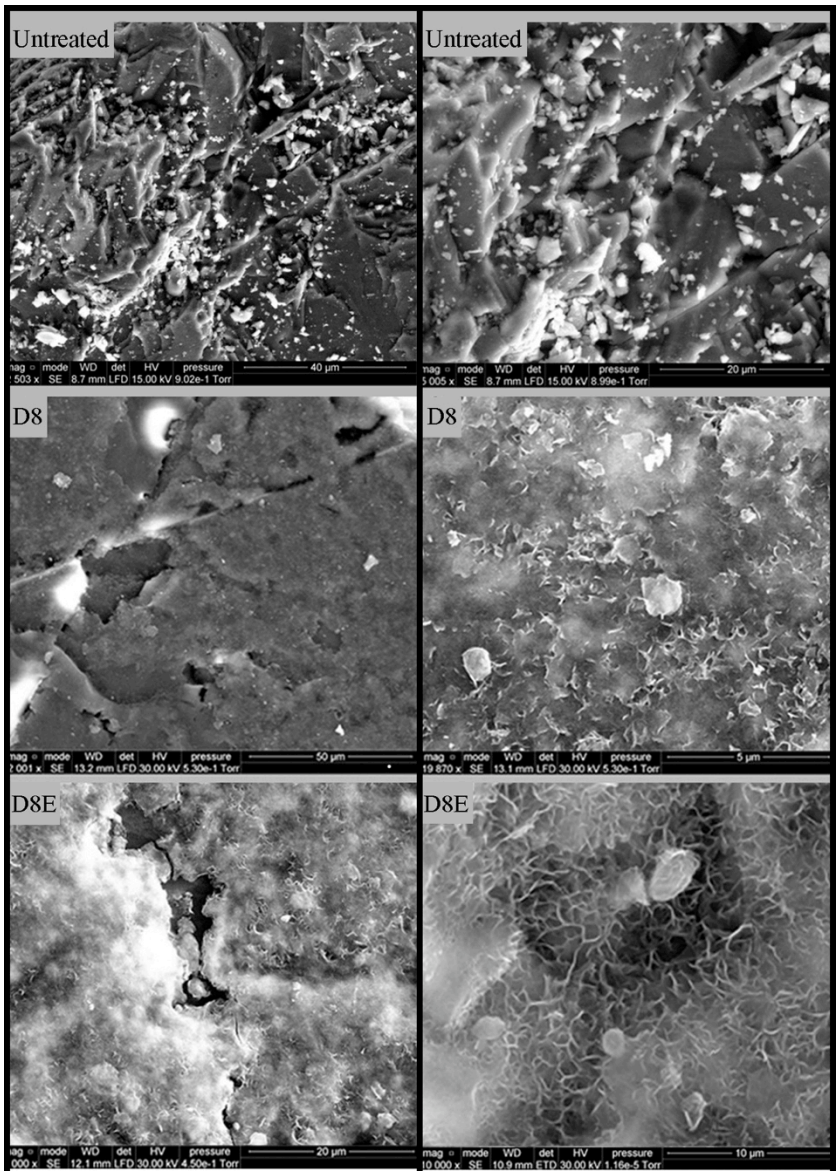

Figure VIII.2: Morphology of calcite powders: untreated, treated with 0.1M DAP + 0.1mM $CaCl_2$ solution (samples "D8"), and the same solution with ethanol addition (samples "D8E")

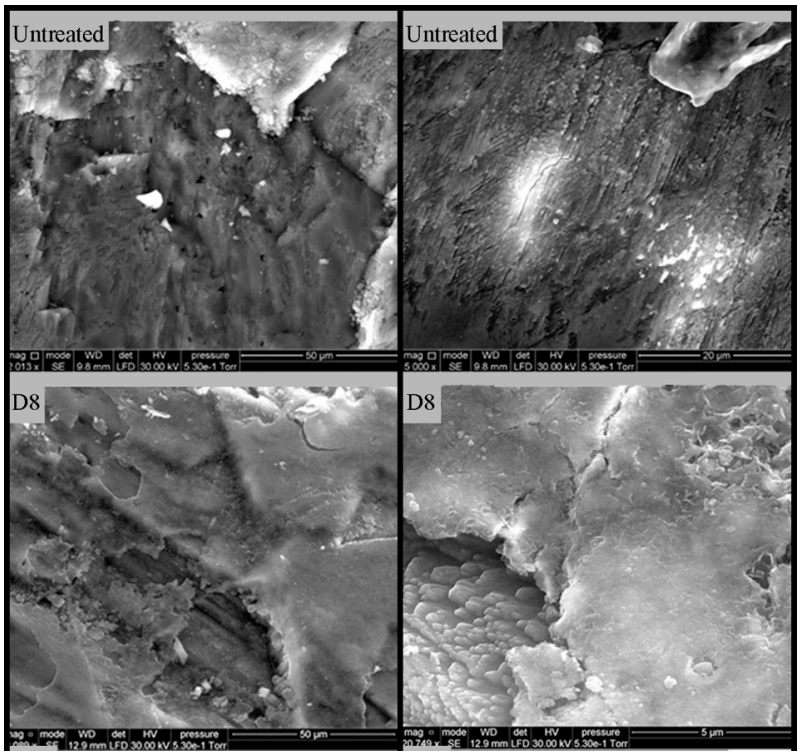

Figure VIII.3: Morphology of untreated powders and samples D8 after acid attack test. Etching of bare calcite surface can be envisaged in untreated powders. It is noticeable that in samples D8 the marble under the HAP layer was attacked by the acid.

VIII.3.2. Effect of pH

Acid attack test results on powders at pH8 and pH11 are reported in Figure VIII.1a. D8 samples are slightly less susceptible to acid attack than bare marble, as the first part of the curve is less steep; however, protection cannot be considered satisfactory, as the curves merge in the latter part. Samples at pH11 exhibit an even lower protection. No benefit was obtained by letting the samples react for a longer time, as the two curves D11 and D11-72 perfectly overlap. The behavior of D8 and D11 samples in acid at pH 3.5 is described in Figure VIII.4b. In this case, the acid resistance of samples treated at pH11 was even lower than that of the untreated reference.

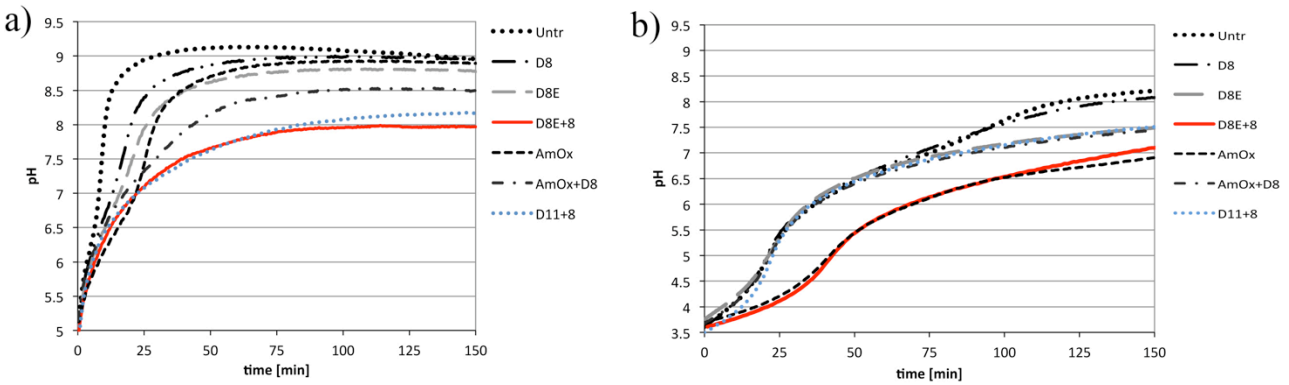

Figure VIII.4: Acid resistance of the most promising formulations at a) pH 5 and b) pH 3.5. Samples D8 and AmOx are also reported for comparison sake. The effect of ethanol addition at different pH can be seen by comparing curves D8 and D8E.

Sample morphology before and after acid attack, investigated by SEM, can be observed in Figure VIII.2 and VIII.3 (D8 samples) and Figure VIII.5 (D11 samples). Relevant EDS data are reported in the Figure VIII.6. D8 samples exhibit a fair, however incomplete, coverage of the substrate. As a result of the incomplete coverage, after acid attack, marble underlying the treated layer was corroded (Figure VIII.3). D11 samples, in contrast, exhibit a complete and uniform coverage. The morphology of D11 samples completely differs from that of samples treated at pH8; images of D11 samples at high magnification are reported in Figure VIII.7. After acid attack the treated layer of D11 samples was found to be consumed (Figure VIII.5).

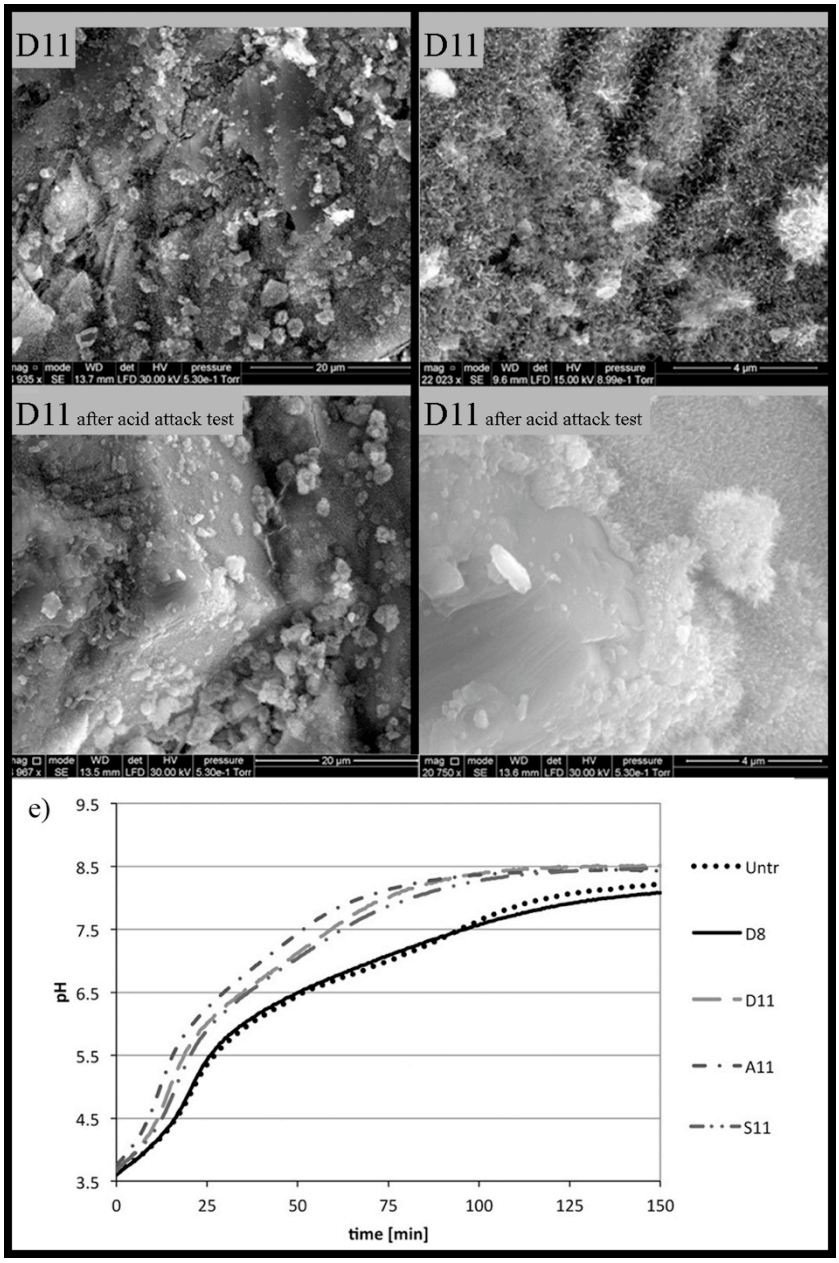

Figure VIII.5: SEM images of samples D11 before and after acid attack test. After acis attack the treated layer was consumed by the acid. In (e) is reported the resistance in acid at pH 3.5 of samples treated at pH11 with and without cationic additions.

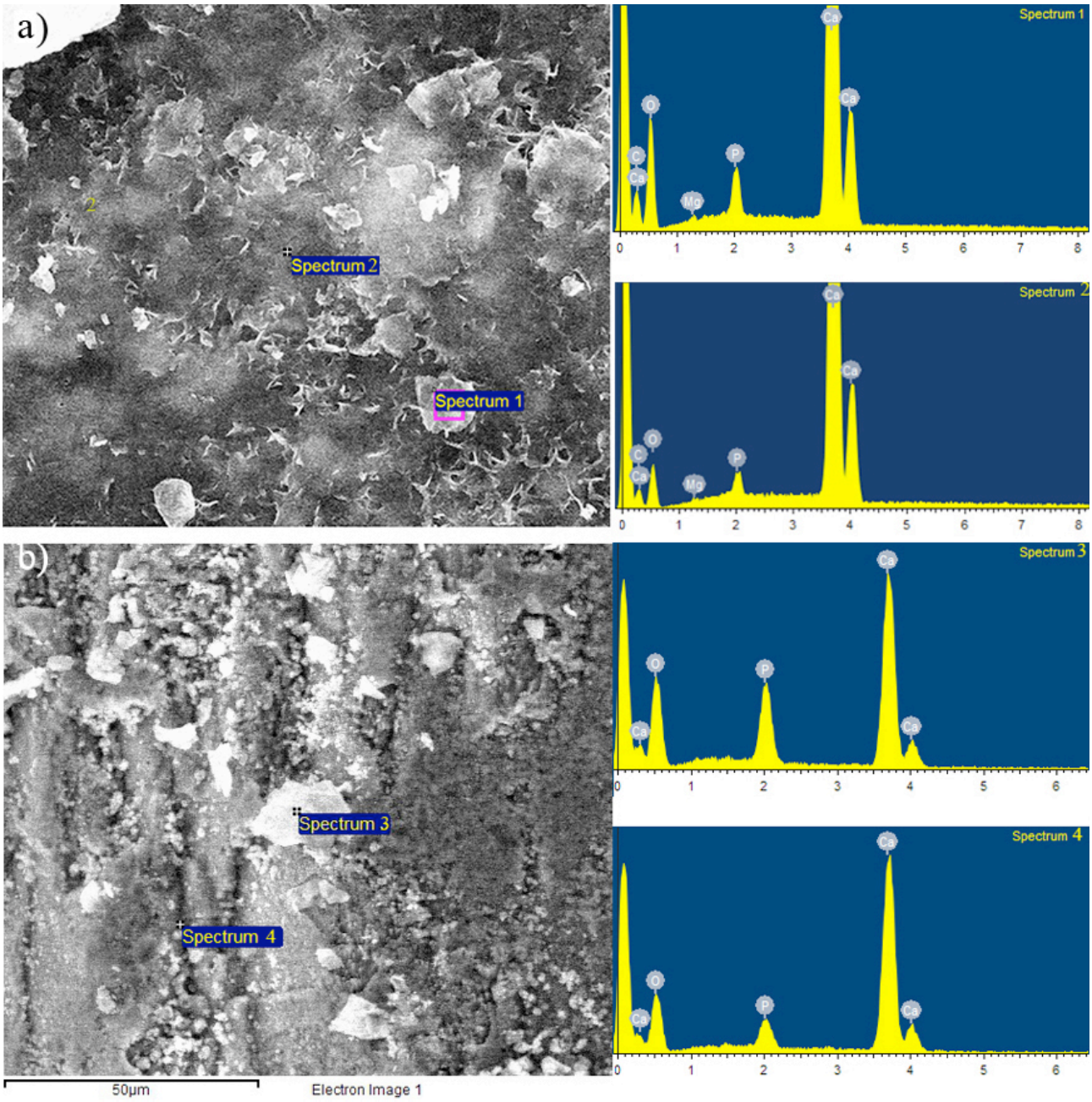

Figure VIII.6: EDS data showing phosphorus in samples (a) D8 and (b) D11. As no phosphorous impurities were found by EDS in bare marble, its presence indicates the formation of phosphatic phases due to the treatment.

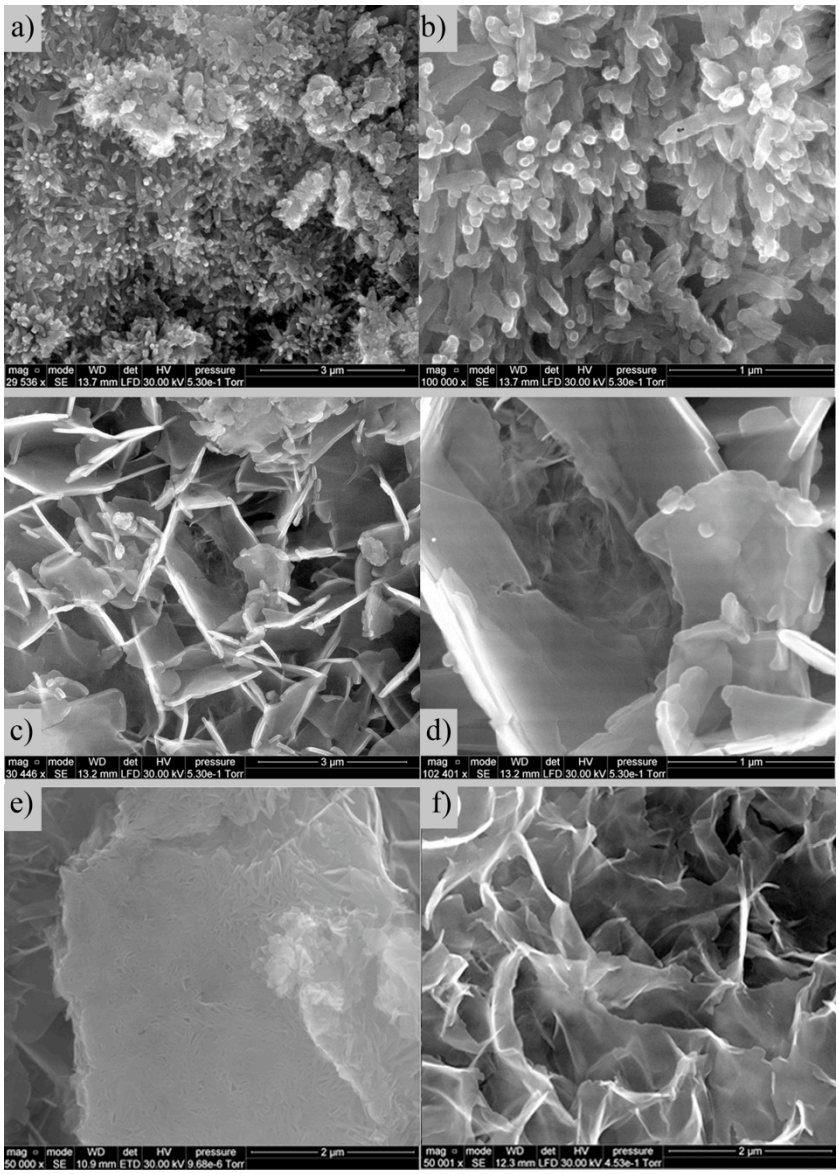

Figure VIII.7: SEM images of D11 (a,b), D11+8 (c,d) and D8E (e,f) samples at high magnification. A flowery morphology was observed in D11 treated layers, while a platy one was found in several areas of sample D11+8 and in sample D8E.

The specific surface area of treated samples is reported in Table VIII.2: a much higher specific surface was found for treated samples (especially D11) compared to bare marble. The increased susceptibility of the same material to acid attack due to larger specific surface area is indicated by the fact that the ground marble curve is much steeper than that corresponding to the powder prior to grinding, and a higher pH value (8.9 instead of 8.1) is reached after 150 minutes, as displayed in Figure VIII.8.

	BET SURFACE AREA [m^2/g]
Untr	0.0534 (±0.0012)
D8	0.6075 (±0.0017)
D11	0.8455 (±0.0015)
M11-H	0.8843 (±0.0018)
M11	0.7011 (±0.0012)
S11-H	0.8407 (±0.0019)
S11	0.5923 (±0.0021)
A11	0.4151 (±0.0017)
A8	0.1291 (±0.0014)

Table VIII.2: Samples BET surface area: samples at high and low pH, with and without cationic additions are considered. Two different concentrations were tested for samples treated with Magnesium and Strontium doped solutions: 0.1 mM $MgCl_2{\cdot}6H_2O$ (sample M11) and 0.2 mM $MgCl_2{\cdot}6H_2O$ (sample M11-H) were used for magnesium chloride, while 0.5 mM $SrCl_2{\cdot}6H_2O$ (sample S11) and 1 mM $SrCl_2{\cdot}6H_2O$ (sample S11-H) for strontium chloride. The formulations causing the lowest increase in specific surface area were selected and further characterized, and are referred to as M11 and S11 elsewhere in the text.

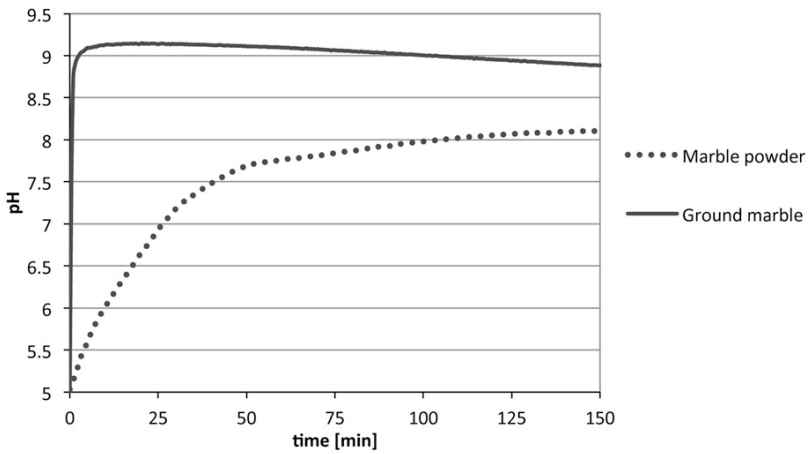

Figure VIII.8: Effect of specific surface on acid attack resistance: Different susceptibility of marble powders to acid attack test, depending on specific surface. Both curves refer to sample "untr" before ("marble powder") and after ("ground marble") manual grinding.

To explain the difference of morphology and acid resistance of D11 treated samples, FT-IR spectroscopy was performed. FT-IR performed on D8 and D11 treated powders (Figure VIII.9) show bands at 1030, 1055 cm^{-1} and 560-570 and 600 cm^{-1}, compatible with the formation of HAP [38,39]. However, FT-IR performed with 16 scans were found to be able to detect only the presence of substances in concentration above 5 wt%, whereas lower concentrations (i.e., 1 wt%) would affect the HAP solubility in acid (see Figure VIII.10). Hence, FT-IR with more scans (Figure VIII.11) were performed, to detect possible soluble phases not detected by FT-IR at lower resolution. Results of FT-IR at 320 scans are shown in Figure VIII.11. Bare marble and D11 curves

match in absorbance at all three calcite peaks (1400, 873 and 700 cm^{-1}). Bands in the region 1100-1000 cm^{-1} and 500-600 cm^{-1}, compatible with ν3 and ν4 phosphate asymmetric stretching and bending modes of HAP, respectively [22], can be seen in D11 samples. Bands at 1100-1000 cm^{-1} appear as broad and shoulders are not well defined.

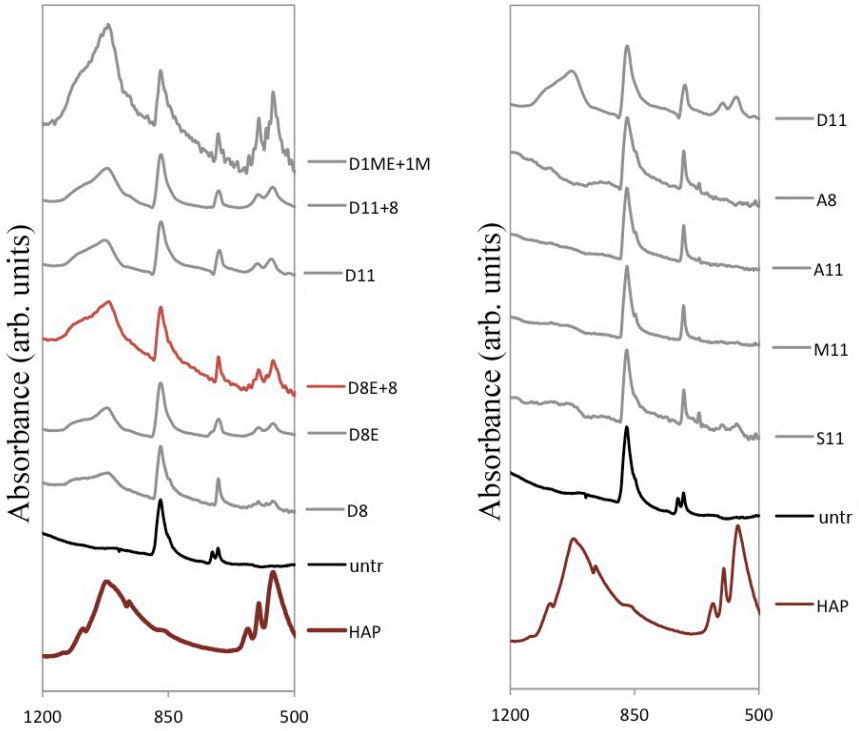

Figure VIII.9: Composition of treated powders as assessed by FT-IR (16 scans): a) most promising formulations and b) samples with cationic additions. Bare marble powder and pure HAP powders were used as references

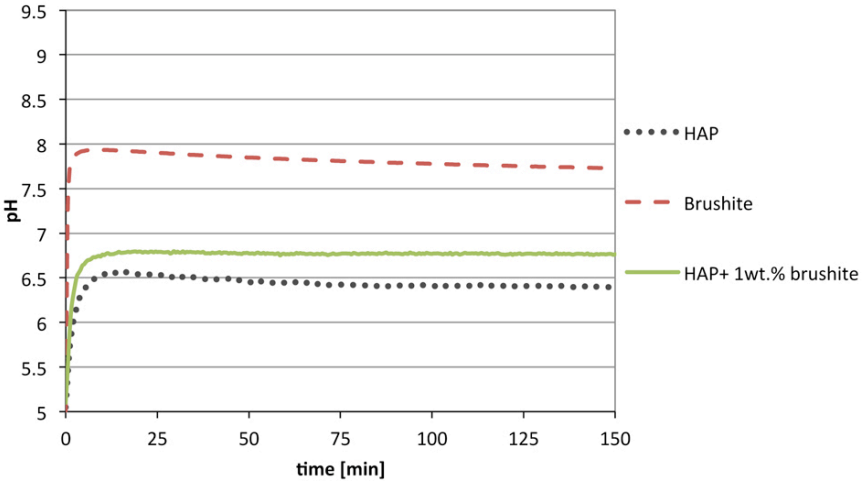

Figure VIII.10: Impact of the addition of 1 wt.% soluble phases on HAP solubility in acid. In this case, brushite was used for the tests as it is more soluble than HAP at pH 5.

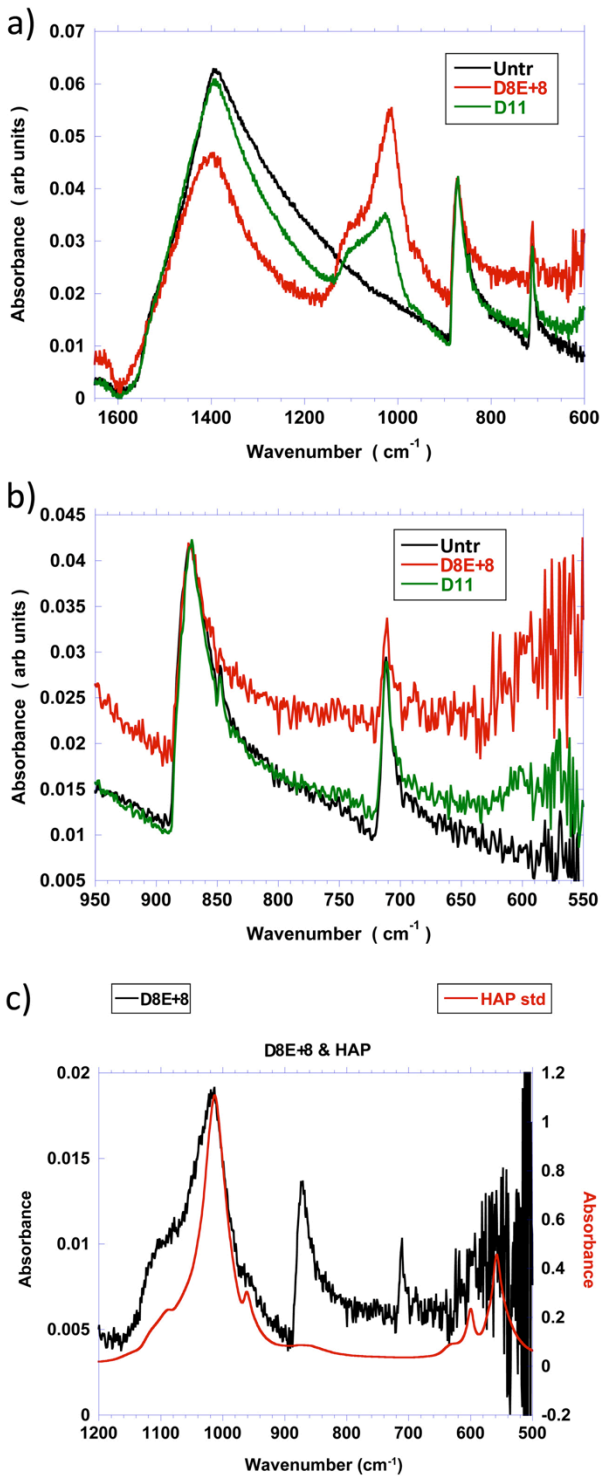

Figure VIII.11: FT-IR at 320 scans of untreated calcite powder and samples D11 and D8E+8. Spectra of untreated (untr) and treated samples (D11 and D8E+8) in a) the 1650-600 cm^{-1} region and b) the 950-550 cm^{-1} region. Curves were shifted to zero at 1600 cm^{-1} and peaks were matched at 873 cm^{-1}

In c) spectrum of sample D8E+8 is compared to a pure HAP reference ("HAP std", courtesy of prof. S.C. Myneni).

VIII.3.3. Effect of cationic additions.

Morphology of samples with cationic additions (Sr^{2+}, Mg^{2+} and Al^{3+}) is reported in Figure VIII.12 and their composition, as assessed by FT-IR is listed in Figure VIII.9. Effects of cationic additions in terms of specific surface alterations and acid attack resistance are reported in Table VIII.2 and Figure VIII.5e, respectively.

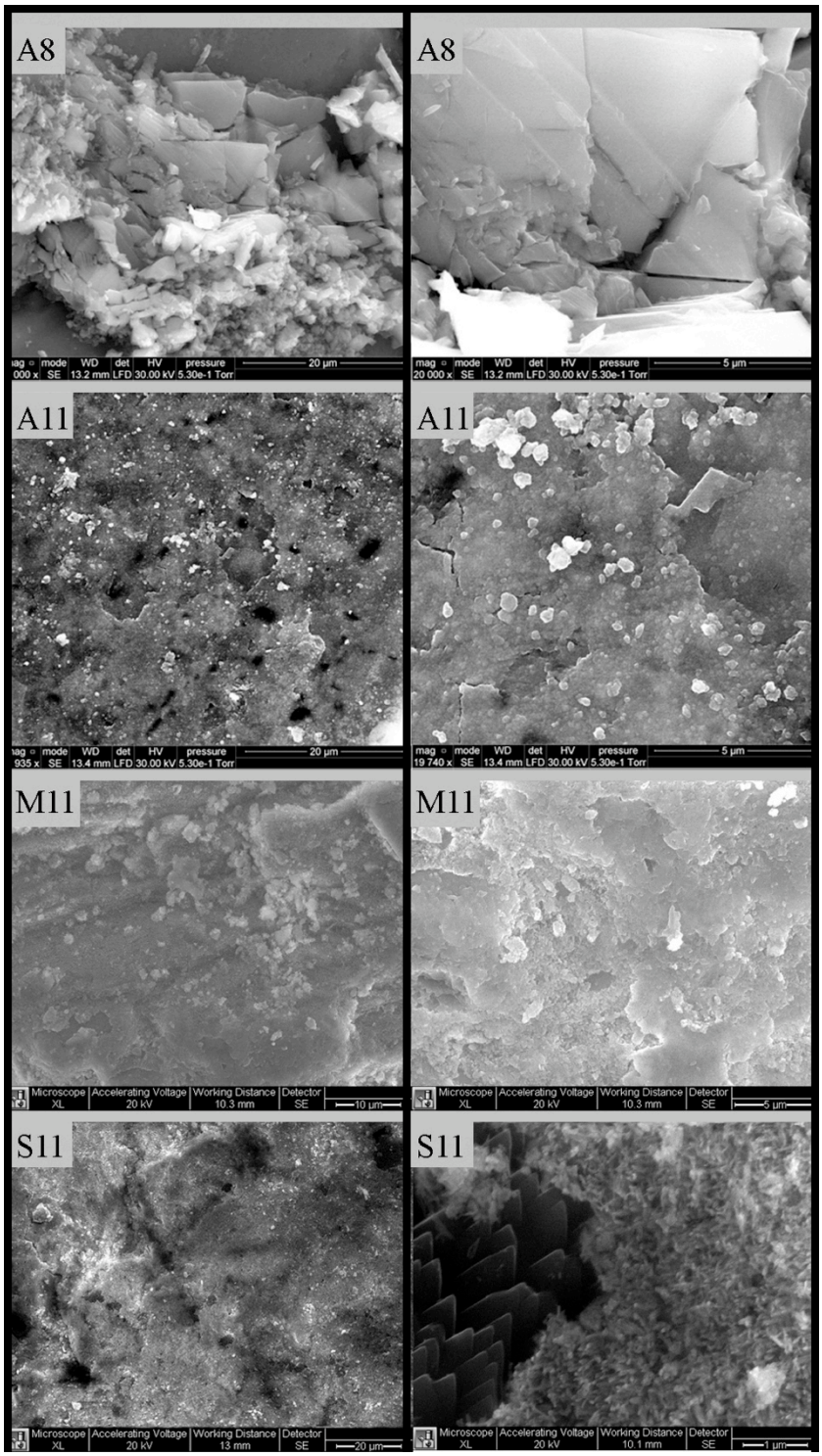

Figure VIII.12: SEM images of samples with cationic additions: aluminum-doped samples at pH 8 "A8" and pH11 "A11"; magnesium-doped samples "M11"; strontium-doped samples "S11".

Only sparse crystals are present on A8 surface, while A11 is essentially bare. A quite uniform treated layer is present on M11 surface, while S11 layer is incomplete and cracked. Each cationic addition largely modifies the coating morphology.

VIII.3.4. Effect of ethanol addition

The effect of the addition of 0.5 wt% ethanol (samples D8E) on the morphology of the treated layer is displayed in Figure VIII.2. The layer appears more uniform and complete; however, some bare marble areas were observed near the grain edges. The effects of increasing the concentration of DAP (while keeping the concentration of ethanol constant) on the acid attack resistance of samples and on the morphology of the treated layer can be seen in Figure VIII.1 and Figure VIII.13. The effects of adding different concentrations of ethanol to the DAP solution and that of varying the DAP concentration on the acid attack resistance of samples are displayed in Figure VIII.1c and d, respectively. The behavior of ethanol-doped samples at pH 3.5 is reported in Figure VIII.4b.

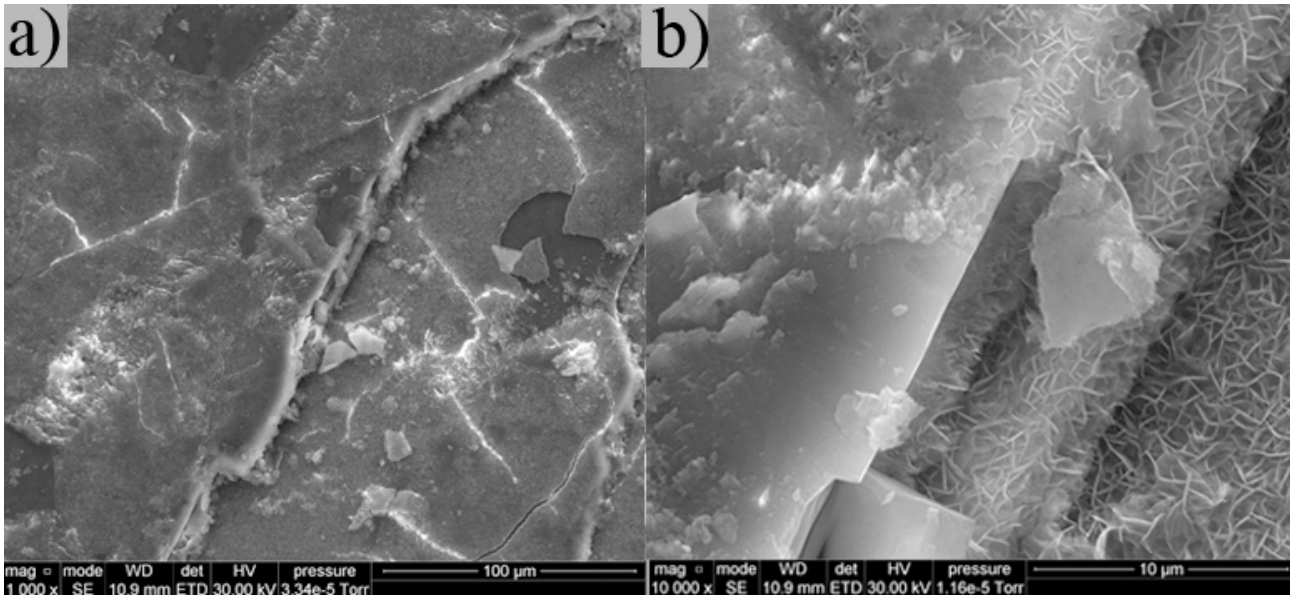

Figure VIII.13: Morphology of sample 1ME: the treated layer appears densely cracked and same parts are peeled off, possibly due to excessive thickness of the layer.

VIII.3.5. Comparison with ammonium oxalate treatment

Ammonium oxalate was found to form a very coherent layer on the powders surface (Figure VIII.14). Acid attack resistance of AmOx treated samples is shown in Figure VIII.1b, in comparison with that of D8 and bare marble. Acid resistance at pH 3.5 is reported in Figure VIII.4b.

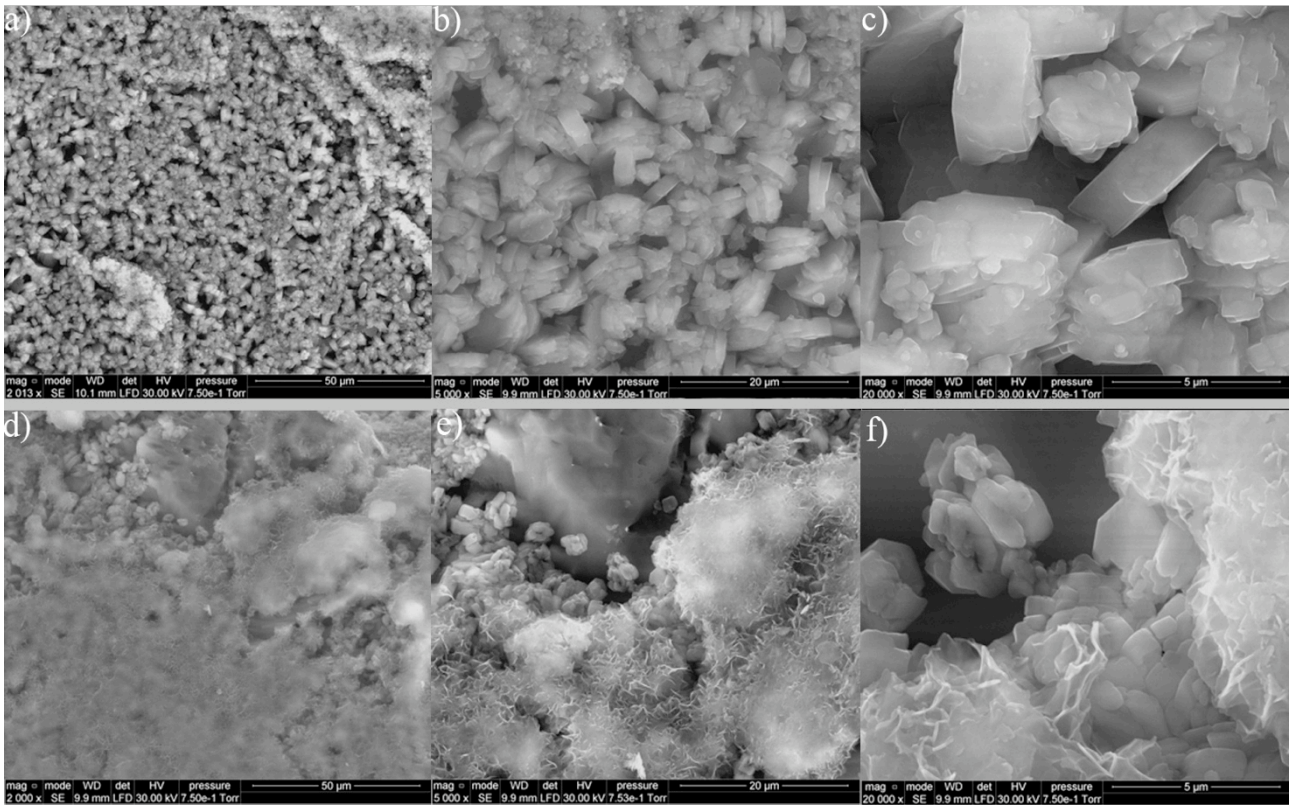

Figure VIII.14: SEM images of (a,b,c) AmOx treated samples and (d,e,f) AmOx+D8 samples.

VIII.3.6. Effect of double treatments

SEM images of samples D8+8, D8+11 and D11+8 are reported in Figure VIII.15. Surface coverage is poor for samples D8+11, which also exhibits cracks, and for D8+8. Sample D11+8 is uniformly coated, but shows some cracks and some flat crystals that might indicate the formation of octacalcium phosphate together with HAP.

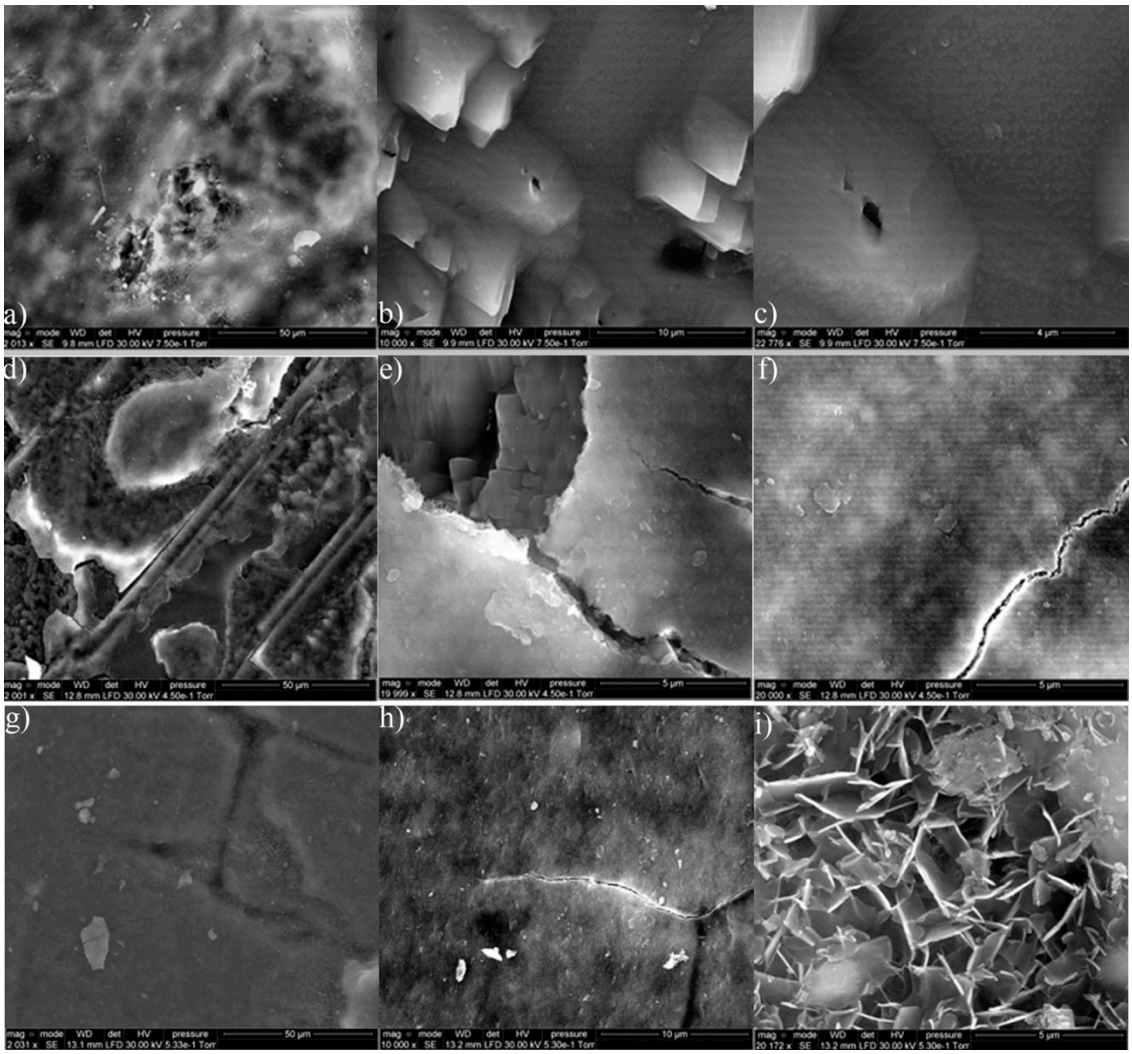

Figure VIII.15: Morphology of samples after DAP double treatments: SEM images of samples (a, b, c) D8+8, (d, e, f) D8+11 and (g, h, i) D11+8. Samples D8+8 and D8+11 exhibit incomplete coverage of the substrate, while sample D11+8, despite sporadic cracking, exhibits a uniform treated layer. Platy morphology (i) can be seen in several areas of sample D11+8.

Acid attack resistance of samples subjected to double treatments is reported in Figure VIII.1e. The best acid resistance was obtained for samples D8E+8, whose morphology is illustrated in Figure VIII.16, and D11+8. The presence of HAP as a result of the most promising treatments (namely, D11+8 and D8E+8) was verified by FT-IR at 16 scans (Figure VIII.9). Both treatments exhibit a good coverage of the support and acid resistance; however, due to the absence of cracks and to the

easier handling of the precursors, and considering the better behavior in acid at pH 3.5 (see Figure VIII.4), D8E+8 was chosen as the most promising treatment, and subjected to further tests.

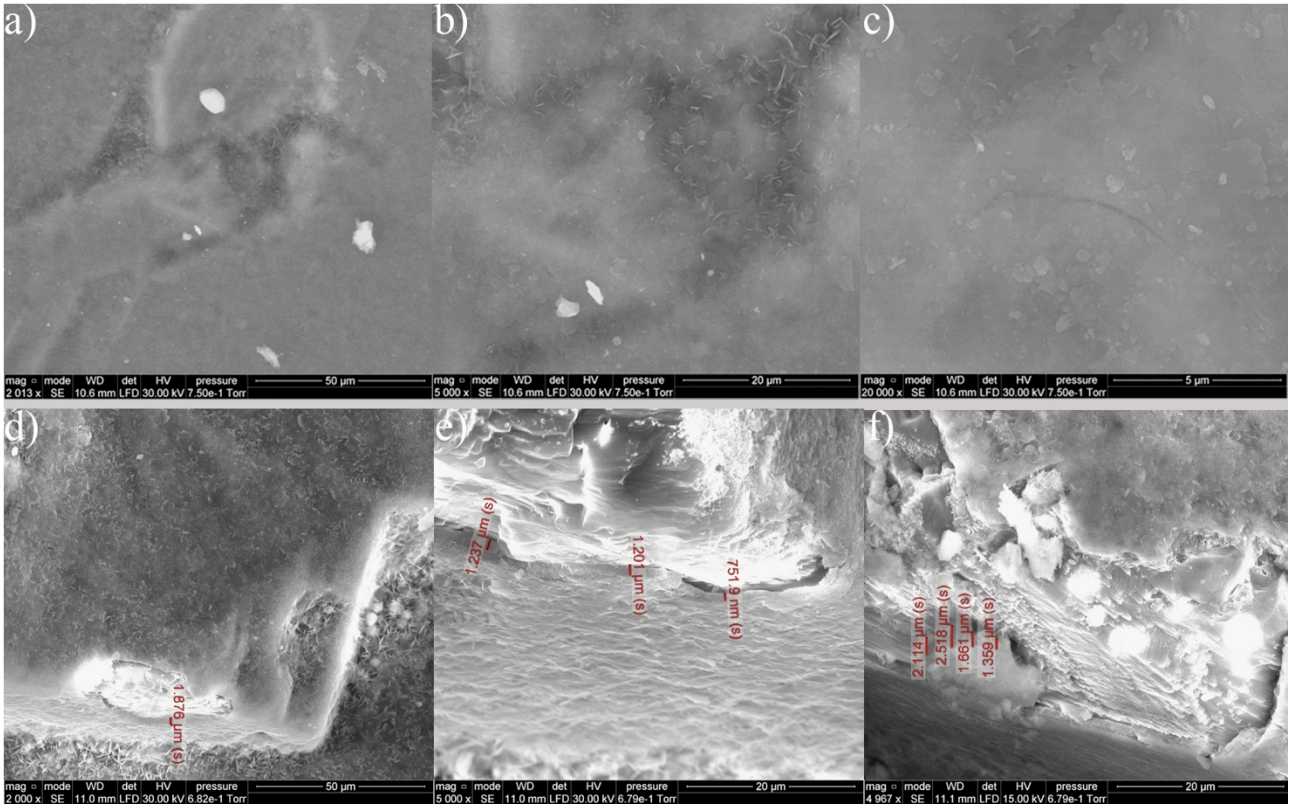

Figure VIII.16: Sample D8E+8 morphology: SEM images of samples double-treated at 1M DAP concentration before (a,b,c) and after (d,e,f) acid attack test.

AmOx+D8 sample morphology and acid resistance are reported in Figure VIII.1 and VIII.14. The behavior in acid is much better than AmOx-treated samples; however, it is still lower than that of D8E+8 samples, probably because the coverage of the substrate is less uniform, as the HAP layer on top of the calcium oxalate one is patchy. Moreover, some bare marble areas can be observed, that are not present in AmOx-treated samples. The addition of ethanol to AmOx did not result in any benefit (Figure VIII.1e).

Using DAP at 1 M concentration, instead of 0.1 M does not represent a benefit in terms of acid attack resistance (Figure VIII.1d). The morphology of 1ME+1M samples is reported in Figure VIII.17: samples are largely cracked and some detachments can be observed after acid attack test. Due to the presence of cracks, it was possible to determine the thickness of the treated layer (1.1 µm to 2.8 µm).

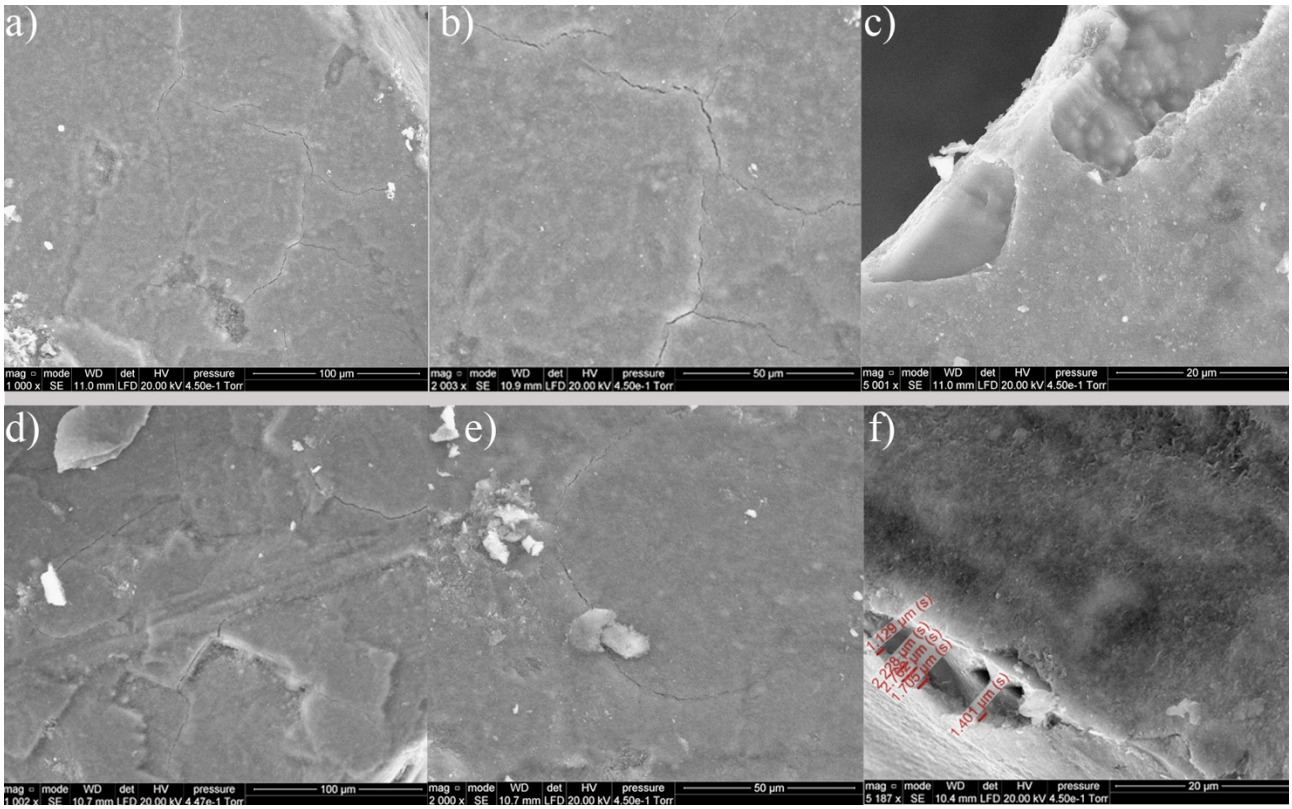

Figure VIII.17: Morphology of D1ME+1M sample before and after acid attack test. Before acid attack test (a,b,c) the treated layer appears uniform, continuous and un-cracked; after attack (d,e,f), some parts of the treated layer were detached, allowing measurement of its thickness.

SEM images of the most promising formulation (sample D8E+8) before and after acid attack are reported in Figure VIII.16. After acid attack, it was possible to measure the thickness of the treated layer (Figure VIII.16d,e,f), that is assessed around 1.6 μm on average, but varies from a minimum of 1.3 μm to a maximum of 2.5 μm.

BET surface before and after acid attack test are reported in Table VIII.3. Some surface roughening (increase in specific surface) can be observed after acid attack, as in the case of untreated marble.

BET SURFACE AREA [m^2/g]

	before acid attack	after acid attack
Untr	0.0534 (±0.0012)	0.0720 (±0.0012)
D8E+8	0.6358 (±0.0027)	0.7321 (±0.0038)

Table VIII.3: Acid attack effect on samples specific surface: BET surface area of samples before and after acid attack

FT-IR results at 320 scans for sample D8E+8 are reported in Figure VIII.11. Calcite bands are less visible than those of D11 (especially that at 1400 cm^{-1}), while phosphate bands at 1100-1000 cm^{-1} are much more pronounced. The shape of the band (broad and with ill-defined shoulders) resembles

that of the D11 sample. Differences can also be assessed in the 650 cm^{-1} area, also corresponding to HAP, where bands are more pronounced for samples D8E+8.

To determine whether the soluble phase would dissolve in acid at pH 5, a second acid attack test was run on samples already subjected to acid attack test, results being shown in Figure VIII.18. For comparison's sake, the same test was carried out on pure HAP powder (Figure VIII.18). The results show that no remarkable differences can be assessed in the behavior of samples D8E+8 during the second test compared to that exhibited during the first one, resembling what seen for bare marble, where the two curves perfectly overlap. Correspondingly, no remarkable differences can be seen in the curves obtained for pure HAP standard, hence indicating no relevant presence of impurities in the powder.

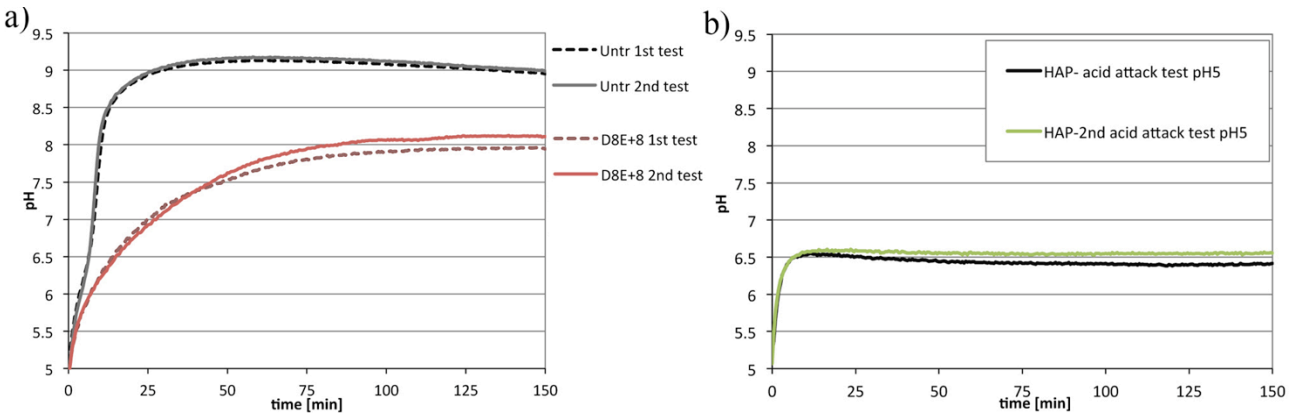

Figure VIII.18: (a) Behavior of untreated and D8E+8 samples after two acid attack tests. (b) Double acid attack tests were also performed on pure HAP powders for comparison.

VIII.3.7. Carrara marble cubes

Treatment D8E+8 was tested on Carrara marble cubes. The acid attack resistance of coarse samples treated with D8E+8, in comparison with that of D8 and untreated cubes is reported in Figure VIII.19a. Acid attack tests on marble cubes was also compared to tests on powders for samples D8E+8 and for untreated references (Figure VIII.19b). Different susceptibility of the materials of powders and cubes was evaluated (Figure VIII.20).

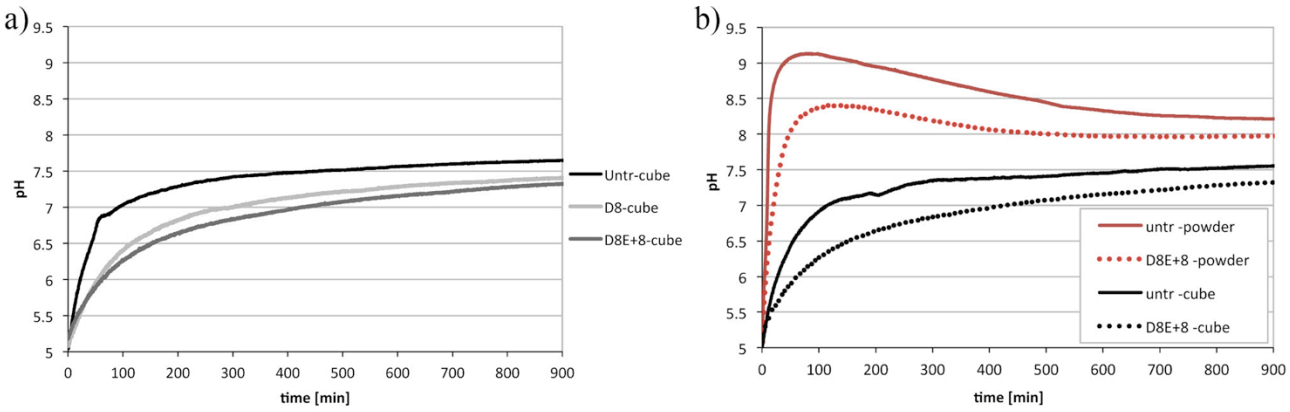

Figure VIII.19: a) Acid attack test on marble cubes and b) comparison between cubes and powders. Differences in the behavior of cubes and powders are also due to the huge difference in their specific surface (Table VIII.4).

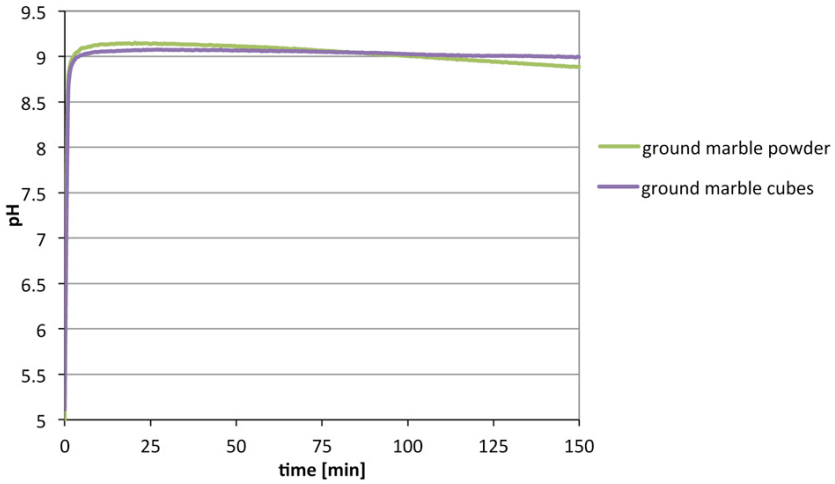

Figure VIII.20: Acid attack resistance of untreated marble powders and Carrara Marble cubes after manual grinding.

	BET SURFACE AREA [m^2/g]
Ground marble powders	0.6217 (±0.0048)
Ground Carrara marble	0.7403 (±0.0073)
HAP powder	1.1471 (±0.0042)

Table VIII.4: BET surface of manually ground marble powders and Carrara marble cubes. Specific surface of commercial HAP powder used for the tests is also reported.

VIII.4. Discussion

Marble powders, composed of magnesium-calcium carbonate, exhibited a marked susceptibility to acid attack at pH 5, resulting in the roughening of the surface, proved by SEM images and by the increase of specific surface area after acid attack (Figures VIII.2 and VIII.3, Table VIII.3).

D8 treatment causes a slight decrease in acid attack compared to untreated references (Figure VIII.1). However, the protection is much less than that expected by theoretical considerations, as the curves merge in the latter part. This can be ascribed to the fact that, when treated layer morphology is observed by SEM (Figure VIII.2), incomplete coverage is found. Bare areas of the samples will act as preferential points for acid attack, as the acid can enter and attack the substrate behind the HAP layer.

Samples treated at pH 11 were less resistant to acid than samples prepared at pH 8 (Figure VIII.1), despite the expectation that a higher amount of PO_4^{3-} would have enhanced the formation of HAP; possible reasons for this behavior are described below. No differences were found in samples left reacting for 72 hours, indicating that increased reaction times did not favor the transformation of possible soluble, metastable phases into more stable HAP, as hypothesized on the basis of [38].

When comparing D8 and D11 samples, the latter exhibit a much more uniform coverage of the substrate, and the layer is neither patchy nor cracked. Nonetheless, poor performances are obtained in the acid attack test, even though the formation of HAP at both pH levels was confirmed by FT-IR results at 16 scans (Figure VIII.9). The reason for the poor behavior of D11 might either be the higher specific surface of the sample (Table VIII.2), insufficient coverage due to high porosity, or formation of soluble phases together with HAP at pH 11. The different morphology of the layer in samples D8 and D11 suggests that different phases are formed in the two treatment conditions.

To test the influence of the specific surface area on the acid attack resistance, given the specific test setup, the test was performed on marble powder ground to different finenesses (specific surface area of the powder can be seen in Table VIII.4). It was found that finer powders are correspondingly more susceptible to acid attack than coarser grains, as expected, confirming what is found in literature for non-porous stones [40]. This will need to be taken into consideration also when comparing powders with marble cubes.

The effect of adding small amounts of soluble phases in a HAP layer was simulated by adding increasing amounts of brushite (which is much more soluble than HAP at pH 5) to pure HAP and performing acid attack tests on the mixes. The solubility in acid was found to be remarkably increased even for 1% addition of the soluble phase (data can be found in Figure VIII.10).

The higher solubility of D11 samples was made even more evident by analyzing the behavior in acid at pH 3.5. In fact, at this pH D11 samples exhibit a higher susceptibility than untreated marble. This behavior is not enhanced by any of the cationic additions tested (Figure VIII.5e). This fact seems to be another confirmation of the formation of soluble phases: in fact, pH 11 treatment produces a much higher specific surface than untreated marble. Cationic additions do limit the increase in the specific surface at pH 11, but do not enhance acid resistance. Finally, comparing the morphology of samples treated at pH 8 and 11 after acid attack (Figures VIII.3 and VIII.5), it can be noticed that in sample D8 the acid has attacked the marble substrate, undercutting the treated layer (Figure VIII.3), while in samples at pH 11 the layer itself was found to be corroded (Figure VIII.5). For this reason, D11 samples were examined by FT-IR at 320 scans (Figure VIII.11). Phosphate bands at 1100-1000 cm^{-1} were found in D11 samples, indicating the formation of HAP. As those bands are broad and shoulders are not well-defined, it is possible to infer that HAP obtained is nanocrystalline or disordered. When the spectrum of sample D11 is compared with that of untreated marble and that of D8E+8 sample, it is clear that all three calcite bands are more marked in sample D11 than D8E+8, while those of phosphates are weaker. The presence of calcite bands comparable to those of untreated marble indicates that a worse coverage was obtained for sample D11 with respect to D8E+8, despite their appearance in SEM images. As SEM images exhibited no bare areas

nor cracks, this indicates that either a porous or a very thin layer was obtained. For this reason, it seems that the evaluation of the presence and intensity of the substrate bands by FT-IR might be an effective method for evaluating the coverage of a protective layer.

No evidence for the presence of soluble phases was obtained by FT-IR; moreover, the spectra were compared to those of brushite and no evidence for its presence was found. However, the higher solubility of D11 samples with respect to bare marble in acid at pH 3.5 indicates that soluble phases must be present in the samples: for this reason, further studies for the detection and the determination of the nature and composition of possible soluble phases are currently in progress.

From the equilibrium constants it might be inferred that using solution at pH11 would result in much more PO_4^{3-}. As pH increases, the calcium activity decreases while phosphate activity increases, and so does the propensity to form HAP around pH 11 [41]. However, the kinetics of deprotonation of HPO_4^{2-} are evidently so fast that there is no practical advantage to using the higher pH; moreover, hydroxylation of Ca and deprotonation of carbonate also play a role in the reactivity of phosphate [41].

Phosphate bands compatible with HAP formation, can be assessed for samples treated with strontium (S11). SEM images, however, reveal cracks and uncoated areas, thus indicating that the layer is discontinuous. Moreover, a sharp band is present at 690 cm^{-1}, whose exact determination is currently in progress.

As a result of the application of the magnesium doped solution, a quite uniform and continuous layer was obtained. Despite the uniformity of the layer, very low HAP bands can be assessed; however, as phosphorous peaks are detected by EDS in essentially all areas of the sample, this might indicate that a very thin layer was obtained.

Aluminum nitrate did not provide any benefit in acid attack resistance at pH 8 or 11. This can be explained by examining the morphology of the treated layers: at pH 8 only sparse cubic crystals were found to form, while the surface is essentially bare; at pH 11, the substrate remains almost uncoated, and the sparse areas that are coated are densely cracked. Consistently, there is no evidence for HAP formation in sample A11, as no phosphate bands could be detected in the FT-IR spectrum, while HAP formation can be detected in sample A8. The same sharp band at 690 cm^{-1} detected in sample M11 was recorded in both aluminum treated samples, though in A11 it is barely visible. The absence of bands in the area around 1000 cm^{-1} seems to make the spectra of sample A11 incompatible with either HAP, brushite or OCP; for this reason, further studies are in progress to determine the exact composition of the treated layer.

It is true that the addition of nitrates was found to reduce the acid resistance of the samples (see the case when calcium nitrate is added to calcium chloride), but the fact that aluminum additions were

not beneficial at all suggests that a different precursor needs to be used. The fact that the surface is essentially bare might be linked to the extremely small amounts of aluminum nitrate added. Higher concentrations resulted in precipitation from the solution, rather than deposition of a layer on the calcite. Further tests are currently in progress to determine a more promising precursor for aluminum additions, that allows for higher amounts to be added before precipitation.

Adding ethanol to the DAP solution results in higher acid resistance. The optimal concentration was found to be 0.5 wt%, as higher concentrations (5 wt%) do not provide any further benefit, or even make the solution too diluted (e.g., 20 wt%.), hence lowering its effectiveness. Ethanol, promotes the growth of the HAP layer, hence guaranteeing a better coverage of the support without leading to the formation of cracks. However, some uncoated areas can still be found, especially near the edges of marble powders. For this reason, the concentrations of DAP was increased, while keeping constant the ratio of ethanol to DAP solution (ethanol/DAP solution: 0.5 wt%). Good coverage was obtained and the acid attack performance of these samples (D1ME) was found to be much better than those of the samples at lower concentrations. However, the HAP layer was found to be densely cracked, thus raising some concerns about its thickness.

Ammonium oxalate treated samples were examined for comparison. AmOx samples exhibit a very uniform coverage of calcium oxalate on the samples. No bare areas were detected. The acid attack performances were found to be better than those of D8 samples, but not yet satisfactory, as the two curves merge in the final part. This might be explained considering that the calcium oxalate layer appears porous (Figure VIII.14) and, moreover, its solubility is higher than that of HAP. Although AmOx samples show better acid resistance than D8 samples, by adding 0.5 wt% ethanol (samples D8E) performance better than AmOx treated samples is achieved.

Due to cracking of D1ME samples, instead of raising the DAP concentration of the starting solutions, double treatments were investigated. The first idea was to treat the samples twice with the same solution (samples D8+8). The acid attack performances were found to be improved with respect to D8 samples; however D8+8 exhibits poor substrate coverage (Figure VIII.15). For this reason, the possibility of creating a first, uniform, but not necessarily insoluble layer and a second insoluble one on top of it, was tested. For this reason D11+8 and AmOx+D8 were tested. Moreover, ethanol additions on the first (D8E+8, D11E+8, AmOxE+D8), second (D8+D8E, AmOx+D8E) or both the formulations were tested. All double treatments performed better than the single treatments; however, samples D8+8 and D8+11 exhibit poor surface coverage and acid attack resistance, hence no further tests were performed.

AmOx+D8 treatment exhibited a much better performance than ammonium oxalate alone; however, as can be noticed in the SEM images, the HAP layer that forms on top of the oxalate is incomplete

and patchy (Figure VIII.14), hence reducing the treatment efficacy. Moreover, some bare marble areas were observed, not present in the samples treated with AmOx alone, thus indicating that some calcium oxalate was dissolved in the HAP solution. In sample AmOx+D8E the addition of ethanol to DAP reduces the surface coverage on top of AmOx, hence further decreasing the treatment efficacy (Figure VIII.1e). This suggests that ethanol does not adsorb on calcium oxalate, however, further investigation is required to determine whether it is so.

In terms of acid attack test the best performances were obtained for samples D11+8 and D8E+8 (Figure VIII.1e). FT-IR on both samples (Figure VIII.9) have shown the formation of HAP alone. Analyzing the morphology of these samples by SEM, it was noticed that both exhibit a very uniform coverage of the samples, but samples D11+8 show some cracks (Figure VIII.15), not present in D8E+8 samples (Figure VIII.16). Moreover, samples D11+8 show some flat crystal areas that suggest the formation of octacalcium phosphate, together with HAP, while the morphology of D8E+8 is more consistent with HAP. However, some "platy" morphology can also be found in HAP [22]. Finally, sample D8E+8 exhibited much better behavior at pH 3.5 (Figure VIII.4b), where its resistance is comparable to that of ammonium oxalate, while that of sample D11+8 is remarkably lower.

These considerations, together with the fact that using very low concentrations of ethanol is preferred for on-site application, rather than employing high pH (especially for handling precautions), led to identify D8E+8 as the most promising treatment, which was then subjected to further characterization. Samples D8E+8 still suffer some damage due to acid attack, probably to be ascribed to the increase in sample specific surface, to some porosity in the layer, and to the presence of some soluble fractions. However, the dissolution is significantly decreased compared to bare marble, hence the treatment can be considered satisfactory.

Double treatments at higher concentration were also tested. However, as the layer becomes too thick, it becomes cracked, hence acid attack resistance is slightly lower than that of D8E+8. Some parts of the treated layer were also found to be detached after acid attack test.

Samples D8E+8 were examined with 320 scans in FT-IR. The spectrum shows much stronger bands in the 1100-1000 cm^{-1} and 650 cm^{-1} areas than D11, indicating a higher formation of HAP (see comparison with HAP standard in Figure VIII.11c). Correspondingly, the calcite peaks are smaller, thus indicating a better substrate coverage. Phosphate bands of sample D8E+8 are broad and no definite shoulders are present, as in the case of D11 samples, again indicating the formation of nanocrystalline/disordered HAP. Samples were subjected to a second acid attack test, to determine whether possible soluble phases would dissolve at pH 5 leaving insoluble HAP or, instead, if the susceptibility of the sample would be higher. The results (Figure VIII.18) showed that

the behavior of the sample is identical in the second acid attack test, as seen in the case of bare marble.

Prior to treating Carrara marble cubes, the different susceptibility of the starting material (due to different mineral composition) of powder and Carrara marble to acid attack was assessed. To make results comparable, both materials were manually ground, and their specific surface was determined (Table VIII.4). Both materials exhibited very similar behavior to acid attack (Figure VIII.20); although a small difference exists in their specific surface, the susceptibility of Carrara marble is very similar to that of the calcite powders. Given the similarity in behavior of the materials, when comparing marble cubes with powders, the difference in dissolution rate can be attributed to the enormous difference in surface area. Differences in the growth of the coating and hence in the coverage of the substrate by HAP or in the phases formed from the reaction, which might also make the behavior of powders with respect to cubes significantly different, are excluded by FTIR and SEM observations. Nevertheless, further tests are currently in progress on coarse marble samples, to better assess the morphology and composition of the layer after treatment with D8E+8 solution and the acid attack resistance of treated samples.

Marble cubes were treated with D8 and D8E+8 and subjected to acid attack test. Treated marble cubes exhibit a higher resistance to acid attack than untreated ones; however, as dissolution is much slower than in powders, the results are much less easy to interpret. Experiments where a continuous flow of acid is channeled over the samples (currently in progress) would be more suitable to investigate the behavior of coarse samples, instead of the set-up presented in this paper where a finite volume of acid is used, as the flow system would prevent too high an accumulation of Ca^{2+}. In fact, dissolution of stone exposed to rainfall might also be affected by the thickness of the water film that forms over the stone, which influences the time needed to reach calcium saturation in the film [42]. The concentration of calcium ions in the solution affects the calcium flux rate in the solution and hence plays a role in the rate of calcite dissolution process [42]. When long tests are performed (Figure VIII.19b), as dissolution proceeds, other mechanisms may occur, thus altering the pH registered and pushing it down to a constant value, independent of the initial behavior of the samples. In powders this phenomenon can be neglected, as it happens over much longer times than those necessary for dissolution, but in coarse sample it cannot be ignored.

VIII.5. Conclusions

The optimization of hydroxyapatite (HAP) treatment for marble protection towards acid rain was investigated and the following conclusions can be derived:

- Samples treated at pH 11, despite the initial assumption that the higher amount of PO_4^{3-} that form as a result of DAP dissociation would enhance HAP growth, are less acid resistant. This is probably due to higher layer porosity and to the formation of soluble phases together with HAP. Moreover, the fast

deprotonation of HPO_4^{2-} makes the practical advantage negligible. None of the tested cationic additions at pH 11 allowed for a better efficacy of the treatments;

- The addition of ethanol in very low concentration remarkably increases the resistance of HAP treated samples and the uniformity of the treated layer, thus making it possible to reduce the concentration of diammonium hydrogen phosphate (DAP) used and control the thickness of the treated layer. Samples treated with DAP and ethanol exhibit better resistance than those treated with ammonium oxalate;
- Adding a layer of HAP on top of calcium oxalate increases its acid resistance. However, the HAP layer remains patchy, thus reducing the treatment efficacy, and the coverage is not improved by adding ethanol to the DAP solution;
- A DAP concentration of 0.1 M was found to leave bare areas of marble allowing acid to penetrate and corrode the substrate underneath the treated layer. However, by increasing the concentration drying cracks might form. Double treatments were found to be more suitable than increases in DAP concentration, as they make it possible to achieve continuous, uncracked layers. It is also noticeable than the sum of the amount of DAP used in double treatments is much lower than that of the 1 M solution used previously [18], with evident economical benefits;
- Among the double treatments tested, the best ones were those where D8 solution was applied on top of D8E and D11 treated samples (i.e. D8+11 and D8E+8). The first was preferred due to the total absence of cracks and flat crystals areas and to the easier handling of the starting solutions, in view of the application on site;
- D8E+8 was effective in obtaining a very uniform and uncracked layer and in sensibly reducing the acid susceptibility of the material. Some dissolution in acid can still be found, probably due to a small presence of soluble phases and possibly to some porosity of the layer; however the protection provided can be considered satisfactory.

Acknowledgments

I am grateful to Prof. Satish Myneny for profitable discussion and for FT-IR analysis, to Dr. John Schreiber for assistance on SEM analysis, to Prof. Bob Cava for collaboration on possible HAP additions, and to Prof. Andy Bocarsly and Dr. James Pander for FT-IR analysis.

References

[1] Graziani G., Sassoni E., Franzoni E., Scherer G.W., Hydroxyapatite coatings for marble protection: Optimization of calcite covering and acid resistance. Appl Surf Sci 368 (2016) 241-257

[2] Naidu S., Liu C., Scherer G.W., Hydroxyapatite based consolidants and the acceleration of hydrolysis of silicate-based consolidants. J Cult Herit 16 (2015) 94-101

[3] Bonazza A., Sabbioni C., Guaraldi C., De Nuntiis P., Climate change impact: Mapping thermal stress on Carrara marble in Europe. Sci Total Environ 407 (2009) 4506-4512

[4] Matteini M., Inorganic treatments for the consolidation and protection of stone artifacts. Conserv Sci Cult Herit 8 (2008) 13–27

[5] Franzoni E., Sassoni E., Correlation between microstructural characteristics and weight loss of natural stones exposed to simulated acid rain. Sci Total Environ 412–413 (2011) 278-285

[6] Bonazza A., Messina P., Sabbioni C., Grossi C.M., Brimblecombe P., Mapping the impact of climate change on surface recession of carbonate buildings in Europe. Sci Total Environ 407 (2009) 2039-2050

[7] Li D., Xu F., Liu Z., Zhu J., Zhang Q., Shao L., The effect of adding PDMS-OH and silica nanoparticles on sol-gel properties and effectiveness in stone protection. Appl Surf Sci 266 (2013) 368-374

[8] Valentini F., Diamanti A., Carbone M, Bauer E.M., Palleschi G., New cleaning strategies based on carbon nanomaterials applied to the deteriorated marble surfaces: A comparative study with enzyme based treatments. Appl Surf Sci 258 (2012) 5965-5980

[9] Liu Q., Zhang B., Shen Z., Lu H., A crude protective film on historic stone and its artificial preparation through biomimetic synthesis. Appl Surf Sci 253 (2006) 2625-2632

[10] Esposito Corcione C., Striani R., Frigione M., UV-cured siloxane-modified methacrylic system containing hydroxyapatite as potential protective coating for carbonate stones. Prog Org Coat 76 (2013) 1236-1242

[11] Cardiano P., Sergi S., Lazzari M., Piraino P., Epoxy-silica polymers as restoration materials. Polymer 43 (2002) 6635-6640

[12] Esposito Corcione C., Frigione M., Influence of stone particles on the rheological behavior of a novel photopolymerizable siloxane-modified acrylic resin. J Appl Polym Sci 122 (2011) 942-947

[13] Ion R.M., Turcanu-Caruţiu D., Fierăscu R.C., Fierăscu I., Bunghez I.R., Ion M.L., Teodorescu S., Vasilievici G., Rădiţoiu V., Caoxite-Hydroxyapatite composition as consolidating material for the chalk stone for basarabi-murfatlar churches ensemble. Appl Surf Sci (2015), in press

[14] Pinna D., Salvadori B., Porcinai S., Evaluation of the application conditions of artificial protection treatments on salt-laden limestone and marble. Constr Build Mater 25 (2011) 2723-2732

[15] Matteini M., Moles A., Giovannoni S., Calcium oxalate as a protective mineral system for wall paintings: methodology and analyses, III Int. Symp. Conservation of Monuments in the Mediterranean Basin, ed. V. Fassina, H. Ott, F. Zezza, 1994.

[16] Conti C., Colombo C., Dellasega D., Matteini M., Realini M., Zerbi G., Ammonium oxalate treatment: Evaluation by μ-Raman mapping of the penetration depth in different plasters. J Cult Herit 12 (2011) 372-379

[17] Meloni P., Manca F., Carangiu G., Marble protection: An inorganic electrokinetic approach. Appl Surf Sci 273 (2013) 377-385

[18] Sassoni E., Naidu S., Scherer G.W., The use of hydroxyapatite as a new inorganic consolidant for damaged carbonate stones. J Cult Herit 12 (2011) 346-355

[19] Franzoni E., Sassoni E., Graziani G., Brushing, poultice or immersion? Role of the application technique on the performance of a novel hydroxyapatite-based consolidating treatment for limestone. J Cult Herit 16 (2015) 173-184

[20] Naidu S., Scherer G.W., Nucleation, growth and evolution of calcium phosphate films on calcite. J Colloid Interf Sci 435 (2014) 128-137

[21] Naidu S., Blair J., Scherer G.W., Acid attack mechanism on Carrara marble and efficacy of a protective hydroxyapatite film. J Am Ceram Soc (in press)

[22] Kanno C.M., Sanders R.L., Flynn S.M., Lessard G., Myneni S.C.B., Novel apatite-based sorbent for defluoridation: synthesis and sorption characteristics of nano-micro-crystalline hydroxyapatite-coated limestone. Envir Sci Tec 48 (2014) 5798-5807

[23] Shanika Fernando M., De Silva R.M., Nalin de Silva K.M., Synthesis, characterization, and application of nano hydroxyapatite and nanocomposite of hydroxyapatite with granular activated carbon for the removal of Pb^{2+} from aqueous solutions. Appl Surf Sci 351 (2015) 95-103

[24] Ji X., Su P., Liu C., Li J., Tan H., Wu F., Yang L., Fu R., Tang C., Cheng B., A novel ethanol induced and stabilized nanorods: hydroxyapatite nanopeanut. J Am Ceram Soc 98 (2015) 1702-1705

[25] Stanić V., Dimitrijević S., Antić-Stanković J., Mitrić M., Jokić B., Plećaš I.B., Raičević S., Synthesis, characterization and antimicrobial activity of copper and zinc-doped hydroxyapatite nanopowders, Appl Surf Sci 256 (2010) 6083-6089

[26] Champion E., Sintering of calcium phosphate bioceramics, Acta Biomater 9 (2013) 5855-5875

[27] Ramesh S., Natasha A.N., Tan C.Y., Bang L.T., Niakan A., Purbolaksono J., Chandran H., Ching C.Y., Ramesh S., Teng W.D., Characteristics and properties of hydroxyapatite derived by sol–gel and wet chemical precipitation methods. Ceram Int (2015)- in press

[28] Sand K.K., Yang M., Makovicky E., Cooke D.J., Hassenkam T., Bechgaard K., Stipp S.L.S., Binding of ethanol on calcite: the role of the OH bond and its relevance to biomineralization. Langmuir 26 (2010) 15239-15247

[29] Dorozhkin S.V., Amorphous Calcium Orthophosphates: Nature, Chemistry and Biomedical Applications. Int J Mater Chem 2 (2012) 19-46

[30] Dorozhkin S.V., Biphasic, triphasic and multiphasic calcium orthophosphates. Acta Biomater 8 (2012) 963–977

[31] Dorozhkin S.V., Calcium orthophosphate coatings on magnesium and its biodegradable alloys. Acta Biomater 10 (2014) 2919–2934

[32] Dorozhkin S.V., Calcium orthophosphates. Biomatter 1:2 (2011) 121-164

[33] Doherty B., Pamplona M., Selvaggi R., Miliani C., Matteini M., Sgamellotti A., Brunetti B., Efficiency and resistance of the artificial oxalate protection treatment on marble against chemical weathering. Appl Surf Sci 253 (2007) 4477-4484

[34] Matteini M., Rescic S., Fratini F., Botticelli G., Ammonium phosphates as consolidating agents for carbonatic stone materials used in architecture and cultural heritage: preliminary research. Int J Archit Herit: Conservation, Analysis, and Restoration 5 (2011) 717-736

[35] Mats S., Johnsson A., Nancollas G.H., The role of Brushite and Octacalcium Phosphate in Apatite Formation. Crit Rev Oral Biol M 3 (1992) 61-82

[36] Sjcoberg E.L., Rickard D.T., The effect of added calcium on calcite dissolution kinetics in aqueous solutions at 25°C. Chem Geol 49 (1985) 405-413

[37] Sugiyama S., Nishioka H., Moriga T., Hayashi H., Moffat J.B., Ion-Exchange Properties of Strontium Hydroxyapatite under Acidic Conditions. Separ Sci Technol 33 (1998) 1999-2007

[38] Tao J., FTIR and Raman Studies of Structure and Bonding in Mineral and Organic–Mineral Composites. Method Enzymol 532 (2013) 533 - 556.

[39] Koutsopoulos S., Synthesis and characterization of hydroxyapatite crystals: A review study on the analytical methods. J Biomed Mater Res 62 (2002) 600-612.

[40] Orkoula M.G., Koutsoukos P.G., Kinetics of dissolution of powdered Pentelic marble in undersaturated solutions: the role of particle characteristics. J Colloid Interf Sci 259 (2003) 287-292

[41] Prof. Satish C. Myneni, personal communication

[42] Kaufmann G., Dreybrodt W., Calcite dissolution in the system $CaCO_3$-H_2O-CO_2 at high undersaturation. Geochim Cosmochim Acta 71 (2007) 1398-1410

CHAPTER IX- Marble protection against acidic rain corrosion: experiments with a simulated rain apparatus

Research Aims

In the previous chapter, hydroxyapatite based treatments have been proposed for the protection of marble artefacts against acidic rain corrosion. Several parameters have been evaluated with the aim of obtaining a complete, crack-free, non-porous HAP layer on top of marble, so as to prevent dissolution. Addition of ethanol to the solution has been found to enhance surface coverage without leading to cracks formation, hence remarkably increasing samples resistance to dissolution in acidic environment. In particular, the most promising treatment consisted in a double application of one ethanol-doped DAP solution followed by DAP alone.

The investigation of the best formulation to be used was carried out on powders by means of an acid attack apparatus with a finite volume of acid to speed up dissolution process and better highlight differences between the different treatments.

In this Chapter, the most promising treatments were applied to Carrara marble specimens. To be closer to real weathering conditions on site and avoid Ca^{2+} accumulation that might occur when using a finite volume of acid, a specifically designed simulated rain apparatus was used, allowing to drop a continuous flux of acidic solution onto the samples.

Results were compared with those of untreated and ammonium-oxalate treated specimens.

IX.1 Introduction

HAP-based treatments have shown promising results for marble protection against dissolution in clean and/or acidic rain [1-4].

In the previous chapter the influence of the pH of the starting solution as well as that of anionic and cationic additions and of ethanol were investigated [3,4]. Promising results have been obtained by adding ethanol to the DAP solution. Ethanol, in fact, has been found to be a calcite growth modifier and to adsorb on calcite and HAP [5,6]. For this reason, its addition to the DAP solution was investigated, to boost acid resistance of marble. Solutions of DAP and ethanol in different concentrations and in single and double applications were tested and their efficacy was compared [3]. At this step, calcite powders and an acid attack testing setup with a finite volume of acid solution were used. Briefly, powders were put in a beaker with the acidic solution kept stirring at a constant speed and pH variations in time were recorded. By using powders, exposure of a high number of grains that differ in crystallographic orientation and impurities was allowed, which otherwise would have required a high number of coarse samples. Moreover, due to very high

specific surface, powders undergo much faster dissolution, hence allowing faster evaluation of treatments efficacy.

At this step, the most promising coatings selected in the previous Chapter, were applied on Carrara marble prisms, to get closer to the real situation experience by samples on site, and a different type of acid attack test was used, consisting in a simulated rain runoff apparatus [8]. Cycles, each consisting in continuous dripping of acidic solution over the samples followed by drying, were performed to prevent too high an accumulation of calcium ions near the dissolving marble surface, which would reduce the marble dissolution rate [7,9]. Ammonium oxalate treated samples were also tested for comparison sake.

IX.2 Materials and Methods

IX.2.1 Materials

Quarry slabs of Carrara marble (Imbellone Michelangelo s.a.s.) were cut into 30×30×20 mm^3 size specimens. DAP (> 99%, Sigma Aldrich), calcium chloride (assay > 99.0%, Sigma Aldrich), ethanol (Fisher-Scientific) and ammonium oxalate (≥ 99.99%, Sigma Aldrich) were used for the treatments. Prior to treating and characterization, prisms were rinsed with water and ethanol to remove possible surface impurities and dried at room temperature.

IX.2.2 Methods

Treatments D8, D8E and double treatment D8E+8 were applied on Carrara Marble prisms. Untreated and AmOx treated samples were also examined for comparison's sake. Treating solutions were the same described in the previous chapter and are summarized in Table IX.1. Briefly, samples D8 were treated with a reference 0.1 M DAP solution, sample AmOx with a 5 wt.% AmOx solution, according to [10] (sample AmOx). To evaluate the effect of ethanol on the formation of HAP, ethanol was added in concentration of 0.5 wt.% to the 0.1 M DAP solution and its effects were evaluated (samples with the letter "E"). In all DAP-treated samples (with and without ethanol addition), calcium ions were externally added by adding $CaCl_2$ to the solution, to prevent dissolution of the substrate. Composition of the most significant solutions are in Table IX.1.

Specimen name	Treating solution
D8	0.1 M DAP + 0.1 mM $CaCl_2$
D8E	0.1 M DAP + 0.1 mM CaCl2 + 0.5 wt.% ethanol
D8E+8	First solution: 0.1 M DAP + 0.1 mM CaCl2 + 0.5 wt.% ethanol
	Second solution 0.1 M DAP + 0.1 mM CaCl
AmOx	5 wt.% AmOx

Table IX.1: Composition and nomenclature of the most significant treatments.

Treatments were performed by immersion, exactly as for the powders.

As calcite dissolution depends on the concentration of Ca^{2+} ions in the solution, a custom designed setup providing a continuous dripping of solution onto the samples was preferred for acid resistance test over that with finite volume of acid (figure IX.1).

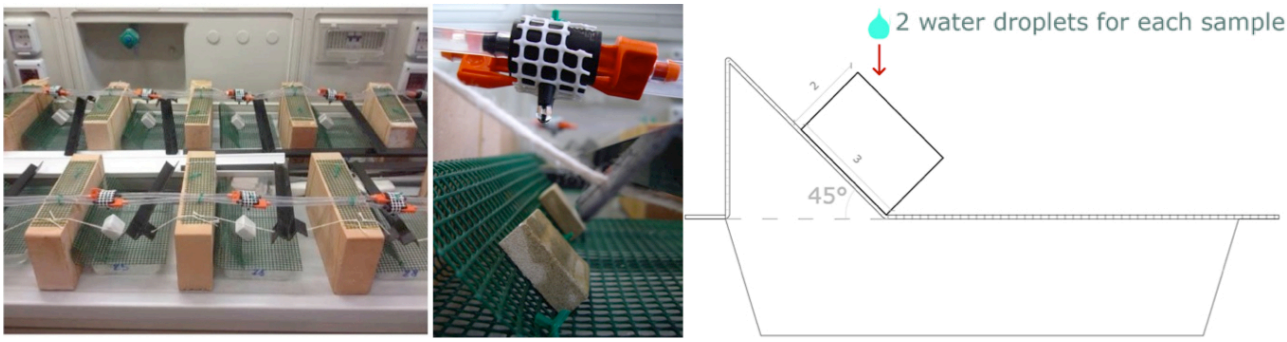

Figure IX.1: Simulated rain apparatus

Deionized water (at initial pH 6.8) was dripped onto the samples (rate of 500 mL/h), alternating periods of dropping (2.5 h) and drying. The apparatus consisted of two dripping lines with separate water supply: one sample for each treating condition was tested for each line. 24 wet/dry cycles were performed (2 cycles per day), thus exposing each sample to an average solution volume of 29 L. Considering the annual average rain in Bologna (800 mm) and the size of the specimens, this volume of solution corresponds to about 40 years of rain.

Runoff water was collected at each cycle and calcium ions and phosphate concentration in the solutions were determined after cycles 1, 2, 8 and 24, to evaluate the dissolution of both the substrate and the coating. Ca^{2+} concentration was determined by HPLC, PO_4^{3-} by spectrometer. Of course, soluble phosphate determination was not performed for AmOx treated samples, as no phosphate originates from calcium oxalate formation reaction. Concentration of calcium ions is expected to be indicative of dissolution of marble substrate and calcium oxalate coating, phosphate of dissolution of HAP-treated samples coating. As HAP is insoluble at the given pH range, phosphate presence might indicate that soluble phases have formed as a result of the reaction. In this case, a contribution of dissolution of these phase would be present in the registered calcium ions concentration. In AmOx samples, calcium ions concentration derives from both dissolution of the substrate and the protective film and it is not possible to discriminate between one contribution and the other.

To investigate the effects of the cycles SEM/EDS was performed after acid resistance test on the most promising formulation, namely sample D8E+8, and compared to untreated reference and

AmOx, for comparison sake. By doing so, it was possible to evaluate the morphology of the treated layer after artificial weathering and the etching of the underlying marble, indicating that the dripping solution has corroded the substrate. EDS was not performed onto AmOx treated samples, as their elemental composition is the same of calcite.

IX.3 Results [8]

Acid resistance of treated samples was evaluated in terms of release of calcium ions and phosphate, respectively.

Calcium ion concentration as measured in the solution after each cycle is reported in figure IX.2, average values for each treating conditions are in Table IX.2. Each value is the average of all measurements taken at all cycles and for the two lines.

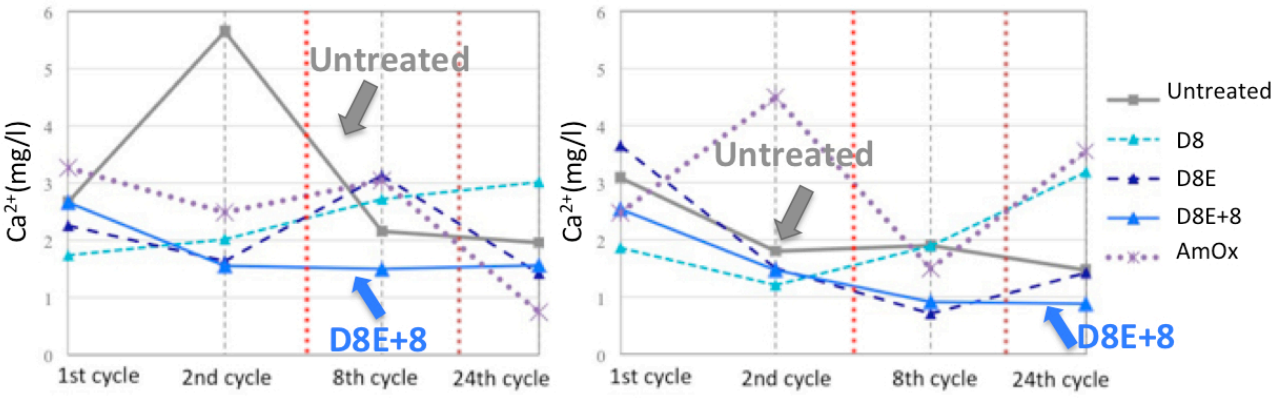

Figure IX.2 : Ca^{2+} ion concentration in the runoff solutions for duplicate samples. Please note that x axis, indicating the number of cycles, is not proportional to the cycles number.

Specimen	Ca^{2+} (mg/L)
Untreated	2.59±1.34
D8	2.21±0.69
D8E	1.97±0.98
D8E+8	1.64±0.65
AmOx	2.69±1.18

Table IX.2: Ca^{2+} concentrations (values are averages for duplicate samples and for all cycles)

Phosphate concentration in the solution are reported in figure IX.3.

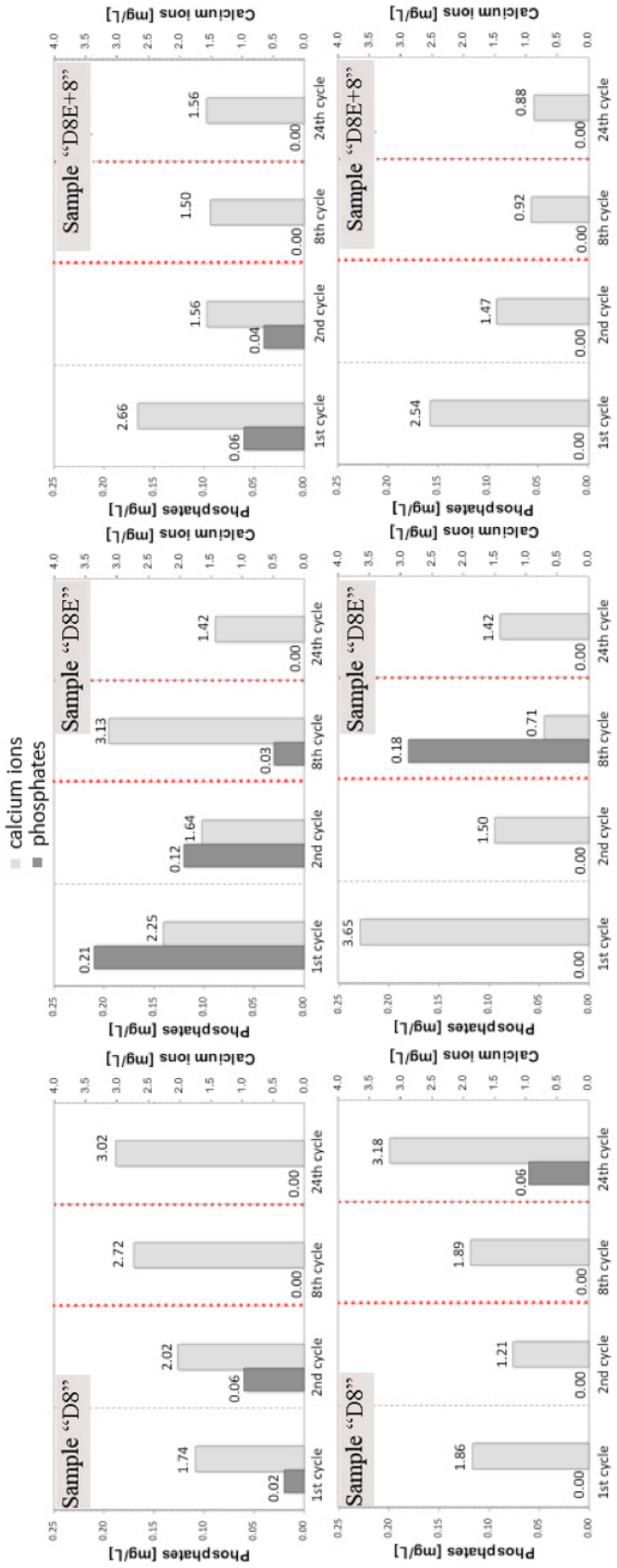

Figure IX.3: $Ca^{2+}$and PO_4^{3-} ion concentrations in the runoff solutions for duplicate samples

Morphology and composition of coating D8E+8 as assessed by SEM/EDS is reported in figure IX.4, in comparison with AmOx and untreated reference.

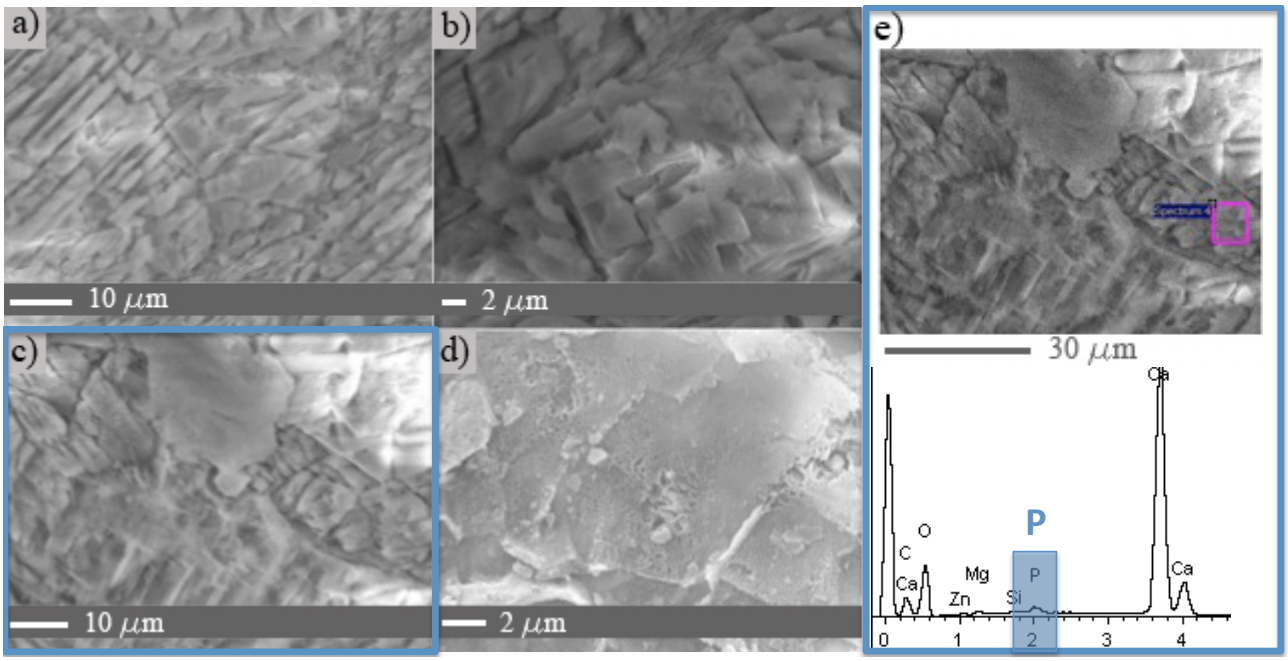

Figure IX.4: Morphology of samples after simulated rain test: a) untreated marble, b) AmOx, c,d) D8E+8; e) EDS on sample D8E+8 in one area that seems uncoated.

IX.4 Discussion

The lowest calcium ions concentration can be assessed for samples D8E+8, thus indicating that these samples suffer the slowest dissolution (Figure IX.2 and Table IX.2). Ethanol addition alone (sample D8E) results in improved behavior with respect to the samples treated with 0.1M solution (sample D8) (Figure IX.2). The effect of ethanol on acid resistance of massive samples, however, is much less evident than that assessed in the case of powders (see §VIII.3).

D8E+8 also exhibits the lowest standard deviation in calcium ion concentration measured for the two duplicate samples and in different cycles, indicating that the behaviour of the samples is more dependent on the coating than on the substrate, that exhibits higher variability.

Phosphate concentration was investigated to assess possible dissolution of the coating (Figure IX.3). As HAP is expected to be insoluble for the given pH, high PO_4^{3-} contents, indicating partial dissolution of the coating, suggest that soluble phases have formed together with HAP.

Phosphate presence is detected in samples D8, even though values are very close to the instrument detectability threshold and can be considered minor. Non-negligible phosphate amounts, instead, are registered in sample D8E suggesting soluble phase formation. For this reason, Ca^{2+} ions found in the solution might derive from the dissolution of both the substrate and the coating. Quite different values are assessed in duplicate samples, thus indicating poor uniformity between different samples.

Sample D8E+8 exhibits the lowest dissolution and a negligible presence of PO_4^{3-} ions (figure IX.3), hence indicating that HAP and not soluble phases were obtained by the treatment. In particular, Ca^{2+} concentration is much lower than that of AmOx samples, where, however, Ca^{2+} ions in solution derive from dissolution of both the substrate and the coating, given the higher solubility of AmOx with respect to HAP.

By comparing calcium ions and phosphate concentration (figure IX.3) it is possible to evaluate whether the substrate, the coating, or both experience dissolution.

Ca^{2+} ion concentration in D8E+8 is lower than that of untreated marble; however, some dissolution occurs in the samples, hence SEM was performed to evaluate weathering of the substrate after the simulated rain test (Figure IX.4). Images of untreated marble and AmOx are also reported for comparison's sake.

After acid attack, untreated samples appear etched, as does AmOx, where the surface seems essentially bare, thus suggesting that both dissolution of the coating and of the substrate has occurred. However, it must be noticed that 40 years of rain were simulated in the tests. Some thick areas of the coating remain visible in sample D8E+8, but many areas appear uncoated and etched, though etching seems less severe than in the untreated reference. However, when EDS is performed (figure IX.4 e), phosphorous signal is detected in all the areas of the sample, including those that seem uncoated. For this reason it might be presumed that a layer of nanometric thickness is preserved: this would be consistent with the fact that, despite the treated layer being almost entirely consumed, the dissolution of the sample is still lower than that of the untreated reference, hence indicating that some protection is still maintained. Further tests are currently in progress to verify the presence of this layer at the nano-scale and for further optimization of the treatment.

IX.5 Conclusions

Ethanol addition was investigated to enhance surface coverage and acid resistance of the coating. Experiments were carried out both on powders and on Carrara marble prisms, by using two different testing setups. Tests on powders highlighted the beneficial effect of ethanol on surface coverage and acid resistance and allowed for choosing the most promising formulation to be used: treatment D8E+8, consisting in a double application of the solution with ethanol addition in the first layer, was successful in providing good coverage on powders without leading to the formation of cracks and hence to slow down dissolution.

For this reason, the efficacy of ethanol additions as well as the performance of the most promising treatment were evaluated on Carrara Marble specimens, by a simulated rain setup. The beneficial effect of ethanol was confirmed, even though improvement with respect to reference solution without ethanol were less dramatic than in the case of powders. Treatment D8E+8 gave good results

slowing down the dissolution of the underlying substrate, also with respect to AmOx treatment. The treatment still offered protection after prolonged simulated rain (corresponding to a period of 40 years in Bologna, Italy). However, as some weathering was found to occur, further optimization is currently in progress to enhance the coating resistance.

Acknowledgements

I am thankful to M.Eng. M. Glorioso for collaboration on dripping tests, to Dr. L. Guadagnini for support on HPLC and to Dr. F. Ospitali for support on SEM analysis.

References

[1] Naidu S., Scherer G.W., Nucleation, growth and evolution of calcium phosphate films on calcite. J Colloid Interf Sci 435 (2014) 128-137

[2] Naidu S., Blair J., Scherer G.W., Acid attack mechanism on Carrara marble and efficacy of a protective hydroxyapatite film. J Am Ceram Soc (in press)

[3] Graziani G., Sassoni E., Franzoni E., Scherer G.W., Hydroxyapatite coatings for marble protection: Optimization of calcite covering and acid resistance. Appl Surf Sci 368 (2016) 241-257

[4] Naidu S., Scherer G.W., Nucleation, growth and evolution of calcium phosphate films on calcite. J Colloid Interf Sci 435 (2014) 128-137

[5] Ji X., Su P., Liu C., Li J., Tan H., Wu F., Yang L., Fu R., Tang C., Cheng B., A novel ethanol induced and stabilized nanorods: hydroxyapatite nanopeanut. J Am Ceram Soc 98 (2015) 1702-1705

[6] Sand K.K., Yang M., Makovicky E., Cooke D.J., Hassenkam T., Bechgaard K., Stipp S.L.S., Binding of ethanol on calcite: the role of the OH bond and its relevance to biomineralization. Langmuir 26 (2010): 15239-15247

[7] Kaufmann G., Dreybrodt W., Calcite dissolution in the system $CaCO_3$-H_2O-CO_2 at high undersaturation. Geochim Cosmochim Acta 71 (2007): 1398-1410

[8] Graziani G., Sassoni E., Franzoni E., Scherer G.W., Marble protection by hydroxyapatite coatings, 13th International Congress on the Deterioration and Conservation of Stone, Glasgow, 6-10 September 2016 (accepted)

[9] Sjcoberg E.L., Rickard D.T., The effect of added calcium on calcite dissolution kinetics in aqueous solutions at 25°C. Chem Geol 49 (1985): 405-413

[10] Doherty B., Pamplona M., Selvaggi R., Miliani C., Matteini M., Sgamellotti A., Brunetti B., Efficiency and resistance of the artificial oxalate protection treatment on marble against chemical weathering. Appl Surf Sci 253 (2007): 4477-4484

Conclusions

A novel hydroxyapatite-based treatment was proposed and fully characterized for consolidation of limestone and for consolidation and protection of marble. In particular, the following conclusions were derived.

Regarding *limestone consolidation*, tests carried out on Globigerina limestone allowed to set up a treating procedure consisting in a 2-step protocol. First, a 3 M DAP solution in deionized water is applied, the concentration being chosen because it is close to saturation: from DAP dissociation, only a limited number of PO_4^{3-} ions are available to form HAP, hence a high concentration is needed to have a sufficient formation of HAP. However, as a great part of DAP remains unreacted (because of dissociation in HPO_4^{2-} and $H_2PO_4^-$) a second step was proposed, consisting in the application of a limewater poultice that is left reacting for 24 hours and then left to dry in contact with the stone. By doing so, additional Ca^{2+} ions are added for further reaction with DAP; moreover, unreacted DAP remained in the stone, as well as possible soluble phases originated by the reaction, can be removed during the drying phase. Curing for 48 hours proved to be sufficient for obtaining the desired improvements in mechanical properties, which is an important advantage of the proposed treatment.
Excellent results were obtained using the proposed treatment under several respects: a good efficacy, in terms of increase in mechanical properties and penetration depth, and remarkable compatibility from aesthetical, microstructural and physical point of view, were found. The application method was found to be very important in determining the final outcome of the treatment, mostly in terms of compatibility and redistribution of the consolidant in the phases after the treatment. The limewater poultice was effective in removing unreacted DAP that otherwise would remain in the stone, also causing higher color change.
When compared to ethyl silicate, the HAP-based treatment exhibits a slightly reduced efficacy (in terms of increase in mechanical properties) but improved compatibility. ES has a shown a good efficacy for the given lithotype because the stone contains some quartzitic fractions that allow for some chemical bonding, though sparse. HAP, however, is much more durable with respect to ES, in terms of all the weathering conditions tested (i.e. wetting drying, freezing-thawing and salt crystallization cycles). Because of the higher durability of HAP, the initial mechanical benefit obtained by ES is rapidly lost after a few accelerated weathering cycles.

Regarding *marble consolidation*, tests carried out on artificially weathered samples confirmed that the treatment conditions applied in the case of Globigerina limestone were the best among those

tested also in the case of marble. These treatment conditions allow to obtain good efficacy and compatibility with the substrate. However, phase characterization indicates that metastable phases are formed as a result of the treatment (namely tetracalcium phosphate-TCP and octacalcium phosphate-OCP): however, these phases, despite being more soluble than HAP, are still much less soluble than calcite, hence their formation does not have to be considered detrimental. The effect of calcium ions addition to the initial DAP solution, aimed at forming HAP without causing dissolution of the substrate (not even millimolar) was investigated. Despite obtaining a less cracked layer, no benefit was obtained in terms of phase composition. Moreover, given the relevant loss of material caused by sugaring, millimolar dissolution of calcite to provide calcium ions necessary for HAP formation was regarded as a minor issue.

Efficacy and compatibility were confirmed when the treatment was applied on a naturally weathered historic specimen, collected in Certosa Monumental Cemetery in Bologna. The slab in exam presented non-uniform weathering conditions and it was affected by a black crust (thus gypsum contamination) and severe sugaring, that caused a marked surface roughening and material loss. The HAP-treatment allowed a remarkable improvement in mechanical properties, without affecting stone microstructure to too high an extent. One of the most relevant findings, though, was that different phases were formed with respect to artificially weathered samples: in particular, only HAP and no metastable phases were detected. This indicates that contamination and surface morphology are crucial in determining phase formation as a result of the reaction: in particular, combined action of gypsum presence and surface roughening appeared to be beneficial for formation of HAP rather than metastable phases. This is a very important finding, as the presence of black crusts as well as sugaring are widely diffused on site and also highlights that the outcome of the treatment is affected by the presence of contaminants. This is in line with the fact that HAP is known to easily incorporate foreign ions that can, in turn, affect its crystallinity and solubility. However, further tests are in progress to investigate and possibly confirm these findings.

The fact that HAP exhibits good efficacy and compatibility for both limestone and marble, that are remarkably different for composition, microstructure, physical and mechanical properties and hence for weathering susceptibility, suggests that it can be successfully used for several lithotypes.

Efficacy and compatibility assessed in laboratory conditions were confirmed when the consolidant was applied on site, as the HAP-based treatment was found to be effective in enhancing stone mechanical properties without affecting its appearance.

Regarding *marble protection*, the following conclusions were derived. By changing treating parameters it is possible to completely modify morphology and acid resistance of the treated layer. In particular, by adding millimolar cationic additions and by changing pH of the starting solution it

was possible to completely alter surface coverage, morphology and composition of the coating. No beneficial effects were obtained in terms of acid resistance by raising solution pH, despite the initial belief that that pH increase would favor DAP dissociation in PO_4^{3-} ions. None of the tested cationic additions caused beneficial effects either, probably because they do not enter the crystal structure. Addition of ethanol, instead, remarkably enhanced surface coverage without causing cracks formation. This, in turn, boosted acid resistance of the treated samples. In fact, by adding ethanol it is possible to obtain complete surface coverage with a 0.1 M DAP solution and thus create a very thin film. In the absence of ethanol, the same solution results in several bare areas that allow corrosion of marble underlying the coating. In both cases, HAP was found to be the only phase that forms as a result of the treatment. By increasing DAP concentration also the thickness of the coating increases and this makes the film prone to cracking during drying. Application of double treatments at reduced concentration, instead, allows a better surface coverage without causing cracks.

The most promising formulation was a double treatment where application of an ethanol-doped 0.1 M DAP solution is followed by a second application of 0.1 M DAP solution. Ethanol addition to the second layer does not result in further improvements. The formulation allowed for a remarkable improvement in acid resistance. Moreover, HAP was the only phase to be detected in the coating.

The effects of ethanol additions, as well as the behavior of the selected formulations were tested by a simulated rain setup, in comparison with untreated and AmOx-treated samples. 40 years of rain were simulates and the beneficial effect of ethanol was confirmed, even though its effect was less dramatic than in the case of powders on which the treatment effects had been previously investigated. The most promising treatment formulation exhibited a reduced dissolution with respect to all the other tested samples and a negligible phosphate release, indicative of negligible presence of soluble phases. When the sample is examined by SEM, however, some etched marble areas can be detected, thus suggesting that some substrate corrosion occurred. However, after 40 years of simulates rain, the protection was maintained (dissolution at the last cycle was still lower than that of untreated references), moreover the presence of phosphorus can still be detected by EDS (P being absent in untreated Carrara marble), which suggests that some nanometric layer is maintained and still offers some protection. This aspect is currently under further investigation.

Summarizing, the hydroxyapatite-based treatment has shown excellent performance for consolidation and protection of carbonate stones. As a consolidant, it exhibited remarkable efficacy and compatibility on limestone and marble, e.g. substrates characterized by very different composition, microstructure and susceptibility to weathering. The results obtained in laboratory conditions were confirmed when the treatment was applied on real historic artifacts and, finally, on

site. As a protective, the use of a diluted ethanol-doped DAP solution allows to obtain a continuous, crack-free HAP layer that guarantees acid resistance to the underlying marble.

Future research
Several aspects are currently under further investigation.

Regarding *limestone consolidation*:

- application of HAP on samples artificially weathered by salt crystallization, both prior to and after desalinization processes. Particular attention is devoted to the phases that form as a result of treatment application on sulfate containing substrates. A comparison between phase formation in presence of gypsum (i.e. calcium sulfate) and sodium sulfate will also be carried out;
- evaluation of the effects of consolidation on contact angle between stone and mercury, also in presence of salts, so as to measure reliability of MIP analyses on treated substrates;
- further comparison between different substrates, with variable calcite content and microstructure.

Regarding *marble consolidation*:

- HAP is currently being investigated for pre-consolidation, mostly for the aspects regarding the possibility to remove possible black crusts after application of the treatment. Also in this case, special attention will be devoted to investigation of phase formation when the consolidant is applied prior to removing the crust;
- Monitoring of Rolandino De' Passeggeri Tomb after one year since the application will be performed.

Regarding *marble protection*:

- further optimization is in progress so as to completely prevent dissolution in acidic rain;
- Investigation of possible formation of nanometric coatings (non-visible by SEM) is in progress.

References

Alvarez de Buergo M., Fort Gonzalez R., Protective patinas applied on stony facades of historical buildings in the past, Constr Build Mater, 17 (2003) 83–89

Amoroso G., Fassina V., Stone decay and conservation. New York: Elsevier; 1983.

Angeli M., Benavente D., Bigas J.P., Menéndez B., Hébert R., David C., Modification of the porous network by salt crystallization in experimentally weathered sedimentary stones. Mater Struct 41 (2008) 1091–1108.

Baglioni M., Berti D., Teixeira J., Giorgi R., Baglioni P., Nanostructured surfactant-based systems for the removal of polymers from wall paintings: A small-angle neutron scattering study. Langmuir 28 (2012) 15193-15202.

Baglioni P., Chelazzi D., Giorgi R., Carretti E., Toccafondi N., Jaidar Y., Commercial $Ca(OH)_2$ nanoparticles for the consolidation of immovable works of art. Appl Phys A 114 (2004) 723–32

Barbacci A., Monumenti di Bologna. Distruzioni e restauri, Bologna, Cappelli, 1977, 44-45

Benavente D., García Del Cura M.A., Bernabéu A., Ordóñez S., Quantification of salt weathering in porous stones using an experimental continuous partial immersion method, Eng Geol 59 (2001) 313–325.

Boanini E., Gazzano M., Bigi A., Ionic substitutions in calcium phosphates synthesized at low temperature. Acta Biomater 6 (2010) 1882-1894

Boivin G., The hydroxyapatite crystal: a closer look. Medicographia 29 (2007) 126–132.

Bonazza A., Messina P., Sabbioni C., Grossi C.M., Brimblecombe P., Mapping the impact of climate change on surface recession of carbonate buildings in Europe. Sci Total Environ 407 (2009) 2039-2050

Brady P.V., Ch. 4 in Physics and Chemistry of Mineral Surfaces, ed. P.V. Brady CRC Press, Boca Raton, FL, 1996.

Brendel T., Engel A., Russel C., Hydroxyapatite coatings by a polymeric route. J Mater Sci Mater Med 3 (1992) 175–179.

C. Miliani, M.L. Velo-Simpson, G.W. Scherer, Particle-modified consolidants: a study on the effect of particles on sol–gel properties and consolidation effectiveness, J Cult Herit 8 (2007) 1–6

Cardell C., Delalieux F., Roumpopoulos K., Moropoulou A., Auger F., Van Grieken R., Salt-induced decay in calcareous stone monuments and buildings in a marine environment in SW France. Constr Build Mater 17 (2003) 165–179.

Cardiano P., Ponterio R.C., Sergi S., Lo Schiavo S., Piraino P., Epoxy-silica polymers as stone conservation materials. Polymer 46 (2005) 1857-1864

Cardiano P., Sergi S., Lazzari M., Piraino P., Epoxy-silica polymers as restoration materials. Polymer 43 (2002) 6635-6640

Carretti E., Dei L., Physicochemical characterization of acrylic polymeric resins coating porous materials of artistic interest. Prog Org Coat 49 (2004) 282–9.

Cassar J., Deterioration of the Globigerina limestone of the Maltese Islands. Geol Soc. Spec Publ 205 (2002) 33–49

Champion E., Sintering of calcium phosphate bioceramics, Acta Biomater 9 (2013) 5855-5875

Charola A.E., Centeno S.A., Normandin K., The New York Public Library: Protective treatment for sugaring marble. Journal of Architectural Conservation 16 (2010) 29-44

Cnudde V., Cnudde J.P., Dupuis C., Jacobs PJS., X-ray micro-CT for the localization of water repellents and consolidants inside natural building stones. Mater Charact 53 (2004) 259-71.

Commission 25-PEM Protection et Erosion des Monuments. Recommended tests to measure the deterioration of stone and to assess the effectiveness of treatment methods. Mater Struct 13 (1980) 175–253.

Conti C., Colombo C., Dellasega D., Matteini M., Reailini M., Zerbi Z., Ammonium oxalate treatment: Evaluation by μ-Raman mapping of the penetration depth in different plasters. J Cult Herit 12 (2011) 372-379

Conti C., Colombo C., Matteini M., Reailini M., Zerbi Z., Micro-Raman mapping on polished cross sections: a tool to define the penetration depth of conservation treatment on cultural heritage. J Raman Spectrosc 41 (2010) 1254-1260

Daniele V., Taglieri G., Quaresima R., The nanolimes in Cultural Heritage conservation: characterization and analysis of the carbonatation process. J Cult Herit 9 (2008) 294-301

Delgado Rodrigues J., Grossi A., Indicators and ratings for the compatibility assessment of conservation actions. J Cult Herit 8 (2007) 32–43.

Direzione generale delle antichità e delle belle arti, La ricostruzione del patrimonio artistico italiano, La Libreria dello Stato, Roma, 1950, 13-107

Doherty B., Pamplona M., Selvaggi R., Miliani C., Matteini M., Sgamellotti A., Brunetti B., Efficiency and resistance of the artificial oxalate protection treatment on marble against chemical weathering. Appl Surf Sci 253 (2007) 4477-4484

Donatti D., Vollet D.R., Effects of the water quantity on the solventless TEOS hydrolysis under ultrasound transmission. J Sol-Gel Sci Tech 17 (2000) 19-24.

Dorozhkin S.V., Amorphous Calcium Orthophosphates: Nature, Chemistry and Biomedical Applications. Int J Mater Chem 2 (2012) 19-46

Dorozhkin S.V., Biphasic, triphasic and multiphasic calcium orthophosphates. Acta Biomater 8 (2012) 963–977

Dorozhkin S.V., Calcium orthophosphate coatings on magnesium and its biodegradable alloys. Acta Biomater 10 (2014) 2919–2934

Dorozhkin S.V., Calcium orthophosphates - Occurrence, properties, biomineralization, pathological calcifications and biomimetic applications. Biomatter 1 (2011) 121-164

Dorozhkin S.V., Calcium orthophosphates in nature, biology and medicine, Materials 2 (2009) 399–498

Dorozhkin S.V., Calcium orthophosphates, Biomatter 1:2 (2011): 121-164

Drdàcky´ M., Lesàk J., Rescic S., Slìzˇkovà Z., Tiano P., Valach J., Standardization of peeling tests for assessing the cohesion and consolidation characteristics of historic stone surfaces. Mater Struct 45 (2012) 505–52.

Dubelaar C.W., Dusar M., Dreesen R., Felder W.M., Nijland T.G., Maastricht limestone: A regionally significant building stone in Belgium and The Netherlands. Extremely weak, yet time-resistant, in: Proceedings of the International Conference on Heritage, Weathering and Conservation, HWC 2006, vol. 1, 2006, pp. 9–14.

E. Franzoni, E. Sassoni, Comparison between different methodologies for artificial deterioration of stone aimed at consolidants testing, Proceedings of 12th International Congress on Deterioration and Conservation of Stone, New York City, USA, 22–26 October 2012 (2014), p. 1-10

E. Franzoni, G. Graziani, E. Sassoni, TEOS-based treatments for stone consolidation: acceleration of hydrolysis-condensation reactions by poulticing. J Sol-Gel Sci Tech 74 (2015) 398-405

E. Sassoni, E. Franzoni, Carrara marble consolidation by hydroxyapatite and behavior towards thermal weathering after consolidation, Proceedings of "Built Heritage 2013. Monitoring

Conservation Management" Springer International Publishing Switzerland, Editors: Lucia Toniolo, Maurizio Boriani, Gabriele Guidi, pp.379-389

E. Sassoni, E. Franzoni, Influence of porosity on artificial deterioration of marble and limestone by heating, Appl Phys A Mater 115 (2014) 809–16

E. Sassoni, E. Franzoni, Sugaring marble in the Monumental Cemetery in Bologna (Italy): characterization of naturally and artificially weathered samples and first results of consolidation by hydroxyapatite. Appl Phys A Mater 117 (2014) 1893–1906.

E. Sassoni, S. Naidu, G.W. Scherer, The use of hydroxyapatite as a new inorganicconsolidant for damaged carbonate stones, J. Cult. Herit. 12 (2011) 346–355.

EN 12370 – Natural stone test methods – Determination of resistance to salt crystallization, 1999.

Esposito Corcione C., Frigione M., Influence of stone particles on the rheological behavior of a novel photopolymerizable siloxane-modified acrylic resin. J Appl Polym Sci 122 (2011) 942-947

Esposito Corcione C., Striani R., Frigione M., UV-cured siloxane-modified methacrylic system containing hydroxyapatite as potential protective coating for carbonate stones, Prog Org Coat 76 (2013) 1236-1242

European Standard EN 12371, Natural stone test methods – Determination of frost resistance, 2010.

European Standard EN 15801. Conservation of cultural property – test methods – determination of water absorption by capillarity; 2010.

European Standard EN 15803. Conservation of cultural property – test methods – determination of water vapor permeability (dp); 2010.

F. Yang, B. Zhang, Y. Liu, W. Guofeng, H. Zhang, W. Cheng, Z. Xu, Biomimic conservation of weathered calcareous stones by apatite, New J Chem 35 (2011) 887–892.

Favaro M, Mendichi R, Ossola F, Russo U, Simon S, Tomasin P, et al. Evaluation of polymers for conservation treatments of outdoor exposed stone monuments. Part I. Photo-oxidative weathering. Polym Degrad Stabil 91 (2006) 3083–96.

Ferreira Pinto A.P., Delgado Rodrigues J., Consolidation of carbonate stones: influence of treatment procedures on the strengthening action of consolidants. J Cult Herit 13 (2012) 154–66.

Ferreira Pinto A.P., Delgado Rodrigues J., Stone consolidation: The role of treatment procedures. J Cult Herit 9 (2008) 38-53

Flatt R.J., Salt damage in porous materials: how high supersaturations are generated. J Cryst Growth 242 (2002) 435–454.

Franzoni E, Sassoni E, Scherer GW, Naidu S. Artificial weathering of stone by heating. J Cult Herit 14S (2013) e85–93.

Franzoni E., Graziani G., Sassoni E., Bacilieri G., Griffa M., Lura P. Solvent based TEOS consolidant for stone: influence of the application technique on penetration depth, efficacy and pore occlusion. Mater Struct 48 (2015) 3503-3515

Franzoni E., Graziani G., Sassoni E., TEOS-based treatments for stone consolidation: acceleration of hydrolysis-condensation reactions by poulticing. J Sol-Gel Sci Tech 74 (2015) 398-405

Franzoni E., Pigino B., Leemann A., Lura P. (2013) Use of TEOS for fired-clay bricks consolidation. Mater Struct 47 (2014): 1175-1184

Franzoni E., Pigino B., The role of moisture in sandstone decay in the monumental cemetery of Bologna (Italy). In: Stefanaggi M., Verges-Belmin V. (eds), Proceeding of Jardins de Pierres, conservation of stone in parks, gardens and cemeteries Conference, Paris, France. XL Print Saint-Etienne, 22-24 June 2011, pp 377

Franzoni E., Sassoni E., Correlation between microstructural characteristics and weight loss of natural stones exposed to simulated acid rain. Sci Total Environ 412–413 (2011) 278-285.

Franzoni E., Sassoni E., Graziani G., Brushing, poultice or immersion? Role of the application technique on the performance of a novel hydroxyapatite-based consolidating treatment for limestone. J Cult Herit 16 (2015) 173-184

Franzoni E., Sassoni E., Scherer G.W., Naidu S., Artificial weathering of stone by heating. J Cult Herit 14S (2013) e85–93.

Giusti A., La competenza umanistica. In: Tiano P., Pardini C., editors. Le patine – Genesi, significato, conservazione, Proceedings of the Workshop ‘‘Le patine – Genesi, significato, conservazione’’, 4–5 May 2004, Florence, Italy, Nardini Editore, Florence; 2005, p. 77–82.

Gräf V., Jamek M., Rohatsch A., Tschegg E., Effects of thermal-heating cycle treatment on thermal expansion behavior of different building stones. Int J Rock Mech Min Sci 64 (2013) 228–35.

Graziani G., Sassoni E., Franzoni E., Consolidation of porous carbonate stones by an innovative phosphate treatment: mechanical strengthening and physical-microstructural compatibility in comparison with TEOS-based treatments, Herit Sci 3 (2015)

Graziani G., Sassoni E., Franzoni E., Experimental study on the salt weathering resistance of fired

clay bricks consolidated by ethyl silicate, Materials and Structures (2015) DOI 10.1617/s11527-015-0665-8

Graziani G., Sassoni E., Franzoni E., Scherer G.W., Hydroxyapatite coatings for marble protection: optimization of calcite covering and acid resistance. Appl Surf Sci 368 (2016): 241-257

Graziani G., Sassoni E., Franzoni E., Scherer G.W., Marble protection by hydroxyapatite coatings, 13th International Congress on the Deterioration and Conservation of Stone, Glasgow, 6-10 September 2016 (accepted)

Hansen E., Dohene E., Fidler J., Larson J., Martin B., Matteini M., Rodrìguez-Navarro C., Pardo E.S., Price C., de Tagle A., Teutonico J. M., Weiss N., A review of selected inorganic consolidants and protective treatments for porous calcareous materials. Reviews in conservation 4 (2003) 13-25

Harouiya N., Chaïrat C., Köhler S.J., Gout R., Oelkers E.H., The dissolution kinetics and apparent solubility of natural apatite in closed reactors at temperatures from 5 to 50°C and pH from 1 to 6. Chem Geol 244 (2007) 554–568.

Hoepfner T.P., Case E.D., An estimate of the critical grain size for microcracks induced in hydroxyapatite by thermal expansion anisotropy. Mater Lett 58 (2004) 489–492.

http://rruff.info/

Ion R.M., Turcanu-Caruţiu D., Fierăscu R.C., Fierăscu I., Bunghez I.R., Ion M.L., Teodorescu S., Vasilievici G., Rădiţoiu V., Caoxite-Hydroxyapatite composition as consolidating material for the chalk stone for basarabi-murfatlar churches ensemble. Appl Surf Sci (2015), in press

Italian Recommendation NORMAL 20/85, Conservazione dei materiali lapidei: Manutenzione ordinaria e straordinaria, Istituto Centrale per il Restauro (ICR), Rome, 1985.

Italian Standard UNI 11186, Cultural heritage – Natural and artificial stones – Methodology for exposure to freeze-thawing cycles, 2008.

Sun J., Wu Z., Cheng H., Zhang Z., Frost R.L., A Raman spectroscopic comparison of calcite and dolomite. Spectrochim Acta A 117 (2014) 158-162

Janson S.J., Hoff W.D., Chemical Injection remedial treatments for rising damp- I. The interaction of damp-proofing fluids with porous building materials. Build Environ 23 (1988) 171-178

Ji X., Su P., Liu C., Li J., Tan H., Wu F., Yang L., Fu R., Tang C., Cheng B., A novel ethanol induced and stabilized nanorods: hydroxyapatite nanopeanut. J Am Ceram Soc 98 (2015) 1702-1705

Jimenez Gonzalez I, Scherer G.W., Effect of swelling inhibitors on the swelling and stress relaxation of clay bearing stones. Environ Geol 46 (2004) 364–377.

Kamiya M., Hatta J., Shimida E., Ikuma Y., Yoshimura M., Monma H., AFM analysis of initial stage of reaction between calcite and phosphate. Mater Sci Eng B 111 (2004) 226–231.

Kanno C.M., Sanders R.L., Flynn S.M., Lessard G., Myneni S.C.B., Novel apatite-based sorbent for defluoridation: synthesis and sorption characteristics of nano-micro-crystalline hydroxyapatite-coated limestone. Envir Sci Tec 48 (2014) 5798-5807

Karampas I.A., Kontoyannis C.G., Characterization of calcium phosphates mixtures. Vib Spectrosc 64 (2013) 126– 133

Kaufmann G., Dreybrodt W., Calcite dissolution in the system $CaCO_3$-H_2O-CO_2 at high undersaturation. Geochim Cosmochim Acta 71 (2007) 1398-1410

Kloprogge J.T., Frost R.L., Raman microscopy at 77 K of natural gypsum CaSO4·2H2O. J Mater Sci Lett 19 (2000) 229-231

Kodati V.R., Tomasi G.E., Turumin J.L., Tu A.T., Raman spectroscopic identification of phosphate-type kidney stones. Appl Spectrosc 45 (1991) 581-583

Koutsopoulos S., Synthesis and characterization of hydroxyapatite crystals: A review study on the analytical methods. J Biomed Mater Res 15 (2002) 600-612

Lazzarini L., Laurenzi Tabasso M., Il restauro della pietra, CEDAM, Padova (Italy), 1986

Leroux L., Vergès-Belmin V., Costa D., Delgado Rodrigues J., Tiano P., Snethlage R., Singer B., Massey S., De Wi E., Measuring the penetration depth of consolidating products: Comparison of six methods. Proceedings of the IX International Congress on the Deterioration and Conservation of Stone, Venice, vol. 2, June 19–24; 2000, 361–370.

Li D., Xu F., Liu Z., Zhu J., Zhang Q., Shao L., The effect of adding PDMS-OH and silica nanoparticles on sol-gel properties and effectiveness in stone protection. Appl Surf Sci 266 (2013) 368-374

Lide D.R. (Ed.), CRC Handbook of Chemistry and Physics, The Chemical Rubber Co, Boca Raton, FL (1999)

Liu C., Huang Y., Shen W., Cui J., Kinetics of hydroxyapatite precipitation at pH 10 to 11. Biomaterials 22 (2001) 301–306.

Liu Q., Zhang B., Shen Z., Lu H., A crude protective film on historic stone and its artificial preparation through biomimetic synthesis. Appl Surf Sci 253 (2006) 2625-2632

Liu Q., Zhang B., Synthesis and characterization of a novel biomaterial for the conservation of historic stone building and sculptures. Mater Sci Forum 675–677 (2011) 317–320.

Liu R., Han X., Huang X., Li W., Luo H., Preparation of three-component TEOS-based composites for stone conservation by sol-gel processes. J Sol-Gel Sci Tech 68 (2013) 19-30.

Lòpez-Arce P., Gomez-Villalba L.S., Pinho L., Fernàndez-Valle M.E., Álvarez de Buergo M., Fort R., Influence of porosity and relative humidityon consolidation of dolostone with calcium hydroxide nanoparticles: effectiveness assessment with non-destructive techniques. Mater Charact 61 (2010) 168–84.

Lourenço P.B., Luso E., Almeida M.G., Defects and moisture problems in buildings from historical city centres: a case study in Portugal. Build Environ 41(2006) 223-234

Lubelli B, van Hees RPJ, Nijland TG, Bolhuis J. A new method for making artificially weathered stone specimens for testing of conservation treatments, J Cult Herit; 205. doi: 10.1016/j.culher.2015.01.002.

Lubelli B., van Hees R.P.J., Nijland T.G., Salt weathering damage: how realistic are existing ageing tests?, in: H. De Clercq (Ed.), Proceedings of SWBSS2014, 3rd International Conference on Salt Weathering of Buildings and Stone sculptures, 14–16 October 2014, pp. 259–273.

Luque A., E. Ruiz-Agudo, G. Cultrone, E. Sebastiàn, S. Siegesmund, Direct observation of microcrack development in marble caused by thermal weathering. Environ Earth Sci 62 (2011) 1375-1386

M. Pamplona, S. Simon, Ultrasonic pulse velocity - A tool for the condition assessment of outdoor marble sculptures, Proceedings of 12th International Congress on Deterioration and Conservation of Stone, New York City (USA), 22-26 October 2012, p. 1-13, http://iscs.icomos.org/pdf-files/NewYorkConf/pampsimo.pdf

M.S.A. Johnsson, G.H. Nancollas, The role of brushite and octacalcium phosphate in apatite formation, Crit Rev Oral Bio M 3 (1992) 61–82.

Malaga-Starzec K., Åkesson U., Lindqvist J.E., Schouenborg B., Microscopic and macroscopic characterization of the porosity of marble as a function of temperature and impregnation. Constr Build Mater 20 (2006) 939–47.

Maravelaki-Kalaitzaki P, Kallithrakas-Kontos N, Agioutantis Z, Maurigiannakis S, Korakaki D. A comparative study of porous limestones treated with silicon-based strengthening agents. Prog Org Coat 62 (2008) 49–60.

Maravelaki-Kalaitzaki P., Black crusts and patinas on Pentelic marble from the Parthenon and Erecteum (Acropolis, Athens): characterization and origin. Anal Chim Acta 532 (2005) 187–98.

Maravelaki-Kalaitzaki P., Kallithrakas-Kontos N., Korakaki D., Agioutantis Z., Maurigiannakis S., Evaluation of silicon-based strengthening agents on porous limestones. Progr Org Coat 57 (2006) 140-148

Martìnez-Martìnez J., Benavente D., Gomez-Heras M., Marco-Castaño L., Garcìa-del-Cura M.A., Non-linear decay of building stones during freeze–thaw weathering processes, Constr Build Mater 38 (2013) 443–454.

Maslen E.N., Streltsov V.A., Streltsova N.R., Ishizawa N., Electron density and optical anisotropy in rhombohedral carbonates. III. Synchroton X-ray studies of $CaCO_3$, $MgCO_3$ and $MnCO_3$. Acta Crystallogr B51 (1995) 929–939.

Mathew M., Takagi S., Structures of biological minerals in dental research, J Res Natl Inst Stand Technol 106 (2001) 1035–1044.

Mats S., Johnsson A., Nancollas G.H., The role of Brushite and Octacalcium Phosphate in Apatite Formation. Crit Rev Oral Biol M 3 (1992) 61-82

Matteini M., Inorganic treatments for the consolidation and protection of stone artifacts. Conserv Sci Cult Herit 8 (2008): 13–27

Matteini M., Moles A., Giovannoni S., Calcium oxalate as a protective mineral system for wall paintings: methodology and analyses, III Int. Symp. Conservation of Monuments in the Mediterranean Basin, ed. V. Fassina, H. Ott, F. Zezza, 1994.

Matteini M., Rescic S., Fratini F., Botticelli G., Ammonium phosphates as consolidating agents for carbonatic stone materials used in architecture and cultural heritage: preliminary research. Int J Archit Herit: Conservation, Analysis, and Restoration 5 (2011) 717-736

Meloni P., Manca F., Carangiu G., Marble protection: An inorganic electrokinetic approach. Appl Surf Sci 273 (2013) 377-385

Mifsud T., Cassar J., The treatment of weathered Globigerina Limestone: the surface conversion of calcium carbonate to calcium oxalate. Proc Int Conf Herit Weather Conserv HWC, 2 (2006) 727–734

Miliani C., Velo-Simpson M.L., Scherer G.W., Particle-modified consolidants: a study on the effect of particles on sol–gel properties and consolidation effectiveness. J Cult Herit 8 (2007) 1–6.

Moropoulou A., Kouloumbi N., Haralampopoulos G., Konstanti A., Michailidis P., Criteria and methodology for the evaluation of conservation interventions on treated porous stone susceptible to salt decay. Prog Org Coat 48 (2003) 259–70.

Mosquera M.J., Pozo J., Esquivias L., Stress during drying of two stone consolidants applied in monumental conservation. J Sol-Gel Sci Tech 26 (2003)1227-1231.

Mudronja D., Vanmeert F., Hellemans H., Fazinic S., Janssens K., Tibljas D., Rogosic M., Jakovljevic S., Efficiency of applying ammonium oxalate for protection of monumental limestone by poultice, immersion and brushing methods. Appl Phys A- Mater 111 (2013) 109-119

Naidu S., Blair J., Scherer G.W., Acid attack mechanism on Carrara marble and efficacy of a protective hydroxyapatite film. J Am Ceram Soc (in press)

Naidu S., Liu C., Scherer G.W., Hydroxyapatite based consolidants and the acceleration of hydrolysis of silicate-based consolidants. J Cult Herit 16 (2015): 94-101

Naidu S., Liu C., Scherer G.W., New techniques in limestone consolidation: Hydroxyapatite based consolidant and the acceleration of hydrolysis of silicate-based consolidants. J Cult Herit 16 (2015) 94-101

Naidu S., Novel Hydroxyapatite Coatings for the Conservation of Marble and Limestone, PhD Thesis.

Naidu S., Sassoni E., Scherer G.W., New treatment for corrosion-resistant coatings for marble and consolidation of limestone, in Stefanaggi M., Vergès-Belmin V. (Eds), "Jardins de Pierres– Conservation of stone in Parks, Gardens and Cemeteries", Paris (F) 22-24 June 2011, p.289-294

Naidu S., Scherer G.W., Development of hydroxyapatite films to reduce the dissolution rate of marble, In: Proceedings of 12th International Congress on Deterioration and Conservation of Stone, New York City (USA), 22-26 October 2012, p. 1-9, http://iscs.icomos.org/pdffiles/NewYorkConf/naidsche.pdf

Naidu S., Scherer G.W., Nucleation, growth and evolution of calcium phosphate films on calcite. J Colloid Interf Sci 435 (2014) 128-137

Nelson D.G.A., Featherstone J.D.B., Duncan J.F., Cutress T.W., Effect of carbonate and fluoride on the dissolution behavior of synthetic apatites, Caries Res 17 (1983) 200–211.

Orkoula M.G., Koutsoukos P.G., Kinetics of dissolution of powdered Pentelic marble in undersaturated solutions: the role of particle characteristics. J Colloid Interf Sci 259 (2003) 287-292

Osaka A., Miura Y., Takeuchi K., Asada M., Takahashi K., Calcium apatite prepared from calcium

hydroxide and orthophosphoric acid. J Mater Sci Mater Med 2 (1991) 51–55.

Pamplona M., Simon S., Ultrasonic pulse velocity - A tool for the condition assessment of outdoor marble sculptures, Proceedings of 12th International Congress on Deterioration and Conservation of Stone, New York City (USA), 22-26 October 2012, p. 1-13

Pinna D., Salvadori B., Porcinai S., Evaluation of the application conditions of artificial protection treatments on salt-laden limestones and marble. Constr Build Mater 25 (2011) 2723-2732

Polikreti K., Maniatis Y., Micromorphology, composition and origin of the orange patina on the marble surfaces of Propylaea (Acropolis, Athens). Sci Total Environ 308 (2003) 111–119

Ramesh S., Natasha A.N., Tan C.Y., Bang L.T., Niakan A., Purbolaksono J., Chandran H., Ching C.Y., Ramesh S., Teng W.D., Characteristics and properties of hydroxyapatite derived by sol–gel and wet chemical precipitation methods. Ceram Int (2015)- in press

RILEM Recommendation MS-A1 Determination of the resistance of wallettes against sulfates and chlorides, Mater. Struct. 31 (1998) 2–19.

RILEM Recommendation MS-A2, Unidirectional salt crystallization test for masonry units, Mater. Struct. 31 (1998) 10–11.

Rodriguez-Navarro C., Doehne E., Sebastian E., How does sodium sulfate crystallize? Implications for the decay and testing of building materials. Cem Concr Res 30 (2000) 1527–1534.

Rothert E., Eggers T., Cassar J., Ruedrich J., Fitzner B., Siegesmund S., Stone properties and weathering induced by salt crystallization of Maltese Globigerina Limestone, in: Přikryl R., Smith B.J. (Eds.), Building stone decay: from diagnosis to conservation. Geol Soc London Spec Publ 271 (2007) 189–198

Rubio F., Rubio J., Oteo J.L., A FT-IR study of the hydrolysis of tetraethylortosilicate [ES]. Spectrosc Lett 3 (1998) 199–219.

Ruedrich J., Kirchner D., Siegesmund S., Physical weathering of building stones induced by freeze-thaw action: a laboratory long-term study. Environ Earth Sci 63 (2011) 1573–1586.

Ruedrich J., Siegesmund S., Salt and ice crystallisation in porous sandstones, Environ Geol 52 (2007) 225–249.

Ruedrich J., Weiss T., Siegesmund S., Thermal behavior of weathered and consolidated marbles. In: Siegesmund S., Weiss T., Vollbrecht A., editors. Natural stone, weathering phenomena, conservation strategies and case studies, Geological Society, London, Special Publications 205 (2002) 255–271.

Naidu S., Scherer G.W., Nucleation, growth and evolution of calcium phosphate films on calcite, J Colloid Interf Sci 435 (2014) 128-137

Saber-Samandaria S., Alamarab K., Saber-Samandaric S., Calcium phosphate coatings: Morphology, micro-structure and mechanical properties. Ceram Int 40 (2014) 563–572

Salazar-Hernandez C., Zarraga R., Alonso S., Sugita S., Calixto S., Cervantes J., Effect of solvent type on polycondensation of TEOS catalysed by DBTL as used for stone consolidation. J Sol-Gel Sci Tech (2009)49:301-310.

Sand K.K., Yang M., Makovicky E., Cooke D.J., Hassenkam T., Bechgaard K., Stipp S.L.S., Binding of ethanol on calcite: the role of the OH bond and its relevance to biomineralization. Langmuir 26 (2010) 15239-15247

Sandrolini F., Franzoni E., Cuppini G., Predictive diagnostics for decayed ashlars substitution in architectural restoration in Malta. Mater Eng 11 (2000) 323–37.

Sandrolini F., Franzoni E., Sassoni E., Diotallevi PP. The contribution of urban-scale environmental monitoring to materials diagnostics: a study on the Cathedral of Modena (Italy). J Cult Herit 12 (2011) 441–450

Sassoni E, Franzoni E. Influence of porosity on artificial deterioration of marble and limestone by heating. Appl Phys A Mater 115 (2014) 809–16.

Sassoni E., Franzoni E., Consolidation of Carrara marble by hydroxyapatite and behavior after thermal ageing, In: Toniolo L. et al. (Eds), Built Heritage: Monitoring Conservation Management, Research for Development, Springer International Publishing, 2015, p. 379-389, DOI: 10.1007/978-3-319-08533-3_32

Sassoni E., Franzoni E., Pigino B., Scherer G.W., Naidu S. Consolidation of calcareous and siliceous sandstones by hydroxyapatite: comparison with a ES based consolidant. J Cult Herit 14S (2013) e103–8.

Sassoni E., Franzoni E., Scherer G.W., Naidu S., Consolidation of a porous limestone by means of a new treatment based on hydroxyapatite, Proceedings of 12th International Congress on Deterioration and Conservation of Stone, New York City (USA), 22–26 October 2012 (2014), p. 1-11

Sassoni E., Franzoni E., Sugaring marble in the Monumental Cemetery in Bologna (Italy): characterization of naturally and artificially weathered samples and first results of consolidation by hydroxyapatite. Appl Phys A Mater 117 (2014) 1893–1906.

Sassoni E., Graziani G., Franzoni E., An innovative phosphate-based consolidant for limestone. Part 1: Effectiveness and compatibility in comparison with ethyl silicate, Constr Build Mater 102 (2016) 918-930

Sassoni E., Graziani G., Franzoni E., An innovative phosphate-based consolidant for limestone. Part 2. Durability in comparison with ethyl silicate. Constr Build Mater 102 (2016) 931-942

Sassoni E., Graziani G., Franzoni E., Repair of sugaring marble by ammonium phosphate: comparison with ethyl silicate and ammonium oxalate and pilot application to historic artifact. Materials and Design 88 (2015) 1145-1157

Sassoni E., Naidu S., Scherer G.W., The use of hydroxyapatite as a new inorganic consolidant for damaged carbonate stones, J Cult Herit 12 (2011) 346-355

Scherer G.W., Crystallization in pores, Cem Concr Res 29 (1999) 1347–1358.

Scherer G.W., Stress from crystallization of salt. Cem Concr Res 34 (2004) 1613–1624.

Scherer G.W., Wheeler G.S., Silicate consolidants for stone. Key Eng Mater 391 (2009) 1–25.

Shanika Fernando M., De Silva R.M., Nalin de Silva K.M., Synthesis, characterization, and application of nanohydroxyapatite and nanocomposite of hydroxyapatite with granular activated carbon for the removal of Pb^{2+} from aqueous solutions. Appl Surf Sci 351 (2015): 95-103

Siegesmund S., Ullemeyer K., Weiss T., Tschegg E.K., Physical weathering of marbles caused by anisotropic thermal expansion. Int J Earth Sci 89 (2000) 170–82.

Sjcoberg E.L., Rickard D.T., The effect of added calcium on calcite dissolution kinetics in aqueous solutions at 25°C. Chem Geol 49 (1985) 405-413

Skinner A.J., LaFemina J.P., Hansen H.J.F., Structure and bonding of calcite: a theoretical study. Am. Mineral 79 (1994) 205–214.

Skoulikidis T., Vassiliou P., Tsakona K., Surface consolidation of Pentelic marble – Criteria for the selection of methods and materials - The Acropolis case. Environ Sci & Pollut Res 12 (2005) 28-33

Slòsarczyk A., Stobierska E., Paskiewicz Z., Gawlicki M., Calcium phosphate materials prepared from precipitates with various calcium: phosphorous Molar Ratios. J Am Ceram Soc 79 (1996) 2539–2544.

Solmi F., Dezzi Bardeschi M., A. Rubbiani: I veri e i falsi storici, Grafis, Casalecchio di Reno, Bologna

Stanić V., Dimitrijević S., Antić-Stanković J., Mitrić M., Jokić B., Plećaš I.B., Raičević S., Synthesis, characterization and antimicrobial activity of copper and zinc-doped hydroxyapatite nanopowders, Appl Surf Sci 256 (2010) 6083-6089

Sugiyama S., Nishioka H., Moriga T., Hayashi H., Moffat J.B., Ion-Exchange Properties of Strontium Hydroxyapatite under Acidic Conditions. Separ Sci Technol 33 (1998) 1999-2007

Sun J., Wu Z., Cheng H., Zhang Z., Frost R.L., A Raman spectroscopic comparison of calcite and dolomite. Spectrochim Acta A 117 (2014) 158-162

Supova M., Substituted hydroxyapatites for biomedical applications: A review. Ceram Int 41 (2015) 9203-9231

Tao J., FTIR and Raman Studies of Structure and Bonding in Mineral and Organic–Mineral Composites. Method Enzymol 532 (2013) 533 - 556.

Toniolo L., Paradisi A., Goidanich S., Pennati G., Mechanical behaviour of lime based mortars after surface consolidation. Constr Build Mater 25 (2011) 1553–9.

Tsakalof A., Manoudis P., Karapanagiotis I., Chryssoulakis I., Panayiotou C., Assessment of synthetic polymeric coatings for the protection and preservation of stone monuments. J Cult Herit 8 (2007) 69-72

Tsui N., Flatt R.J.,. Scherer G.W., Crystallization damage by sodium sulfate. J Cult Herit 4 (2003) 109–115.

Tugrul A., The effect of weathering on pore geometry and compressive strength of selected rock types from Turkey. Eng Geol 75 (2004) 215–27.

Tulliani J.M., Formia A., Sangermano M., Organic-inorganic material for the consolidation of plaster. J Cult Herit 12 (2011) 364-371

Vacchiano C.D., Incarnato L., Scarfato P., Acierno D., Conservation of tuff-stone with polymeric resins. Constr Build Mater 22 (2008) 855–65.

Valentini F., Diamanti A., Carbone M, Bauer E.M., Palleschi G., New cleaning strategies based on carbon nanomaterials applied to the deteriorated marble surfaces: A comparative study with enzyme based treatments. Appl Surf Sci 258 (2012) 5965-5980

Van Balen K., Papayanni I., Van Hees R., Binda L., Waldum A., Introduction requirements for and functions and properties of repair mortars. Mater Struct 38 (2005) 781–5.

Verges-Belmin V., Orial G., Garnier D., Bouineau A., Coignard R., Impregnation of badly decayed Carrara marble by consolidating agents: Comparison of seven treatments, In: La conservation des

monuments dans le bassin metiterraneen: Actes du 2° symposium international, Geneve, 19-21/11/1991, 1992, 421-437

Wangler T., Scherer G.W., Clay swelling mechanism in clay-bearing sandstones. Environ Geol 56 (2008) 529–534.

Weiss T., Rasolofosaon P.N.J., Siegesmund S., Ultrasonic wave velocities as a diagnostic tool for the quality assessment of marble, In: Siegesmund S., Weiss T., Vollbrecht A., Natural stone, weathering phenomena, conservation strategies and case studies, Geological Society, London, Special Publications, 205 (2002) 149-164

Wheeler G., Alkoxysilanes and the Consolidation of Stone (Research in conservation), The Getty Conservation Institute, Los Angeles, 2005

Wheeler G.S., Fleming S.A., Ebersole S., Evaluation of some current treatments for marble, In: La conservation des monuments dans le bassin mediterraneen: Actes du 2° symposium international, Geneve, 19-21/11/1991, 1992, 439-443

Xu F., Li D., Effect of the addition of hydroxyl-terminated polydimethylsiloxane to TEOS-based stone protective materials. J Sol-Gel Sci Tech 65 (2013) 212-219.

Xu J., Gilson D.F.R., Butler I.S., FT-Raman and high pressure FT-infrared spectroscopic investigation of monocalcium phosphate monohydrate $Ca(H_2PO_4)2{\cdot}H_2O$. Spectrochim Acta A 54 (1998) 1869-1878

Yamini D., Devanand Venkatasubbu G., Kumar J., Ramakrishan V., Raman scattering studies on PEG funcionalized hydroxyapatite nanoparticles. Spectrochim Acta A 117 (2014) 299-303

Yang F., Zhang B., Liu Y., Guofeng W., Zhang H., Cheng W., Xu Z., Biomimic conservation of weathered calcareous stones by apatite. New J Chem 35 (2011) 887–892

Yang F.W., Liu Y., Zhu Y.C., Long S.J., Zuo G.F., Wang C.Q., Guo F., Zhang B.J., Jiang S.W., Conservation of weathered historic sandstones with biomimetic apatite. Chin Sci Bull 57 (2012) 2171–2176

Yavuz H., Ugur I., Demirdag S., Abrasion resistance of carbonate rocks used in dimension stone industry and correlations between abrasion and rock properties. Int J Rock Mech Min Sci 45 (2008) 260–267

Yoshimura M., Suda H., Okamoto K., Ioku K., Hydrothermal synthesis of biocompatible whiskers. J Mat Sci 29 (1994) 3399–3402.

Zendri E., Biscontin G., Nardini I., Riato S., Characterization and reactivity of silicatic

consolidants. Constr Build Mater 21 (2007) 1098–106.

Zhu Y., Zhanga X., Chena Y., Xiea Q., Lana J., Qiana M., He N., A comparative study on the dissolution and solubility of hydroxylapatite and fluorapatite at 25°C and 45°C. Chem Geol 268 (2009) 89–96.